Final Report

UPDATING FLORIDA DEPARTMENT OF TRANSPORTATION'S (FDOT) PILE/SHAFT DESIGN PROCEDURES BASED ON CPT & DTP DATA

BD-545, RPWO #43
UF Project #00005780

Submitted by:

David Bloomquist, P.E.
Mike McVay
Zhihong Hu

Department of Civil and Coastal Engineering
University of Florida
Gainesville, Florida 32611

Developed for the

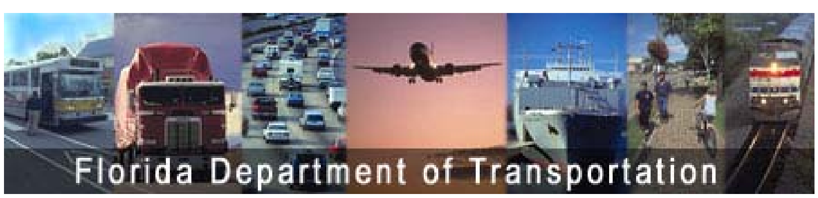

Project Managers:
David Horhota, PhD., P.E.
Peter Lai, P.E.
September 2007

Disclaimer

The opinions, findings, and conclusions expressed in this publication are those of the author and not necessarily those of the State of Florida Department of Transportation.

SI (MODERN METRIC) CONVERSION FACTORS (from FHWA)

Table 0-1. Approximate conversions to SI units

SYMBOL	WHEN YOU KNOW	MULTIPLY BY	TO FIND	SYMBOL
LENGTH				
in	inches	25.4	millimeters	Mm
ft	feet	0.305	meters	M
yd	yards	0.914	meters	M
mi	miles	1.61	kilometers	Km
SYMBOL	WHEN YOU KNOW	MULTIPLY BY	TO FIND	SYMBOL
AREA				
in^2	Square inches	645.2	square millimeters	mm^2
ft^2	Square feet	0.093	square meters	m^2
yd^2	square yard	0.836	square meters	m^2
ac	acres	0.405	hectares	Ha
mi^2	square miles	2.59	square kilometers	km^2
SYMBOL	WHEN YOU KNOW	MULTIPLY BY	TO FIND	SYMBOL
VOLUME				
fl oz	fluid ounces	29.57	milliliters	Ml
gal	gallons	3.785	liters	L
ft^3	cubic feet	0.028	cubic meters	m^3
yd^3	cubic yards	0.765	cubic meters	m^3
NOTE: volumes greater than 1000 L shall be shown in m^3				
SYMBOL	WHEN YOU KNOW	MULTIPLY BY	TO FIND	SYMBOL
MASS				
oz	ounces	28.35	grams	G
lb	pounds	0.454	kilograms	Kg
T	short tons (2000 lb)	0.907	megagrams (or "metric ton")	Mg (or "t")
SYMBOL	WHEN YOU KNOW	MULTIPLY BY	TO FIND	SYMBOL
TEMPERATURE (exact degrees)				
^oF	Fahrenheit	5 (F-32)/9 or (F-32)/1.8	Celsius	^oC
SYMBOL	WHEN YOU KNOW	MULTIPLY BY	TO FIND	SYMBOL
ILLUMINATION				
fc	foot-candles	10.76	lux	Lx
fl	foot-Lamberts	3.426	candela/m^2	cd/m^2
SYMBOL	WHEN YOU KNOW	MULTIPLY BY	TO FIND	SYMBOL
FORCE and PRESSURE or STRESS				

lbf	Pound force	4.45	newtons	N
lbf/in^2	Pound force per square inch	6.89	kilopascals	kPa

Table 0-2. Approximate conversions to English units

SYMBOL	WHEN YOU KNOW	MULTIPLY BY	TO FIND	SYMBOL
LENGTH				
mm	millimeters	0.039	inches	In
m	meters	3.28	feet	Ft
m	meters	1.09	yards	Yd
km	kilometers	0.621	miles	Mi
SYMBOL	WHEN YOU KNOW	MULTIPLY BY	TO FIND	SYMBOL
AREA				
mm^2	square millimeters	0.0016	square inches	in^2
m^2	square meters	10.764	square feet	ft^2
m^2	square meters	1.195	square yards	yd^2
ha	hectares	2.47	acres	Ac
km^2	square kilometers	0.386	square miles	mi^2
SYMBOL	WHEN YOU KNOW	MULTIPLY BY	TO FIND	SYMBOL
VOLUME				
mL	milliliters	0.034	fluid ounces	fl oz
L	liters	0.264	gallons	Gal
m^3	cubic meters	35.314	cubic feet	ft^3
m^3	cubic meters	1.307	cubic yards	yd^3
SYMBOL	WHEN YOU KNOW	MULTIPLY BY	TO FIND	SYMBOL
MASS				
g	grams	0.035	ounces	Oz
kg	kilograms	2.202	pounds	Lb
Mg (or "t")	megagrams (or "metric ton")	1.103	short tons (2000 lb)	T
SYMBOL	WHEN YOU KNOW	MULTIPLY BY	TO FIND	SYMBOL
TEMPERATURE (exact degrees)				
^oC	Celsius	1.8C+32	Fahrenheit	^oF
SYMBOL	WHEN YOU KNOW	MULTIPLY BY	TO FIND	SYMBOL
ILLUMINATION				
lx	lux	0.0929	foot-candles	Fc
cd/m^2	$candela/m^2$	0.2919	foot-Lamberts	Fl
SYMBOL	WHEN YOU KNOW	MULTIPLY BY	TO FIND	SYMBOL
FORCE and PRESSURE or STRESS				
N	newtons	0.225	Pound force	Lbf
kPa	kilopascals	0.145	Pound force per square inch	lbf/in^2

*SI is the symbol for the International System of Units. Appropriate rounding should be made to comply with Section 4 of ASTM E380.(Revised March 2003

Table 0-3. Technical Report Documentation Page

<table>
<tr><td>1. Report No.</td><td>2. Government Accession No.</td><td colspan="2">3. Recipient's Catalog No.</td></tr>
<tr><td colspan="2" rowspan="2">4. Title and Subtitle

UPDATING FLORDA DEPARTMENT OF TRANSPORTATION'S (FDOT) PILE/SHAFT DESIGN PROCEDURES BASED ON CPT & DTP DATA

BD-545, RPWO # 43
UF Project 00005780</td><td colspan="2">5. Report Date
July 2007</td></tr>
<tr><td colspan="2">6. Performing Organization Code</td></tr>
<tr><td colspan="2">7. Author(s)
David Bloomquist, Mike McVay, Zhihong Hu</td><td colspan="2">8. Performing Organization Report No.</td></tr>
<tr><td colspan="2" rowspan="2">9. Performing Organization Name and Address
Department of Civil and Coastal Engineering
365 Weil Hall
University of Florida
Gainesville, Florida 32611</td><td colspan="2">10. Work Unit No. (TRAIS)</td></tr>
<tr><td colspan="2">11. Contract or Grant No.
BC-545, RPWO #43</td></tr>
<tr><td colspan="2" rowspan="2">12. Sponsoring Agency Name and Address
Florida Department of Transportation
605 Suwannee Street, MS 30
Tallahassee, FL 32399</td><td colspan="2">13. Type of Report and Period Covered
Final Draft Report
12/2004 – 7/2007</td></tr>
<tr><td colspan="2">14. Sponsoring Agency Code</td></tr>
<tr><td colspan="4">15. Supplementary Notes</td></tr>
<tr><td colspan="4">16. Abstract
Fourteen pile design methodologies (Schmertmann, LCPC, etc.) using CPT results have been evaluated using the LRFD resistance factor method s (Philipponnat Method) has been modified to propose a new method to improve future FDOT pile design. This research also involves identifying cemented soils using DTP since cementation is a critical issue in pile design procedures.</td></tr>
<tr><td colspan="2">17. Key Words
Concrete piles, cemented sand, Dual Tip Penetrometer, Cone Penetration Test, ultimate pile capacity</td><td colspan="2">18. Distribution Statement
No restrictions.</td></tr>
<tr><td>19. Security Classif. (of this report)
Unclassified.</td><td>20. Security Classif. (of this page)
Unclassified.</td><td>21. No. of Pages
199</td><td>22. Price</td></tr>
</table>

TABLE OF CONTENTS

LIST OF TABLES

LIST OF FIGURES

Figure page

LIST OF ABBREVIATIONS

α	empirical factor to calculate tip resistance in Zhou et al. Method
α_C	penetrometer to pile friction ratio in clay in Schmertmann Method
α_S	penetrometer to pile friction ratio in sand in Schmertmann Method
α_s	empirical factor to calculate skin friction in Philipponnat Method
A_S	surface area for the calculation of skin friction
ASTM	American society for testing and materials
β	adhesion factor in De Ruiter and Beringen Method and Zhou et al. Method
β_T	target reliability index
C_S	pile skin friction factor in Eslami and Fellenius Method
CPT	cone penetration test
COV (Q)	load coefficients of variation
COV (R)	resistance coefficient of variation
COV_{QD}	dead load coefficient of variation
COV_{QL}	live load coefficient of variation
δ_f	pile-soil interface friction angle at the maxmum shear stress
δ_{cv}	constant volume interface friction angle between sand and pile
D	diameter or side length of pile
D_{CPT}	diameter of cone penetrometer
D_{int}	the internal diameter for pipe pile
DTP	dual tip penetrometer
Δr	interface dilation
$\Delta\sigma'_{rd}$	the net dilatant component
Φ	LRFD resistance factor
F_b	empirical factor to calculate tip resistance in Aoki and De Alencar Method
F_s	empirical factor to calculate skin friction in Aoki and De Alencar Method
F_S	empirical factor to calculate skin friction in Philipponnat Method
FDOT	Florida department of transportation
FORM	First Order Reliability Method
FOSM	First Order Second Moment
f_L	loading coefficient
f_S	pile unit skin friction
f_{sa}	average CPT sleeve friction
ϕ	friction angle
G	the sand shear modulus, failure equation in terms of random variables
G_{max}	maximum shear modulus
γ_D	dead load factor
γ_L	live load factor
h	the hight above the pile tip
I-295	Interstate 295

I-95	Interstate 95
K_c	earth pressure coeffient after equilization
k	pile tip resistance factor in MTD Method
k_1	pile skin friction factor in Almeida et al. Method and Powell et al. Method
k_2	pile tip resistance factor in Almeida et al. Method and Powell et al. Method
k_b	pile tip resistance factor
k_S	pile skin friction factor
L	pile embedment length
LCPC	Laboratoire Central des Ponts et Chaussées
LRFD	load and resistance factor design
γ_i	load factors
λ_{QD}	dead load bias factor
λ_{QL}	live load bias factor
λ_R	the mean bias
λ_{Ri}	the ratio of measured to predicted pile capacities
MTD	marine technology directorate
MN/m^2	mega Newton per square meters
m	pile skin friction factor in Tumay and Fakhroo Method
N	the number of cases, or SPT blow count
N_C	bearing capacity factor
N_k	cone factor in De Ruiter and Beringen Method
N_{kt}	cone factor in Powell et al. Method
N_s	cone factor to estimate sensitivity
NCHRP	National Cooperative Highway Research Program
OCR	over consolidation ratio
PI	plasticity index
Pa	atmosphere pressure
PPC	precast-prestressed-concrete
PL-AID	pile load settlement analysis from *insitu* data
psi	pound per square inches
Q	random variable for load
Qc/N	the ratio of CPT tip resistance to the SPT blow count
Q_I	force effects
Q_D	dead load
$Q_{Davisson}$	Davisson capacity
Q_L	live load ratio
Q_D/Q_L	dead to live load ratio
Q_S	pile total tip resistance
$Q_{S\ ult}$	ultimate pile skin friction
$Q_{T\ ult}$	ultimate pile tip resistance
q_c	CPT tip resistance
q_{ca}	average CPT tip resistance
q_e	the average of the effective cone resistance within the calculation layer
q_{eg}	the geometric average of the effective cone resistance
q_{eq} (tip)	average tip resistance within 1.5 D above and 1.5 D below the pile tip

q_t	pile unit tip resistance
R	the diameter of the pile in the MTD method, random variable for resistance
R_{cla}	the pile's center-line-average roughness
R_{design}	design capacity
R_{mi}	measured capacity from load test data
R_{ni}	predicted capacity form CPT data
R_n	nominal resistance
R.D.	relative density
SMO	state material office
SPT	standard penetration test
S_t	clay sensitivity
S_u	undrained shear strength
σ_R	the standard deviation of λ_{Ri}
σ'_{rc}	radial effective stress on side after equalization
σ'_{rf}	radial effective stress at maximum shear stress
σ_{v0}	the total overburden stress
σ'_{v0}	the effective overburden stress
T1	DTP first tip resistance
T2	DTP second tip resistance
tsf	tons per square feet
UF	the University of Florida
UWA	the university of Western Australia
VAR	variance
YSR	yield stress ratio
y	the distance between the surface and the skin friction calculating point
η	load modifier for importance, redundancy and ductility

EXECUTIVE SUMMARY

The Florida Department of Transportation (FDOT) is developing a geotechnical – materials-construction database that includes information on piles and drilled shafts. Specifically, *insitu* (SPT, CPT, etc.) and load test data which it began accumulating in the early 1990s. More recently, FDOT sponsored a novel research project to develop a new *insitu* device, the Dual Tip Penetrometer (DTP), to identify cemented soils and thereby contribute to the database. The objective of this research program is to evaluate current pile design methodologies (Schmertmann, LCPC, etc.) using CPT, DTP, and SPT and to modify a current method or methods or propose a new one to improve future FDOT pile design. This research also involves identifying cemented soils using the DTP, since cementation is a critical issue in pile design predictions.

This research explores 14 pile-capacity-design methods based on the CPT currently used in the States, and assesses LRFD (Load and Resistance Factor Design) resistance factors for each method using 21 cases in Florida soil and 28 cases in Louisiana soil. The resulting resistance factors were not satisfactory for any of the methods. Therefore, a new design method was proposed, taking into account cementation and spatial variability. The LRFD resistance factor was also assessed for this new method. DTP tests were performed at cemented-soil sites to verify the cemented-soil identification (T2/T1, [Tip 1/Tip 2], and Friction Ratio) from the DTP. The ratio T2/T1 was finally determined to be an excellent identifier in locating cemented sand.

The new method provides better LRFD resistance factors for both Florida and Louisiana soils. It portends to be a promising method to improve pile designs. From the DTP tests in cemented soils, it was concluded that the DTP could be an efficient tool to identify cemented sands and thereby better predict pile capacity.

CHAPTER 1
INTRODUCTION

From the 1960s to the 1980s, FDOT sponsored research at the University of Florida to evaluate the methods used for calculating static pile capacity based on the CPT (Cone Penetration Test). After years of research, Dr. Schmertmann (1978) proposed the method which was later named after him. This method was adopted by FDOT in their pile design software and termed, PL-AID. This method has been used successfully in the Districts of Florida on 16” to 18” precast-prestressed-concrete (PPC) piles. However, during the last two decades, the size of piles have increased to 24” to 30”, primarily due to higher strength concrete and steel as well as larger pile driving equipment. The Schmertmann Method thus became conservative in evaluating pile capacity based on the comparison between the predictions and static load test results.

During the 1980s, there were several other methods developed around the world. These included the Aoki, N. and de Alencar Method (1975), Penpile Method (Clisby, M.B., et al. 1978), de Ruiter, J., and F.L. Beringen Method (1979), Philipponnat, G. Method (1980), Bustamante, M., and L. Gianeeselli Method (LCPC) (1982), Price, G. and Wardle, I.F. Method (1982), and Tumay, M.T., and Fakhroo, M. Method (1982). Most of these methods were generated by matching the CPT and load test database in the local area. None of the methods have been evaluated in Florida soils. The Louisiana Transportation Research Center did evaluate these methodologies in predicting the axial ultimate capacity of square PPC piles driven into Louisiana clays. Based on the results, the de Ruiter and Beringen and Bustamante and Gianeselli (LCPC) methods showed the best performance in prediction pile capacity. However, that may or may not be the case in Florida.

From 1990 until the present, many new methods have been proposed. They include the Almeida et al. Method (1996), Jardine and Chow Method (1996), Eslami and Fellenius Method (1997), Powell et al. Method (2001), and UWA-05 Method (Lehane, B.M., et al. 2005). Most of these methods take into account the pore pressure from the CPTU to improve their accuracy. The Zhou et al. Method (1982) was proposed in 1982 using load test data and CPT results performed in eastern China. However, it hadn't been evaluated in other areas outside of this region. Again, none of these methods have been evaluated in Florida. Details of these methods are provided in the following chapters.

There are a total of 21 cases (load test data with CPT results close to them) in Florida and 28 in Louisiana. All previous methods were evaluated using these cases. The LRFD resistance factor for each method was calculated and compared. One of the most accurate and simplest method, the Philipponnat Method, was chosen and modified to form the proposed UF method. Both Florida and Louisiana soil data were used for validation.

One of the more challenging soil types in Florida is cemented sand. Cementation in sands improves strength, but the strength increase depends on the degree of cementation. The bond strength should be considered when designing foundations on or in cemented sands. Since this material cannot be identified by a CPT test, none of the methods mentioned above had taken into account the cementation issue. This means they may overestimate the pile capacity, which may produce a serious design flaw. Recently, the FDOT funded the University of Florida to develop a new cone penetrometer, termed the Dual Tip Penetrometer (DTP), which appears to be able to identify cemented sands. UF's new proposed design method takes into account the cementation issue and results in the highest Φ/λ_R (ratio of resistance factor to mean bias - 0.62 for Florida soils and 0.67 for Louisiana soil) among all the methods as well has having the lowest coefficient of variation (0.27 for Florida soil and 0.23 for Louisiana soil).

CHAPTER 2
LITERATURE REVIEW

Cemented Sand

The term "cemented sand" is a generic term used for a wide variety of soils. King, R.W. (Lunne et al. 1997) proposed a classification system for a variety of cemented carbonate soils (Table 2-1). One of the main problems of this table is that degree of cementation is only a function of penetrometer resistance q_c, and does not take into account the sand's relative density. For example, non-cemented dense sand may have a cone resistance q_c higher than 10 MN/m^2, with no cementation. It will be very useful for design engineers, if better identifiers or parameters for cemented sand can be found.

Table 2-1. Classification system for calcareous soils proposed by King et al. (Lunne et al. 1997)

			FINE GRAINED		MEDIUM-COARSE GRAINED			
	DEGREE OF INDURATION	CONE RESISTANCE q_c MN/m^2	INCREASING GRAINSIZE 0.002mm	0.006mm, 0.02mm, 0.06mm (fine, med, c'se)	0.2mm, 0.6mm, 2mm (fine, med, coarse)	6mm, 20mm, 60mm (fine, med, coarse)	DEGREE OF CEMENTATION	CONE RESISTANCE q_c MN/m^2
SOIL	VERY WEAKLY INDURATED	0-2	CARBONATE MUD	CARBONATE SILT	CARBONATE SAND clastic/bioclastic/oolitic	CARBONATE GRAVEL clastic/bioclastic	VERY WEAKLY CEMENTED	0-2
SOIL	WEAKLY INDURATED	2-4					WEAKLY CEMENTED	2-4
SOIL	FIRMLY INDURATED	4-10					FIRMLY CEMENTED	4-10
ROCK	WELL INDURATED	>10	CALCILUTITE (carb mudstone)	CALCISILTITE (carb siltstone)	CALCARENITE (carb sandstone) clastic/bioclastic/oolitic	CALCIRUDITE (carb congl. or breccia) clastic/bioclastic	WELL CEMENTED	>10
ROCK			FINE GRAINED LIMESTONE		DETRITAL LIMESTONE clastic/bioclastic/oolitic	CONGLOMERATE LIMESTONE clastic/bioclastic		
ROCK			CRYSTALLINE LIMESTONE		CRYSTALLINE LIMESTONE			

Classification of Carbonate Sediments (90–100% carbonate)
(modified after Clark and Walker, 1977)

Cemented sands exist in many areas of the United States, including California, Texas, Florida, and along the banks of the lower Mississippi River. They also exist in Norway, Australia, Canada, and Italy (Puppala et al. 1995). Calcareous cemented sands are a feature of warm water seas mainly due to the sedimentation of the skeletal remains of marine organisms (Lunne et al. 1997).

Cemented sand, as the name implies, is a cohesionless material in which a calcium-carbonate chemical bond develops - to some extent. This chemical bond is the result of the deposition of calcium at the particle-to-particle contacts and the chemical reaction occurs between calcium and sand over a long period of time. The strength of these chemical bonds depends on the degree of cementation as well as the distribution. This kind of cementation leads to a significant increase in modulus (Briaud). Ahmadi et al. modeling the CPT penetrating process and found that the modulus of sand is the key factor in CPT tip resistance (Ahmadi et al. 2005). This is the primary reason why cementation tends to increase tip resistance. This phenomenon was also found by Puppala et al. (Puppala et al. 1995).

From a mechanical point of view, cemented sand belongs to an intermediate class of geo-materials placed between classical soil mechanics and rock mechanics. Often, no physical or mathematical models are able to integrate this kind of material in a consistent and unified framework (Gens and Nova 1993). During loading, cemented sand shows a very stiff behavior before yielding, which is governed by cementation. After stresses reach the yielding stress, it suddenly changes into a ductile material. Leroueil and Vaughan (1990) discovered that the structure of chemical bonds and its effects on soil behavior is a very important factor in determining the soil stress-strain behavior as well as other factors, such as the relative density, consolidation ratio, etc. However, the structure of chemical bonds is an unpredictable and very difficult issue to identified, let alone quantify.

An understanding of the effect of a low degree of cementation on a sand's strength is increasingly important in geotechnical engineering design and analysis. In the current design procedure, the effect of cementation is often neglected because cementation often improves the strength. However, preliminary studies indicate that light cementation increases the tip and friction resistances while decreasing the CPT friction ratio (Rad and Tumay 1986). This could be explained by the bonds increasing the resistance during the penetration. However, the bonds tend to be break during pile driving, and the CPT cannot "sense" this reduction in strength.

The degree of cementation in sands can be an issue for geotechnical engineers. For well cemented sands, the strength can be so high that engineers will neglect the cementation issue. However, in these cases, even though the CPT couldn't totally break the chemical bond within the sand particles, large diameter driven piles may indeed do so, resulting in a much lower pile capacity than that predicted by the CPT results. For lightly cemented sand, a breakdown of the "cohesion" bonds can also occur from a disturbance such as an earthquake. One such example is when the Loma Prieta San Francisco earthquake caused slope failures along the cemented sand northern Daly City bluffs (Puppala et al. 1995). Other similar slope failures have occurred due to earthquakes and heavy rains (Rad and Tumay 1986).

If the sands tested with a CPT are not known to be cemented, the high bearing readings may be misinterpreted as being due to high relative densities. This can lead to an underestimation of the liquefaction potential of the soil and an overestimation of the ultimate pile capacity. None of the CPT prediction methods evaluated to date take into account the reduction of strength in cemented sand. The concern was proved legitimate by the CPT and DTP testing performed at the Port Orange Relief Bridge in Jacksonville Florida. A comparison between the prediction methods and the load test result shows that most of the methods over-predict the pile capacity (some by over 100%).

Some researchers have performed laboratory tests on cemented sands obtained in the field. Both Clough et al. (1981) and Puppala et al. (1998) have tested naturally cemented sands in triaxial tests and unconfined compressive strength tests. The cemented sands were obtained by trimming samples using an SPT split spoon sample. The retreival of undisturbed, lightly cemented sands was quite difficult since the bonds tended to break under light finger pressure.

Due to the difficulty in sampling, *insitu* testing has become a more popular method of testing naturally occurring cemented sands. The CPT test is a popular device for testing cemented sands. The CPT test has been used to test both naturally occurring cemented sands in the field (Puppala et al. 1998) and artificially cemented sands in calibration chambers (Rad & Tumay 1986; and Puppala et al. 1995). In both the 1985 and 1996 calibration chamber studies, Monterrey No. 0/30 sand was cemented with 1% and 2% Portland cement. An attempt was made to relate the tip bearing and friction sleeve values to the sand properties, including cement content, relative density, confining stress and friction angle. Puppala (1995) did this by using the bearing capacity equations of Durgunoglu & Mitchell (1975) and Janbu & Senneset (1974). To include the effect of cementation or cohesion on tip bearing, the other parameters that affect the tip, mainly relative density and confining stress, needed to be known and included in the equations proposed by Puppala. Even though the calibration chamber study is time-efficient and makes it easy to control the cementation ratio, there are several drawbacks; first, the cementation structure in nature is almost impossible to duplicate in the chamber and, as is discussed above, this is a very important issue in determining a soil's strength. Secondly, the stress state in the field is different from those in the calibration chamber, especially for deeply occurring cemented soil, due to size limitations of the chamber. Therefore, the literature indicates that the best approach in dealing with this issue is to test materials insitu (e.g., CPT test) and somehow identify when cementation is present.

Since the main problem of cemented sands is providing "cohesion" on tip bearing resistance, it may be possible to obtain more accurate bearing capacity predictions if this effect could be removed from the tip bearing resistance. One way to accomplish this would be to design an *insitu* device that could measure the bearing strength of the cemented sands both before and after the cohesive bonds have been broken. This is the rationale that led to the development of the Dual Tip Penetrometer developed at the University of Florida. Since it is simply an enhanced CPT, a brief history of this versatile instrument is provided below.

CPT (Cone Penetration Test)

The cone penetration test is considered one of the most cost-effective and reliable methods for soil classification. The CPT (Figure 2-1) pushes a cone into the soil at a constant rate by means of cylindrical rods that are connected in series with the cone located at the base of the string of rods. During the test, the sleeve friction and tip resistance are measured and recorded. These two parameters are used to classify soil and to estimate strength and deformation characteristics of soils.

In 1917, the Swedish Railways was the first to introduce the CPT. Ten years later, Danish Railways started using the CPT. The first apparatus was simply a cone and a string of outer rods. In 1936, the Dutch Mantle cone was introduced. This cone has an area of 10 cm^2 and an apex angle of 60°, which is similar to the current ones in use. But the cone was pushed by hand and there was a limitation on the capacity and penetration depth. In addition, it could not penetrate very dense sand or cemented soils.

Figure 2-1. Conventional cone penetrometer

In the 1940's and early 1950's, hydraulic jacks were introduced that allowed for much more reactive force being applied, thereby increasing penetration depths. This advancement dramatically increased CPT usage. In 1948, the first electric cone penetrometer was developed. Strain gages were used to measure the soil resistance, which increased its accuracy dramatically, since the bridge circuit made it more sensitive to small changes in soil resistance. The most important feature of electric CPT is that it can provide a continuous reading of a soil's resistance during the test (typically logged every 5 cm). This provides a wealth of subsurface information for geotechnical engineers.

One of the most important improvements of the CPT was made in 1953. Begemann proposed the use of a separate sleeve located just behind the tip that allows the penetrometer to measure both tip resistance q_c and sleeve friction resistance f_s. The friction sleeve has an area of 150 cm^2 and was used in conjunction with the traditional Begemann mechanical cone in the late 1950s. In 1968, an electric cone penetrometer with the friction sleeve was developed in Australia.

The first ASTM standard (ASTM D-3441-75T) for the cone penetrometer was published in 1975. In 1979 and 1986, ASTM D-3441-79 and ASTM D-3441-86 were published to revise the previous standard. In 1988, an international reference test procedure was developed by the International Society of Soil Mechanics and Foundation Engineering.

Currently, there are two diameters for the cone: 1.41 in (10 cm^2 cross section) and 1.71 in (15 cm^2 cross section) with both having a 60° angle. The first one is the most commonly used.

CPT Based Pile Capacity Prediction Methods

Using CPT data for design is considered one of the most promising methods to predict pile capacities for the following reasons:

1. The shape of a cone penetrometer is very similar to a cylindrical driven pile except at the bottom. However, during driving, the soil under the pile tip is densified and forms a cone-shaped failure envelope similar to the cone penetrometer's 60° tip.
2. The soil state during cone penetration is comparable to that during pile driving.
3. The testing process is quasi-static, which is more representative of a static load test compared to other in-situ tests.
4. Because the cone penetrometer actually penetrates the soil, causing an ultimate failure (punching failure) condition, it should be possible to predict the ultimate failure of the pile - including ultimate skin friction and ultimate tip resistance. These two predictions can also be useful during pile driving in order to prevent damage during the driving process.
5. The speed of conducting a test allows for more CPT soundings at a particular site and coupled with load test data make it possible to generate improved pile capacity prediction methods.

There are also issues involved in the prediction of pile capacities using the CPT which have to be solved by empirical correlations:

1. The scale effect caused by the difference between the diameter of the penetrometer and that of the piles. This will influence soil densification. The larger the diameter, the more densification the soil can achieve. It will also influence the size of the "stress bulb" which will influence the zone of resistance near the pile tip. If the soil is not uniformly distributed and the soil layer is not horizontal, one CPT may not be able represent the full scale pile – particularly large diameter piles.
2. The CPT cannot be used to identify cemented soils. It tends to misidentify the material as simply a denser soil state, due to the high q_c values.
3. When a CPT is performed in saturated clayey soils, especially with low permeability, high excess pore pressure will be generated during penetration and will cause higher q_c values. However, when a pile is driven into the same soil, much higher excess pore pressure will be generated and will dissipate slowly depending on the permeability.

In order to propose a better method to predict pile capacities, many existing methods have been investigated. An extensive literature search was conducted, specifically looking for axial pile prediction methods based on CPT cone soundings. The following methods were identified as those used by a number of DOTs, consultants or contractors: the Schmertmann Method, the de Ruiter and Beringen Method, the Penpile Method, the Price and Wardle Method, the Tumay and Fakhroo Method, the Aoki and De Alencar Method, the Philipponnat Method, and the LCPC (Bustamante and Gianeselli) Method. Most of the above methods were developed in 1980's. From 1990 until now, several new methods have been proposed. They are the Almeida et al. Method, the MTD (Jardine and Chow) Method, the Eslami and Fellenius Method, the Lee and

Salgado Method, the Powell et al. Method, and the UWA-05 Method. The Zhou et al. Method was proposed in 1982 using load test data and CPT performed in eastern China. A discussion of each of the methods is presented in the following section of this chapter.

Schmertmann Method (1978)

This method was first proposed by Schmertmann in 1978. It uses both tip resistance and sleeve friction to predict pile capacity. The pile's unit tip capacity is calculated by the minimum path rule shown in Figure 2-2. Schmertmann set an upper limit of 150 tsf for the unit tip capacity.

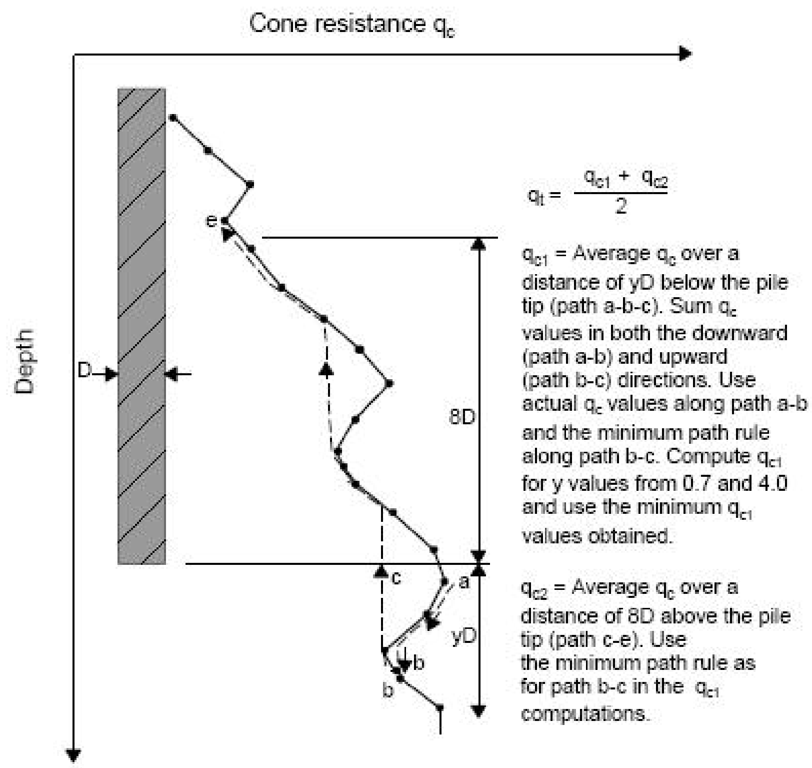

Figure 2-2. Calculation of average tip resistance using the Minimum Path Rule in the Schmertmann method

The pile's unit skin friction:

In clay: $f_s := \alpha_c \cdot f_{sa} \le 1.2\text{tsf}$

where: α_c is a function of f_{sa} as shown in Figure 2-3.

In sand: $$Q_s := \alpha_s \cdot \left(\sum_{y=0}^{8D} \frac{y}{8D} \cdot f_{sa} \cdot A_s + \sum_{y=8D}^{L} f_{sa} \cdot A_s \right) \qquad f_{sa} \le 1.2\text{tsf}$$

where: α_S is a function of pile depth to width ratio as shown in Figure 2-4.

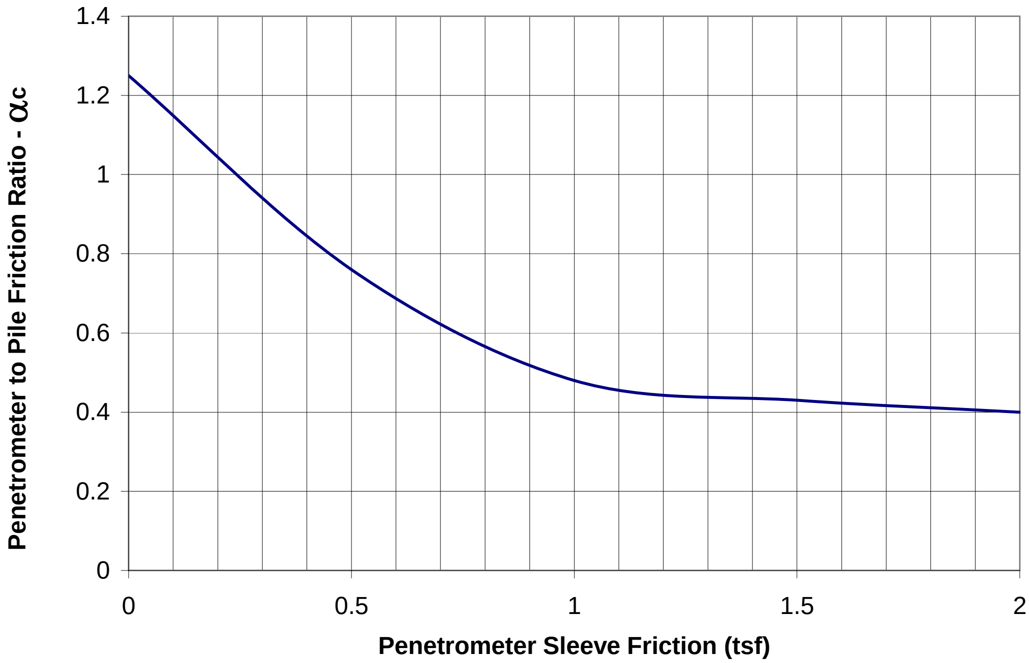

Figure 2-3. Design curve for concrete pile side friction in clay (Schmertmann method)

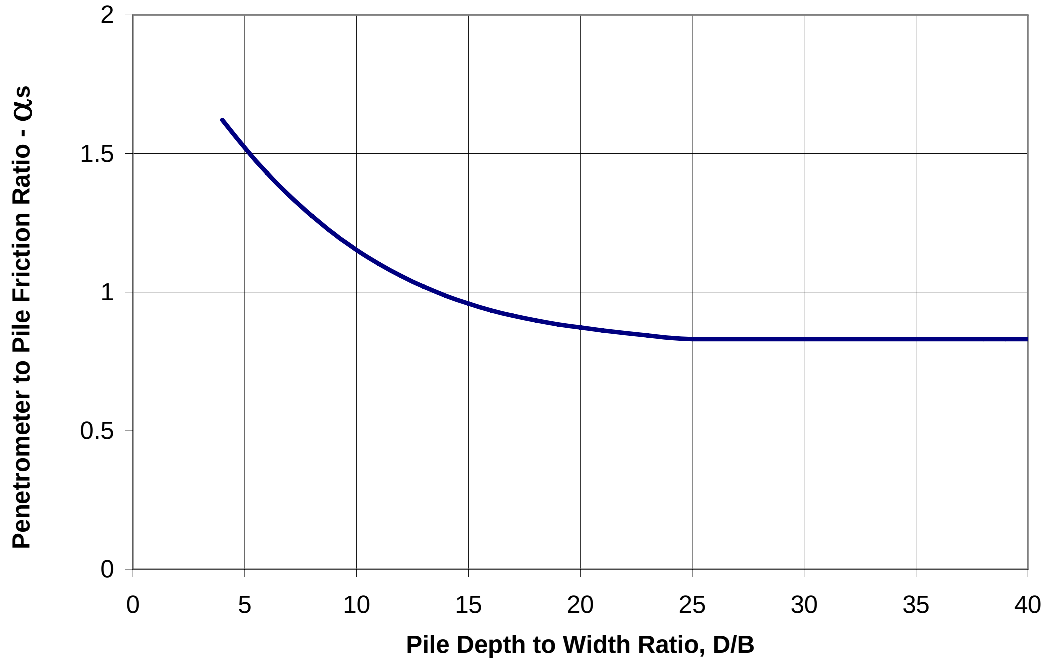

Figure 2-4. Design curve for concrete pile side friction in sand (Schmertmann method)

De Ruiter and Beringen Method (1979)

This method was proposed by de Ruiter and Beringen from their study of the soil near the North Sea. It uses both tip resistance and sleeve friction to predict the pile capacity.

The pile's unit tip capacity:

In clay: $q_t := N_c \cdot S_u(\mathrm{tip})$ $\qquad S_u(\mathrm{tip}) := \dfrac{q_c(\mathrm{tip})}{N_k}$

where: $N_C = 9$, constant, bearing capacity factor;

q_c (tip) is the average cone tip resistance around the pile tip - similar to Schmertmann method (minimum path rule);

$N_k = 15{\sim}20$, constant, cone factor, (20 was used in the current study since it yielded better results).

In sand: $$q_t := \frac{q_{c1} + q_{c2}}{2} \le 150 \cdot tsf$$

The calculation of tip capacity is simular to the Schmertmann Method.

The pile's unit skin friction:

In clay: $$f_s := \beta \cdot S_u(side) \qquad S_u(side) := \frac{q_c(side)}{N_k}$$

where: β constant, adhesion factor, 1 for N.C., 0.5 for O.C., (1 was used in the current study);

q_c (side) is the average cone tip resistance within the calculated layer along the pile.

In sand: $$f_s := \min\left[f_{sa}, \frac{q_c(side)}{300}(compression), \frac{q_c(side)}{400}(tension), 1.2tsf\right]$$

where: f_{sa} is the average sleeve friction within the calculated layer along the pile.

Penpile Method (1980)

This method was invented by Clisby et al. for the Mississippi Department of Transportation. It uses both cone tip resistance and sleeve friction to predict the pile's axial capacity.

The pile's unit tip capacity:

In clay: $$q_t := 0.25 \cdot q_{ca}$$

In sand: $q_t := 0.125 \cdot q_{ca}$

where: q_{ca}: the average of three cone tip resistances near the pile tip.

The pile's unit skin friction: $$f_s := \frac{f_{sa}}{1.5 + 0.1 \cdot f_{sa}}$$

where: f_{sa}: the average sleeve friction within the calculated layer along the pile.

f_s, f_{sa} are expressed in psi (lb/in^2).

Prince and Wardle Method (1982)

This method uses both the CPT tip resistance, q_c, and sleeve friction, f_s, to predict the axial pile capacity.

The pile's unit tip capacity: $q_t := k_b \cdot q_{ca}(\text{tip}) \le 150 \cdot \text{tsf}$

The pile's unit skin friction: $f_s := k_s \cdot f_{sa} \le 1.2 \cdot \text{tsf}$

where: k_b and k_S are factors that depend on pile type;

$k_b = 0.35$ for driven pile, 0.3 for jacked pile;

$k_S = 0.53$ for driven pile, 0.62 for jacked piles, and 0.49 for drilled shafts;

q_{ca} (tip) is the average CPT tip resistance within 4D below and 8D above the pile tip (there is no reference regarding the influence zone, therefore for better results, 4D below and 8D above were chosen).

Tumay and Fakhroo Method (1982)

This method was proposed by Tumay and Fakhroo for estimating pile capacity in clayey soil. In order to see how this method performed for Florida soil, it was also evaluated. It uses both tip resistance and sleeve friction to predict capacity.

The pile's unit tip capacity: $q_t := \dfrac{q_{c1} + q_{c2}}{2} \le 150 \cdot tsf$

The pile's unit skin friction:

$$f_s := m \cdot f_{sa} \le 0.72 \cdot tsf \qquad m := 0.5 + 9.5 \cdot e^{-9 \cdot f_{sa}}$$

where: f_{sa} is the average sleeve friction within the calculated layer along the pile in tsf (ton/ft^2),

Aoki and De Alencar Method (1975)

This method only uses the CPT tip resistance to predict the pile capacity.

The pile's unit tip capacity: $q_t := \dfrac{q_{ca}(tip)}{F_b} \le 150 \cdot tsf$

The pile's unit skin friction: $f_s := q_{ca}(side) \cdot \dfrac{\alpha_s}{F_s} \le 1.2 \cdot tsf$

where: F_b, F_s are empirical factors that depend on pile type (Table 2-2), α_S is a function of soil type (Table 2-3).

q_{ca} (tip) is the average CPT tip resistance within 4D below and 8D above the pile tip.

Table 2-2. Empirical factors F_b, F_S for Aoki and De Alencar Method

Pile Type	F_b	F_s
Bored	3.5	7.0
Franki	2.5	5.0
Steel	1.75	3.5
Precast concrete	1.75	3.5

Table 2-3. Empirical factors α_S for Aoki and De Alencar Method

Soil Type	α_S (%)	Soil Type	α_S (%)
Sand	1.4	Clayey sand	3.0
Silty sand	2.0	Silt	3.0
Sandy silt	2.2	Silt clay with sand	3.0
Silty sand with clay	2.4	Clayey silt with sand	3.0
Sandy Clay	2.4	Clayey silt	3.4
Sandy silt with clay	2.8	Silty clay	4.0
Clayey sand with silt	2.8	Clay	6.0
Sandy clay with silt	2.8		

Philipponnat Method (1980)

This is another method which uses tip resistance, q_c, to predict the axial pile capacity.

The pile's unit tip capacity: $q_t := k_b \cdot q_{ca}(\text{tip})$

The pile's unit skin friction: $f_s := q_{ca}(\text{side}) \cdot \frac{\alpha_s}{F_s} \le 1.27 \cdot \text{tsf}$

where: q_{ca} (tip) is the average tip resistance 3D below and 3D above the pile tip;

k_b and F_S are functions of soil type, see Tables 2-4, 2-5 for k_b and F_S;

α_s is determined by pile type = 1.25 for precast prestressed concrete piles.

Table 2-4. Bearing factors k_b for the Philipponnat Method

Soil Type	k_b
Gravel	0.35
Sand	0.40
Silt	0.45
Clay	0.50

Table 2-5. Empirical factors F_S for Philipponnat Method

Soil Type	F_s
Clay and calcareous clay	50
Silt, sandy clay, and clayey sand	60
Loose sand	100
Medium dense sand	150
Dense sand and gravel	200

LCPC (Bustamante and Gianeselli) Method (1982)

This method only uses cone tip resistance for predicting axial pile capacity. It was proposed by Bustamante and Gianeselli for the French Highway Department after the study of 197 piles in Europe. It is also called the French method.

The pile's unit tip capacity: $$q_t := k_b \cdot q_{eq}(tip)$$

where: q_{eq} (tip) is the average of tip resistance within 1.5 D above and 1.5 D below the pile tip after eliminating abnormal data (out of the range of ±30% of the average value);

k_b is a function of soil and pile type and can be found from Table 2-6.

The pile's unit skin friction is obtained by first noting pile type (Table 2-7), then determining the Curve No. from Tables 2-8, 2-9 and 2-10, and finally looking at Figures 2-5, 2-6 and 2-7.

Table 2-6. Bearing factors k_b for the LCPC Method

Soil Type	Bored Piles	Driven Piles
Clay-Silt	0.375	0.60
Sand-Gravel	0.15	0.375
Chalk	0.20	0.40

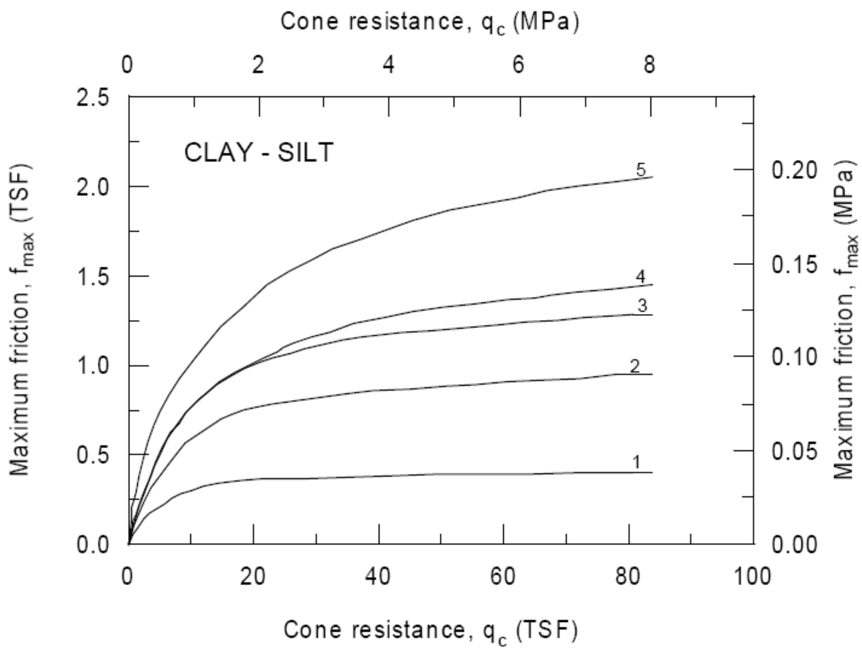

Figure 2-5. Ultimate skin friction curves for clay and silt from the LCPC method

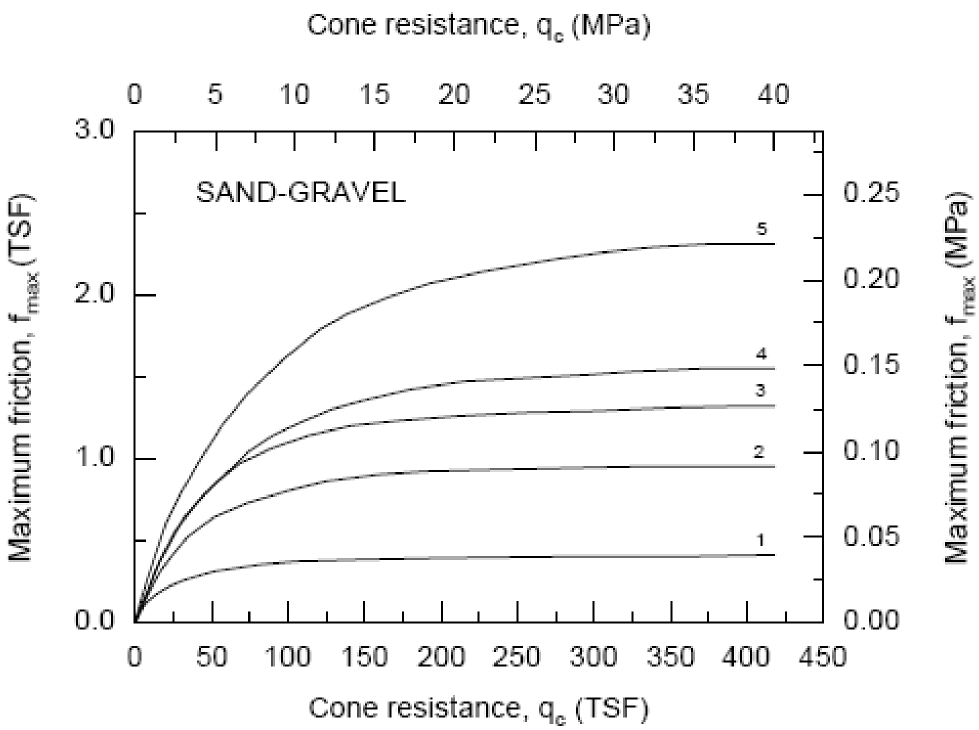

Figure 2-6. Ultimate skin friction curves for sand and gravel from the LCPC method

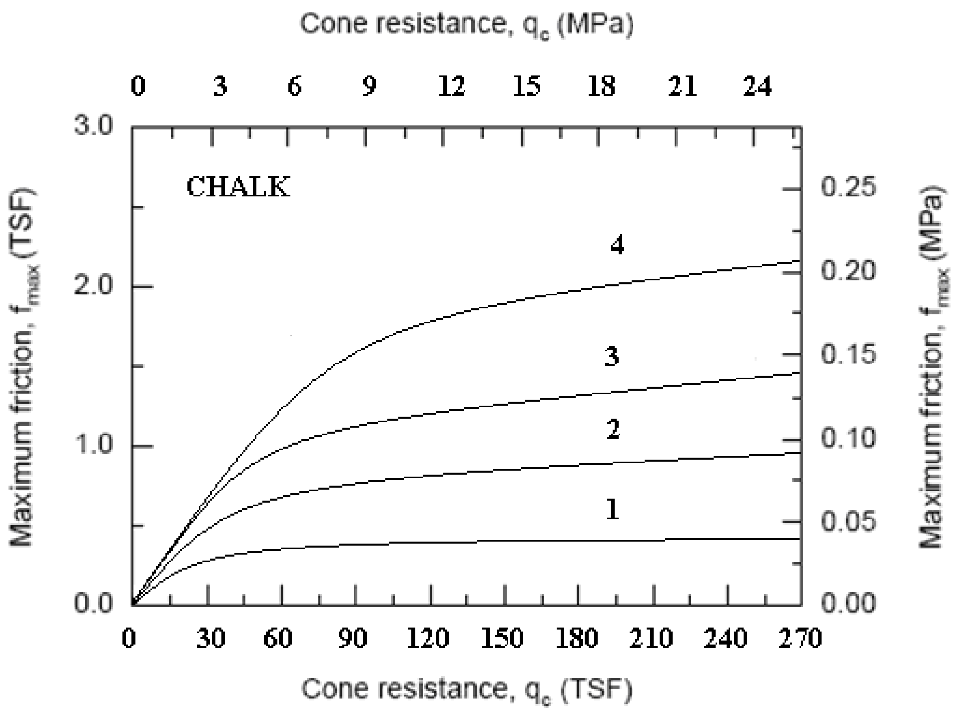

Figure 2-7. Ultimate skin friction curves for chalk from the LCPC method

Table 2-7. Pile type from the LCPC Method

Pile type	Descriptions
1. FS drilled shaft with no drilling mud	Installed without supporting the soil with drilling mud. Applicable only for cohesive soils above the water table.
2. FB drilled shaft with drilling mud	Installed using mud to support the sides of the hole. Concrete is poured from the bottom up, displacing the mud.
3. FT drilled shaft with casting (FTU)	Drilled within the confinement of a steel casing. As the casing is retrieved, concrete is poured in the hole.
4. FTC drilled shaft, hollow auger (auger cast piles)	Installed using a hollow stem continuous auger having a length at least equal to the proposed pile length. The auger is extracted without turning while, simultaneously, concrete is injected through the auger stem.
5. FPU Pier	Hand excavated foundations. The drilling method requires the presence of workers at the bottom of the excavation. The sides are supported with retaining elements or casing.
6. FIG Micropile type I (BIG)	Drilled pile with casing. Diameter less than 250 mm (10 in). After the casing has been filled with concrete, the top of the casing is plugged. Pressure is applied inside the casing between the concrete and the plug. The casing is recovered by maintaining the pressure against the concrete.
7. VMO screwed-in piles	Not applicable for cohesionless or soils below water table. A screw type tool is placed in front of a corrugated pipe which is pushed and screwed in place. The rotation is reversed for pulling out the casing while concrete is poured.
8. BE driven piles, concrete coated	- Pile piles 150 mm (6 in) to 500 mm (20 in) external diameter. - H piles. - Caissons made of 2, 3, or 4 sheet pile sections. The pile is driven with an oversized protecting shoe. As driving proceeds, concrete is injected through a hose near the oversized shoe producing a coating around the pile.
9. BBA driven prefabricated piles	Reinforced or prestressed concrete piles installed by driving or vibrodriving.
10. BM steel driven piles	Piles made of steel only and driven in place. - H piles. - Pipe piles. - Any shape obtained by welding sheet-pile sections.
11. BPR prestressed tube pile	Made of hollow cylinder elements of lightly reinforced concrete assembled together by prestressing before driving. Each element is generally 1.5 to 3 m (4-9 ft) long and 0.7 to 0.9 m (2-3 ft) in diameter. The thickness is approximately 0.15 m (6 in). The piles are driven open ended.
12. BFR driven pile, bottom concrete plug	Driving is achieved through the bottom concrete plug. The casing is pulled out while low slump concrete is compacted in it.
13. BMO driven piles, molded	A plugged tube is driven until the final position is reached. The tube is filled with medium slump concrete to the top and the tube is extracted.
14. VBA concrete piles, pushed-in	Pile is made of cylindrical concrete elements prefabricated or cast-in-place, 0.5 to 2.5 m (1.5 to 8 ft) long and 30 to 60 cm (1 to 2 ft) in diameter. The elements are pushed in by a hydraulic jack.
15. VME steel piles, pushed-in	Piles made of steel only are pushed in by a hydraulic jack.
16. FIP micropile type II	Drilled pile < 250 mm (10 in) in diameter. The reinforcing cage is placed in the hole and concrete placed from bottom up.
17. BIP high pressure injected pile, large diameter	Diameter > 250 mm (10 in). The injection system should be able to produce high pressures.

Table 2-8. Curve No. for clay and silt from the LCPC Method

Curve number	qc (ksf)	Pile type	Comments on insertion procedure
1	< 14.6 > 14.6	1-17 1, 2	- Very probable values when using tools without teeth or with oversized blades and where a remolded layer of material can be deposited along the sides of the drilled hole. Use these values also for deep holes below the water table where the hole must be cleaned several times. Use these values also for cases when the relaxation of the sides of the hole is allowed due to incidents slowing or stopping the pouring of concrete. For all the previous conditions, experience shows, however, that q_s can be between curve 1 and 2; use an intermediate value of q_s if such value is warranted by a load test.
2	> 25.1	4, 5, 8, 9, 10, 11, 13, 14, 15	- For all steel piles, experience shows that in plastic soils, q_s is often as low as curve 1; therefore, use curve 1 when no previous load test is available. For all driven concrete piles use curve 3 in low plasticity soils with sand or sand and gravel layers or containing boulders and when q_c > 52.2 ksf.
	> 25.1	7	- Use these values for soils where q_c < 52.2 ksf and the rate of penetration is slow; otherwise use curve 1. Also for slow penetration, when q_c > 93.9 ksf, use curve 3.
	> 25.1	6	- Use curve 3 based on previous load test.
	> 25.1	1, 2	- Use these values when careful method of drilling with an auger equipped with teeth and immediate concrete pouring is used. In the case of constant supervision with cleaning and grooving of the borehole walls followed by immediate concrete pouring, for soils of q_c > 93.9 ksf, curve 3 can be used.
	> 25.1	3	- For dry holes. It is recommended to vibrate the concrete after taking out the casing. In the case of work below the water table, where pumping is required and frequent movement of the casing is necessary, use curve 1 unless load test results are available.
3	> 25.1 < 41.8	12	- Usual conditions of execution as described in DTP 13.2
5	> 14.8	16, 17	- In the case of injection done selectively and repetitively at low flow rate it will be possible to use curve 5, if it is justified by previous load test.

Table 2-9. Curve No. for sand and gravel from the LCPC Method

Curve number	qc (ksf)	Pile type	Comments on insertion procedure
1	< 73.1	2 - 4, 6 -15	
2	> 73.1	6, 7, 9 -15	- For fine sands. Since steel piles can lead to very small values of q_s in such soils, use curve 1 unless higher values can be based on load test results. For concrete piles, use curve 2 for fine sands of q_c > 156.6 ksf.
	> 104.4	2, 3	- Only for fine sands and bored piles which are less than 30m (100 ft) long. For piles longer than 30 m (100 ft) in fine sand, q_s may vary between curves 1 and 2. Where no load test data is available, use curve 1.
	> 104.4	4	- Reserved for sands exhibiting some cohesion.
3	> 156.6	6, 7, 9 - 11, 13 - 15, 17	- For coarse gravelly sand or gravel only. For concrete piles, use curve 4 if it can be justified by a load test.
	> 156.6	2, 3	- For coarse gravelly sand or gravel and bored piles less than 30 m (100 ft) long. - For gravel where q_c > 83.5 ksf, use curve 4.
4	> 156.6	8, 12	- For coarse gravelly sand and gravel only.
5	> 104.4	16, 17	- Use of values higher than curve 5 is acceptable if based on load test.

Table 2-10. Curve No. for chalk from the LCPC Method

Curve number	q_c (ksf)	Pile type	Comments on insertion procedure
1	<62.6	1, 2, 3, 4, 6, 7, 8, 9, 10, 11, 12, 13, 14, 15	
3	>62.6	7, 8, 9, 10, 11, 13, 14, 15	- Experience shows that in some chalks where q_c< 146.1 ksf, below water table, steel or smooth concrete piles may exhibit q_s values as low as those of curve 2. When no load test is available, use curve 2 for q_c < 146.1 ksf. For chalk of q_c > 250.5 ksf use curve 4 based on a load tests.
	>93.9	6, 8	- For bored piles above the water table and concrete poured immediately after boring. For type 7 piles, use a slow penetration thus creating corrugations along the hole walls. Also for chalk above the water table and for q_c > 250.5 ksf use curve 4 if based on a load test.
	>93.9	1, 2, 3, 5, 7	- Below the water table and with tools producing a smooth wall or when a deposit of remolded chalk is left on the walls of the hole, experience shows that q_s can drop to values given by curve 2. Use higher values only on the basis of load tests.
4	>93.9	12	- Higher values than curve 4 can be used if based on a load test.
	>93.9	16, 17	

Almeida et al. Method (1996)

This method was proposed by Almeida et. al. based on the analysis of 43 load tests on driven and jacked piles in clay in Norway and Britain. Most of the load tests were performed in tension with only 4 tested in compression. The parameters used in this prediction method are penetrometer tip resistance and overburden stress.

The pile's unit skin friction: $f_s := \dfrac{q_c - \sigma_{v0}}{k_1}$ $\quad k_1 := 11.8 + 14.0\log\left(\dfrac{q_c - \sigma_{v0}}{\sigma'_{v0}}\right)$

where: q_C is CPT tip resistance, with pore pressure correction for piezocones,

σ_{v0} is the total overburden stress,

σ'_{v0} is the effective overburden stress.

In order to calculate the effective overburden stress, hydrostatic pressure is used. A reduction in k_1 needs to be applied if L/D >60. The reduction factor is recommended by both Semple and Rigden (1948) and is included in the procedure suggested by Randolph and Murphy (1985).

The pile's unit tip capacity: $q_t := \dfrac{q_c - \sigma_{v0}}{k_2}$

where: k_2 is a function of both pile type and material: k_2 = 2.7 for driven pile = 1.5 for jacked pile in soft clay, and = 3.4 for jacked pile in stiff clay. In order to prevent a nonrealistic result in sand, a limitation of highest unit skin friction is set at 1.2 tsf.

MTD (Jardine and Chow) Method (1996)

The method proposed by Jardine and Chow is from intensive field tests using 4 inch (102 mm) diameter, closed-ended instrumented piles at two sand sites in France. In addition, data acquired from field tests on high-quality instrumented displacement piles in a large range of clay soils performed by MIT, Oxford University, NGI and Imperial College over 15 years was utilized.

The pile's unit tip capacity:

In clay:

$$q_t := k \cdot q_{ca}$$

where: $k = 0.8$ for drained loading, $= 1.3$ for undrained loading. q_{ca} is the average cone tip resistance within 1.5D above and 1.5D below the pile tip.

In sand:

$$q_t := \left(1 - 0.5 \cdot \log\left(\frac{D}{D_{CPT}}\right)\right) \cdot q_{ca}$$

where: D is the diameter of the pile and

D_{CPT} is the diameter of cone penetrometer which is 1.4 inch (36 mm). q_t has the lower bound value of 0.13* q_{ca} when D is greater than 6.56 ft (2 m).

The pile's unit skin friction:

In clay:

$$f_s := f_L \cdot K_c \cdot \sigma_{v0}' \cdot \tan\left(\delta_f\right)$$

$$K_c := \left(2.2 + 0.016\,YSR - 0.870\log\left(S_t\right)\right)\,YSR^{0.42} \cdot \left(\frac{h}{R}\right)^{-0.20}$$

where: f_L: loading coefficient, = 0.8;

K_c: earth pressure coeffient after equilization;

YSR: yield stress ratio (yield stress determined in an oedometer test divided by the vertical effective stress). In case the YSR is not available, Lehane et.al (2000) provides the following relationship between YSR and cone tip resistance;

$$\mathrm{YSR} := 0.04427\left(\frac{q_c}{\sigma'_{v0}}\right)^{1.667}$$

S_t: clay sensitivity, and in case S_t is not available, Robertson and Campanella (1983) proposed the relationship between S_t and friction ratio;

$$S_t = \frac{10}{R_f(\%)}$$

h: the hight above the pile tip. In order to prevent too large a K_C value, $h/R \geq 8$;

R: the diameter of the pile;

σ'_{v0}: effective over-burden pressure;

δ_f: pile-soil interface friction angle at the maxmum shear stress. Because the large variations are possible, it is recommended by Lehane et.al (2000) to use a ring shear test to obtain the direct measurement; in case direct measurement is not available, Jardine and Chow proposed a relationship between δ and clay plasticity index for steel piles (Figure 2-8). δ_f will be between peak (δ_{peak}) and ultimate ($\delta_{ultimate}$) depending on relative displacement between pile and soil. If the PI of the deposit is not available for determining δ_f for clay, Schmertmann (1978a) suggests assuming an average normally consolidated ratio of 0.33 for most post-pleistocene clay which corresponds to a PI of 0.59. From Figure 2-8, 0.2 was determined to be tan (δ_f).

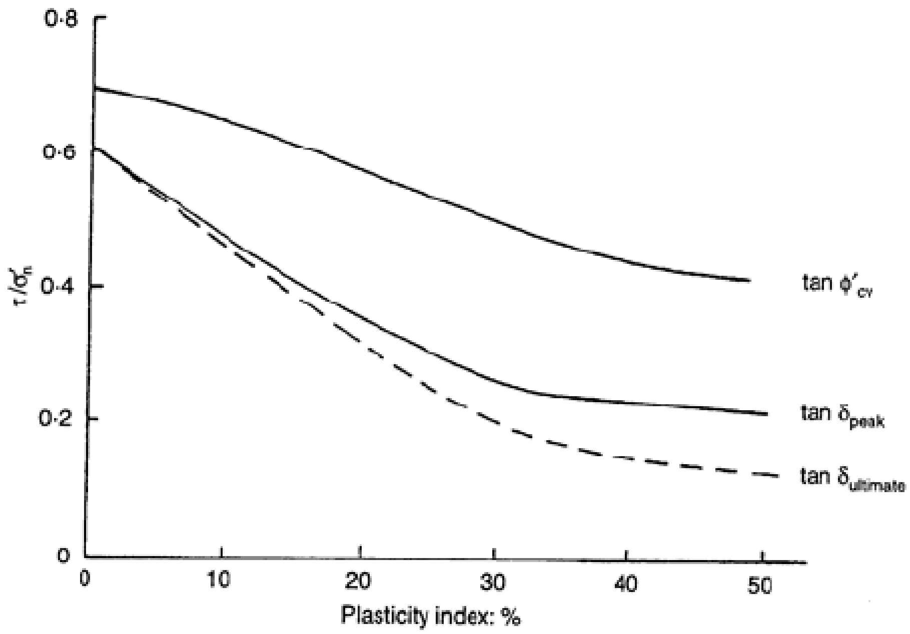

Figure 2-8. Proposed design δ values for steel piles after Jardine and Chow

In sand: $$f_s := \sigma'_{rf} \tan(\delta_f)$$

$$\sigma'_{rf} := \sigma'_{rc} + \Delta\sigma'_{rd}$$ For compression pile

$$\sigma'_{rf} := 0.8\sigma'_{rc} + \Delta\sigma'_{rd}$$ For tension pile

$$\sigma'_{rc} := 0.029 q_c \cdot \left(\frac{\sigma'_{v0}}{Pa}\right)^{0.13} \cdot \left(\frac{h}{R}\right)^{-0.38}$$

$$\Delta\sigma'_{rd} := \frac{4G \cdot R_{cla}}{R}$$

$$G := q_c \cdot \left(0.0203 + 0.00125 \frac{q_c}{\sqrt{Pa \cdot \sigma'_{v0}}} - 1.216 \, 10^{-6} \cdot \frac{q_c^{\,2}}{Pa \cdot \sigma'_{v0}} \right)^{-1}$$

where:

σ'_{rf}: the radial effective stress at maximum shear stress;

σ'_{rc}: the radial effective stress on side after equalization;

$\Delta\sigma'_{rd}$: the net dilatant component;

Pa: the atmosphere pressure;

G: the sand shear modulus;

R_{cla}: the pile's center-line-average roughness. It is qual to 10^{-5} for steel pile, 10^{-4} for very rough casing of concrete pile and $3*10^{-5}$ for prestressed concrete pile;

δ_f: pile-soil interface friction angle at the maxmum shear stress. Jardine and Chow (1996) recommend using an interface-direct or a ring-shear test with the same roughness and hardness as the pile material and same effective normal stress as in the field; in case direct measurement is not possible, Jardine and Chow recommended using the relationship between δ_{cv} (critical state interface friction angle) and sand mean particle size (d_{50}) for steel pile (Figure 2-9) and assume δ_f is equal to δ_{cv}. From correspondence with the authors, it was found that they are currently conducting sets of interface shear tests on sands sheared against concrete but are yet not finished. Hence, currently they recommend users assume δ_f between concrete pile and sand is similar to δ_f between a steel pile and sand. From Figure 2-9 and D_{50} of Florida soil (somewhere between 0.1 mm and 0.3 mm), it was decided to use 30° as δ_f.

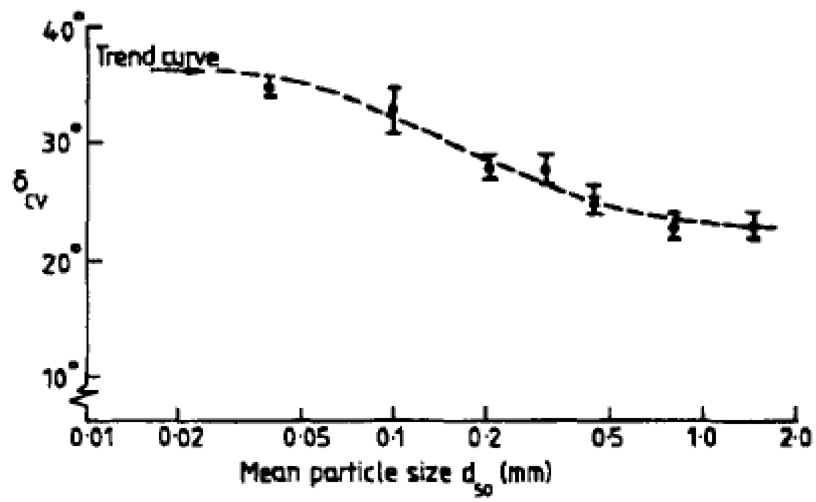

Figure 2-9. The relationship between critical state interface friction angle with grain size for granular soils shearing against a steel interface with 10 μm CLA roughness; after Jardine et. al. (1992)

Eslami and Fellenius Method (1997)

This method was proposed by Eslami and Fellenius from the study of 102 cases around the world. This method uses cone tip resistance (q_c) and pore pressure (u) to predict the axial pile capacity. CPT sleeve friction is only used to identify the soil type.

The pile's unit tip capacity: $q_t = q_{eg}$

where: q_{eg} is the geometric average of the effective cone resistance. The effective cone resistance is calculated by subtracting the hydrostatic pressure from the cone resistance if pore pressure data is not available.

The influence zone proposed by the Eslami and Fellenius is as follows:

2D above and 4D below the pile tip when the pile is installed through a dense soil into a weak soil.

8D above and 4D below the pile tip when the pile is installed through a weak soil into a dense soil.

The pile's unit skin friction: $f_s = c_s * q_e$

where: C_S is functions of soil type. The soil type and C_S can be obtained from Figure 2-10 and Table 2-11.

q_e is average of the effective cone resistance within the calculation layer. The effective cone resistance is calculated by subtracting the hydrostatic pressure from the cone resistance if pore pressure data is not available.

Table 2-11. Shaft correlation coefficient C_s in Eslami and Fellenius Method

Soil Type	**C_S (%)**
Soft Sensitive Soil	8.0
Clay	5.0
Stiff Clay and Mixture of Clay and Silt	2.5
Mixture of Silt and Sand	1.0
Sand	0.4

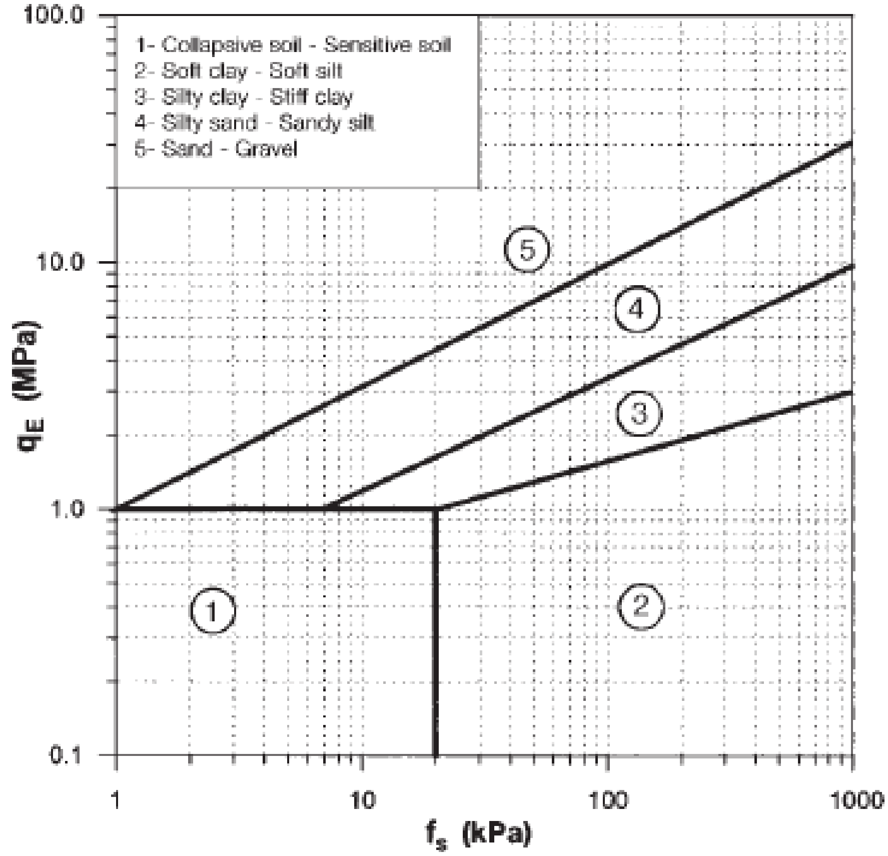

Figure 2-10. Soil profile from Eslami and Fellenius Method

Powell et al. Method (2001)

This method was proposed by Powell et al. from the study of 63 steel driven or jacked piles. The soil conditions ranged from soft normal-consolidated clay to stiff over-consolidated clay and two sand sites. The parameters used by this method are cone tip resistance (q_c) and pore pressure (u), undrained shear strength (s_u), and a soil profile to predict the axial pile capacity.

The pile's unit skin friction: $$f_s := \frac{q_c - \sigma_{v0}}{k_1} \qquad k_1 := 10.5 + 13.3\log\left(\frac{q_c - \sigma_{v0}}{\sigma'_{v0}}\right)$$

where: q_C is CPT tip resistance, with pore pressure correction for piezocones,

σ_{v0} is the total overburden stress,

σ'_{v0} is the effective overburden stress.

In order to calculate the effective overburden stress, hydrostatic pressure has been used. A reduction in k_1 needs to be applied if L/D >60. The reduction factor is recommended by both Semple and Rigden (1948) and is included in the procedure suggested by Randolph and Murphy (1985).

The pile's unit tip capacity: $$q_t := \frac{q_c - \sigma_{v0}}{k_2} \qquad k_2 := \frac{N_{kt}}{9}$$

where: N_{kt} is the cone factor, ranging from 10 to 20 based on local experience. A value of 15 was used in the current study.

UWA-05 Method (2005)

This method was proposed by Lehane et al. in 2005. This method is primarily used to predict ultimate pile capacity in sands only.

The pile's unit tip capacity: $$q_t := q_{ca} \cdot \left[0.15 + 0.45 \cdot \left(1 - \frac{D_{int}^{\,2}}{D^2}\right)\right]$$

where: q_{ca} is calculated by minimum path rule shown in Figure 2-2.

D_{int} is the internal diameter for pipe pile,

D is the outer diameter of the pile.

The unit skin friction: $$f_s := 0.03 q_c \cdot \left(1 - \frac{D_{int}^2}{D^2}\right)^{0.3} \cdot \left[\left(\max\left(\frac{h}{D}, 2\right)\right)^{-0.5} + 4 \cdot G \cdot \frac{\Delta r}{D}\right] \cdot \tan\left(\delta_{cv}\right)$$

$$G := q_c \cdot 185 \cdot \left(\frac{\frac{q_c}{Pa}}{\sqrt{\frac{\sigma'_{v0}}{Pa}}}\right)^{-0.7}$$

where: q_c is the average CPT tip resistance within the calculated soil layer;

Pa is the atmosphere pressure;

G is the sand shear modulus;

h is the hight above the pile tip. In order to prevent too large a K_C value, $h/R \geq 8$;

σ'_{v0} is the effective over-burden pressure;

Δr is the interface dilation, (0.02 mm was used in the current study);

δ_{cv} is the constant volume interface friction angle between sand and pile.

Since large variations are possible, it is recommended that a ring shear test be used to obtain a direct measurement; In the absence of lab tests, the trends between δ_{cv} and D_{50} recommended by ICP-05 with the upper limit of 0.55 for the $\tan(\delta_{cv})$ are considered reasonable (Figure 2-11). From D_{50} of Florida soil (somewhere between 0.1 mm and 0.3 mm), it was decided to use 29° as δ_{cv}, which yields the $\tan(\delta_{cv}) = 0.55$.

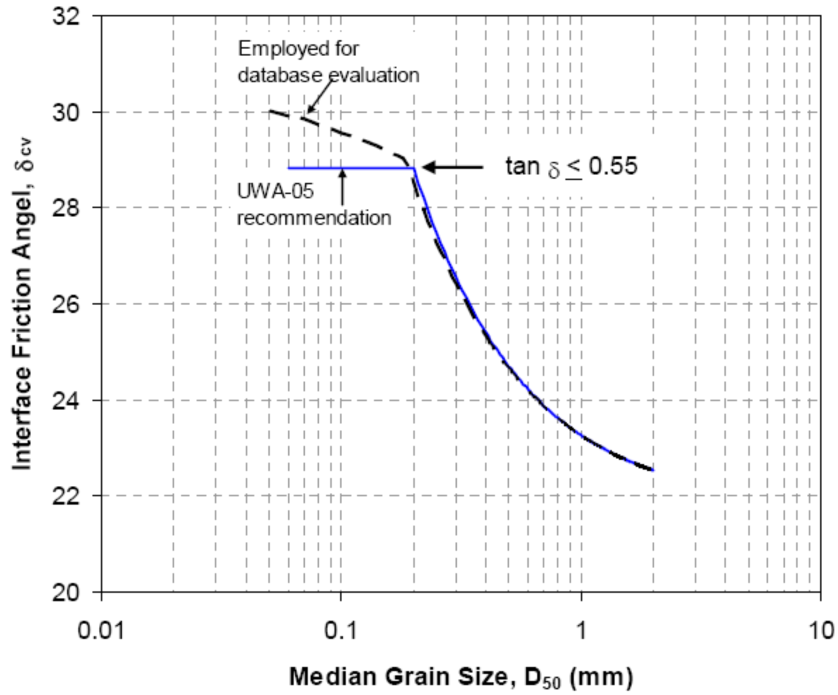

Figure 2-11. Relationship between δ_{cv} and D_{50} (modified from ICP-05 guidelines)

Zhou et al. Method (1982)

This method was proposed by Zhou et al. after the study of 96 pre-cast driven concrete piles in several eastern Chinese provinces. It provides satisfactory predictions (80% of the predicted errors are within 20% of the true load test results). The soil conditions ranged from sand to clayey soil. The parameters used by this method are cone tip resistance (q_c) and sleeve friction (f_s) to predict the axial pile capacity. One of the interesting points about this method is that it predicts limit load capacity instead of ultimate load capacity. The limit load is defined as the load near the starting point of the straight line portion on the load test curve, the point where the shaft resistance of pile would be fully mobilized, while the end resistance is only partially mobilized. If the point is not obvious from the data, they recommend using the load at a relative settlement of 0.4 – 0.5. This is the ratio of settlement to the ultimate settlement (punching failure).

The pile's unit tip capacity: $q_t := \alpha \cdot q_{ca}$

where: q_{ca} is the average CPT tip resistance within 4D above and 4D below the pile tip;

Soil type is defined as: Soil Type I: $q_{ca} > 2$ MPa and $f_{sa} / q_{ca} < 0.014$

Soil Type II: other than Soil Type I.

α is a function of soil type and q_{ca}, see Figure 2-12 or use the following equations to calculate a α value;

Soil Type I: $\alpha := 0.71 \cdot q_{ca}^{-0.25}$

Soil Type II: $\alpha := 1.07 \cdot q_{ca}^{-0.35}$

The pile's unit skin friction: $f_s := \beta \cdot f_{sa}$

where: f_{sa} is the average CPT sleeve friction along the calculated soil layer;

β is the function of soil type and f_{sa}, see Figure 2-13 or use the following equations to calculate β value:

Soil Type I: $\beta := 0.23 \cdot f_{sa}^{-0.45}$

Soil Type II: $\beta := 0.22 \cdot f_{sa}^{-0.55}$

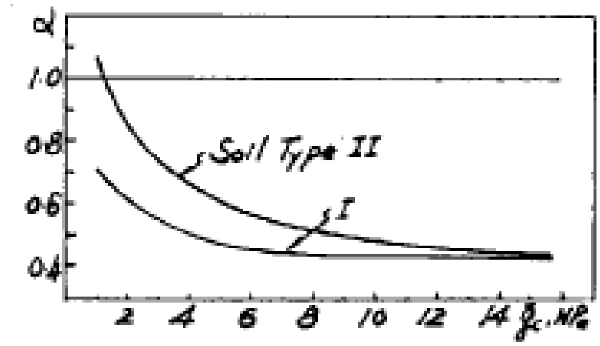

Figure 2-12. α vs q_{ca} in Zhou et al. Method

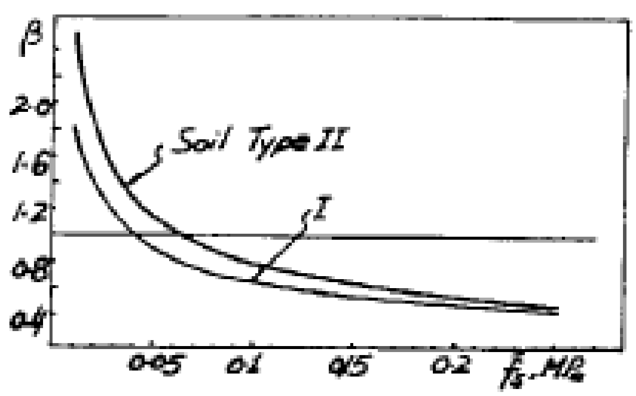

Figure 2-13. β vs f_{sa} in Zhou et al. Method

Relationship between CPT data and Soil Properties

Since the CPT penetration process dramatically changes the soil's stress – strain conditions, it is very difficult to model CPT penetration. Most of the relationships between CPT and soil properties are empirical, i.e., based on either chamber or field tests, and then comparing the CPT data and soil properties, determining correlations. The following section will briefly discuss the correlations between CPT results and traditional soil properties.

Soil Classification

The most comprehensive work on soil classification from CPT data was undertaken by Douglas and Olsen (1981). Figure 2-14 shows their soil type classification chart. This chart used two parameters (friction ratio and cone resistance) to correlate to soil type. The correlation came from CPT and SPT boring data obtained from California, Oklahoma, Utah, Arizona and Nevada (Martin and Douglas, 1981).

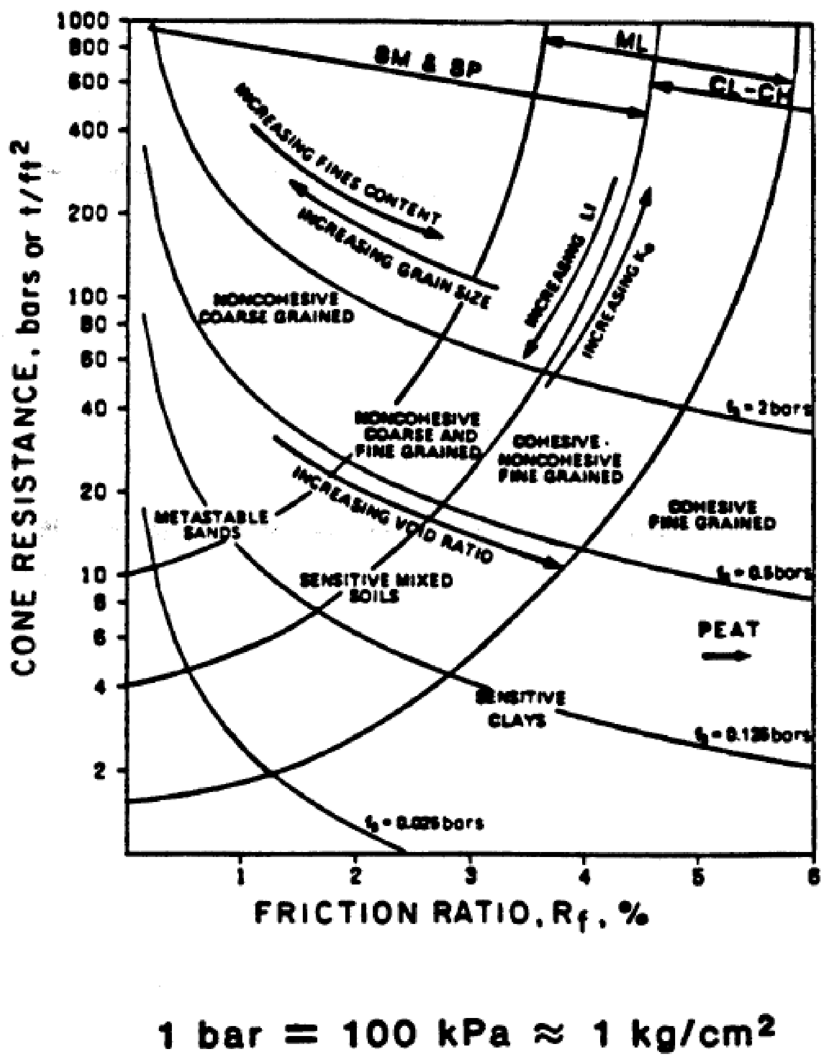

Figure 2-14. Soil type classification chart for the CPT (after Douglas and Olsen 1981)

Unfortunately, this chart was considered too complicated for practical design use. Therefore, Robertson et al (1986) proposed a simplified soil type classification chart, shown in Figure 2-15. It uses the same parameters as the Douglas and Olsen (1981) chart, but divides the soil into 12 types. The soil drainage condition had been also included. The software program Coneplot, which is produced by Hogentogler & Co. Inc. and used extensively, uses the 1983 Robertson & Campanella 12-zone chart. All CPT data analyzed in this research report used this chart.

One drawback of the Robertson et al.'s simplified soil type classification chart (1986) is that it does not take into account the depth of soil. Some error will be generated when the chart is used to identify soils below 100 feet (30 m). Fortunately, most onshore deep foundations are within this range. Therefore, this drawback should not pose a problem using this chart to identify soil types in this research. However, for offshore foundations, especially for soils located deeper than 100 feet, Robertson (1988) proposed a new soil type classification chart using the normalized cone tip resistance and friction ratio. Figure 2-16 shows this new chart.

Cohesionless Soil

There are several properties that are very important for cohesionless soil, such as relative density (R.D.), friction angle (ϕ), shear modulus (G). The correlation between the CPT data and each of these properties are presented as follows.

Relative density

Most work of relative density correlation with the CPT was done in the calibration chambers; (Veismanis, 1974, Chapman and Donald, 1981, Baldi et al, 1981, Parkin et al, 1980 and Villet and Mitchell, 1981). From the test results, one conclusion that can be drawn is that there is no unique relationship between relative density and cone resistance for cohesionless soils. Figure 2-17 shows the relationship of relative density with the cone tip resistance in sand with different compressibility.

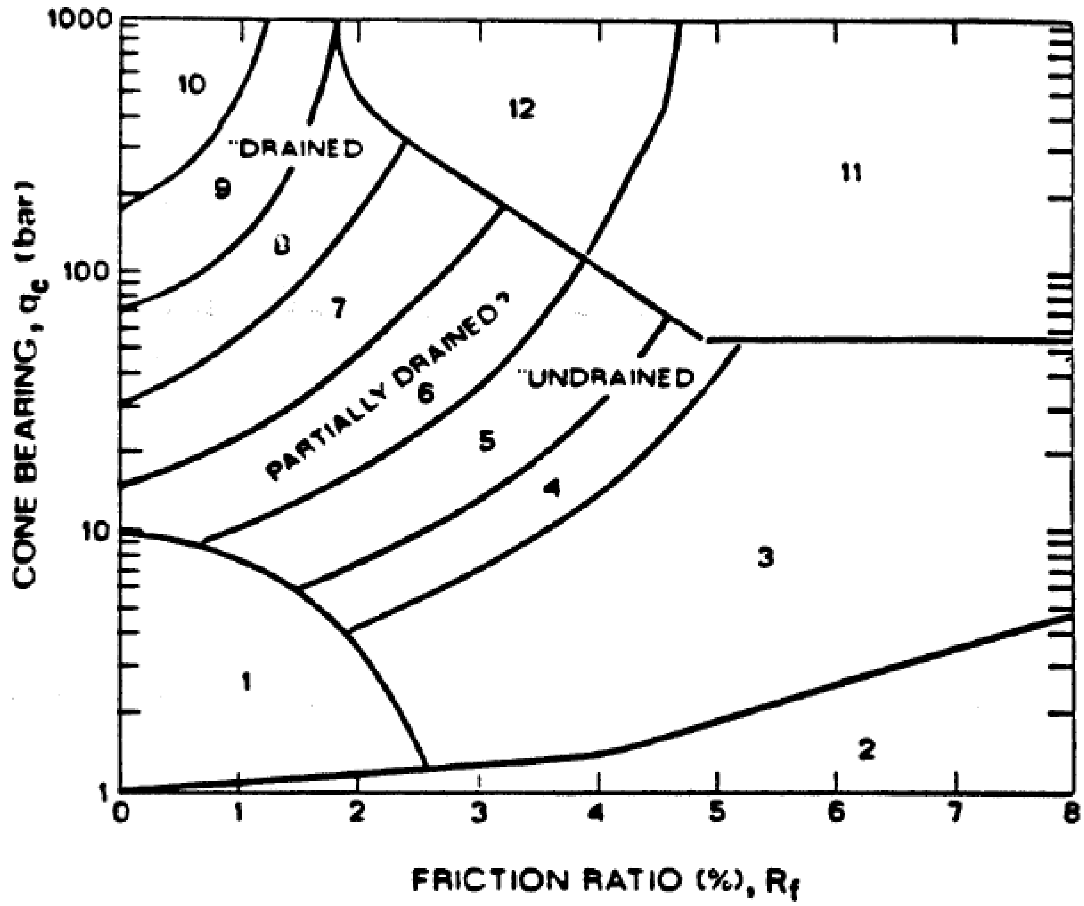

Zone	q_c/N	Soil Behaviour Type
1)	2	sensitive fine grained
2)	1	organic material
3)	1	clay
4)	1.5	silty clay to clay
5)	2	clayey silt to silty clay
6)	2.5	sandy silt to clayey silt
7)	3	silty sand to sandy silt
8)	4	sand to silty sand
9)	5	sand
10)	6	gravelly sand to sand
11)	1	very stiff fine grained (*)
12)	2	sand to clayey sand (*)

(*) overconsolidated or cemented

Figure 2-15. Soil type classification chart for the CPT (after Robertson et al. 1986)

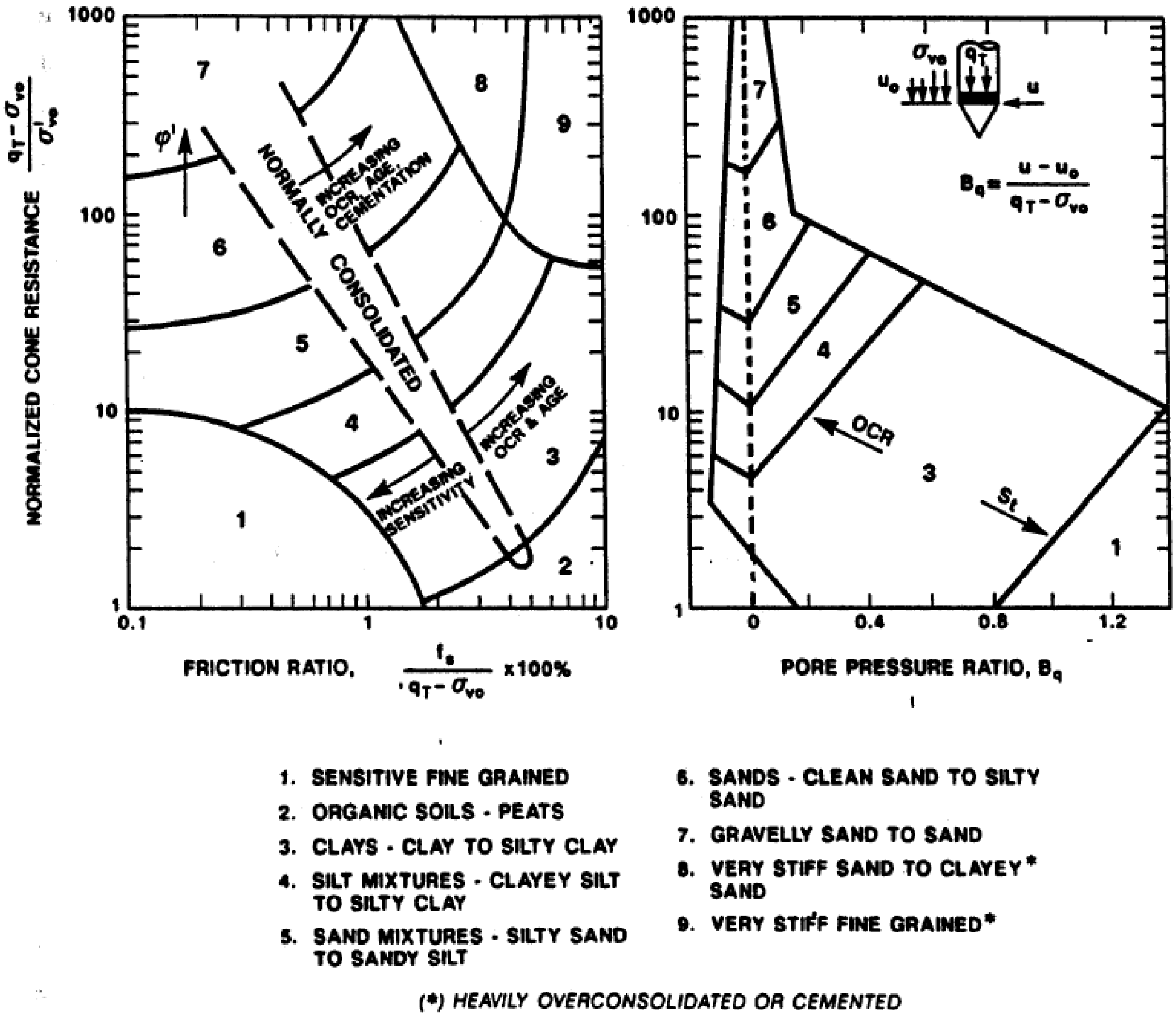

Figure 2-16. Soil classification for the CPT using normalized tip resistance (Robertson 1988)

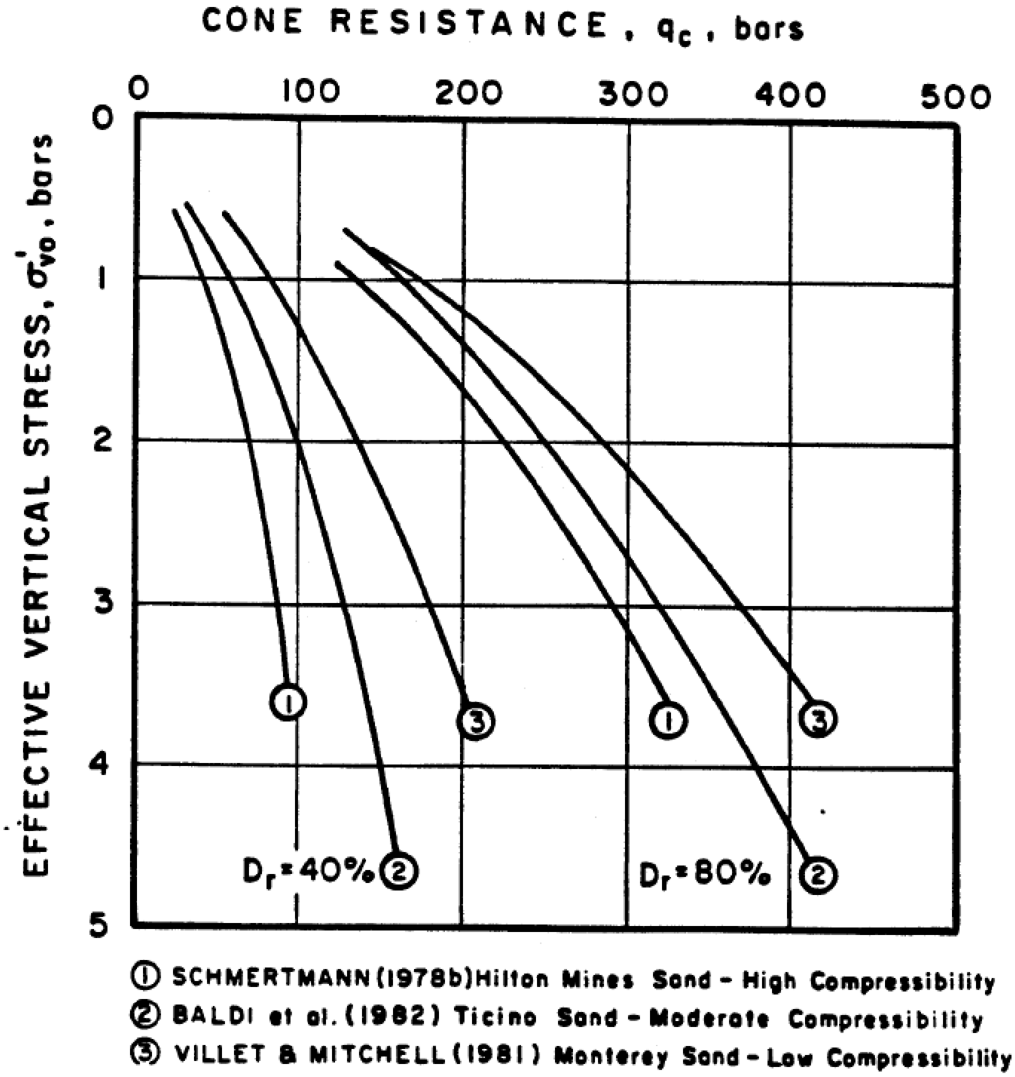

Figure 2-17. Comparison of relative density relationships (Robertson and Campanella 1983a)

Figure 2-18 shows Baldi's relationship between relative density, vertical effective stress and cone resistance. This chart uses Ticino Sand which has moderate compressibility and is representative of most quartz sands. Research from Joustra and de Gijt (1982) shows that the variation in compressibility for most quartz sands is relatively small, but there is substantial difference in the sands 'angularity. In the proposed CPT based pile capacity prediction method discussed later, the sand density condition (loose, medium and dense sand) was determined using this chart.

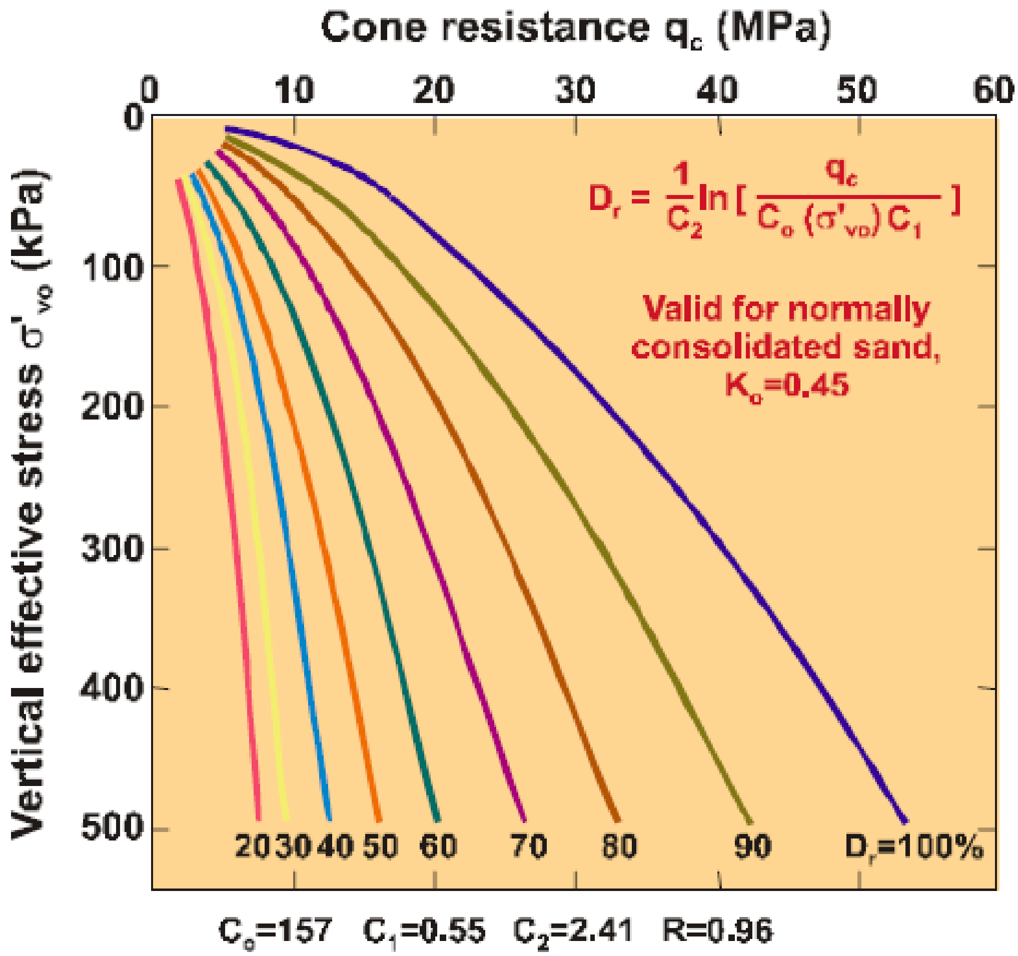

Figure 2-18. Relative density relationship for N.C. moderately compressible, non-cemented, unaged quartz sands (after Baldi et al. 1986)

Friction angle

Vesic (1963) performed research that shows there is no unique relationship between friction angle and CPT tip resistance. There are other factors that could influence the relationship such as the compressibility and shear strength of soil particles. Robertson and Campanella (1983a) proposed the relationship of CPT tip resistance and friction ratio (shown in Figure 2-19) after the study of the previous calibration chamber test results. The friction angle was measured from a drained triaxial test and the CPT tip resistance was obtained from the calibration chamber test. Figure 2-19 is considered to provide reasonable estimates for normally consolidated, non-cemented, moderately incompressible, quartz sands. It tends to give lower predictions of friction angle for highly compressible sands.

Shear modulus

Many researchers (Seed and Idriss, 1970, Hardin and Drnevich, 1972) have performed laboratory tests to obtain a correlation between the maximum shear modulus (G_{max}) and CPT tip resistance. Based on these results, Robertson (1982) proposed a correlation that is shown in Figure 2-20. This plot is suitable for normally consolidated, non-cemented, quartz sands. Baldi et al. (1986) proposed the estimation of G_{max} from CPT tip resistance, shown in Figure 2-21. The sand used in their research was non-cemented silica sands from Italy. In 1991, Rix and Stokoe (1991) proposed a relationship between G_{max}, q_c and effective overburden pressure using the following equation:

$$G_{max} = 1634(q_c)^{0.250}(\sigma'_v)^{0.375}$$

This relationship is based on field tests in Italy and on calibration chamber tests.

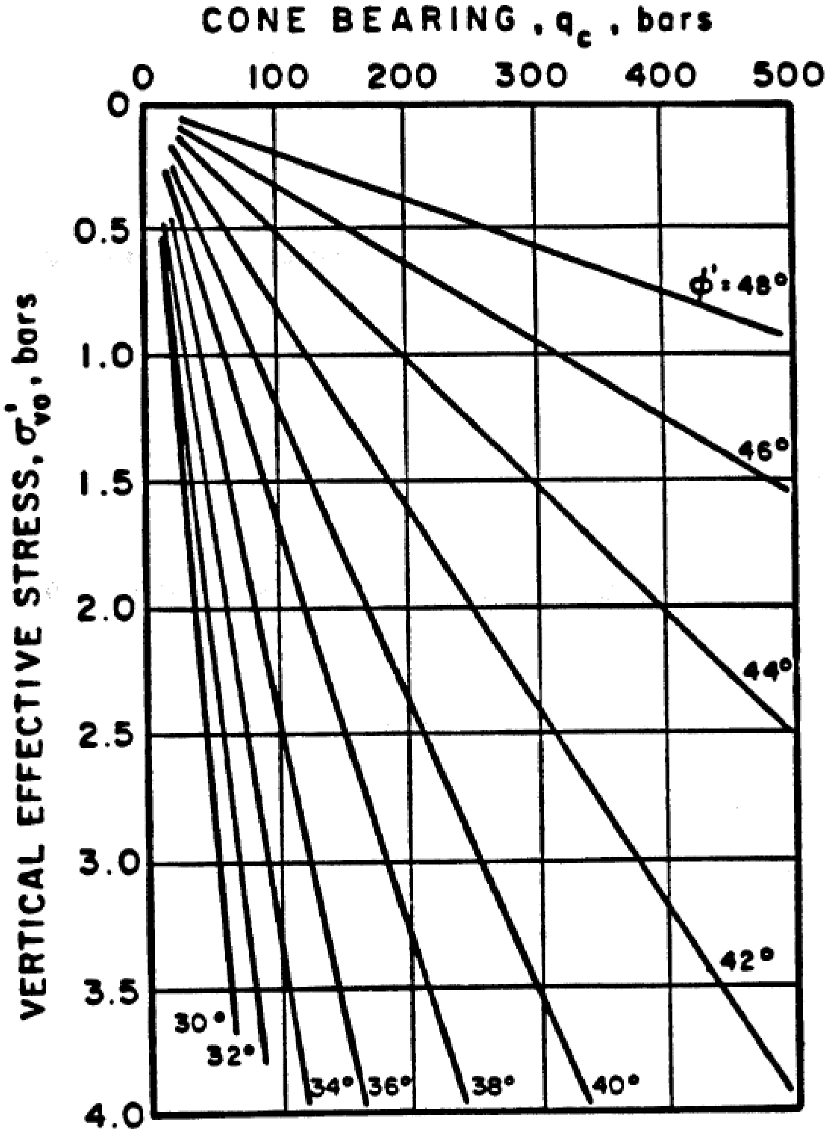

Figure 2-19. Correlation between CPT tip resistance and peak friction angle for non-cemented quartz sands (after Robertson and Campanella 1983a)

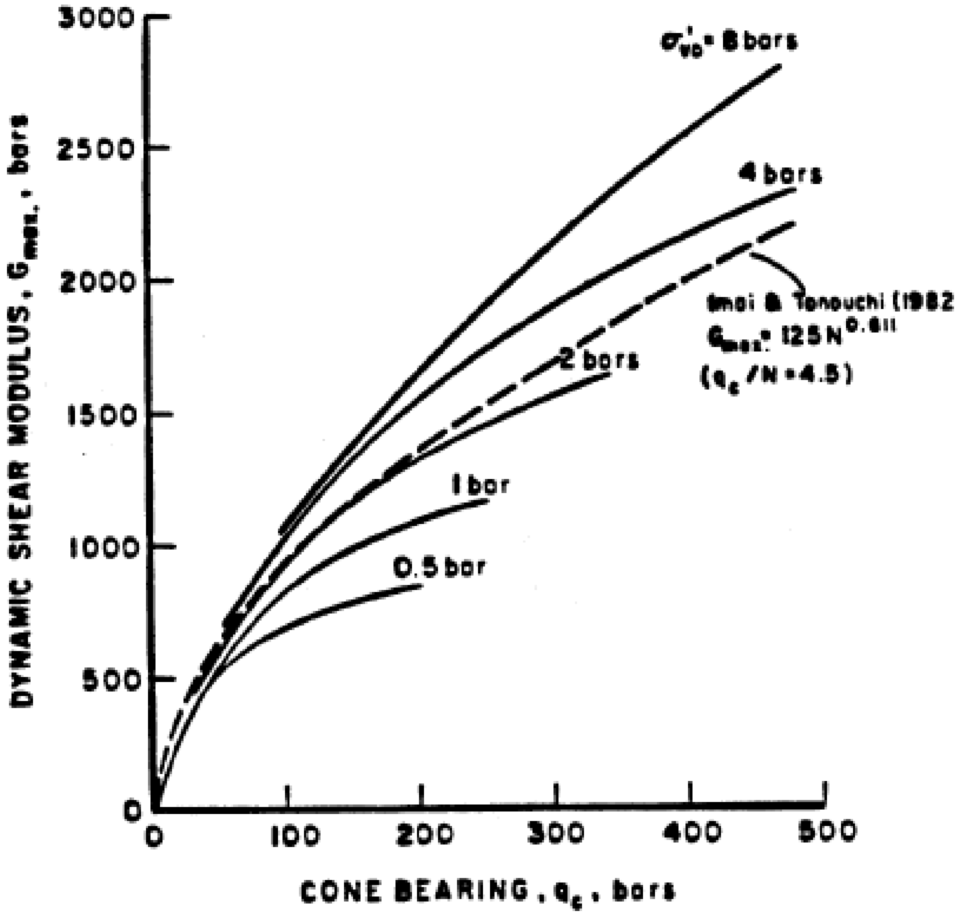

Figure 2-20. Correlation between CPT tip resistance and dynamic shear modulus for normally consolidated, non-cemented quartz sands (after Robertson and Campanella 1983a)

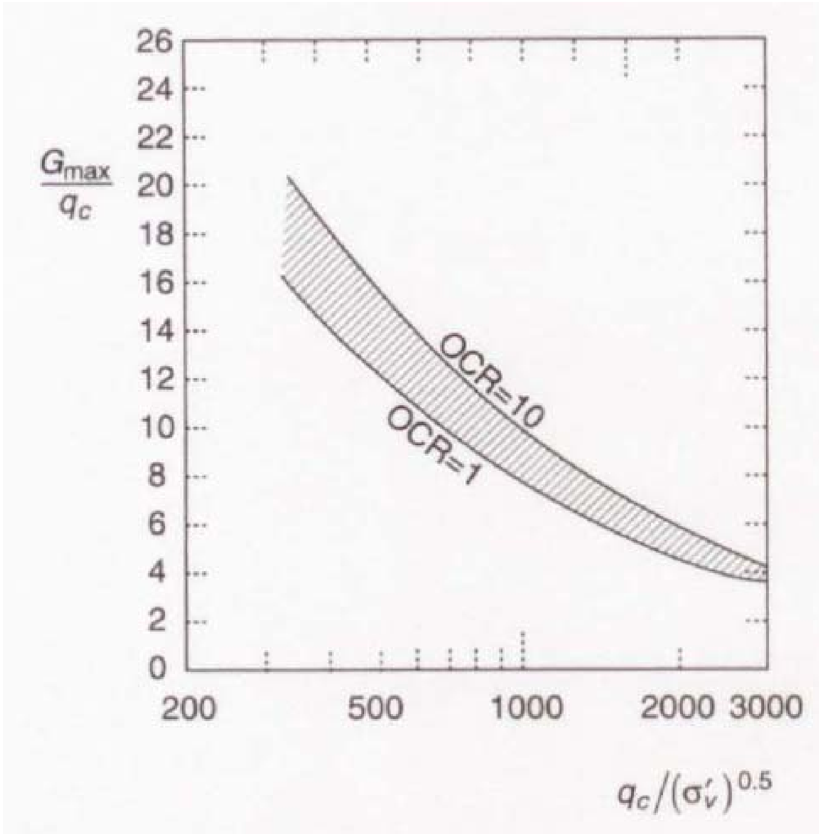

Figure 2-21. Correlation between CPT tip resistance and maximum shear modulus for non-cemented silica sands (after Baldi et al. 1989)

After a maximum shear modulus is estimated, the modulus reduction factor can be used to calculate the shear modulus at any strain level. The modulus reduction factor was proposed by Seed and Idriss in 1970. For cohesionless and cohesive soil, the modulus reduction factors were plotted on different charts. Recent research has found a gradual transition between the modulus reduction factor of cohesionless soil and cohesive soil. After reviewing experimental results of a wide range of soil, Dobry and Vucetic (1987) and Sun et al. (1988) found that the key factor that influences the shape of the modulus reduction curve is the plasticity index and not the void ratio. Vucetic and Dobry (1991) proposed modulus reduction curves as a function of plasticity index (shown in Figure 2-22). The interesting part in this figure is that the reduction curve with PI = 0 is very similar to the average modulus reduction curve that was commonly used for sands proposed by Seed and Idriss (1970).

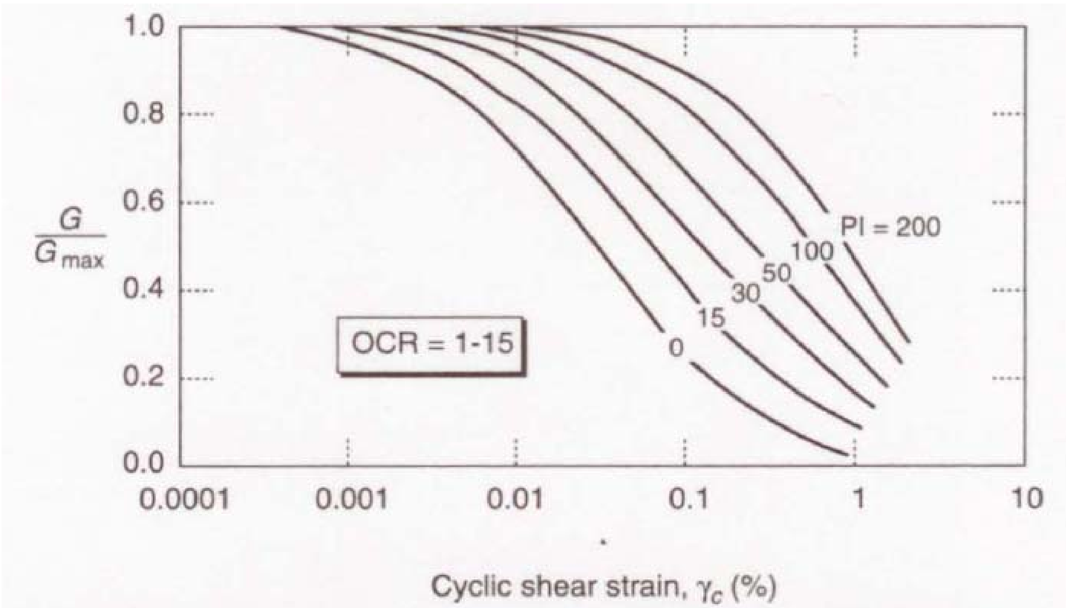

Figure 2-22. Modulus reduction curves for fine-grained soils of different plasticity (after Vucetic and Dobry 1991)

Cohesive Soil

The most important soil properties for cohesive soils are the undrained shear strength (s_u), over-consolidation ratio (OCR), sensitivity (S_t), and shear modulus (G).

Undrained shear strength (s_u)

There are many researchers (Baligh et al. [1980], Lunne and Kleven [1981], Jamiolkowski et al. [1982], and Robertson et al. [1986]) who have done extensive work on the evaluation of s_u from CPT data. Campanella (1995) recommended using the following equation to estimate s_u:

$$s_u := \frac{q_c - \sigma_{v0}}{N_k}$$

In the cone factor $N_{k,}$ it is recommended that 15 be used as a preliminary assessment of s_u. However, for sensitive cohesion soil, N_k should be reduced to approximatly 10 or less depending on the degree of sensitivity.

Over-consolidation ratio (OCR)

The following procedure suggested by Schmertmann (1975) and modified by Campanella (1995) can be used to estimate the over-consolidation ratio from CPT testing:

1. estimate the undrained shear strength (s_u) from cone tip resistance using the above method
2. calculate the vertical effective stress (σ'_{vo}) from the soil profile and unit weight
3. estimate the average normally consolidated $(s_u/\sigma'_{vo})_{NC}$ ratio from its plasticity index (PI) using Figure 2-23. If the PI is not available, 0.33 was recommended by Schmertmann (1978a) for the estimation of $(s_u/\sigma'_{vo})_{NC}$ for most post-pleistocene clays
4. estimate OCR from correlations proposed by Ladd and Foott (1974) and normalized by Schmertmann (1978a) as shown in Figure 2-24

It was pointed out by Campanella (1995) that the empirical relationship for estimating OCR should be used to obtain only qualitative information on the OCR within the relatively same homogeneous deposit.

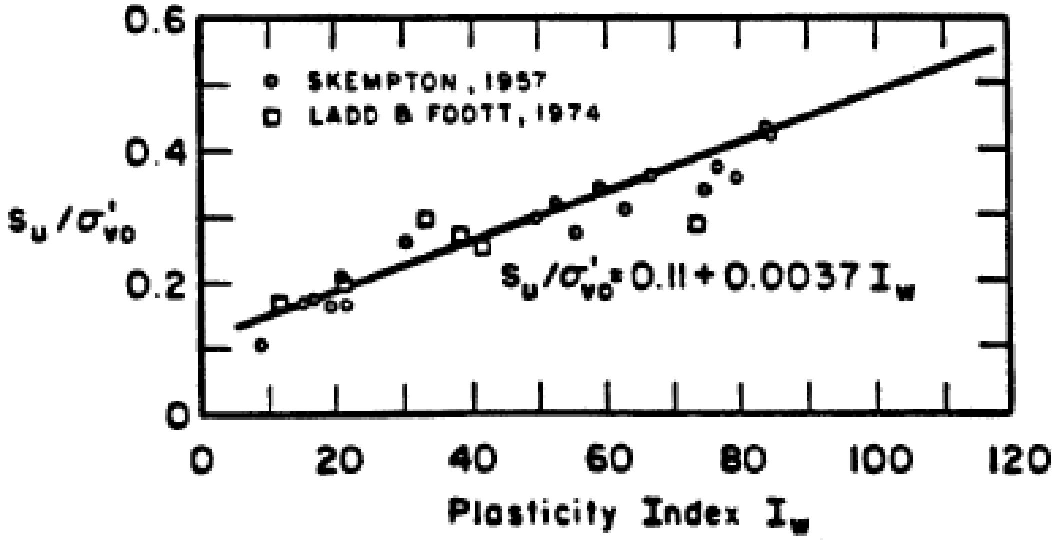

Figure 2-23. The relationship between s_u/σ'_{vo} ratio and Plasticity Index for normally consolidated clays

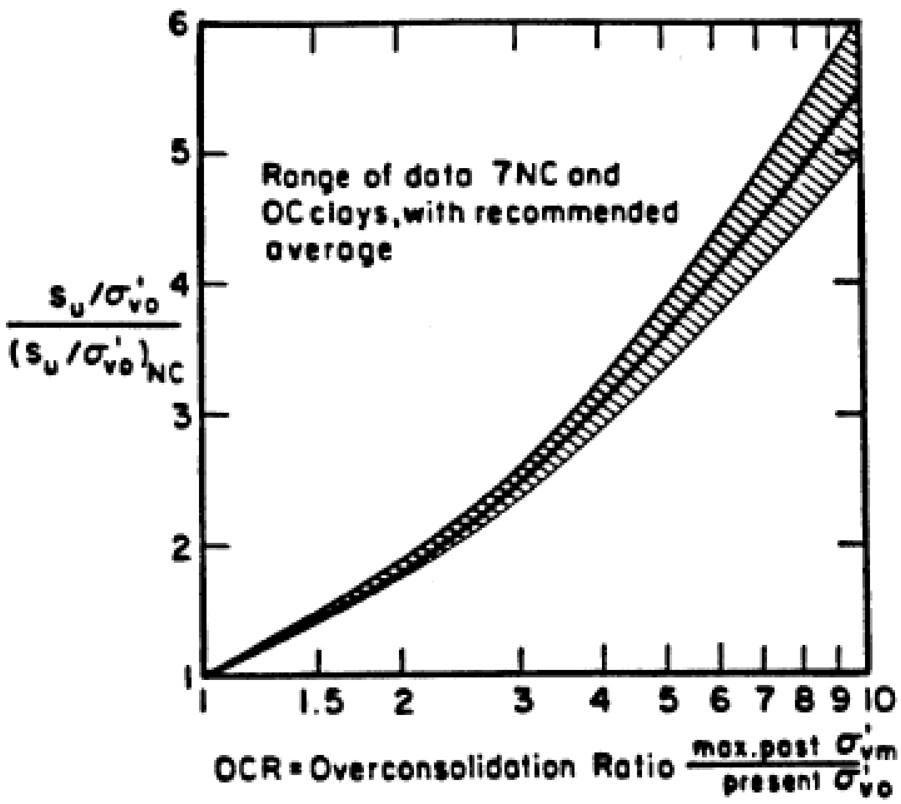

Figure 2-24. The relationship between normalized s_u/σ'_{vo} ratio and over-consolidated ratio

Sensitivity (S_t)

The sensitivity (S_t) is the ratio of undisturbed strength to totally remolded strength. It can be estimated from the CPT friction ratio using the following equation:

$$S_t := \frac{N_s}{FR(\%)}$$

Based on the work of Schmertmann (1978a), Robertson and Campanella (1983b), and Greig (1986), Campanella (1995) recommended using $N_s = 6$ as the initial assessment of sensitivity if no other measurement of S_t is available.

Shear modulus (G)

Campanella (1995) suggested using the relationship between maximum shear modulus and CPT tip resistance as shown in Figure 2-25 to estimate the maximum shear modulus. Notice that the maximum shear modulus is highly related to the over-consolidation ratio (OCR). Using the correlation proposed by Vucetic and Dobry (1991) shown in Figure 2-22, the shear Modulus (G) can be estimated at any strain level.

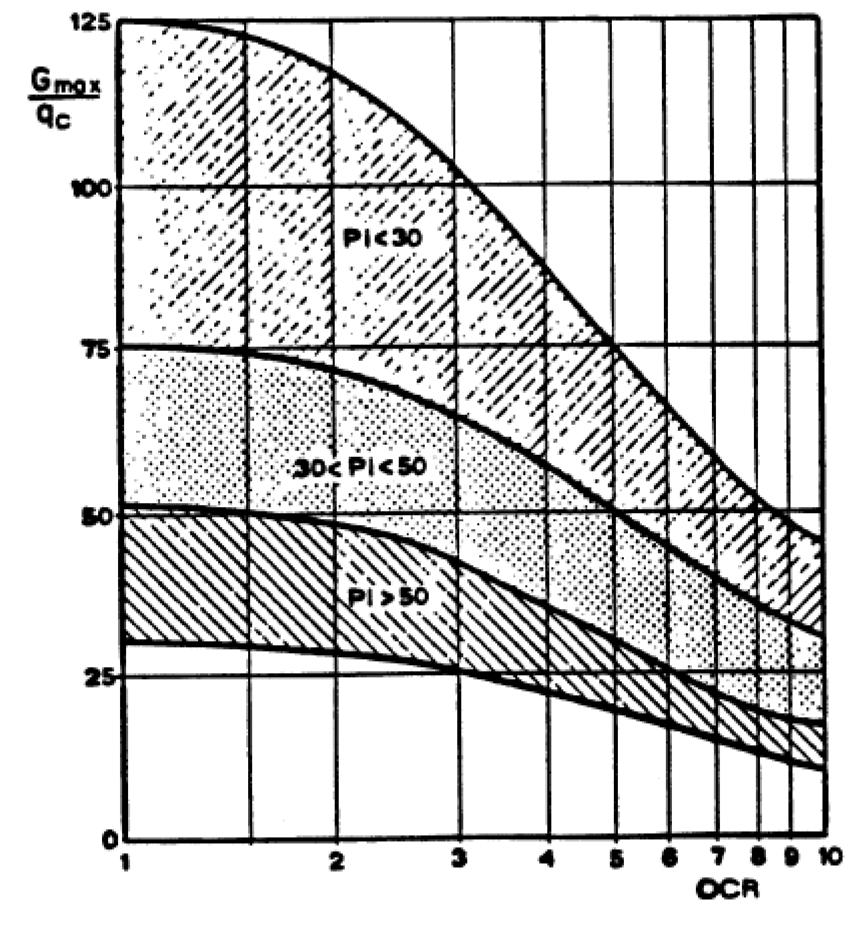

Figure 2-25. Tentative correlation for estimating maximum shear moduli in cohesive soil (Campanella 1995)

CHAPTER 3
MATERIALS AND METHODS

DTP (Dual Tip Penetrometer)

The DTP is the latest version of a series of devices developed at the University of Florida intended for identifying cemented sands. Daniel Hart developed the first version of the device in 1996 while he was a graduate student at the University of Florida. This unfunded research project created a lip that was welded to the top of the friction sleeve. However, this meant that the bearing reading measured by the lip was added to the frictional component measured by the friction sleeve strain gauge. The lip also made it difficult to remove the cone from the ground. In 1998, Randell Hand eliminated the welded lip and welded a bearing annulus onto the friction reducer coupler. The annulus was therefore located about 20 inches above the top of the cone's friction sleeve. Strain gages were used to measure resistance in the annulus. The voltage output was translated into a second "q_c" (tip resistance) reading. Steve Kiser and Hogentogler & Co. Inc. improved on the design and came up with the Dual Tip Penetrometer in 1999. In 2004, Hogentogler & Co. Inc. converted the DTP from analog into a digital cone, which is the latest version of DTP equipped in the cone penetrometer vehicle at the Florida Department of Transportation State Materials Office.

The DTP is similar to conventional cone penetrometers except for a second tip (actually an annulus) just above the friction sleeve as shown in Figure 3-1. The second tip has the same angle (60°) and bearing area (10 cm^2) as the regular cone. The first tip was originally designed to break down the cohesive bonds of cemented sand while the second tip was meant to measure the residual or broken-up bearing resistance. Based on the relationship of Tip 1 and Tip 2 along with the soil profile, through a large number of experiments, cemented sand identifiers would be identified.

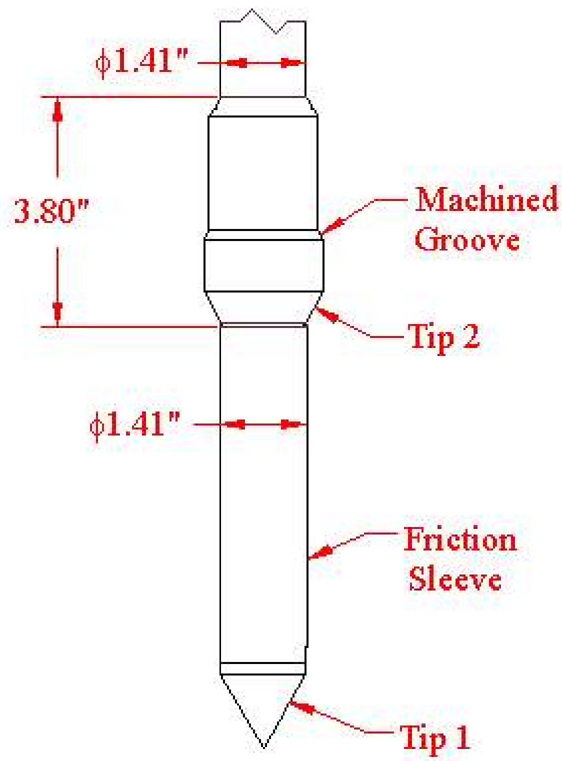

Figure 3-1. Dual Tip Penetrometer

Location of Cemented Sites

Cemented sands exist in many areas of the United States, including California, Texas, Florida, and along the banks of the lower Mississippi River. Lightly cemented sands are usually misidentified in the CPT test, which can cause design problems. SPT borings log are one resource used to identify cemented sand. However, if the cementation is very weak and can be easily broken by finger pressure, it might not be noticed by the field technicians.

In order to incorporate cemented sands into the new proposed design method, strongly cemented and lightly cemented sand sites were identified using two databases, FDOT and UF. There are hundreds of insitu and load test data in these two databases. Both SPT data and boring logs were searched to identify cemented sand sites. CPT data were also searched and combined with SPT N (Q_c/N) as well. All previous project reports were reviewed to find soil and load test data. In case of sites where load test and SPT data were available, (but no CPT data) the sites were flagged for future CPT and DTP testing.

There were a total of 21 cases where load test, SPT and CPT (DTP in some cases) are all available. Figure 3-2 shows the relative locations of these 21 sites. These cases were used to calibrate the ultimate pile capacity prediction methods and their corresponding LRFD resistance factors, Φ.

Axial Ultimate Pile Capacity Prediction Methods

There are a total of 14 prediction methods that have been analyzed in this research. They are; the Schmertmann Method, de Ruiter and Beringen Method, Penpile Method, Price and Wardle Method, Tumay and Fakhroo Method, Aoki and De Alencar Method, Philipponnat Method, LCPC (Bustamante and Gianeselli) Method, Almeida et al. Method, MTD (Jardine and Chow) Method, Eslami and Fellenius Method, Powell et al. Method, UWA-05 Method, and Zhou et al. Method. Because most of the methods involve complicated calculations and digital CPT data make these calculations time intensive, a MathCAD program was used to calculate each of the predictions. For each method there is a MathCAD program that is provided in the appendix.

Figure 3-3 shows the program for the Philipponnat method. The colored fields are inputs. The CPT data input is an Excel file formatted with four columns (depth, tip resistance, sleeve friction, and pore pressure). Other inputs are diameter or edge length of pile, embedment length, layer depths. After all required fields have been inputted, the program will calculate ultimate tip resistance, ultimate skin friction and Davisson capacity (1/3 of ultimate tip resistance + ultimate skin friction).

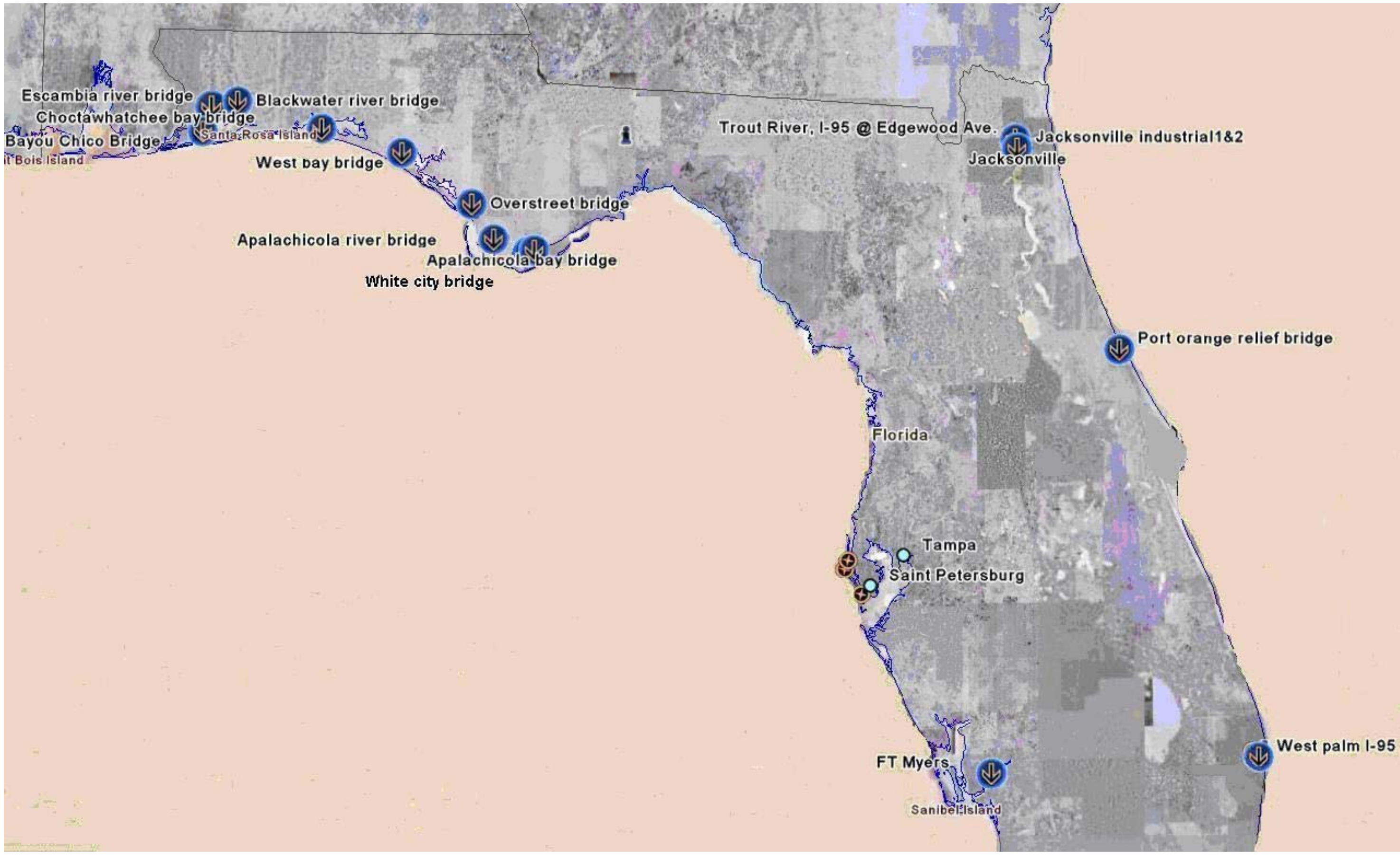

Figure 3-2. Locations of 21 sites with load test and CPT data

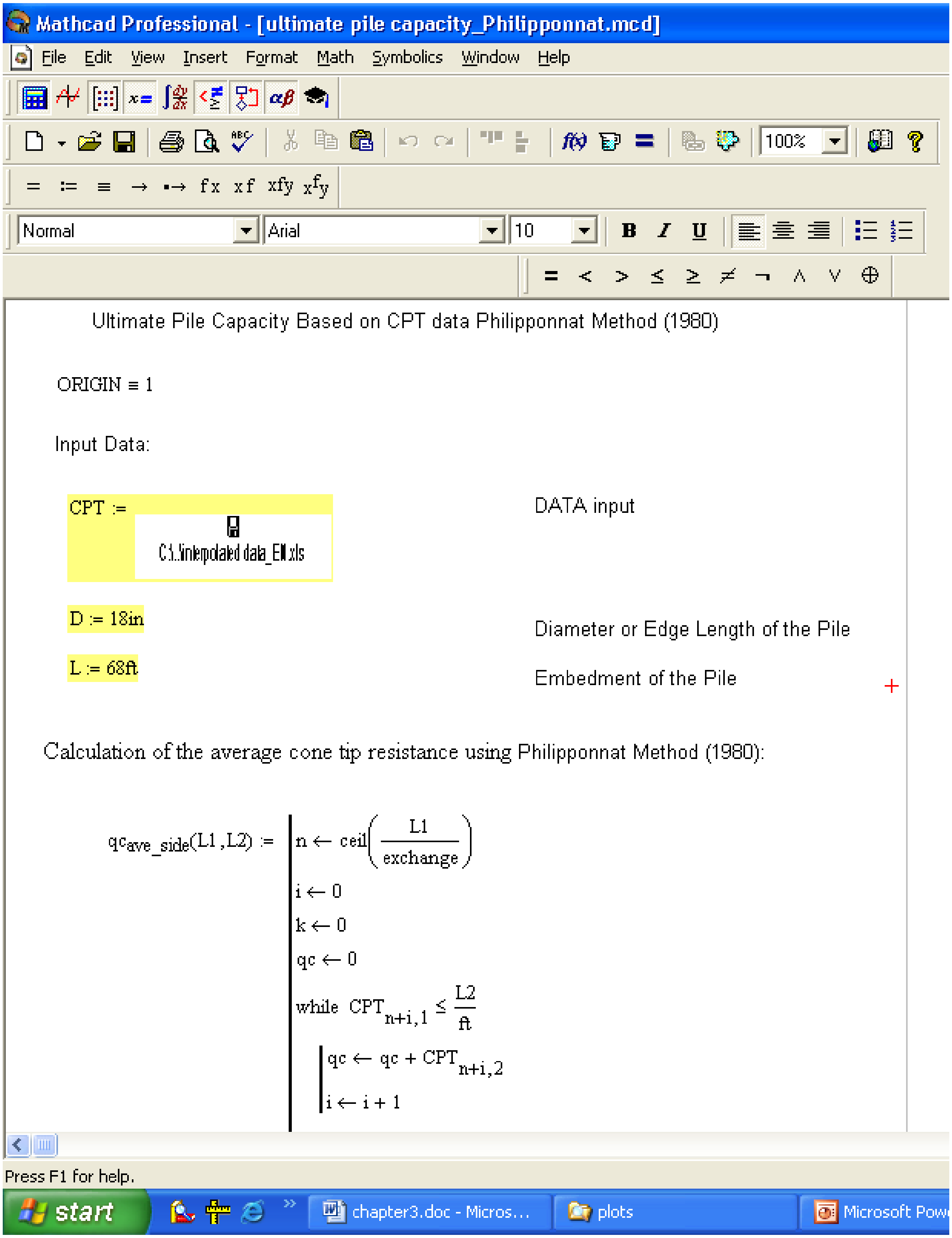

Figure 3-3. MathCAD program for the Philipponnat Method

LRFD (Load and Resistance Factor Design)

Over the past two decades, Load and Resistance Factor Design (LRFD) has been incorporated in structural and geotechnical designs. One of the benefits of LRFD is its consistent reliability in design practice. Many state DOT's, including FDOT, are now implementing AASHTO (American Association of State Highway and Transportation Officials) LRFD Specifications. Hence, the objective of this research is to update FDOT's pile/shaft design procedure based on CPT and DPT data and assess the LRFD resistance factor for each pile capacity prediction method. Even though LRFD requires both load and resistance factors, the resistance factor is considered a variable for each static pile capacity prediction method whereas load factors are typically a constant, based on local experience.

Modified First Order Second Moment (FOSM) Approach

The LRFD approach used in this research is the modified FOSM (First Order Second Moment Approach). The modification was developed at the University of Florida due to the differences between FORM (First Order Reliability Method) and FOSM resistance factors provided in NCHRP Report 507. The modified portion in FOSM is the term COV (Q). The previous method assumes COV (Q) = COV (Q_D) + COV (Q_L). It was found that this equation was incorrect and a modified COV (Q) was formulated as:

$$COV(Q) := \sqrt{\frac{\frac{Q_D^{\,2}}{Q_L^{\,2}}\cdot\lambda_{QD}^{\,2}\cdot COV_{QD}^{\,2} + \lambda_{QL}^{\,2}\cdot COV_{QL}^{\,2}}{\frac{Q_D^{\,2}}{Q_L^{\,2}}\cdot\lambda_{QD}^{\,2} + 2\cdot\frac{Q_D}{Q_L}\cdot\lambda_{QD}\cdot\lambda_{QL} + \lambda_{QL}^{\,2}}}$$

where: Q_D/Q_L = Dead to live load ratio, varies from 1.0 to 3.0 (spans, L = 57-170 ft. Since it is not very sensitive, a value of 2.0 is used herein);

λ_{QD}, λ_{QL} = Dead load and live load bias factors, λ_{QD} = 1.08, λ_{QL} = 1.15 (recommended by AASHTO 1996/2000),

COV_{QD}, COV_{QL} = Dead load and live load coefficients of variation,

COV_{QD} = 0.128, COV_{QL} = 0.18 (recommended by AASHTO)

Based on this modified FOSM, it was concluded that the difference between FORM and FOSM was slight. Since FORM involves a complicated calculation process, the modified FOSM is the approach used in this research.

The following section provides a detailed deviation of the LRFD resistance factor using the modified FOSM approach.

Limit state equation

In this approach, load and resistance are assumed to be a lognormal distribution. Therefore, the limit state equation is as follows:

$$G := \ln(R) - \ln(Q)$$

$$E(G) := E(\ln(R)) - E(\ln(Q))$$

$$E(\ln(R)) := \ln(E(R)) - \frac{1}{2}\cdot\ln\left[1 + (COV(R))^2\right]$$

$$E(\ln(Q)) := \ln(E(Q)) - \frac{1}{2}\cdot\ln\left[1 + (COV(Q))^2\right]$$

$$E(G) := \ln\left[\frac{E(R)\cdot\sqrt{1 + (COV(Q))^2}}{E(Q)\cdot\sqrt{1 + (COV(R))^2}}\right]$$

It is assumed that R and Q are statistically independent, therefore σ_G:

$$\sigma_G := \sqrt{VAR(\ln(R)) + VAR(\ln(Q))}$$

$$\sigma_G := \sqrt{\ln\left[\left[1 + (COV(R))^2\right]\cdot\left[1 + (COV(Q))^2\right]\right]}$$

where: COV(R), COV(Q) = Resistance, load coefficient of variation

Reliability index $$\beta := \frac{E(G)}{\sigma_G}$$

$$\beta := \frac{\ln\left[\dfrac{E(R)\cdot\sqrt{1 + (COV(Q))^2}}{E(Q)\cdot\sqrt{1 + (COV(R))^2}}\right]}{\sqrt{\ln\left[\left[1 + (COV(R))^2\right]\cdot\left[1 + (COV(Q))^2\right]\right]}}$$

$$E(R) := \frac{E(Q)\cdot\exp\left[\beta\cdot\sqrt{\ln\left[\left[1 + (COV(R))^2\right]\cdot\left[1 + (COV(Q))^2\right]\right]}\right]}{\sqrt{\dfrac{1 + (COV(Q))^2}{1 + (COV(R))^2}}}$$

Resistance factor Φ

The LRFD equation:

$$\phi R_n \geq \Sigma\, \eta\, \gamma_i\, Q_i$$

where: Φ = Resistance factor

R_n = Nominal Resistance

η = Load modifier for importance, redundancy and ductility

γ_i = Load factors

Q_i = Force effects

Load modifier η is set equal to 1 which leaves all uncertainty on the resistance factor ϕ.

For driven pile design, two load effects, dead load Q_D and live load D_L are considered. Therefore, γ_D and γ_L are considered as load factors for dead load and live load, respectively. The LRFD equation becomes:

$$\phi R_n \geq \gamma_D Q_D + \gamma_L Q_L$$

$$\phi \geq \frac{\gamma_D \cdot Q_D + \gamma_L \cdot Q_L}{R_n}$$

Since: $$E(R) := \lambda_R \cdot R_n$$

where: λ_R = Mean bias (mean of resistance bias factor);

$$\lambda_R := \frac{\sum_{i=1}^{N} \lambda_{Ri}}{N}$$

$$\lambda_{Ri} := \frac{R_{mi}}{R_{ni}}$$

R_{mi} = Measured capacity from load test data

R_{ni} = Predicted capacity from CPT data

N = The number of cases

$$\phi \geq \frac{\gamma_D \cdot Q_D + \gamma_L \cdot Q_L}{\frac{E(R)}{\lambda_R}}$$

By inserting E(R) into the above equation, the follow equation can be derived:

$$\phi \geq \frac{\lambda_R \cdot \left(\gamma_D \cdot Q_D + \gamma_L \cdot Q_L\right) \cdot \sqrt{\frac{1 + (COV(Q))^2}{1 + (COV(R))^2}}}{E(Q) \cdot \exp\left[\beta \cdot \sqrt{\ln\left[\left[1 + (COV(R))^2\right] \cdot \left[1 + (COV(Q))^2\right]\right]}\right]}$$

Since the dead load and live load are considered statistically independent, E (Q) can be expressed as follows:

$$Q := \gamma_D \cdot Q_D + \gamma_L \cdot Q_L$$

$$E(Q) := \lambda_{QD} \cdot Q_D + \lambda_{QL} \cdot Q_L$$

where: λ_{QD}, λ_{QL} = Dead load and live load bias factors;

λ_{QD}=1.08, λ_{QL} = 1.15 (recommended by AASHTO 1996/2000)

By inserting E(Q) into the equation for resistance factor, and dividing both numerator and denominator by Q_L, the follow equation results:

$$\phi \geq \frac{\lambda_R \cdot \left(\gamma_D \cdot \frac{Q_D}{Q_L} + \gamma_L\right) \cdot \sqrt{\frac{1 + (COV(Q))^2}{1 + (COV(R))^2}}}{\left(\lambda_{QD} \cdot \frac{Q_D}{Q_L} + \lambda_{QL}\right) \cdot \exp\left[\beta \cdot \sqrt{\ln\left[\left[1 + (COV(R))^2\right] \cdot \left[1 + (COV(Q))^2\right]\right]}\right]}$$

This equation was traditionally used to calibrate the resistance factor using FOSM in AASHTO's specifications by assuming COV (Q) ^{2} = COV (QD) ^{2} + COV (QL) ^{2}. However, as mentioned previously, this assumption is incorrect. The correct derivation is as follows:

$$VAR(Q) := Q_D^{2} \cdot VAR(\gamma_D) + Q_L^{2} \cdot VAR(\gamma_L)$$

$$QD := \gamma_D \cdot Q_D$$

$$QL := \gamma_L \cdot Q_L$$

$$COV(QD)^2 := \frac{VAR(\gamma_D) \cdot Q_D^{2}}{\lambda_{QD}^{2} \cdot Q_D^{2}}$$

$$COV(QL)^2 := \frac{VAR(\gamma_L) \cdot Q_L^{2}}{\lambda_{QL}^{2} \cdot Q_L^{2}}$$

$$VAR(\gamma_D) := \lambda_{QD}^{2} \cdot COV(QD)^2$$

$$VAR(\gamma_L) := \lambda_{QL}^{2} \cdot COV(QL)^2$$

$$VAR(Q) := Q_D^{2} \cdot \lambda_{QD}^{2} \cdot COV(QD)^2 + Q_L^{2} \cdot \lambda_{QL}^{2} \cdot COV(QL)^2$$

$$COV(Q)^2 := \frac{VAR(Q)}{E(Q)^2}$$

$$COV(Q)^2 := \frac{\frac{Q_D^{2}}{Q_L^{2}} \cdot \lambda_{QD}^{2} \cdot COV(QD)^2 + \lambda_{QL}^{2} \cdot COV(QL)^2}{\frac{Q_D^{2}}{Q_L^{2}} \cdot \lambda_{QD}^{2} + 2 \cdot \frac{Q_D}{Q_L} \cdot \lambda_{QD} \cdot \lambda_{QL} + \lambda_{QL}^{2}}$$

Inserting the COV (Q) into the resistance equation, the following equation can be obtained:

$$\phi \geq \frac{\lambda_R \cdot \left(\gamma_D \cdot \frac{Q_D}{Q_L} + \gamma_L\right) \cdot \sqrt{\frac{1 + \frac{\frac{Q_D^2}{Q_L^2} \cdot \lambda_{QD}^2 \cdot COV(QD)^2 + \lambda_{QL}^2 \cdot COV(QL)^2}{\frac{Q_D^2}{Q_L^2} \cdot \lambda_{QD}^2 + 2 \cdot \frac{Q_D}{Q_L} \cdot \lambda_{QD} \cdot \lambda_{QL} + \lambda_{QL}^2}}{1 + (COV(R))^2}}}{\left(\lambda_{QD} \cdot \frac{Q_D}{Q_L} + \lambda_{QL}\right) \cdot \exp\left[\beta \cdot \sqrt{\ln\left[\left[1 + (COV(R))^2\right] \cdot \left(1 + \frac{\frac{Q_D^2}{Q_L^2} \cdot \lambda_{QD}^2 \cdot COV(QD)^2 + \lambda_{QL}^2 \cdot COV(QL)^2}{\frac{Q_D^2}{Q_L^2} \cdot \lambda_{QD}^2 + 2 \cdot \frac{Q_D}{Q_L} \cdot \lambda_{QD} \cdot \lambda_{QL} + \lambda_{QL}^2}\right)\right]}\right]}$$

where: γ_D = Dead load factor (1.25, recommended by AASHTO (1996/2000*1*)),

γ_L = Live load factor (1.75, recommended by AASHTO 1996/2000),

Q_D/Q_L = Dead to live load ratio, varies from 1.0 to 3.0 (spans, L = 57-170 ft, is not very sensitive, a value of 2.0 used herein)

λ_R = Mean of resistance bias factor,

COV (R) = Resistance coefficient of variation ,

λ_{QD}, λ_{QL} = Dead load and live load bias factors,

λ_{QD} = 1.08, λ_{QL} = 1.15 (recommended by AASHTO 1996/2000),

COV_{QD}, COV_{QL} = Dead load and live load coefficients of variation,

COV_{QD} = 0.128, COV_{QL} = 0.18 (recommended by AASHTO)

β_T = Target reliability index, AASHTO and FHWA recommend values from 2.0 to 3.

Of major importance in estimating the LRFD resistance factor, Φ, are the resistance's bias factor (λ_R), and the resistance's coefficient of variation (COV(R)). Both are computed from: 1) the nominal predicted resistance, R_{ni} (predicted pile capacity), and 2) the measured pile capacity, R_{mi}, i.e., load test results. Based on the ratio of measured to predicted pile capacities, λ_{Ri}, for each of the sites, the mean, λ_R, standard deviation, σ_R, and coefficient of variation, COV(R), were determined for all 14 CPT methods. Using these inputs, the LRFD resistance factors, Φ, were determined with a reliability index, β of 2.5 for each method. Because driven piles are usually in groups and redundancy will provide higher reliability, 2.5 was used in this research.

Differentiating Ultimate Skin Friction and Tip Resistance from Load Test Data

All of the load tests were conventional top-down static load tests performed for which load-settlement data exist (see Figure 3-4.). Using FDOT's load testing protocol (i.e. Specification Section 455), the Davisson Capacity was assessed for each load versus settlement curve. The Davisson Capacity, referred to as the measured capacity, R_m, generally occurs for settlements that are tolerable (i.e. less than 1"), under service loading conditions. These values were subsequently used with the predicted capacities, R_n, (where $R_n = Q_{S\ ult} + 1/3 * Q_{T\ ult}$) to assess the LRFD resistance factor, Φ for each of the fourteen CPT methods.

However, the load versus settlement curve does not provide the ultimate skin friction and tip resistance. In order to evaluate the accuracy of each prediction method for ultimate skin friction and tip resistance separately, each needs to be estimated using this load test curve. Figure 3-5 shows the proposed process that was developed to separate the two attributes. For the majority of the tests, the piles were not loaded sufficiently to induce a plunging failure. While the ultimate skin friction is likely fully mobilized at small displacements (0.1"), the tip resistance is not. Thus, it is not possible to determine the ultimate tip resistance (i.e., the tests ended after one inch displacement was reached, whereas two inches of displacement or approximately D/10 [D is in inches] is typically needed to induce a plunging failure) unless the load test curve is extrapolated to the two inch value. The idea of extending the load test curve follows from deBeer's method for determining pile capacity.

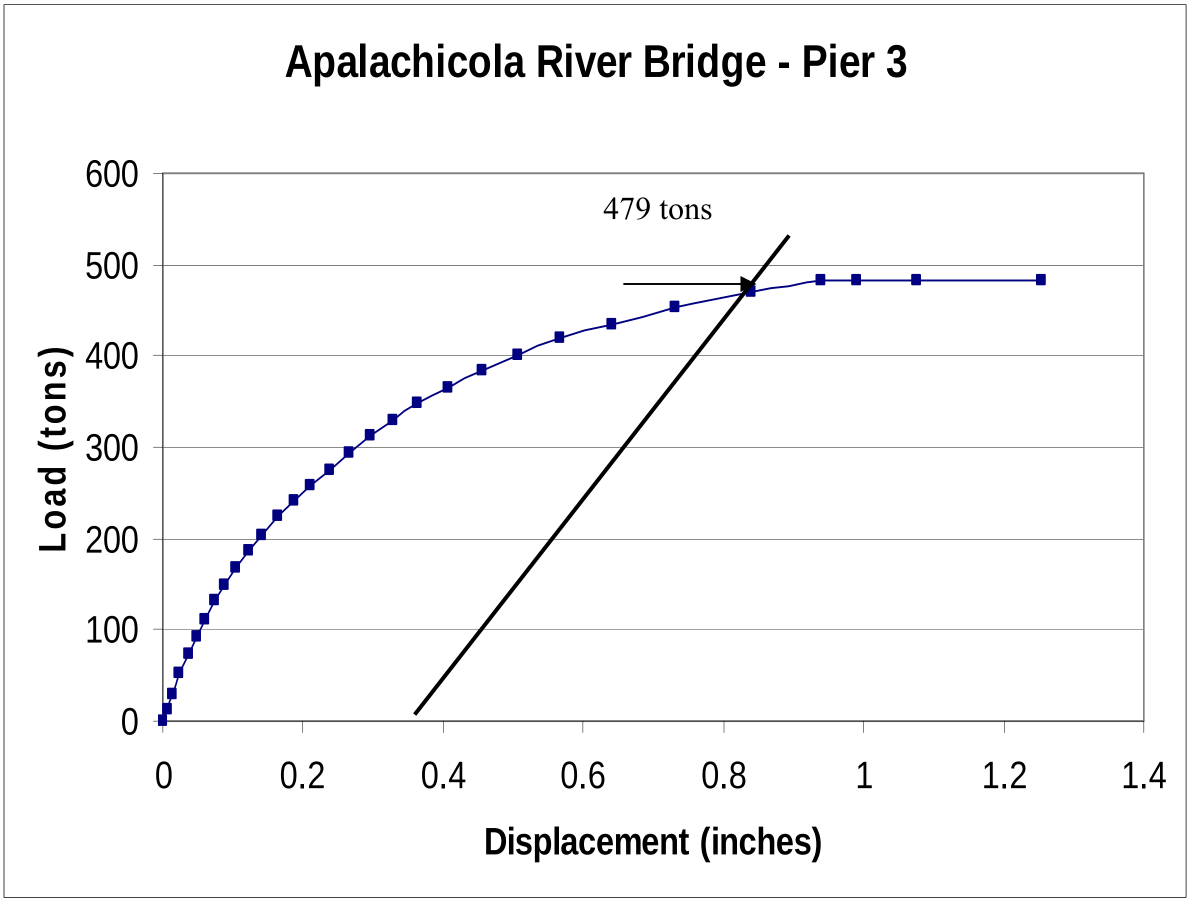

Figure 3-4. Static load test, Apalachicola Bay Bridge (pier 3)

The proposed differentiate method is as follows (see Figure 3-5 for an example of the process):

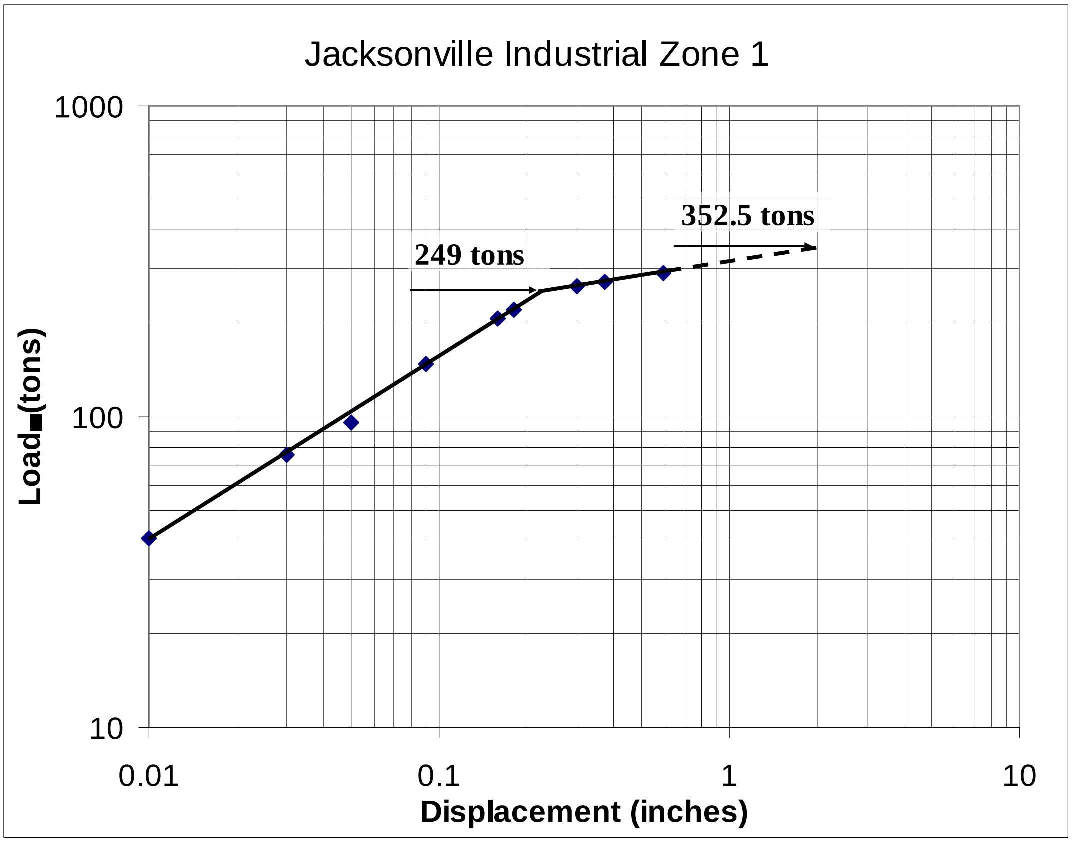

Example:

S + 5 % T = 249 tons
S + T = 352.5 tons
S = 243.5 tons
T = 109 tons
S : Ultimate Skin Friction
T : Ultimate Tip Resistance

Figure 3-5. Separating the ultimate skin friction and tip resistance

a. The load test is plotted in log-log space.

b. Two straight trend lines are drawn among the data points, with the second line extended or extrapolated to two inches.

c. Two distinct loads are indentified: the first occurs at the intersection of the two sloped lines and the other at the presumed displacement of two inches.

d. Since the first load typically occurred at a displacement of approximately 0.1 to 0.2 inches, (i.e., 5% to 10% of the extrapolated value), it was assumed that 5% of the ultimate tip resistance was mobilized. Therefore, the first load is assumed to be the sum of the ultimate skin friction and 5% of the tip resistance, while the second load is the ultimate skin plus tip resistance. Therefore, the separate contributions of ultimate tip and skin friction can be calculated.

The Proposed UF Method

The proposed method uses the following equation to estimate the ultimate pile unit tip resistance, q_t, from the CPT tip resistance, q_c:

$$q_t = k_b * q_{ca}(tip) \leq 150 \text{ tsf}$$

where: k_b is a factor that depends on the soil type as shown in Table 3-1.

The soil type was determined using the soil classification chart for the standard electronic friction cone (Robertson et al, 1986) which includes tip resistance and sleeve friction. Soil cementation was determined by SPT samples, DTP tip2/tip1 ratio or SPT q_c/N ratio (>10).

$q_{ca}(tip)$: the average CPT tip resistance, which is calculated as follows:

$$q_{ca}(tip) = (q_{ca\ above} + q_{ca\ below}) / 2$$

$q_{ca\ above}$: average q_c measured from the tip to 8 D above the tip;

$q_{ca\ below}$: average q_c measured from the tip to 3 D below the tip for sand or 1D below the tip for clay;

Impose the condition: $q_{ca\ above} \leq q_{ca\ below}$, which means if $q_{ca\ above} \geq q_{ca\ below}$, let q_{ca} (tip) be equal to $q_{ca\ below}$.

The proposed method uses the following equation to estimate the ultimate skin friction resistance of the pile, f_s, from the CPT tip resistance, q_c:

$$f_s = q_{ca}\,(\text{side}) * 1.25 / F_s \leq 1.2 \text{ tsf}$$

where: F_s: friction factor that depends on the soil type as shown in Table 3-2. Figure 2-16 was used to determine the relative density of the sand and the following criterion was used to determine the sand state: loose sand (R.D. < 40 %), medium dense sand (40 % < R.D. < 70 %), and dense sand (R.D. >70 %).

q_{ca} (side) : the average q_c within the calculating soil layers along the pile.

Table 3-1. Ultimate unit tip resistance factor k_b

Well Cemented Sand	Lightly Cemented Sand	Gravel	Sand	Slit	Clay
0.1	0.15	0.35	0.4	0.45	1

Table 3-2. Ultimate unit skin friction empirical factor, F_s

Well Cemented Sand	Lightly Cemented Sand	Gravel and Dense Sand	Medium Dense Sand	Loose Sand	Silt, Sandy Clay, Clayey Sand	Clay
300	250	200	150	100	60	50

CHAPTER 4
RESULTS

This chapter includes two parts. The first provides a synopsis of the DPT and CPT results from various sites and a discussion of the cemented sand identifiers. The second part is the evaluation of current axial ultimate pile capacity prediction methodologies using the LRFD statistical method and the proposed method, including its verifications.

Identification of Cemented Sand

Cemented sands exist in many areas of the United States, including California, Texas, Florida, and along the banks of the lower Mississippi River. They also exist in Norway, Australia, Canada, and Italy (Puppala et al. 1995). If the sands found with a CPT test are not known to be cemented, the high bearing readings may be misinterpreted as being due to high relative densities. This can lead to an underestimation of the liquefaction potential of the soil and overestimate the ultimate pile capacity. It is a very challenging soil type for geotechnical engineers. It is therefore important to identify such soil before the design of foundation. In previous practice, engineers used SPT borings and CPT (Q_c/N) to identify cemented sand. However, there are two drawbacks: firstly, lightly cemented sand may not be able to be identified by field technicians since the strength between sand particles is very weak, and secondly, the SPT provides discontinuous data so that engineering judgment is required to estimate the N value between data points for calculating the Q_c /N ratio. It would be very beneficial if the DTP could be used to identify cemented sand.

DTP & CPT Test Data at FDOT Bridge Sites

Many FDOT's bridge sites have been revisited and had DTP and CPT tests performed. DTP and CPT tests were usually performed in pairs for comparison. All field tests were conducted by personnel from the State Materials Office (SMO). The sites were chosen so that load tests and SPT data were available, and several sites also had cemented sand presented. The sites include: Archer Landfill (Archer, FL), I-95 at Edgewood Avenue (Jacksonville, FL), Apalachicola River Bridge, Pier 3 (Apalachicola, FL), West Bay Bridge, Pier 20 (Bay County, FL), Port Orange Relief Bridge (Port Orange, FL), University of Central Florida (Orlando, FL), I-295 at Blanding Blvd (Jacksonville, FL), I-295 at Normandy Blvd. (Jacksonville, FL), and White City Bridge, Pier 5 and Pier 8 (White City, FL).

Archer Landfill Site

This site is one of the first sites used for DTP testing. The Archer landfill is an excellent site for initial scrutiny. Located in Archer, Florida, this site contains a very clean, fine sand deposit peripheral to the outside of the clay liner boundary. This area has been used for many years as a borrow area, where clean sands were mined for daily cover of the landfill debris.

No SPT data is available for this site. Figure 4-1 shows the CPT tip resistance, DTP Tip 1 and Tip 2 resistances. The Tip 1 and CPT tip resistance are very close to each other. Therefore, the second tip (the one above the friction sleeve) does not influence the reading of the first tip (the one at the same location as the CPT). This phenomenon was found in all paired CPT and DTP tests, which means the distance between these two tips is sufficient enough to eliminate the interaction between each other. Another finding is that the relative magnitudes between DTP Tip 2 reading (T2) and Tip 1 reading (T1) for the clear fine sand equal 0.5.

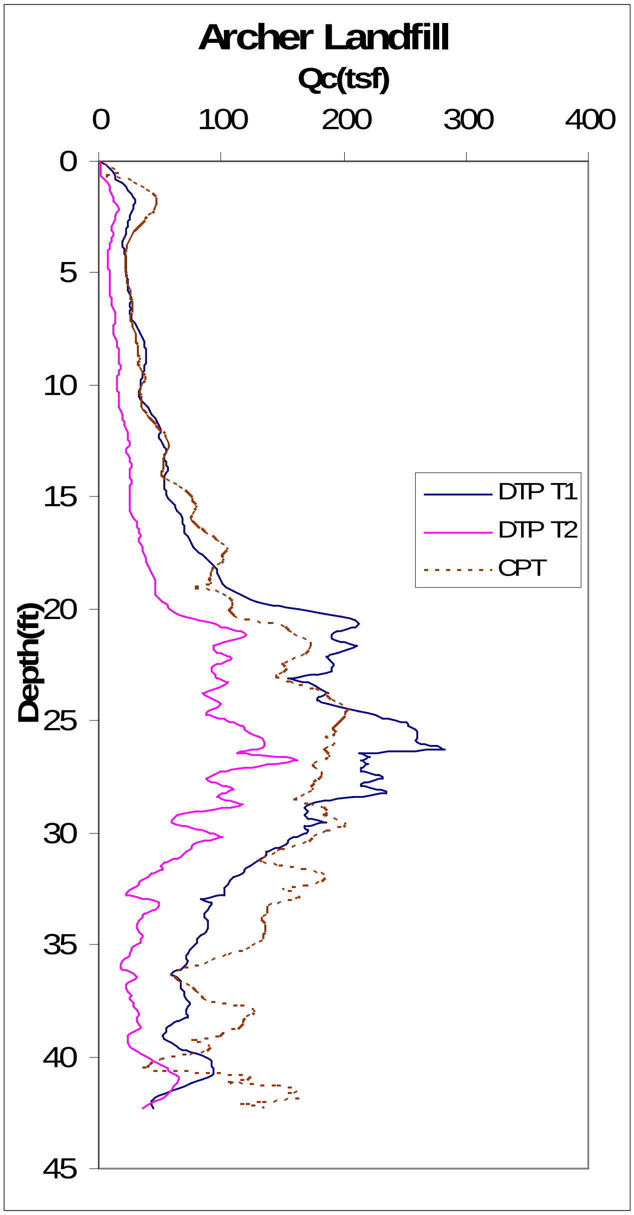

Figure 4-1. CPT and DTP test data from Archer Landfill site

Figure 4-2 shows the comparison between friction ratios of CPT and DTP. From the plot, it was found that the friction ratio of the DTP is much higher than that of the CPT for sand (~ 3 times). The main reason for this increase is the normal stress adjacent to the friction sleeve due to the second tip. Therefore, the shear stress near the friction sleeve is also increased. The discrepancy in friction ratios between the DTP and CPT does not allow for soil classification unless a new soil classification chart for the DTP is created. However, the main purpose of the DTP is to identify cemented sand using cemented sand identifiers (T2/T1 ratio). This ratio is presented below in the following analysis.

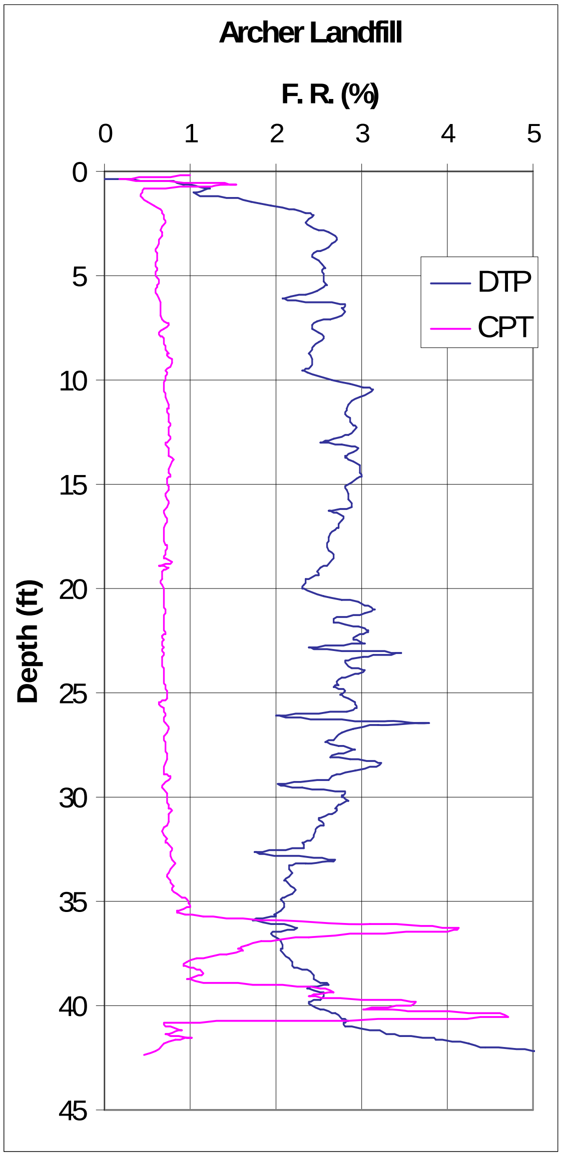

Figure 4-2. Friction ratio of CPT and DTP rest from Archer Landfill site

I-95 at Edgewood Avenue Site

This site is located in Jacksonville and is a FDOT bridge site. Figure 4-3 shows the CPT tip resistance, DTP Tip 1 and Tip 2 resistances. The Tip 1 and CPT tip resistance are very close to each other. It was found that the T2/T1 ratio varies with depth. Since the depth is a function of soil type, T2/T1 is a function of soil type, depth, or both. Through later test results, it was found that the T2/T1 ratio is solely a function of soil type.

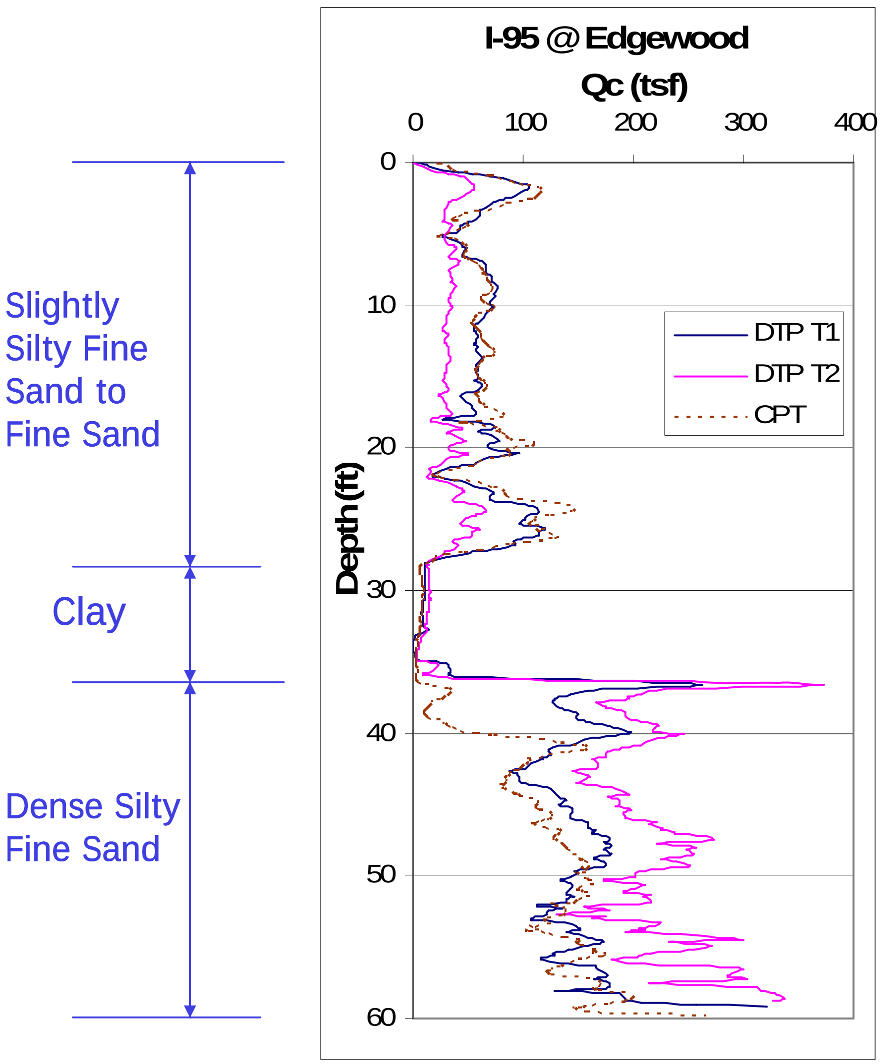

Figure 4-3. CPT and DTP test data from I–95 at the Edgewood Avenue site

Figure 4-4 shows the comparison between the friction ratios of the CPT and DTP. From the plot, it can be observed that the DTP's is again higher than the CPT's for sandy soil (also 3 times), but it is close to the CPT's in clayey soil. Since the friction ratio of the DTP is different from the CPT and hence could not be used to classify the soil, the friction ratio for the following cases will not be presented.

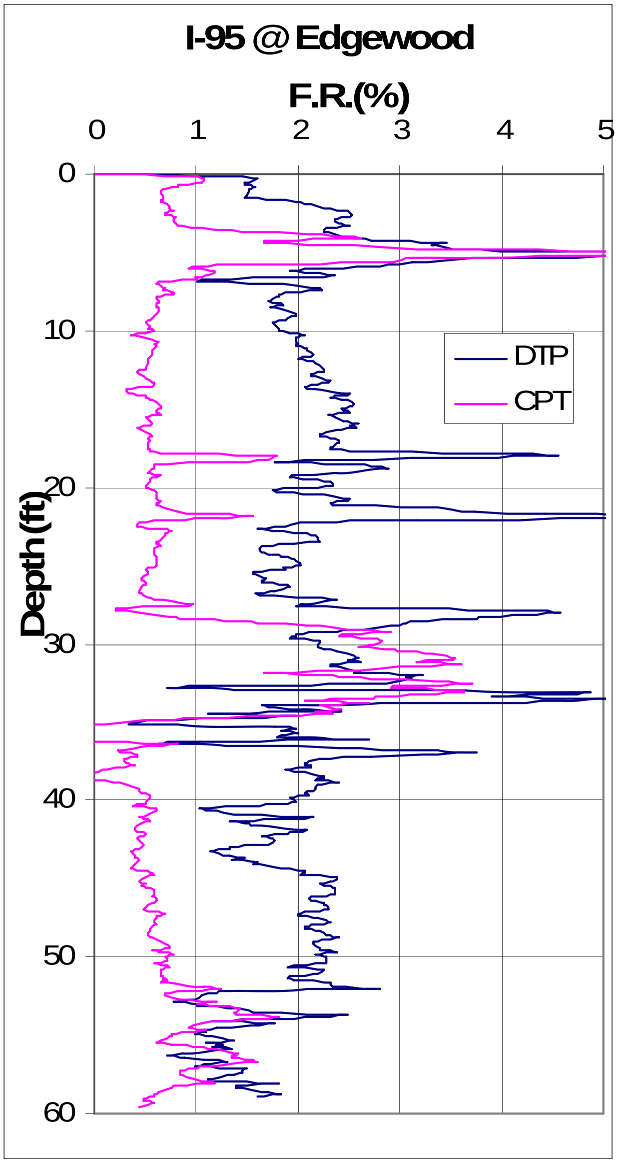

Figure 4-4. Friction ratio of CPT and DTP tests from I–95 at Edgewood Avenue site

Figure 4-5 shows the comparison between the T2/T1 ratio and Q_c/N ratio with depth. Generally speaking, when the Qc/N ratio is less than 3, the soil is considered as a clayey, silty soil. With Q_c/N ratios between 3 to 10, the soil is considered a regular sand, and above 10, cemented sand may be encountered. For the I-95 at Edgewood site, the soil profile is as follows: loose to medium dense sand with a thin layer of silt (0 feet – 27 feet), clay (27 feet – 36 feet), and dense, silty fine sand (36 feet – 59 feet). This was confirmed by the Qc/N ratio. The T2/T1 ratio is 0.5 for loose to medium dense sand, greater than or equal to 1 for clayey silty soil, and greater than 1 for very dense, silty sand.

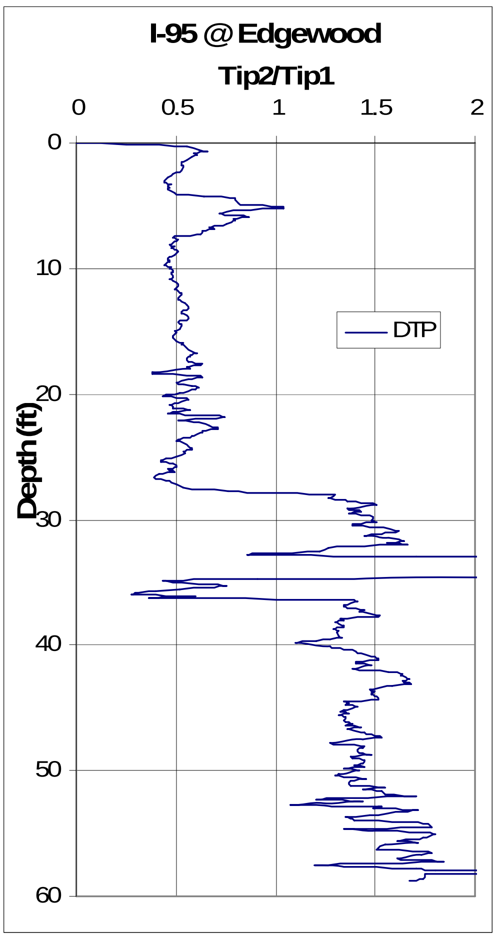

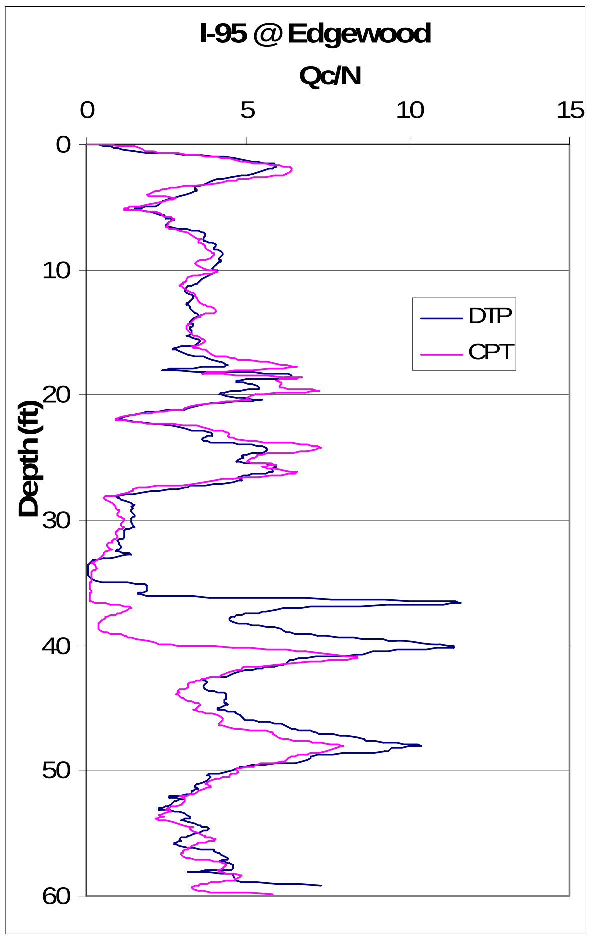

Figure 4-5. Tip2/Tip and Q_c/N ratio for CPT and DTP tests at I–95 at Edgewood Avenue site

Apalachicola River Bridge Site

This site is also a FDOT bridge site located in Apalachicola, FL. Figure 4-6 shows the CPT tip resistance, DTP Tip 1 and Tip 2 resistances. Tip 1 and CPT tip resistances are very close to each other. The soil profile in this site is as follows: two lightly cemented sand layers (0 feet – 25 feet), sandy silt (25 feet – 45 feet), silty clay (45 feet – 60 feet), and lightly cemented sand layer (under 60 feet). Figure 4-7 shows the comparison between the T2/T1 ratio and Q_c/N ratio with depth at the Apalachicola River Bridge site. The T2/T1 ratio is less than 0.5 for lightly cemented sand, between 0.5 to 1 for sandy silt and silty clay soil.

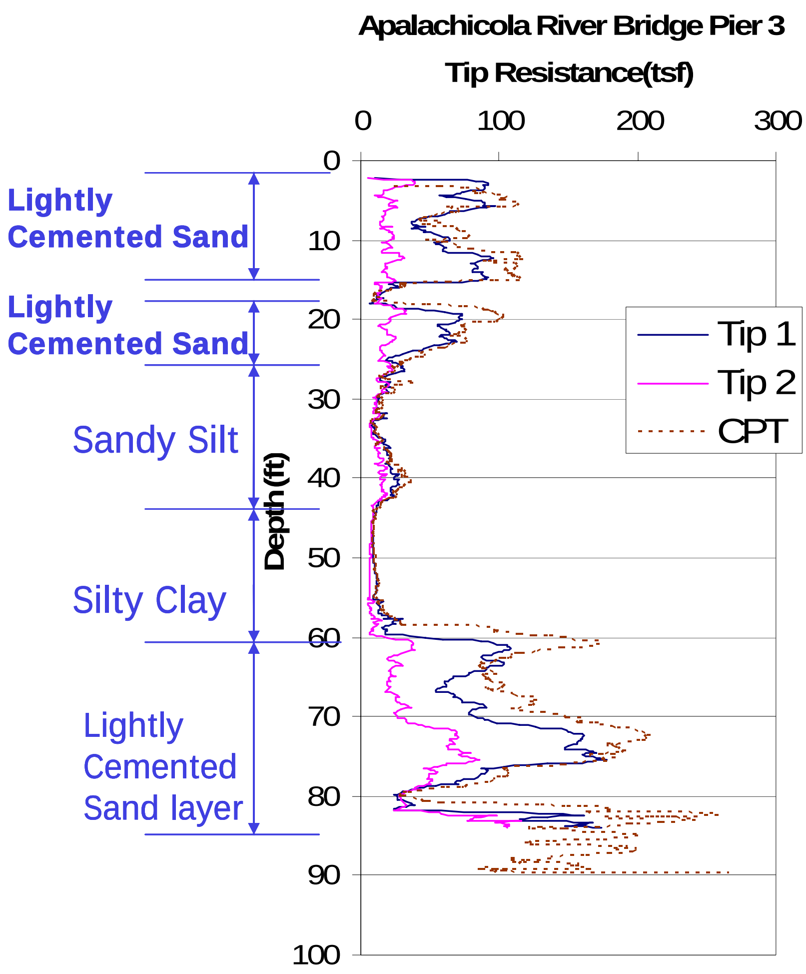

Figure 4-6. CPT and DTP test data from the Apalachicola River Bridge site

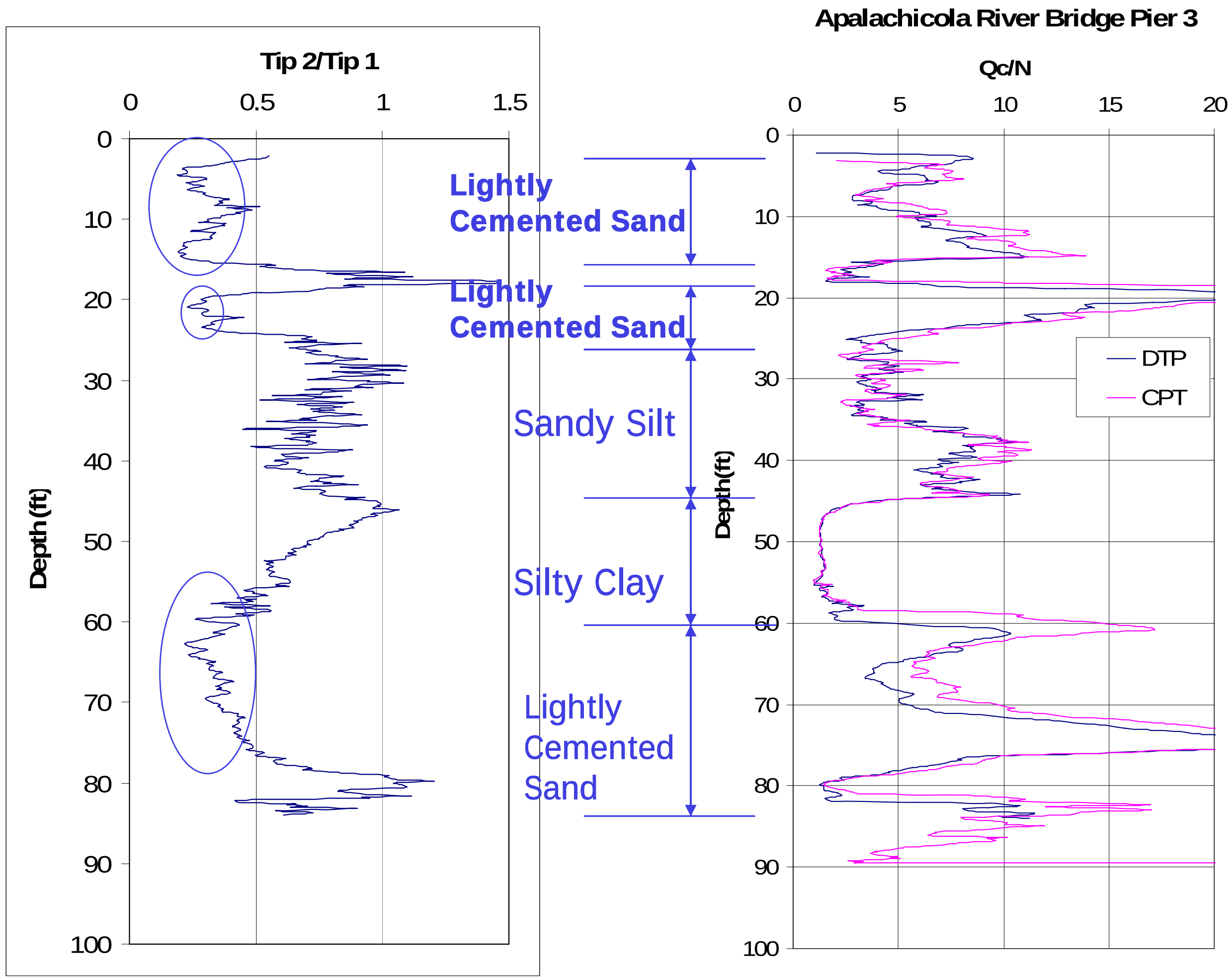

Figure 4-7. Tip2/Tip and Q_c/N ratios from Apalachicola River Bridge site

West Bay Bridge Site

This site is a FDOT bridge site located in Bay County, FL. Figure 4-8 shows two CPT tip resistances, DTP Tip 1 and Tip 2 resistances. The reason for presenting two CPTs is to show that there is significant spatial variability at this site. These two CPTs are within 100 feet and are totally different. The DPT Tip 1 and CPT1 Tip resistances are very close at 68 feet but DTP T1 is much higher than CPT1 tip resistance at the same depth. However, DTP T1 is very similar to the CPT2 tip resistance at the depth above 64 feet but significant smaller at the depth below 64 feet. In this site, there are two lightly cemented sand layers and one well cemented sand layer. Figure 4-9 provides a comparison between T2/T1 ratio and Q_c/N ratio along the depth at this site. The T2/T1 ratio is less than 0.5 for lightly cemented sand, and close to 1 for well cemented sand.

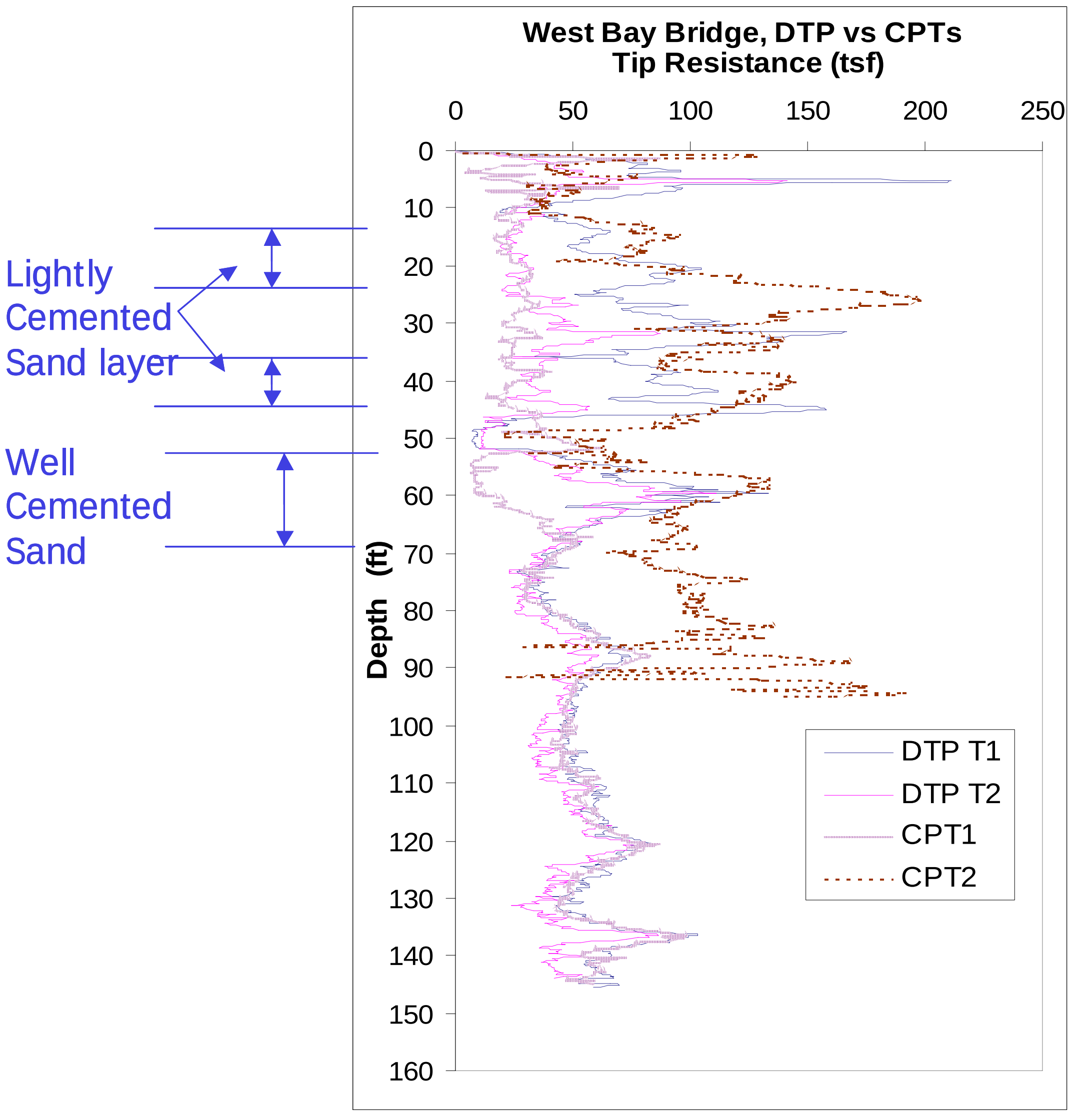

Figure 4-8. CPT and DTP test data from West Bay Bridge site

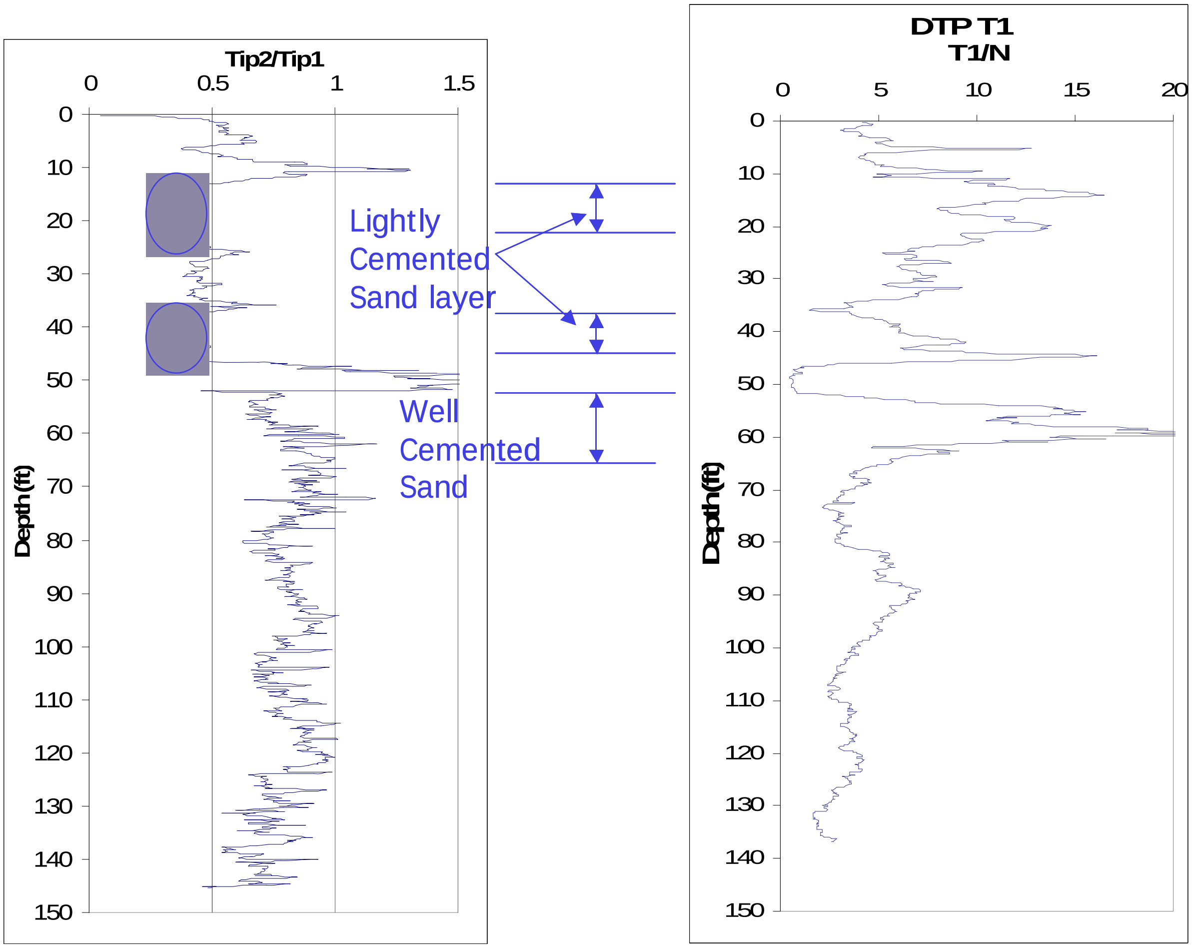

Figure 4-9. Tip2/Tip1and Q_c/N ratios from the West Bay Bridge site

Port Orange Relief Bridge

This site is a FDOT bridge site located in Port Orange, FL. Figure 4-10 shows CPT tip resistance, DTP Tip 1 and Tip 2 resistances. The DPT Tip 1 and CPT1 Tip resistances are very similar to one another. At this site, there are two well cemented sand layers with one clayey silt and one lightly cemented sand layer in the middle.

Figure 4-11 shows a comparison between T2/T1 and Q_c/N with depth. The T2/T1 ratio is less than 0.5 for lightly cemented sand and clayey silt and close to 1 for well cemented sand. The interesting finding in this figure is that the Q_c/N ratio is higher for lightly cemented sand than that for well cemented sand. The lightly cemented sand is loose to medium dense sand with very low N blow counts; therefore, it does not require a high tip resistance (q_c) to produce very large Qc/N ratios. Therefore, this ratio cannot indicate the relative degree of cementation.

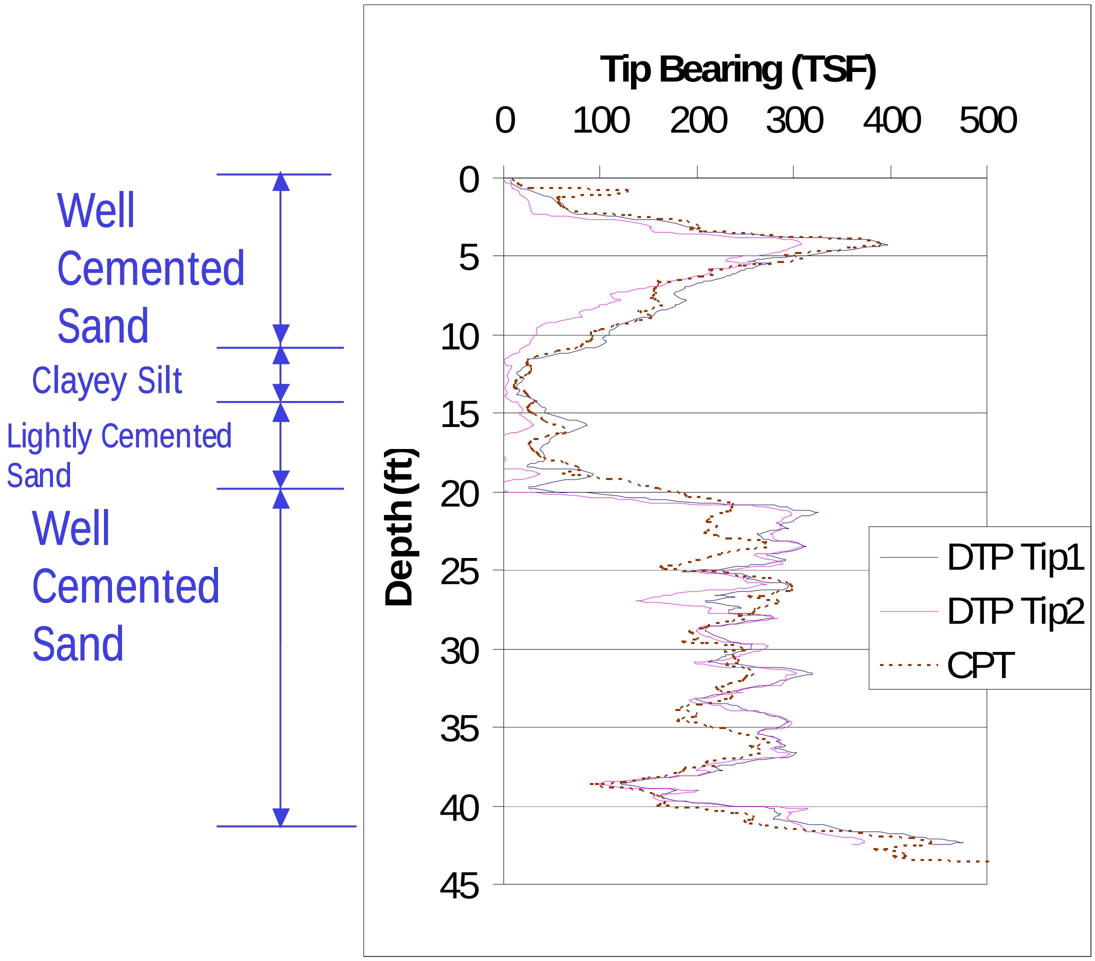

Figure 4-10. CPT and DTP test data from the Port Orange Relief Bridge site

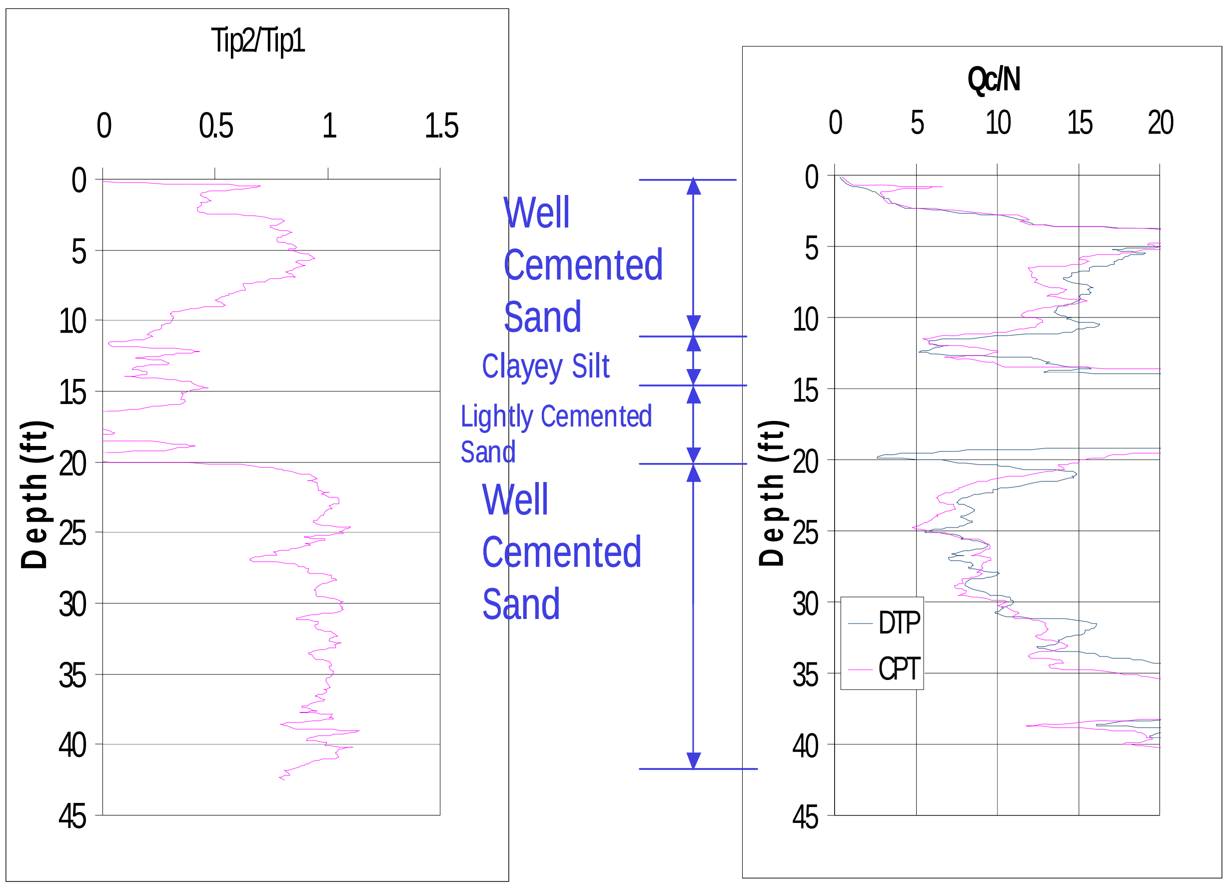

Figure 4-11. Tip2/Tip1 and Q_c/N ratios from the Port Orange Relief Bridge site

University of Central Florida

This site is located at the University of Central Florida, Orlando, FL. Figure 4-12 shows CPT tip resistance, DTP Tip 1 and Tip 2 resistances. The DPT Tip 1 and CPT1 Tip resistances are similiar. At this site, there are two lightly cemented sand layers (T2/T1 <0.5) and four well cemented sand layers (T2/T1 ≈ 1) with one clayey silt layer with shell (38 feet – 53 feet) and two clay layers (4 feet – 6 feet, 30 feet – 34 feet).

Figure 4-13 shows a comparison between T2/T1 and Q_c/N with depth. The T2/T1 ratio is less than 0.5 for lightly cemented sand, close to 1 for well cemented sand, and less than 0.5 for clay and clayey silt. The interesting finding at this site is that the T2 values in clay and clayey silt are very low and even negative. That means that the clay is highly sensitive and looses its shear strength dramatically after the disturbance of the first tip.

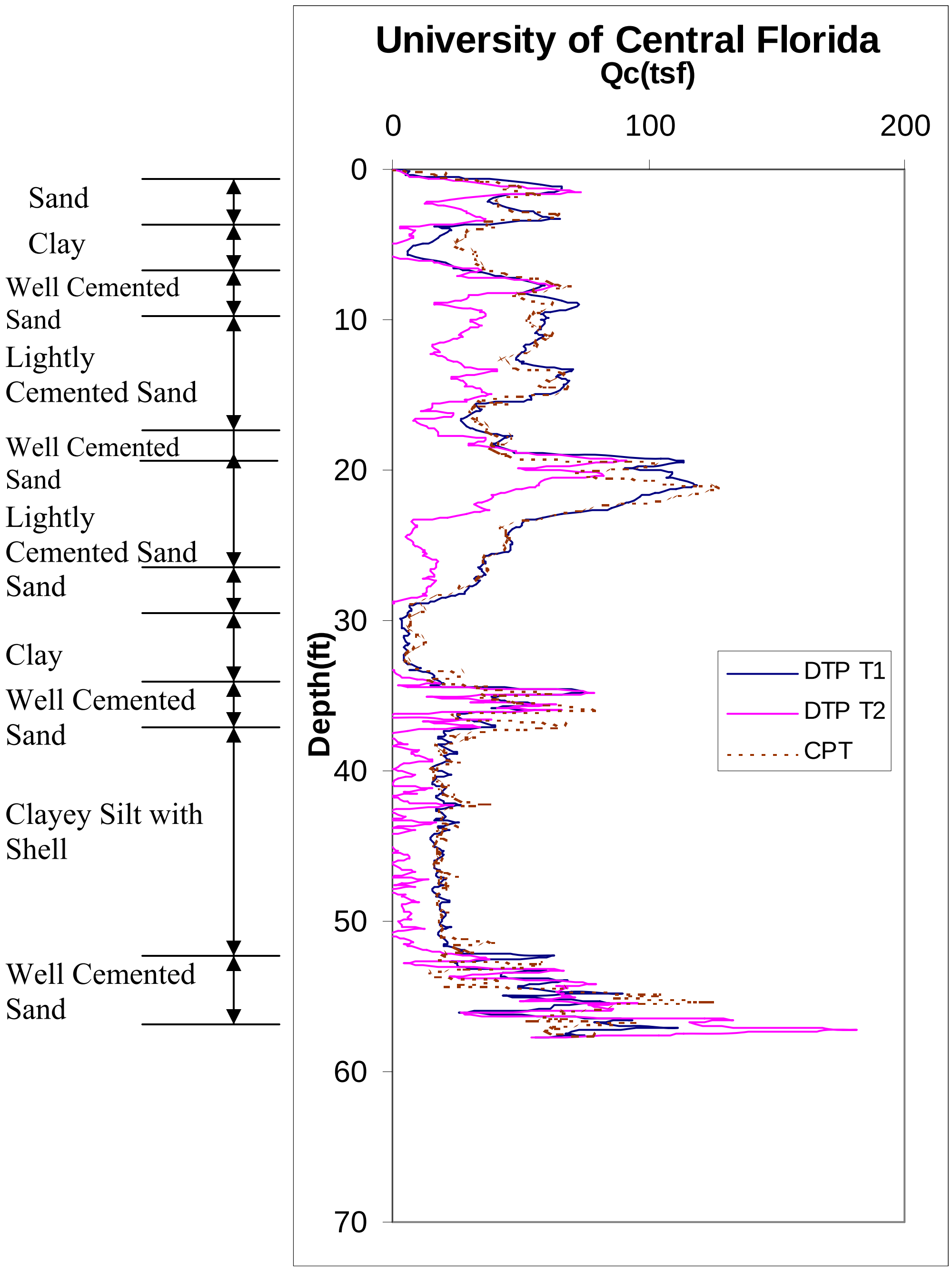

Figure 4-12. CPT and DTP test data at the University of Central Florida site

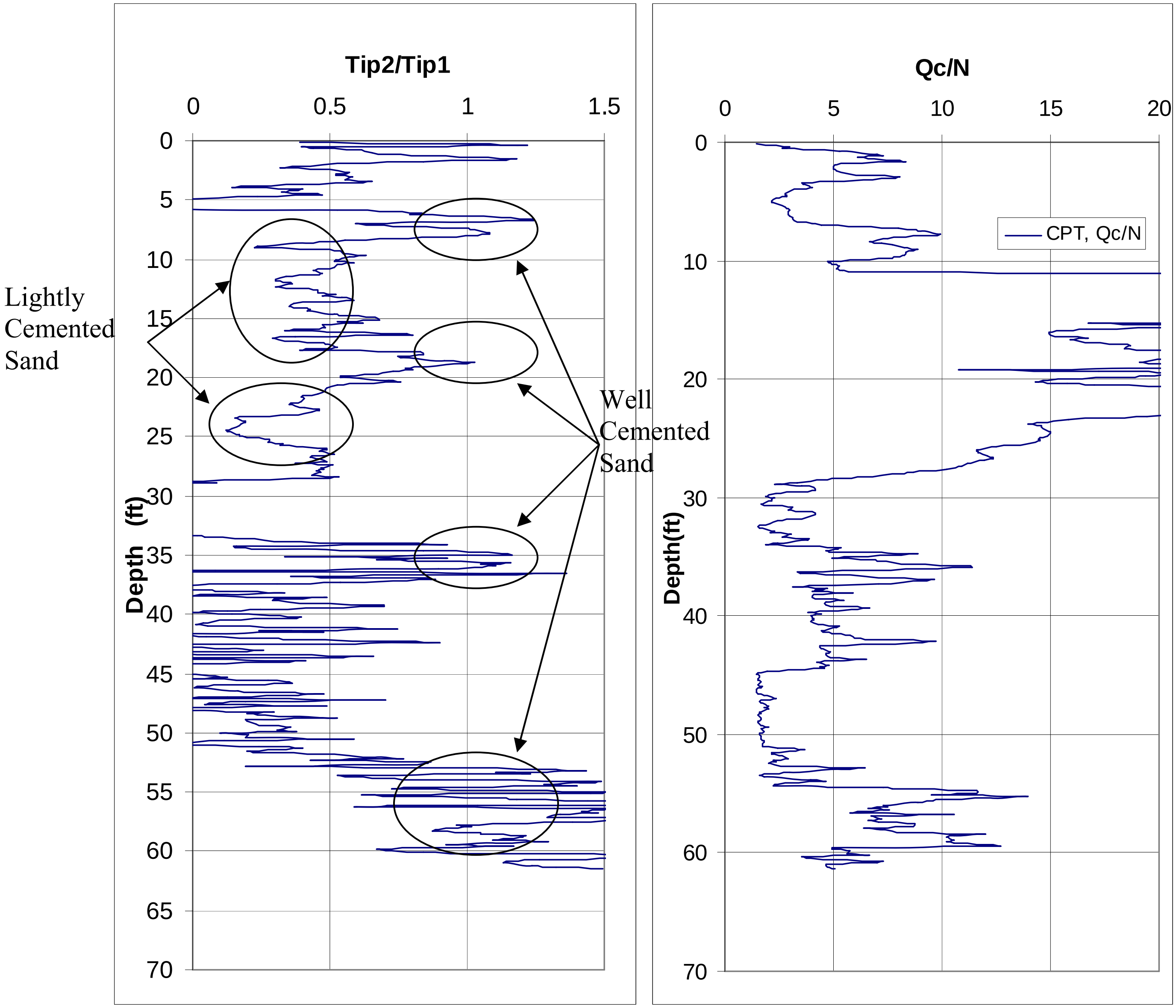

Figure 4-13. Tip2/Tip1 and Q_c/N ratios at the University of Central Florida site

I-295 at Blanding Blvd Site

This is a site in Jacksonville, FL. Figure 4-14 shows CPT tip resistance, DTP Tip 1 and Tip 2 resistances. In this site, there are two sand layers (0 feet – 32 feet, 53 feet – 58 feet) with four lightly cemented sand layers within (T2/T1 <0.5) and one clayey silt layer (32 feet – 53 feet) with one lightly cemented sand within. Figure 4-15 show the comparison between T2/T1 and Q_c/N with depth. The T2/T1 ratio is less than 0.5 for lightly cemented sand, close to or greater than 1 for clayey silt.

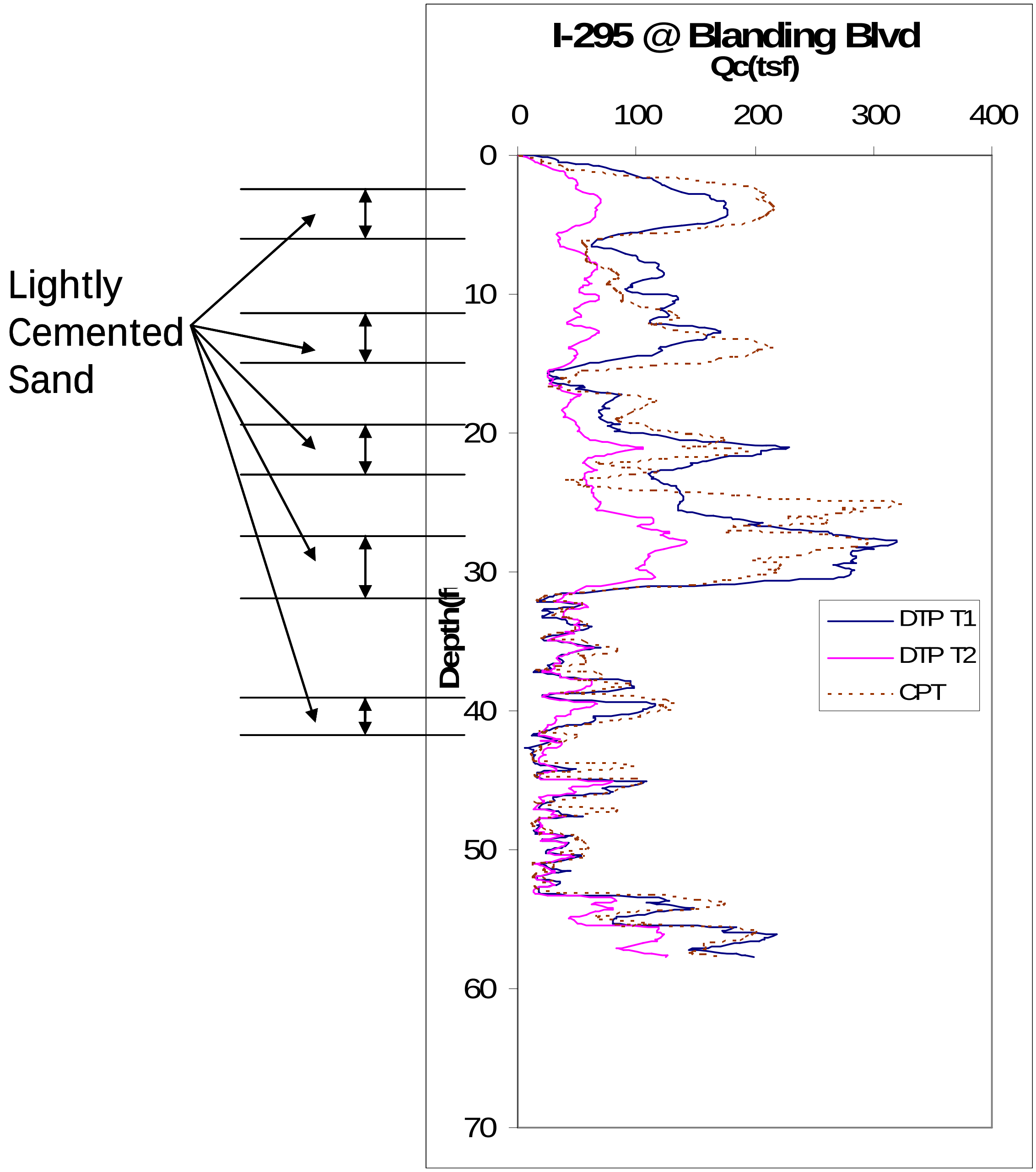

Figure 4-14. CPT and DTP test data at I-295 at Blanding Blvd site

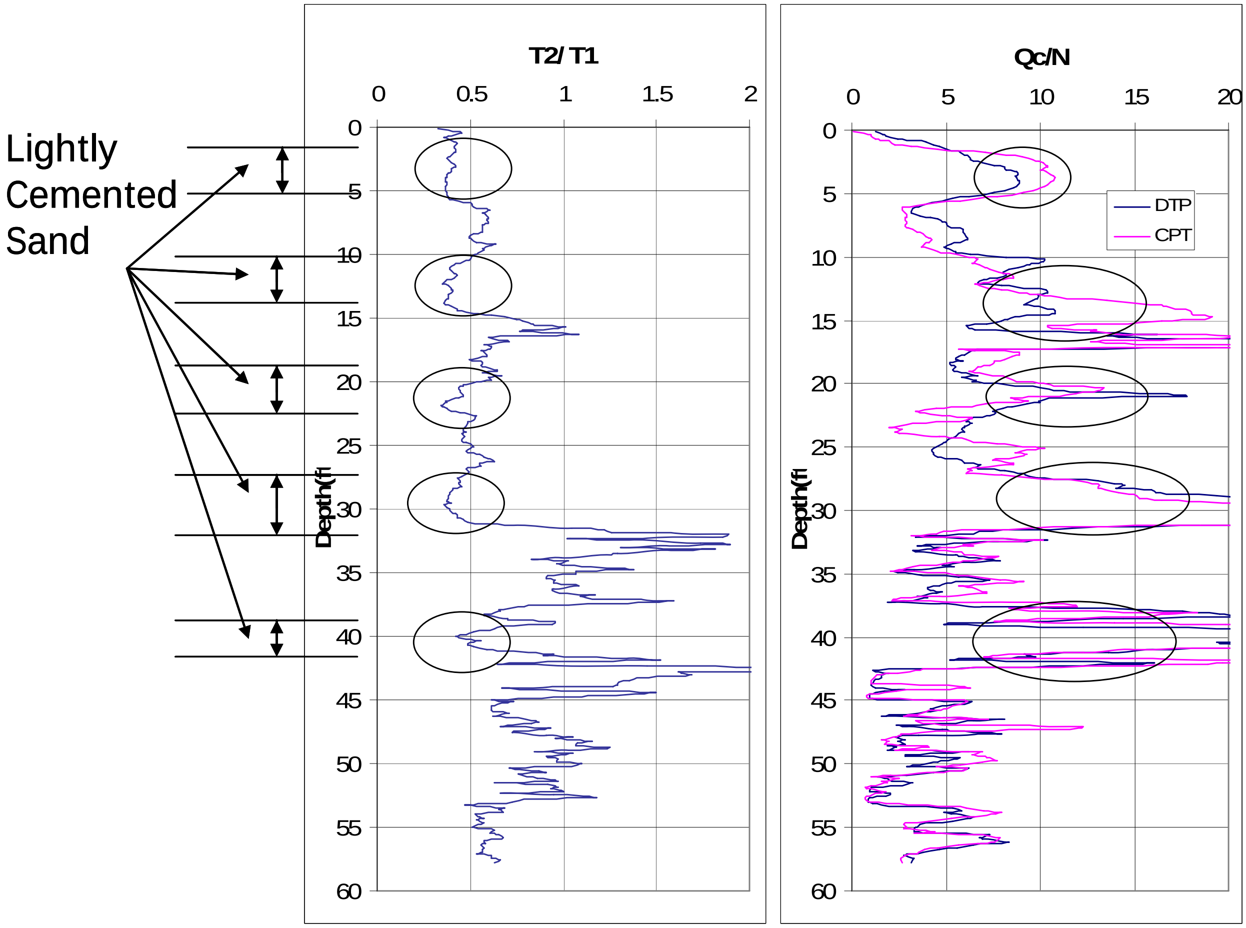

Figure 4-15. Tip2/Tip1 and Q_c/N ratios at the I-295 - Blanding Blvd site

I-295 at Normandy Blvd. Site

This is another site in Jacksonville, FL. Figure 4-16 shows the CPT tip resistance and DTP Tip 1 and Tip 2 resistances. At this site, there are three lightly cemented sand layers (T2/T1 <0.5). Figure 4-17 shows a comparison between T2/T1 and Q_c/N ratios with depth. The T2/T1 ratio is less than 0.5 for lightly cemented sand.

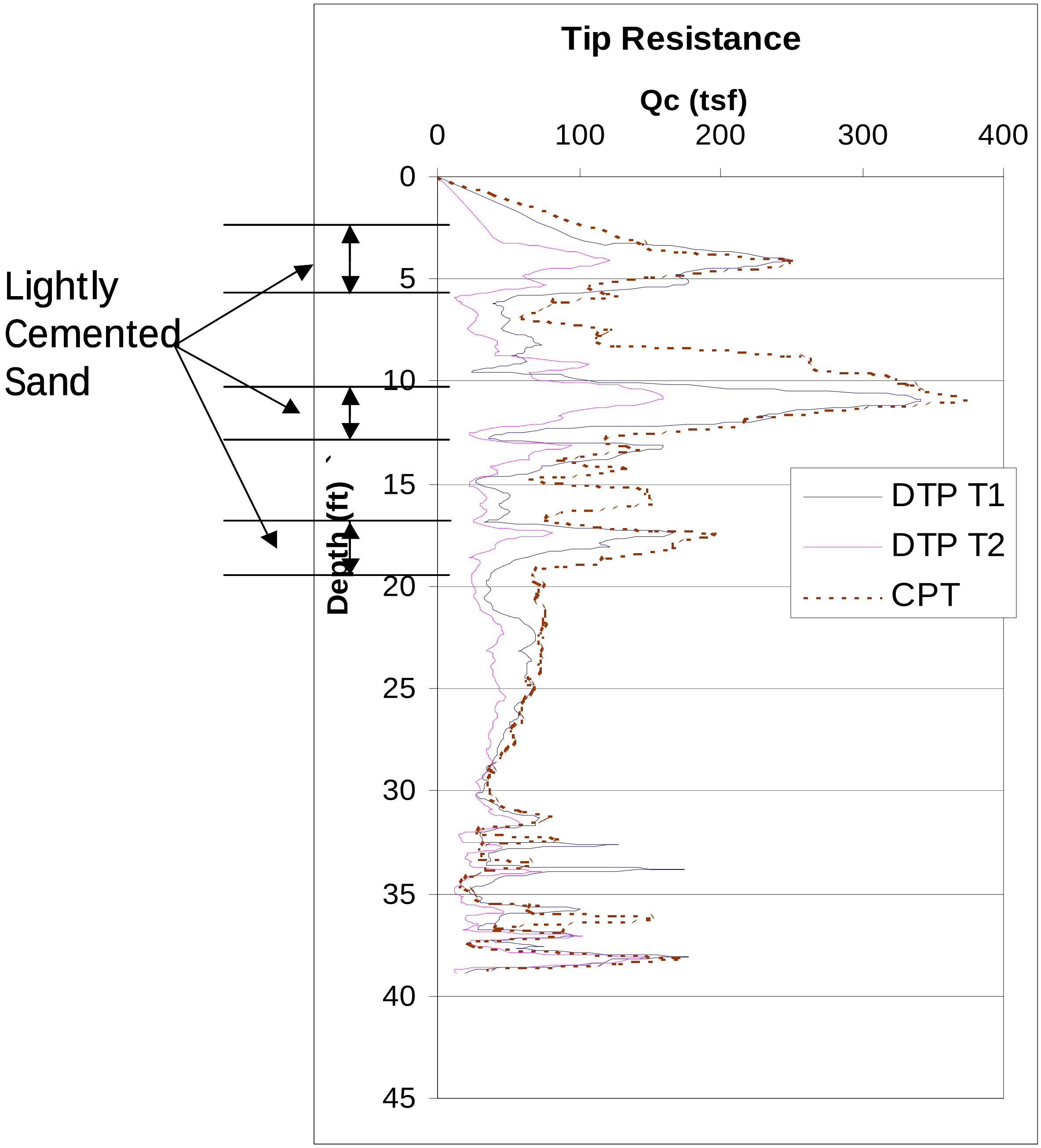

Figure 4-16. CPT and DTP test data at I-295 at the Normandy Blvd. site

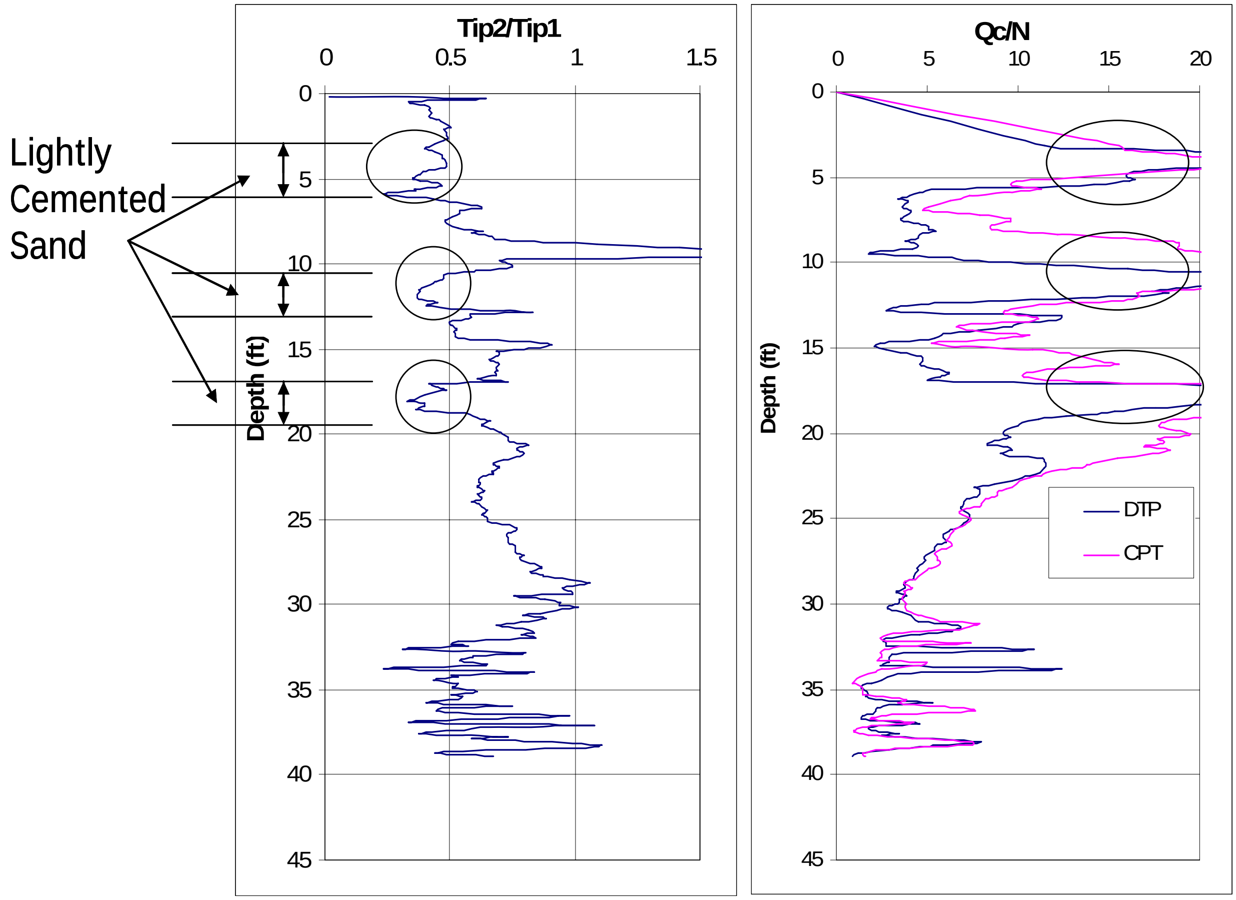

Figure 4-17. Tip2/Tip1 and Q_c/N ratios at the I-295 - Normandy Blvd. site

White City Bridge Site (Pier 5)

This is a site in White City, FL. Figure 4-18 shows CPT tip resistances and DTP Tip 1 and Tip 2 resistances. At this site, there are three lightly cemented sand layers, two silty sand layers and three clay layers. Figure 4-19 indicates the comparison between T2/T1 and Q_c/N with depth. The T2/T1 ratio is less than 0.5 for lightly cemented sand, between 0.5 – 1 for silty sand and close to or greater than 1 for clay.

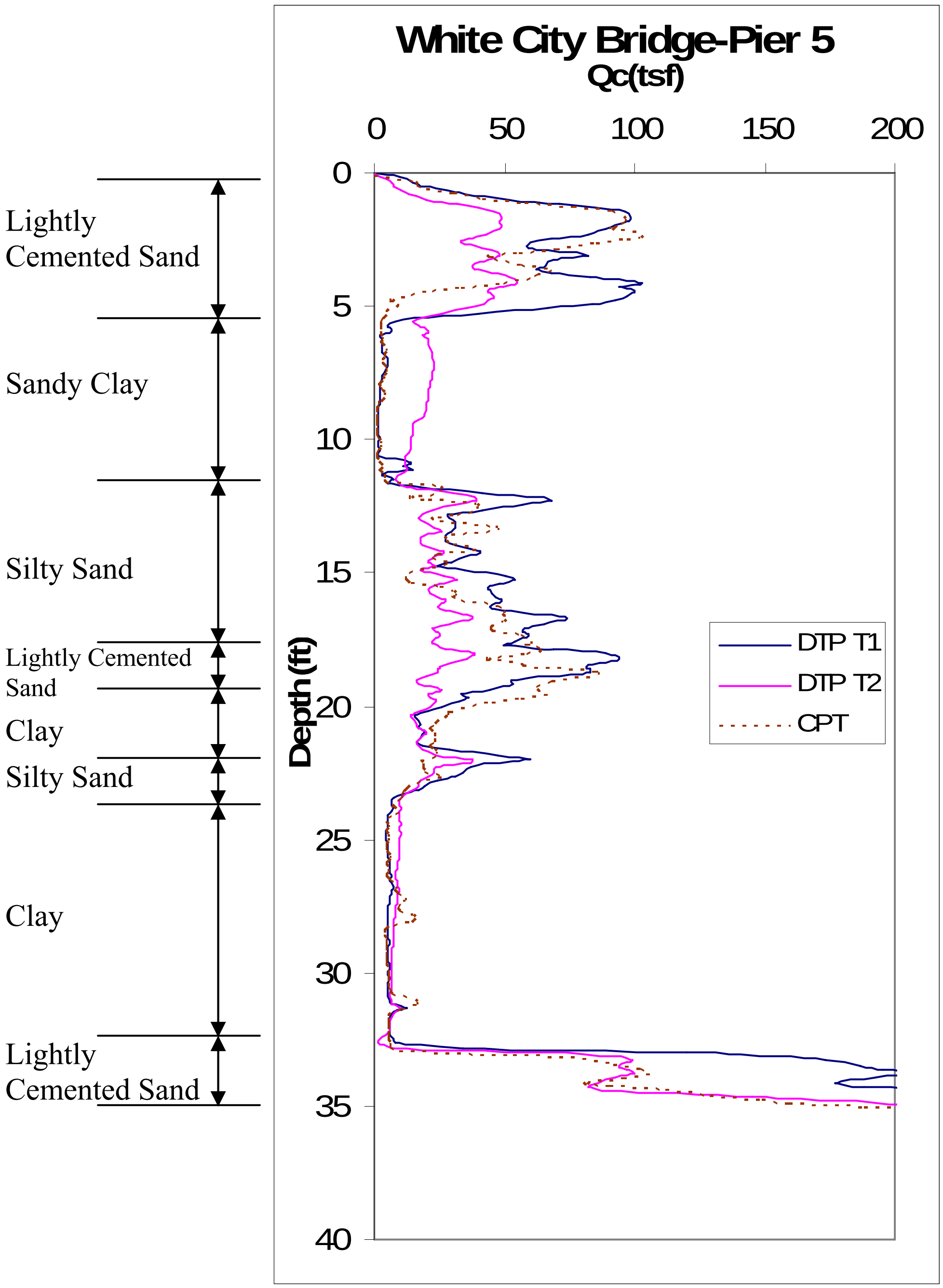

Figure 4-18. CPT and DTP test data at the White City site (pier 5)

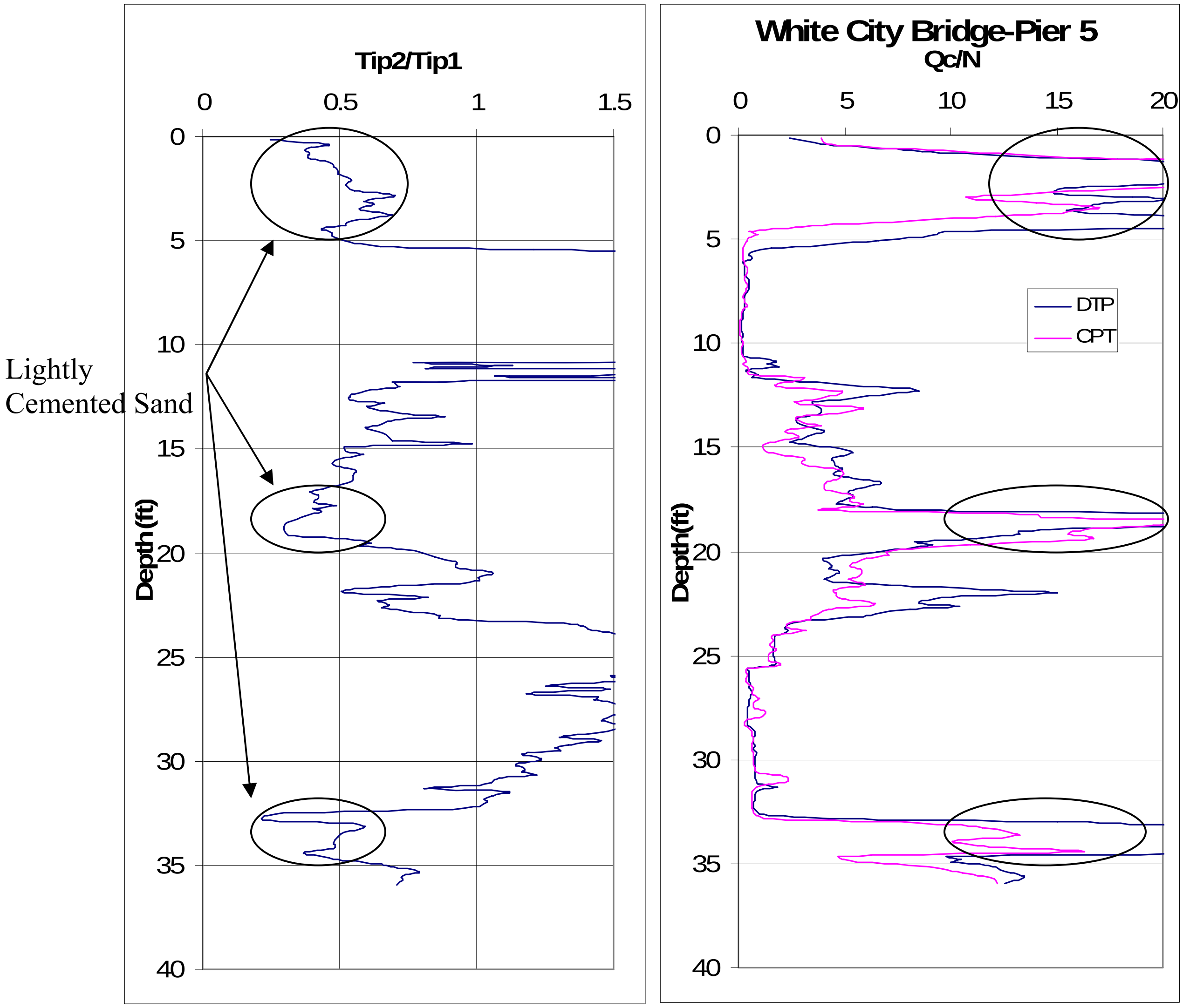

Figure 4-19. Tip2/Tip1 and Q_c/N ratios at the White City site (pier 5)

White City Bridge Site (Pier 8)

This is the second pier at White City Bridge site in White City, FL. Figure 4-20 shows CPT tip and DTP Tip 1 and Tip 2 resistances. There are three lightly cemented sand layers, one silty sand layer, one clay layer, and one sand layer. Figure 4-21 provides a comparison between T2/T1 and Q_c/N with depth. The T2/T1 ratio is less than 0.5 for lightly cemented sand, is between 0.5 and 1 for silty sand, greater than 1 for clay and 0.5 for sand.

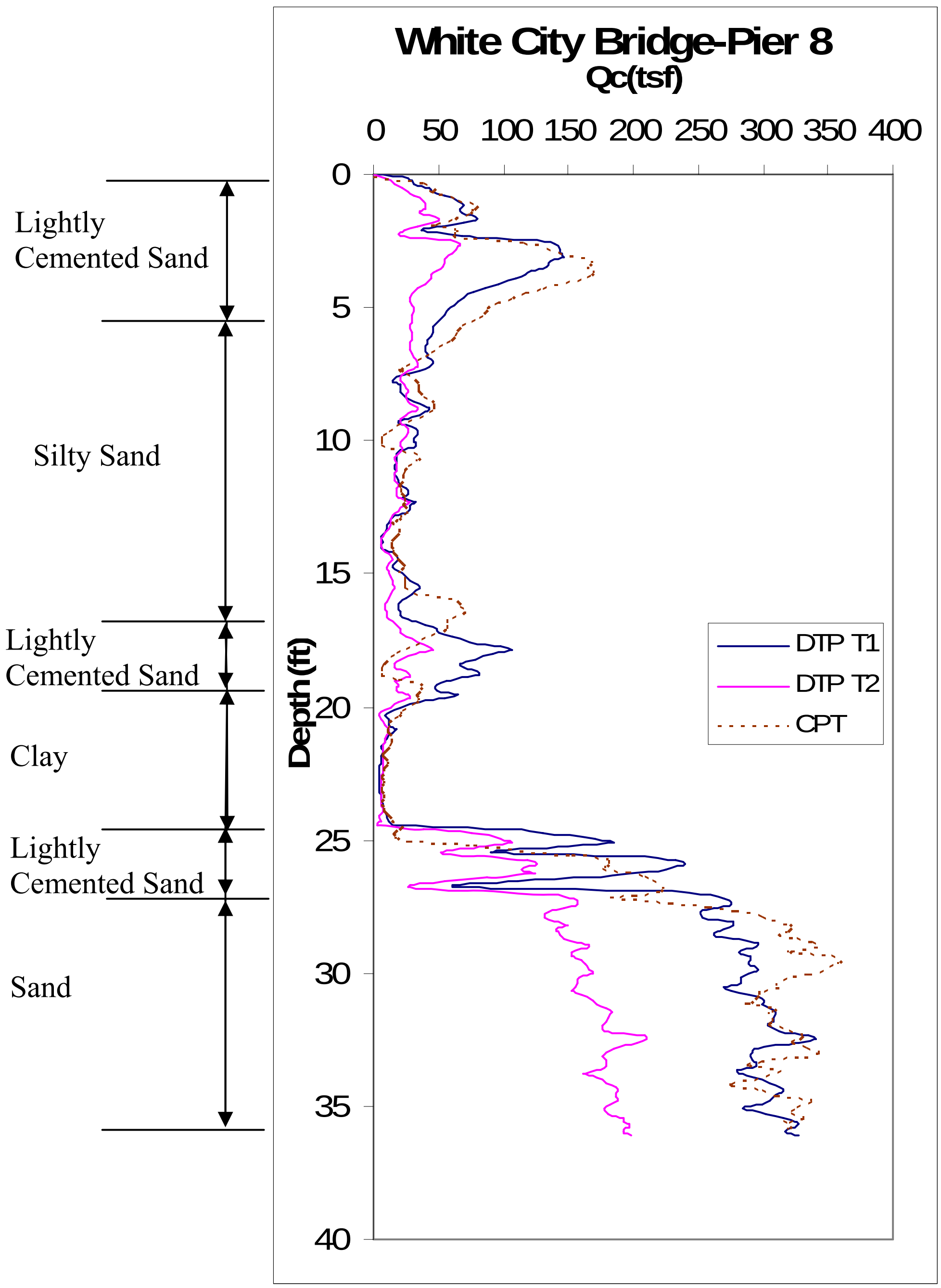

Figure 4-20. CPT and DTP test data at the White City site (pier 8)

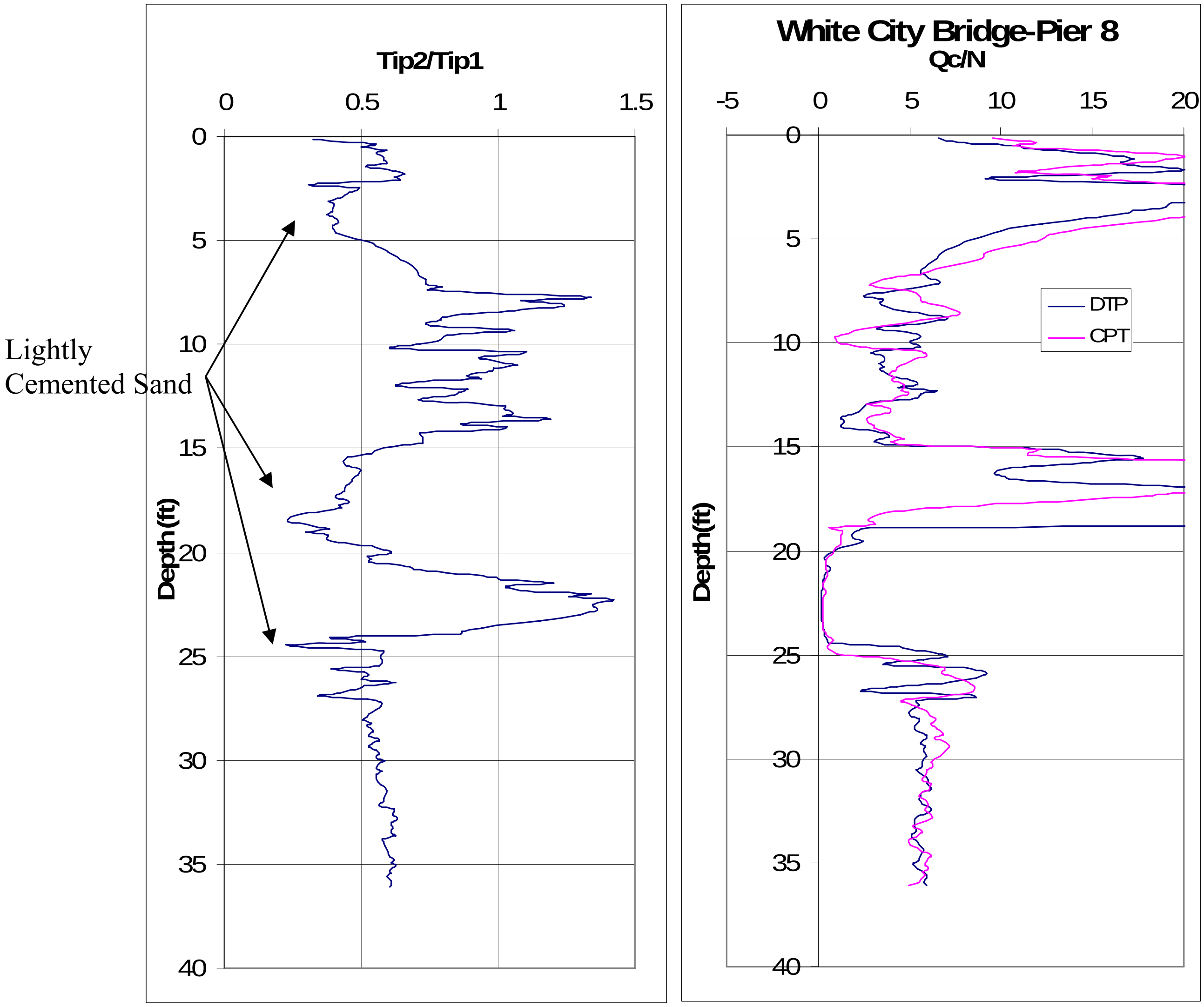

Figure 4-21. Tip2/Tip1 and Q_c/N at the White City site (pier 8)

Identifier for Cemented Sand Summarized from DTP Data

Based on the data collected to date, the T2/T1 ratio appears to be a reasonable predictor or identifier for cemented sand. The following ranges for each soil type are based on the limited data collected in Florida. It may be different elsewhere and more data needs to be collected to verify these values.

T2/T1:

≈ 0.5	Non-Cemented Sand (Loose and Medium Dense Sand)
= 0.3~0.5	Lightly Cemented Sand
≈ 1	Strongly Cemented Sand
= 0.5~1	Silty Sand, Sandy Silt and Silty Clay
< 0.5	Highly Sensitive Clay
> 1	Dense Silty Sand
≥1	Clayey Silt, Silty Clay and Clay

The reasons for the identifiers having different values for different soil types may seem ambiguous. However, the following is one possible explanation that will have to be verified by additional testing.

For non-cemented sand (loose and medium dense sand), T2 is less than T1 due to the compression of the sand after the first tip penetrates the soil. The 0.5 value for the identifier is function of the location of the second tip. Therefore, it is an artifact of the unique shape of the DTP. However, for dense sand, due to the dilation of sand particles after the disturbance of the first tip, T2 is greater than T1. For highly sensitive clay, the disturbance of the first tip dramatically reduces the shear strength of clay that results in the T2/T1 ratio of less than 0.5. For lightly cemented sand, the cementation bonds are totally broken after penetration of the first tip so that T2 is the same as that for non-cemented sand. However, T1 for lightly cemented sand is higher than that for non-cemented sand, which causes the T2/T1 ratio to be less than 0.5. For well cemented sand, the cementation bonds are so strong that they cannot all be broken or are only partially destroyed. Therefore, T2 is close to T1 for well-cemented sands.

For low sensitive clay, clayey silt and silty clay, the penetration of the first tip may reduce the shear strength of the soil and the reduction depends on the strength of clay. However, the excess pore pressure generated by the intrusion of the first tip also increases T2. The resultant effects causes the T2/T1 ratio to be less than, close to or greater than 1. For a mixed soil such as silty sand and sandy silt, T2 /T1 is between 0.5 and 1 due to their combining effects.

Assessing LRFD Resistance Factors, Φ, Based on Reliability (Risk)

Two set of data were used for the LRFD assessment. They include 21 Florida sites and 28 in Louisiana. The data for both Florida and Louisiana are analyzed separately to see how each method works for their respective soil type (Florida: predominantly sand, Louisiana: predominantly clay).

Criteria Used to Quantify Pile Capacity from Load Test Data

The criteria used to quantify pile capacity from load test data are the same as provided in FDOT Specifications. It is defined as the load that causes a pile tip deflection equal to the calculated elastic compression plus 0.15 inches plus 1/120 of the pile width in inches for piles 24 inches or less in width. For piles greater than 24 inches, it is equal to the calculated elastic compression plus 1/30 of the pile width (FDOT Specification 2007, 455-2.2.1). The criteria are similar to Davisson's capacity except for piles greater than 24 inches. All methods predict the ultimate pile tip and skin capacity, therefore the nominal capacities are calculated by the sum of ultimate skin capacity and 1/3 of ultimate tip capacity ($R_n = Q_{S\,ult} + 1/3 * Q_{T\,ult}$). The ratio of measured capacity (FDOT failure load) to the nominal capacity is used to assess the LRFD resistance factor.

Since clay is the predominant soil type in Louisiana, a typical load test curve is shown in Figure 4-22. The ultimate pile capacity is less than the peak load. Therefore, it is not appropriate to compare the predicted nominal capacities ($R_n = Q_{S\ ult} + 1/3 * Q_{T\ ult}$) with Davisson capacity ($Q_{Davisson}$). Thus it was decided to compare the predicted ultimate pile capacity ($R_{ult} = Q_{S\ ult} + Q_{T\ ult}$) with the ultimate capacity from the load test (load at 2 inches of displacement). According to FDOT specifications, the allowable load of any pile tested must be either 50% of the maximum applied load or 50% of the failure load, whichever is smaller.

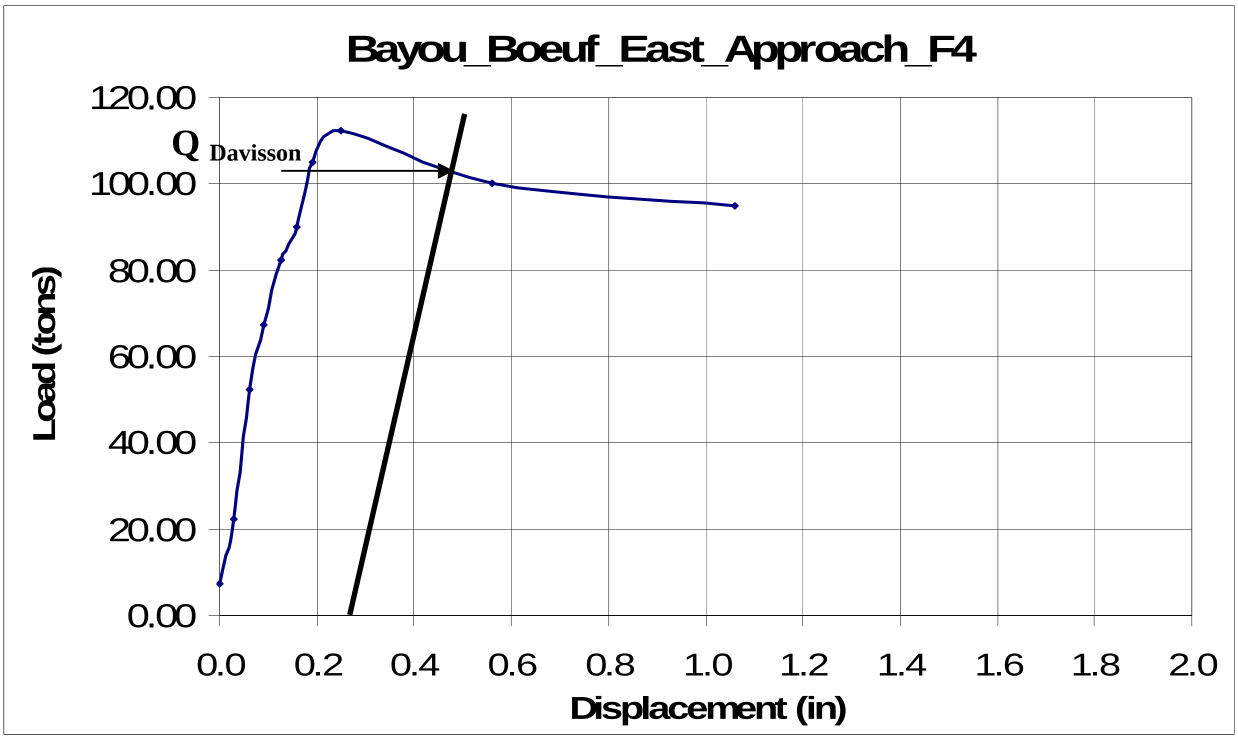

Figure 4-22. Typical load test curve in Louisiana soil

LRFD Resistance Factor, Φ, for Florida Soil

Using the 14 CPT methods with the cone data from the 21 load test sites in Florida, (see Tables 4-1, 4-2, and 4-3) the ultimate skin friction, ultimate tip resistance, and Davisson capacities were determined for each test pile. Also shown in these tables are the measured ultimate skin friction, ultimate tip resistance, Davisson Capacity (from load test curve and the proposed process to separate skin and tip). The highlighted cases represent cemented sand sites. Shown in Figure 4-23 is a plot of the ratio (measured Davisson capacity/predicted Davisson capacity) for each method for all 21 piles. The methods above the value of one are conservative. Next, the LRFD resistance factors, Φ, were assessed for each method.

Based on the ratio of measured to predicted pile capacities, λ_{Ri}, for each of the sites, the mean, λ_R, standard deviation, σ_R, and coefficient of variation, COV_R, were determined for all 14 CPT methods. Using the computed mean, λ_R and coefficient of variation, COV_R, the LRFD resistance factors, Φ, were determined with a reliability index, β of 2.5 (recommended for redundant foundation elements) for each method. Tables 4-4, 4-5, and 4-6 are the LRFD resistance factors for ultimate skin friction, ultimate tip resistance, and Davisson capacity. The last method is the one proposed by UF and was created by modifying the most promising method, the Philipponnat Method (1980).

Evident from Tables 4-4, 4-5, and 4-6, many of the methods result in higher resistance factors, Φ. However, if the method has a substantial amount of scatter (a high COV_R), Table 4-4 (e.g. Schmertmann, Prince, etc.), then the LRFD resistance factor, Φ, will be adjusted downward.

Of strong interest is a ranking of the 14 CPT methods investigated. The latter may be determined as follows:

$$R_{design} = \Phi R_n \text{ (i.e. predicted capacity from individual method)}$$

However $\lambda_R = R_m$ (i.e. Davisson) / R_n (predicted capacity)

Substituting the above equation into the R_{design} equation for R_n

$$R_{design} = (\Phi / \lambda_R)\, R_m$$

Table 4-1. Predicted ultimate skin friction for 14 CPT methods (Florida soil)

Load Test No.	Site Name	Pier (Bent/Slab) No.	Diameter (in)	Length (ft)	Schmertmann	De-Ruiter & Beringen	Bustamante & Gianeselli (LCPC)	Aoki & de Alencar	Penpile	Philipponnat	Prince & Wardle	Turmay & Fakhroo	Almeida et al.	Eslami & Fellenius	Jardine & Chow (MTD)	Powell et al. Method	UWA-05 Method	Zhou et al. Method	Proposed Method	**Davisson Capacity (Load Test)**
1	FT Myers		14	67	110	172	183	92	66	150	79	106	288	140	110	296	59	136	150	**133**
2	Apalachicola river bridge	Bent 16	18	60.2	139	151	222	112	85	177	110	134	264	143	170	234	117	193	154	**123**
3	Port orange relief bridge	Bent 19	18	33.5	129	110	166	120	65	198	93	99	232	128	212	233	186	114	126	**103**
4	West palm I-95	Bent 4	18	52.6	111	120	268	151	66	273	75	95	368	151	258	368	222	124	192	**162**
5	West palm I-95	Bent 9	18	45.8	118	109	246	117	74	191	100	110	323	146	184	324	127	137	195	**187**
6	Apalachicola bay bridge	Bent 22	18	68	93	92	235	127	65	194	72	115	372	127	179	373	120	126	194	**165**
7	Trout River, I-95 @ Edgewood Drive	Bent 1	18	48.5	84	84	216	83	55	157	63	98	293	106	135	294	100	116	157	**147.5**
8	Jacksonville industrial1		20	46	150	183	347	220	89	343	119	115	368	228	393	368	305	163	280	**243.5**
9	Jacksonville industrial2		20	36	136	136	214	164	85	257	132	125	286	165	284	286	214	153	247	**119.4**
10	Apalachicola river bridge	Pier 3A	24	88.4	191	126	534	217	114	376	133	104	656	273	391	667	239	234	308	**311**
11	Apalachicola river bridge	Pier 3B	24	88.4	320	298	469	251	177	393	233	283	641	346	436	652	241	379	307	**311**
12	Choctawhatchee bay bridge	Slab 3	24	81.7	169	265	267	154	111	257	116	214	576	264	229	604	111	271	231	**237**
13	Choctawhatchee bay bridge	Slab 26	24	69	143	234	335	141	90	254	94	188	459	203	190	467	93	221	255	**374**
14	Overstreet bridge	Pier16	24	65.6	208	248	328	192	102	290	134	216	370	251	303	381	150	231	248	**205**
15	Bayou Chico Bridge	Pier 15	24	26.7	83	103	230	128	48	201	55	64	246	129	234	246	216	93	201	**250**
16	Black water bay bridge	Bent 20	24	84.9	237	187	437	216	114	348	149	204	530	250	400	534	266	224	348	**360.5**
17	Escambia river bridge	Bent 5	24	87	316	365	725	389	164	605	204	245	752	403	621	755	351	323	605	**382**
18	Escambia river bridge	Bent 77	24	61.4	161	217	473	230	89	388	106	185	474	254	356	483	215	185	388	**695**
19	White City Bridge	Pier 5	24	37.2	80.5	170	167	77	51	124	70	130	174	125	183.5	179	112	120	114	**102**
20	White City Bridge	Pier 8	24	28.5	71	161	170	67	41	137	48	88	183	102	134	190	102.5	93	120	**96**
21	West bay bridge	Pier 20	30	104	224	146	268	191	159	302	163	361	973	349	294	1008	157	365	302	**390**

Table 4-2. Predicted ultimate tip resistance for 14 CPT methods (Florida soil)

Load Test No.	Site Name	Pier (Bent/Slab) No.	Diameter (in)	Length (ft)	Schmertmann	De-Ruiter & Beringen	Bustamante & Gianeselli (LCPC)	Aoki & de Alencar	Penpile	Philipponnat	Prince & Wardle	Turmay & Fakhroo	Almeida et al.	Eslami & Fellenius	Jardine & Chow (MTD)	Powell et al. Method	UWA-05 Method	Zhou et al. Method	Proposed Method	**Davisson Capacity (Load Test)**
1	FT Myers		14	67	6	3	4	3	1.5	3	2	6	1	3	8	1.4	3.5	9	6	**7**
2	Apalachicola river bridge	Bent 16	18	60.2	257	257	126	170	47	142	104	257	110	209	150	179	154	122	46	**77**
3	Port orange relief bridge	Bent 19	18	33.5	265	265	186	283	57	202	170	265	187	487	221	304	159	151	51	**45**
4	West palm I-95	Bent 4	18	52.6	338	338	316	338	104	327	224	338	230	304	376	338	309	235	220	**266**
5	West palm I-95	Bent 9	18	45.8	143	143	81	137	24	102	96	251	82	164	107	133	86	112	91	**261**
6	Apalachicola bay bridge	Bent 22	18	68	338	338	211	258	97	190	158	338	159	227	232	258	206	157	154	**160**
7	Trout River, I-95 @ Edgewood Drive	Bent 1	18	48.5	213	213	119	181	40	120	89	214	94	179	141	153	128	108	104	**110**
8	Jacksonville industrial1		20	46	276	276	263	383	96	277	248	334	249	724	283	403	166	204	235	**109**
9	Jacksonville industrial2		20	36	417	417	216	297	85	215	182	417	185	485	235	300	268	185	76	**159**
10	Apalachicola river bridge	Pier 3A	24	88.4	358	358	207	327	57	233	187	362	194	490	219	308	215	216	202	**273**
11	Apalachicola river bridge	Pier 3B	24	88.4	254	254	227	284	69	226	174	301	164	352	240	266	153	208	218	**273**
12	Choctawhatchee bay bridge	Slab 3	24	81.7	14	6	17	16	4	49	63	65	54	38	37	87	8.5	66	14	**12**
13	Choctawhatchee bay bridge	Slab 26	24	69	254	254	154	213	61	149	137	337	130	70	143	210	155	158	146	**242**
14	Overstreet bridge	Pier16	24	65.6	23	10	28	32	12	188	176	477	133	175	73	216	14	192	43	**45**
15	Bayou Chico Bridge	Pier 15	24	26.7	600	600	442	600	148	495	379	600	403	848	448	600	562	364	383	**376**
16	Black water bay bridge	Bent 20	24	84.9	202	202	194	309	59	239	189	300	189	543	216	306	121	190	190	**169.5**
17	Escambia river bridge	Bent 5	24	87	455	455	202	334	72	258	240	600	238	599	224	385	273	237	265	**85**
18	Escambia river bridge	Bent 77	24	61.4	77	77	88	128	14	136	136	135	139	196	86	224	46	140	133	**105**
19	White City Bridge	Pier 5	24	37.2	600	600	507	460	172	399	281	600	294	154	470	476	442	302	321	**323**
20	White City Bridge	Pier 8	24	28.5	600	600	440	434	159	357	266	600	279	244	426	453	409	279	304	**281**
21	West bay bridge	Pier 20	30	104	255	255	107	163	36	121	116	275	108	289	96	176	153	148	126	**53**

Table 4-3. Predicted Davisson capacity for 14 CPT methods (Florida soil)

Load Test No.	Site Name	Pier (Bent/Slab) No.	Diameter (in)	Length (ft)	Schmertmann	De-Ruiter & Beringen	Bustamante & Gianeselli (LCPC)	Aoki & de Alencar	Penpile	Philipponnat	Prince & Wardle	Turmay & Fakhroo	Almeida et al.	Eslami & Fellenius	Jardine & Chow (MTD)	Powell et al. Method	UWA-05 Method	Zhou et al. Method	Proposed Method	**Davisson Capacity (Load Test)**
1	FT Myers		14	67	112	174	184	94	66	150.6	80.2	108	289	141	113	296	60	144	152	**140**
2	Apalachicola river bridge	Bent 16	18	60.2	224	237	264	169	101	224	145	219	301	212	220	333	167	315	170	**165**
3	Port orange relief bridge	Bent 19	18	33.5	217	198	228	213	84	264	150	187	295	290	286	334	239	265	143	**103**
4	West palm I-95	Bent 4	18	52.6	223	232	374	263	100	382	150	208	444	253	383	481	325	359	266	**250**
5	West palm I-95	Bent 9	18	45.8	166	157	273	169	82	225	132	193	351	201	220	368	155	249	225	**266**
6	Apalachicola bay bridge	Bent 22	18	68	205	205	305	213	97	257	125	227	425	202	257	459	189	284	245	**213**
7	Trout River, I-95 @ Edgewood Drive	Bent 1	18	48.5	155	155	255	131	68	197	92	169	324	166	182	345	142.5	223	192	**194**
8	Jacksonville industrial1		20	46	242	275	434	355	121	358	201	226	451	469	487	502	360	367	358	**283**
9	Jacksonville industrial2		20	36	275	275	286	263	113	329	193	265	347	327	362	386	304	338	272	**185**
10	Apalachicola river bridge	Pier 3A	24	88.4	311	245.5	603.5	319	133	443	194.8	224.8	720	436	464	769	310.5	426	375	**479**
11	Apalachicola river bridge	Pier 3B	24	88.4	405	383	545	346	200	462	291	383	696	463	516	740	292	595	380	**479**
12	Choctawhatchee bay bridge	Slab 3	24	81.7	174	268	273	189	113	272	138	236	594	277	242	633	114	337	236	**249**
13	Choctawhatchee bay bridge	Slab 26	24	69	229	319	387	197	111	281	140	300	503	226	238	537	145	379	303	**480**
14	Overstreet bridge	Pier16	24	65.6	216	252	337	288	106	353	193	375	415	310	328	453	155	424	262	**250**
15	Bayou Chico Bridge	Pier 15	24	26.7	283	303	378	328	97	366	181	264	380	411	383	446	403	457	329	**393**
16	Black water bay bridge	Bent 20	24	84.9	304	255	501	319	134	411	212	304	593	431	472	636	306	414	411	**438**
17	Escambia river bridge	Bent 5	24	87	468	517	792	520	188	691	284	445	831	603	695	884	442.5	559	693	**425**
18	Escambia river bridge	Bent 77	24	61.4	187	243	502	304	94	432	151	230	520	320	385	558	231	326	432	**735**
19	White City Bridge	Pier 5	24	37.2	280.5	370	336	230	108	256.5	164	330	272	176.5	340	338	259	422	221	**332**
20	White City Bridge	Pier 8	24	28.5	271	361	317	212	94	256	136	288	276	183	276	341	239	372	221	**250**
21	West bay bridge	Pier 20	30	104	309.5	231	304	255	171	382	202	452	1009	446	326	1066	208.5	513	344	**425**

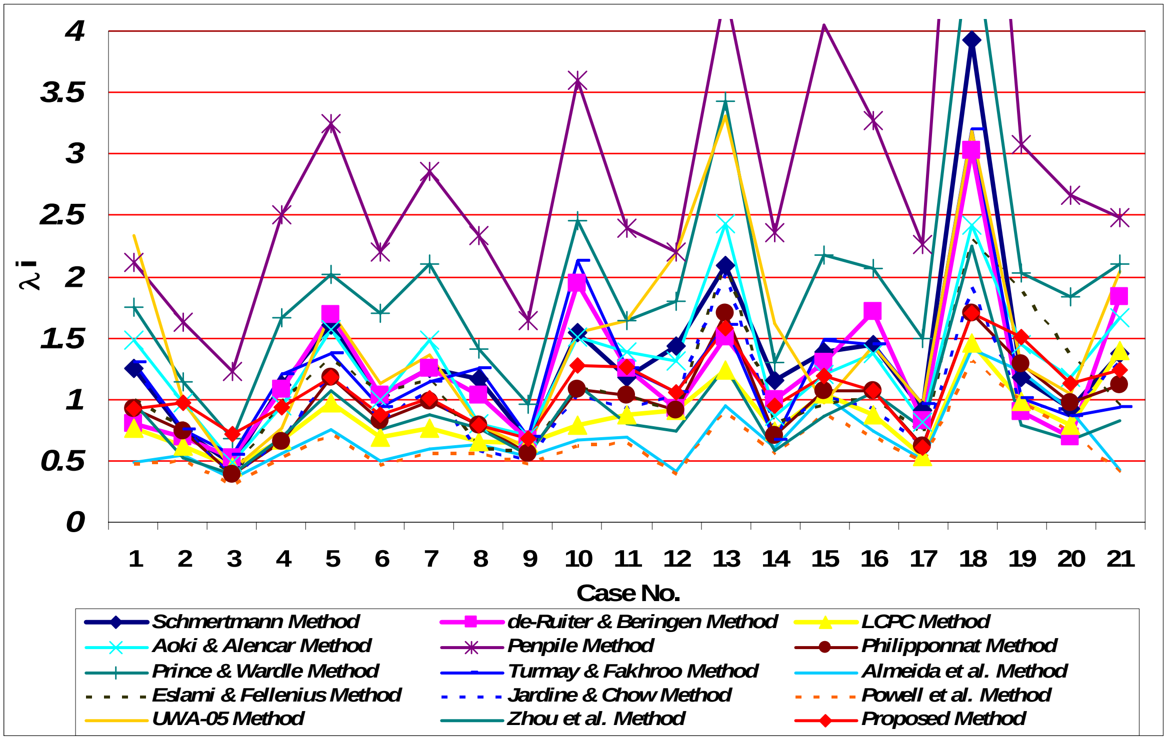

Figure 4-23a. Comparison (ratio of measured/predicted) for 14 methods (Florida soil)

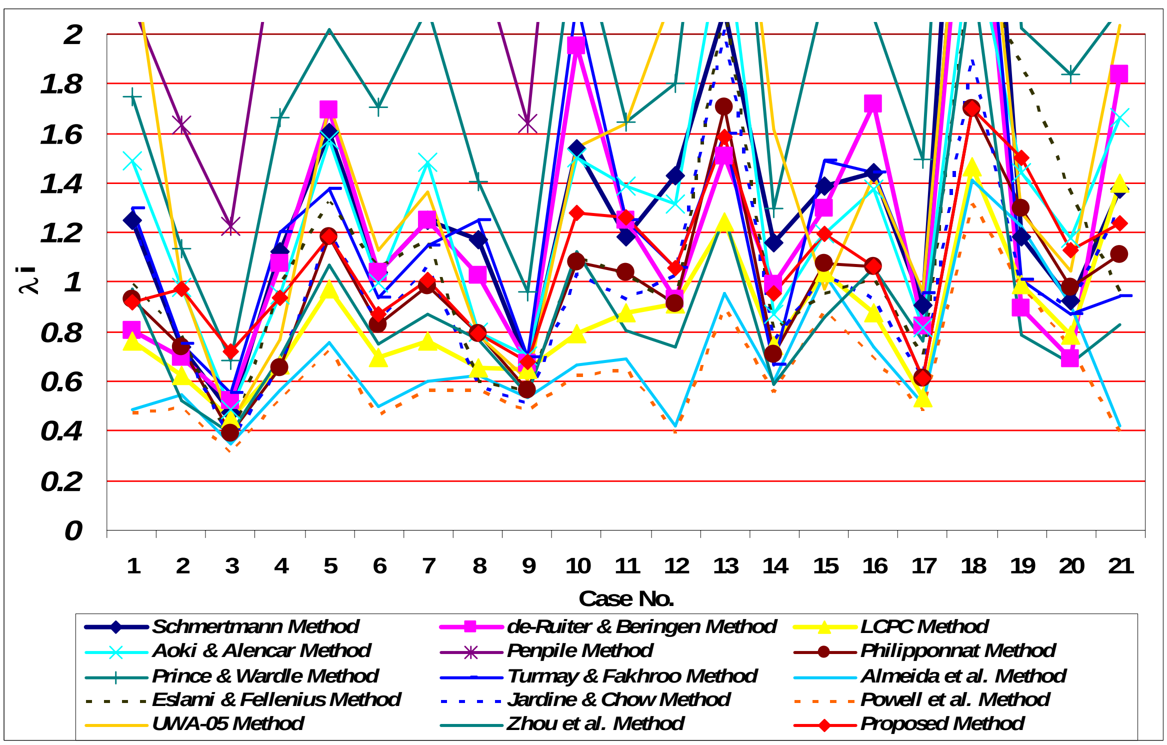

Figure 4-23b. Comparison (ratio of measured/predicted) for 14 methods, (y-scale expanded from Figure 4-23a)

Table 4-4. LRFD resistance factors,Φ, for all CPT based methods
(ultimate skin friction, Florida soil)

Analysis Method	λ_R	COV_R	Φ	Φ/λ_R
Schmertmann Method (1978)	1.619	0.507	0.548	0.339
de Ruiter and Beringen Method (1979)	1.460	0.509	0.492	0.337
Bustamante and Gianeselli(LCPC) (1982)	0.777	0.358	0.382	0.491
Aoki & de Alencar Method (1975)	1.492	0.378	0.697	0.467
Penpile Method (Clisby et al. 1978)	2.737	0.531	0.873	0.319
Philipponnat Method (1980)	0.899	0.361	0.439	0.488
Prince and Wardle Method (1982)	2.285	0.570	0.663	0.290
Tumay and Fakhroo Method (1982)	1.653	0.537	0.520	0.314
Almeida et al. Method (1996)	0.588	0.426	0.243	0.414
Eslami & Fellenius Method (1997)	1.190	0.405	0.520	0.437
Jardine & Chow (MTD) Method (1996)	0.926	0.453	0.358	0.387
Powell et al. Method (2001)	0.582	0.423	0.243	0.418
UWA-05 Method (2005)	1.502	0.585	0.420	0.280
Zhou et al. Method (1982)	1.326	0.537	0.417	0.315
Proposed Method (2006)	**0.975**	**0.292**	**0.565**	**0.580**

Table 4-5. LRFD resistance factors,Φ, for all CPT based methods
(ultimate tip resistance, Florida soil)

Analysis Method	λ_R	COV_R	Φ	Φ/λ_R
Schmertmann Method (1978)	0.755	0.663	0.175	0.233
de Ruiter and Beringen Method (1979)	0.986	1.023	0.106	0.107
Bustamante and Gianeselli(LCPC) (1982)	1.001	0.655	0.238	0.237
Aoki & de Alencar Method (1975)	0.795	0.669	0.182	0.229
Penpile Method (Clisby et al. 1978)	3.172	0.747	0.608	0.192
Philipponnat Method (1980)	0.879	0.714	0.182	0.207
Prince and Wardle Method (1982)	1.090	0.745	0.210	0.193
Tumay and Fakhroo Method (1982)	0.530	0.575	0.152	0.287
Almeida et al. Method (1996)	1.276	1.155	0.106	0.083
Eslami & Fellenius Method (1997)	0.823	1.054	0.083	0.101
Jardine & Chow (MTD) Method (1996)	0.829	0.611	0.218	0.263
Powell et al. Method (2001)	0.826	1.262	0.057	0.069
UWA-05 Method (2005)	1.202	0.708	0.252	0.210
Zhou et al. Method (1982)	0.885	0.567	0.259	0.293
Proposed Method (2006)	**1.141**	**0.504**	**0.390**	**0.341**

Table 4-6. LRFD resistance factors,Φ, for all CPT based methods
(Davisson capacity, Florida soil)

Analysis Method	λ_R	COV_R	Φ	Φ/λ_R
Schmertmann Method (1978)	1.327	0.522	0.433	0.327
de Ruiter and Beringen Method (1979)	1.224	0.474	0.449	0.367
Bustamante and Gianeselli(LCPC) (1982)	0.852	0.309	0.473	0.555
Aoki & de Alencar Method (1975)	1.289	0.385	0.591	0.459
Penpile Method (Clisby et al. 1978)	2.869	0.478	1.045	0.364
Philipponnat Method (1980)	0.969	0.342	0.495	0.511
Prince and Wardle Method (1982)	1.935	0.456	0.744	0.385
Tumay and Fakhroo Method (1982)	1.229	0.471	0.455	0.370
Almeida et al. Method (1996)	0.692	0.396	0.309	0.447
Eslami & Fellenius Method (1997)	1.094	0.446	0.430	0.394
Jardine & Chow (MTD) Method (1996)	0.982	0.415	0.419	0.426
Powell et al. Method (2001)	0.628	0.375	0.295	0.471
UWA-05 Method (2005)	1.492	0.516	0.494	0.331
Zhou et al. Method (1982)	0.873	0.436	0.353	0.404
Proposed Method (2006)	**1.079**	**0.267**	**0.665**	**0.617**

The term (Φ / λ_R) in the above equation identifies the percentage of measured Davisson capacity that is available for design. Obviously, the higher the (Φ / λ_R) term, the better the method. Shown in Tables 4-4, 4-5, and 4-6 are (Φ / λ_R) terms for each method. Clearly, Philipponnat & LCPC are the better methods. Interestingly, both the Philipponnat & LCPC methods use just the CPT tip resistance, q_c, to predict axial pile capacity. Finally, the proposed UF method provides a value of 0.617 for Φ / λ_R, which means that 61.7% of the measured load test capacity can be used for design.

LRFD Resistance Factors, Φ, for Louisiana Soils

Tables 4-7, 4-8, and 4-9 show the ultimate skin friction, ultimate tip resistance, and ultimate pile capacity using the 14 CPT methods with cone data from 28 load test sites in Louisiana. Shown in Figure 4-24 is a plot of the ratio (measured ultimate capacity/predicted ultimate capacity) for each method. Again, methods above one are conservative. Tables 4-10, 4-11, and 4-12 show the LRFD resistance factors for ultimate skin friction, ultimate tip resistance, and ultimate pile capacity.

Shown in Tables 4-10, 4-11, and 4-12 are the (Φ / λ_R) terms for each method. From each table, it is found that the ranking of prediction methods are different from the Florida data. Jardine & Chow (MTD) & Philipponnat Methods are the better methods. However, both the Jardine & Chow (MTD) and Philipponnat Methods use only the CPT tip resistance, q_c, to predict axial pile capacity. The proposed UF method provides a value of 0.673 for Φ / λ_R, which is the second best method, and only slightly less than the MTD method.

In summation, it appears that the proposed UF method works very well for both sands (Florida soil) and clays (Louisiana soil).

Evaluating the Prediction Methods Using the Bootstrap Method

After calculating the λ_i (Measured/Predicted) for each method and performing an LRFD resistance factor analysis, one question remains: how representative is the data to the population? Is there sufficient data to predict the pile capacity with a certain level of confidence? Fortunately, a very powerful tool is available, termed the Bootstrap method.

This method estimates the sampling distribution of an estimator by resampling with replacements from the original sample. For instance, there are total of 21 cases involving Florida soil. We have 21 λs which are original samples from the whole population of λs. We want to know how good the samples' mean and standard deviations are.

Table 4-7. Predicted ultimate skin friction for 14 CPT based methods (Louisiana soil)

Load Test No.	Site Name	Pier (Bent/Slab) No.	Diameter (in)	Length (ft)	Schmertmann	De-Ruiter & Beringen	Bustamante & Gianeselli (LCPC)	Aoki & de Alencar	Penpile	Philipponnat	Prince & Wardle	Turmay & Fakhroo	Almeida et al.	Eslami & Fellenius	Jardine & Chow (MTD)	Powell et al. Method	UWA-05 Method	Zhou et al. Method	Proposed Method	**Ultimate Skin Friction (Load Test)**
1	Houma_ICW_Bridge	TP 1	14	80	181	187	208	87	83	132	111	153	221	192	115	230	55	208	132	**106.4**
2	Houma_ICW_Bridge	TP 2	14	70	99	201	164	47	59	89	66	117	129	110	86	140	29.5	158	89	**43**
3	Houma_ICW_Bridge	TP 3	14	80	140	159	140	68	68	108	84.5	147	174	176	107	182	42	178	108	**116.5**
4	Houma_ICW_Bridge	TP 4	14	81	123	156	138	57	61	93	71	151	136.5	140	83	145	36	175	93	**105**
5	Bayou_Boeuf_Main_Span	TP 2	14	70	89	227	151	45	50	106	53	120	149	141	85	161	36	142	106	**97**
6	Bayou_Boeuf_Main_Span	TP 5	14	80	59	150	105	42	32	72	30	161	96	147	64.5	104	27	109	72	**115**
7	Bayou_Boeuf_West_Approach	TP 1	14	89.5	131	177	119	56	76.5	90	82	131	120	131	85	131	31	206	90	**105**
8	Bayou_Boeuf_West_Approach	TP 3	14	63.5	91	138	115	46	53	80.5	60	107	119	130	72	126	43	145	80.5	**125.5**
9	Bayou_Boeuf_East_Approach	F 1	14	68	88.5	138.5	87.5	47.5	51	69	52	107	92	142	59	100	25	146	69	**90**
10	Bayou_Boeuf_East_Approach	F 2	14	71	91	131	86	40	50	63	50	116	87	122	60	95	24	149	63	**90**
11	Bayou_Boeuf_East_Approach	F 3	14	77.5	99	176.5	113	50	55	87	56	129	117	149.5	76	128	30	164	87	**82**
12	Bayou_Boeuf_East_Approach	F 4	14	79	107.5	248	181	58	59	114	60	125	157	148	94	171	36	171	114	**95**
13	Bayou_Boeuf_East_Approach	F 5	14	79	96	185	113	40	53	81	53	135.5	130	168	75	142	31	161	81	**70**
14	Houma_ICW_Bridge	TP 5	16	71.5	111	127	88	44	62.5	64	64	126	85	106	65	93	23	180	64	**85**
15	Bayou_Boeuf_West_Approach	TP 4	16	70	126	166	140	66	79	102	98	129	140	152	90	149	37	203	102	**80**
16	Bayou_Ramos_Bridge	TP 1	16	78	118	163	136	59	65	101	68	148	165	158	88	175	43	186	101	**98**
17	Bayou_Ramos_Bridge	TP 7	16	77	129	169	126	61	71	103	78	140	136	149	89	146	34	198	98	**107.6**
18	Houma		18	105	187	316	202.5	102	102	173	106	215	248.5	257	146	268	52	294	173	**160**
19	Tickfaw_River_Bridge	TP 1	30	59.3	283	606	412	145	170	286	238	251	387	307.5	280	418	67	396	286	**407**
20	Bayou_Boeuf_West_Approach	TP 2	30	110	429	492	374.5	170	242	278	281	344	437	387	301	473	83	625	278	**285**
21	Bayou_Ramos_Bridge	TP 2	30	88	437	407	523	198	213	398	283	343	617	442	354	635	156	497	398	**365**
22	Bayou_Ramos_Bridge	TP 3	30	104	453	551	466	253	256	490	341	406	778	500	380	805	141	603	490	**353**
23	Bayou_Ramos_Bridge	TP 4	30	99.3	464	542	451	212	213	497	285	411	614	444	393	641	188	523	497	**454**
24	Bayou_Ramos_Bridge	TP 5	30	113	434	557	375	208	217	345	267	404	421	456	365	452	170	584	345	**307**
25	Bayou_Boeuf_East_Approach	F 6	30	110	332	676	487	154	186	213.5	197	378.5	440	519	311	479	73.5	532	313.5	**280**
26	Gibson_Raceland_Highway	TP 1	30	116	319	553	377	169	169	315	175	435	428	455	300	464	93	504	315	**364**
27	Gibson_Raceland_Highway	TP 4	30	124	412	648	447	211	203	400	245.5	505	521	526	358	559	135	573	400	**387**
28	Luling_Bridge		30	112	491	516	408	209	228	420.5	311	500	698	582	362	724	160	582	420.5	**424**

Table 4-8. Predicted ultimate tip resistance for 14 CPT based methods (Louisiana soil)

Load Test No.	Site Name	Pier (Bent/Slab) No.	Diameter (in)	Length (ft)	Schmertmann	De-Ruiter & Beringen	Bustamante & Gianeselli (LCPC)	Aoki & de Alencar	Penpile	Philipponnat	Prince & Wardle	Turmay & Fakhroo	Almeida et al.	Eslami & Fellenius	Jardine & Chow (MTD)	Powell et al. Method	UWA-05 Method	Zhou et al. Method	Proposed Method	**Ultimate Tip Resistance (Load Test)**
1	Houma_ICW_Bridge	TP 1	14	80	14	6	9	8.5	4	7	5	14	3	12	20	5	8	16	15	**32.6**
2	Houma_ICW_Bridge	TP 2	14	70	5	2	5.5	6	4	3.5	4	5	2	3	12	3	3	10	9	**12**
3	Houma_ICW_Bridge	TP 3	14	80	12	5	8	8	3	7	5	12	3	11	21	5	7	15	14	**8**
4	Houma_ICW_Bridge	TP 4	14	81	11	5	7	7	3	6	4	11.5	2	9	16	3	7	14	12	
5	Bayou_Boeuf_Main_Span	TP 2	14	70	24	11	29.5	26	15	19	16	26	16	31	61	25	14	31	21	**19**
6	Bayou_Boeuf_Main_Span	TP 5	14	80	2.5	1	8	5	3	4	3	2.5	1	1	18	2	1.5	9	8	
7	Bayou_Boeuf_West_ Approach	TP 1	14	89.5	9.5	4	6.5	11	2	18	7	16	4	13.5	14	7	6	19	18.5	
8	Bayou_Boeuf_West_ Approach	TP 3	14	63.5	93.5	93.5	62.5	64.5	22	55	39.5	98	40	64	83	64	56	52	45	**39.5**
9	Bayou_Boeuf_East_ Approach	F 1	14	68	15	7	10	9	4	8	6	15	4	13.5	21.5	6	9	17	16	
10	Bayou_Boeuf_East_ Approach	F 2	14	71	12	5	8	8	3	7	5	12	3	10	17	5	7	14.5	13	
11	Bayou_Boeuf_East_ Approach	F 3	14	77.5	12	5	8	7	4	6.5	5	12	3	10	18	4	7	14	13	
12	Bayou_Boeuf_East_ Approach	F 4	14	79	19.5	9	13	12	6	9.5	7	19.5	5.5	17	29	9	12	19	9	
13	Bayou_Boeuf_East_ Approach	F 5	14	79	12	6	9	8	3.6	7	5	12	3	11	19	5	7	15	14	
14	Houma_ICW_Bridge	TP 5	16	71.5	11	5	8	7	3	6	4	11	2	9	17.5	3	7	15	12	
15	Bayou_Boeuf_West_ Approach	TP 4	16	70	17	8	11	12	4	9	7	17	5	15	24	8	10	20	18	
16	Bayou_Ramos_Bridge	TP 1	16	78	48	48	23	47	6.4	28	29	70	25.5	66	30	41	29	40	31	**43**
17	Bayou_Ramos_Bridge	TP 7	16	77	15	7	15	12	5	10	7	15	5	12	35.5	8.6	9	21	10	**8.4**
18	Houma		18	105	24	11	17	17	7	14	10	25	6	21	37	9	15	28	28	**56**
19	Tickfaw_River_Bridge	TP 1	30	59.3	122	55	90	79	38	68.5	48.5	125	43	116	195	69	73	123	61	**77**
20	Bayou_Boeuf_West_ Approach	TP 2	30	110	113	113	123	119	48	88	73	117	67	150.5	101	109	68	146	88	
21	Bayou_Ramos_Bridge	TP 2	30	88	212	212	107	252	15	155	154	212	155	380	95	250	127	168	177	**162**
22	Bayou_Ramos_Bridge	TP 3	30	104	183	183	151	173	56	131	106	187	102	246	113	166	110	199	125	**147**
23	Bayou_Ramos_Bridge	TP 4	30	99.3	78	78	151	315	29	175	193	264.5	176.5	439	141	286	47	268	175	**146**
24	Bayou_Ramos_Bridge	TP 5	30	113	455	455	381	511	163	452	313	729	296	303	359	480	273	378	336	**268**
25	Bayou_Boeuf_East_ Approach	F 6	30	110	97	44	67	60	27	46	97	100	24	90	145	39	58	96	46	
26	Gibson_Raceland_ Highway	TP 1	30	116	252	252	170	322	58	220	197	521	164	162	162.5	265	151	247	193	**275**
27	Gibson_Raceland_ Highway	TP 4	30	124	310	310	302	415	90	310	254	668	217	211.5	260	352	186	359	252	**254**
28	Luling_Bridge		30	112	378.5	378.5	396	641	54	390	392.5	937.5	330	383	347	534	227	396	372	**76**

Table 4-9. Predicted ultimate pile capacity for 14 CPT based methods (Louisiana soil)

Load Test No.	Site Name	Pier (Bent/Slab) No.	Diameter (in)	Length (ft)	Schmertmann	De-Ruiter & Beringen	Bustamante & Gianeselli (LCPC)	Aoki & de Alencar	Penpile	Philipponnat	Prince & Wardle	Turmay & Fakhroo	Almeida et al.	Eslami & Fellenius	Jardine & Chow (MTD)	Powell et al. Method	UWA-05 Method	Zhou et al. Method	Proposed Method	**Ultimate Pile Capacity (Load Test)**
1	Houma_ICW_Bridge	TP 1	14	80	195	194	217	95	87	135	117	167	224	204	134.8	235	63	224	147	**139**
2	Houma_ICW_Bridge	TP 2	14	70	104	203	170	53	62	92	70	122	131	113	98	143	32	168	98	**55**
3	Houma_ICW_Bridge	TP 3	14	80	151.5	164	148	76	71.5	115.5	89	159	177	187	128.5	187	49	193	122	**125**
4	Houma_ICW_Bridge	TP 4	14	81	135	161	145	64	64	99	75	162	139	149	98	148	43	189	105	**105**
5	Bayou_Boeuf_Main_Span	TP 2	14	70	113	237	181	71.5	65.5	125	69	146	164	171	146	186	50	174	127	**116**
6	Bayou_Boeuf_Main_Span	TP 5	14	80	61	151	113.5	47	36	76	33	164	97	148	83	107	28.5	118	80	**115**
7	Bayou_Boeuf_West_Approach	TP 1	14	89.5	140	182	125	67	79	108	88.5	146.5	124	144	99	138	37	224	109	**105**
8	Bayou_Boeuf_West_Approach	TP 3	14	63.5	184	231	178	110	75	136	100	205	159	194	156	191	99	197	126	**165**
9	Bayou_Boeuf_East_Approach	F 1	14	68	103	145	97	57	55	77	58	122	96	155	80	107	33.6	163	85	**90**
10	Bayou_Boeuf_East_Approach	F 2	14	71	103	136	94	48	53	70	55	129	90	133	77	100	31	163	76	**90**
11	Bayou_Boeuf_East_Approach	F 3	14	77.5	111	182	121	57	59	94	60.5	141	120	160	94	132	37	178	100	**82**
12	Bayou_Boeuf_East_Approach	F 4	14	79	127	257	194	70	65	123	68	144	163	165	123	180	48	191	123	**95**
13	Bayou_Boeuf_East_Approach	F 5	14	79	108	190	122	48	56.5	88	58	148	133.5	179	93	147	39	176	95	**70**
14	Houma_ICW_Bridge	TP 5	16	71.5	122	132	95.5	50	66	69.5	68.5	138	87	115	82	96	29	195	76	**85**
15	Bayou_Boeuf_West_Approach	TP 4	16	70	143	174	151	78	83.5	111	105	146.5	145	166.5	113	157	47	223	120	**80**
16	Bayou_Ramos_Bridge	TP 1	16	78	167	211	159	107	72	130	97	218	190	224	118	216	72	227	132	**140**
17	Bayou_Ramos_Bridge	TP 7	16	77	144	175.5	142	73	76	113	85	155	141	161	124.5	154	43	219	108	**116**
18	Houma		18	105	211	327	220	119	109	186	116.5	240	254	278	183	277	66	322	201	**216**
19	Tickfaw_River_Bridge	TP 1	30	59.3	405	660.5	502	224	208	355	287	376	430	424	475	487	140	519	347	**484**
20	Bayou_Boeuf_West_Approach	TP 2	30	110	542	606	497.5	289	290	366	354	461.5	505	538	402	582	151	771	367	**285**
21	Bayou_Ramos_Bridge	TP 2	30	88	649	618	636	449	228	553	437	556	772	822	449	885	283	665	575	**527**
22	Bayou_Ramos_Bridge	TP 3	30	104	636	735	617	426	312	554	447	593	880	746	493	971	251	802	615	**500**
23	Bayou_Ramos_Bridge	TP 4	30	99.3	542	620	602	527	241	672	478	676	790	883	533.5	927	235	791	672	**578**
24	Bayou_Ramos_Bridge	TP 5	30	113	889	1012	756	719	381	796	579.5	1133	717.5	759	724.5	932	443	962	681	**577**
25	Bayou_Boeuf_East_Approach	F 6	30	110	429.5	720	554	214	213	360	234	478	464	609	456	518	132	628	360	**280**
26	Gibson_Raceland_Highway	TP 1	30	116	571	805	547.5	491	227	535	372	955.5	592	617	463	729	245	750	508	**639**
27	Gibson_Raceland_Highway	TP 4	30	124	722	958	749	626	293	710	499	1173	738.5	738	618	911	321	932	652	**641**
28	Luling_Bridge		30	112	870	895	804	850	282	810	704	1438	1027	965	709	1258	387	978	793	**500**

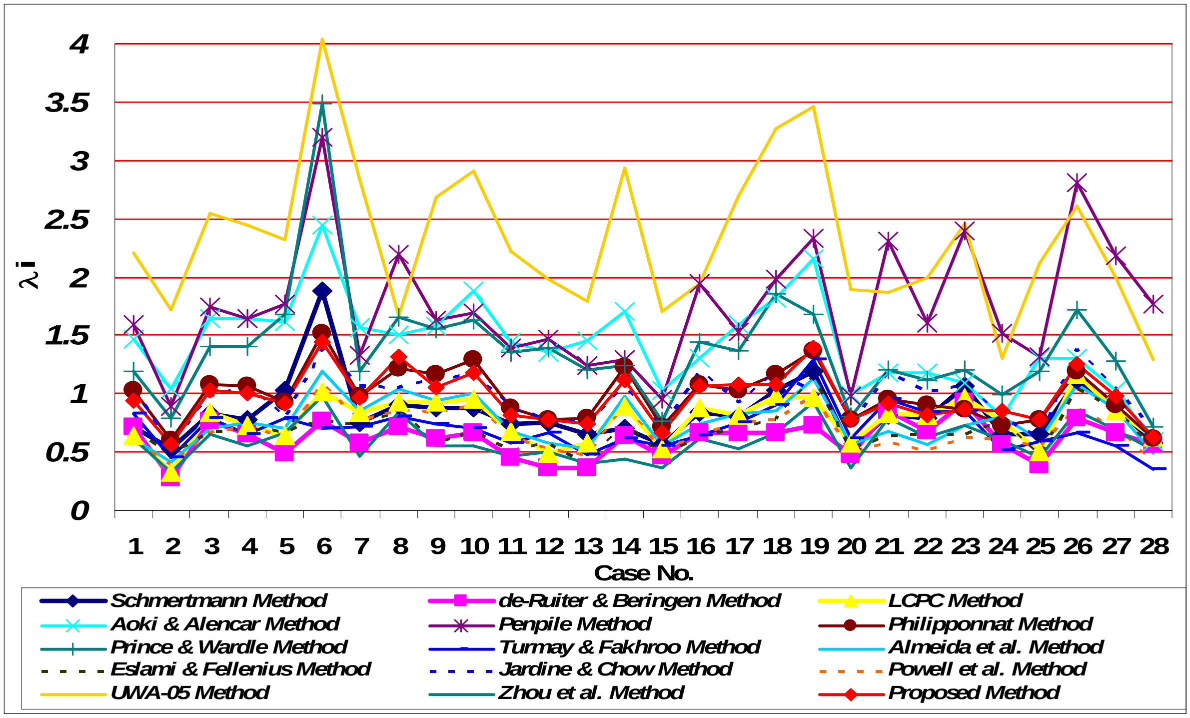

Figure 4-24a. Comparisons (ratio of measured/predicted) for 14 methods (Louisiana soil)

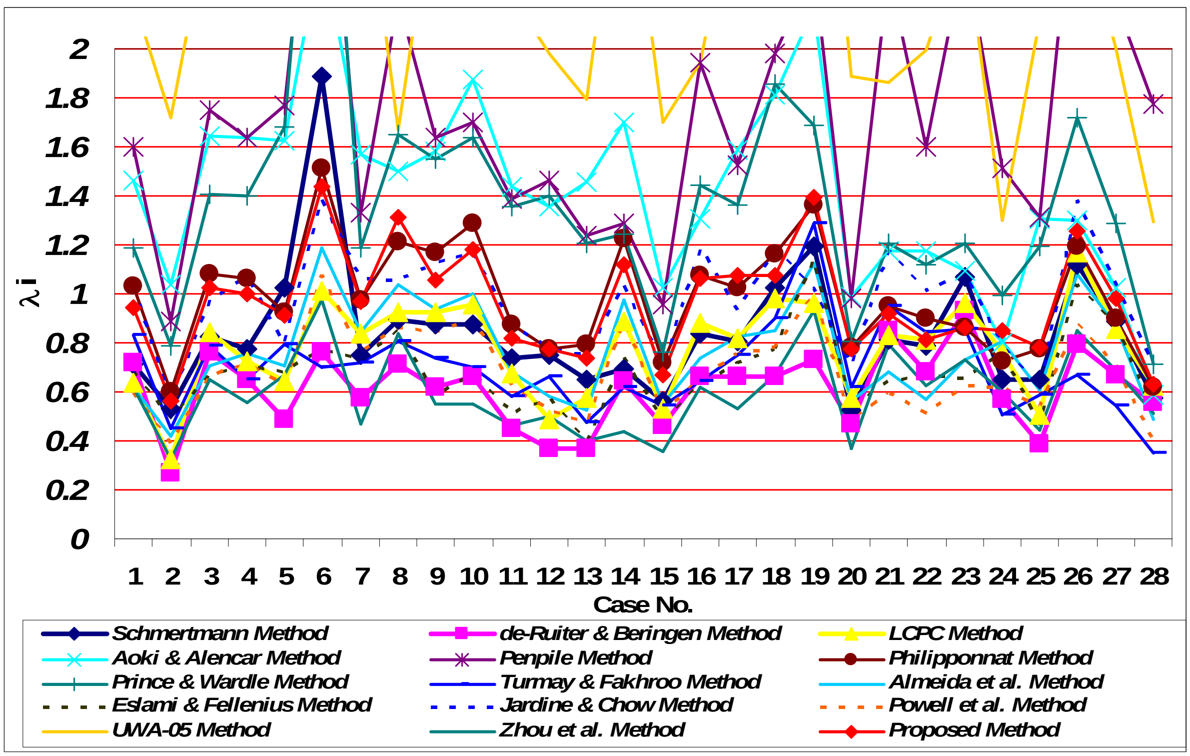

Figure 4-24b. Comparisons (ratio of measured/predicted) for 14 methods, (y-scale expanded from 0 to 2)

Table 4-10. LRFD resistance factors,Φ, for CPT based methods
(ultimate skin friction, Louisiana soil)

Analysis Method	λ_R	COV_R	Φ	Φ/λ_R
Schmertmann Method (1978)	0.910	0.322	0.489	0.537
de Ruiter and Beringen Method (1979)	0.608	0.269	0.373	0.613
Bustamante and Gianeselli(LCPC) (1982)	0.800	0.255	0.507	0.634
Aoki & de Alencar Method (1975)	1.846	0.239	1.218	0.660
Penpile Method (Clisby et al. 1978)	1.690	0.315	0.924	0.547
Philipponnat Method (1980)	1.053	0.248	0.679	0.645
Prince and Wardle Method (1982)	1.504	0.378	0.703	0.467
Tumay and Fakhroo Method (1982)	0.803	0.283	0.476	0.593
Almeida et al. Method (1996)	0.734	0.282	0.436	0.594
Eslami & Fellenius Method (1997)	0.713	0.259	0.448	0.628
Jardine & Chow (MTD) Method (1996)	1.145	0.240	0.752	0.657
Powell et al. Method (2001)	0.684	0.275	0.413	0.604
UWA-05 Method (2005)	2.983	0.306	1.667	0.559
Zhou et al. Method (1982)	0.614	0.290	0.357	0.582
Proposed Method (2006)	**1.040**	**0.248**	**0.670**	**0.644**

Table 4-11. LRFD resistance factors,Φ, for CPT based methods
(ultimate tip resistance, Louisiana soil)

Analysis Method	λ_R	COV_R	Φ	Φ/λ_R
Schmertmann Method (1978)	1.073	0.678	0.241	0.224
de Ruiter and Beringen Method (1979)	1.869	1.000	0.209	0.112
Bustamante and Gianeselli(LCPC) (1982)	1.342	0.728	0.269	0.200
Aoki & de Alencar Method (1975)	1.133	0.910	0.152	0.135
Penpile Method (Clisby et al. 1978)	4.024	0.727	0.807	0.201
Philipponnat Method (1980)	1.519	0.856	0.229	0.151
Prince and Wardle Method (1982)	1.864	0.937	0.237	0.127
Tumay and Fakhroo Method (1982)	0.876	0.844	0.136	0.155
Almeida et al. Method (1996)	2.721	1.163	0.224	0.082
Eslami & Fellenius Method (1997)	1.168	0.913	0.156	0.134
Jardine & Chow (MTD) Method (1996)	0.941	0.590	0.261	0.277
Powell et al. Method (2001)	1.710	1.176	0.137	0.080
UWA-05 Method (2005)	1.794	0.678	0.403	0.225
Zhou et al. Method (1982)	0.889	0.578	0.253	0.285
Proposed Method (2006)	**1.107**	**0.447**	**0.435**	**0.393**

Table 4-12. LRFD resistance factors,Φ, for CPT based methods
(ultimate pile capacity, Louisiana soil)

Analysis Method	λ_R	COV_R	Φ	Φ/λ_R
Schmertmann Method (1978)	0.838	0.320	0.452	0.539
de Ruiter and Beringen Method (1979)	0.613	0.257	0.387	0.631
Bustamante and Gianeselli(LCPC) (1982)	0.776	0.250	0.498	0.641
Aoki & de Alencar Method (1975)	1.417	0.280	0.845	0.596
Penpile Method (Clisby et al. 1978)	1.740	0.312	0.958	0.551
Philipponnat Method (1980)	0.985	0.231	0.663	0.673
Prince and Wardle Method (1982)	1.376	0.372	0.652	0.474
Tumay and Fakhroo Method (1982)	0.698	0.263	0.434	0.622
Almeida et al. Method (1996)	0.766	0.266	0.473	0.618
Eslami & Fellenius Method (1997)	0.676	0.246	0.438	0.648
Jardine & Chow (MTD) Method (1996)	0.971	0.222	0.668	0.687
Powell et al. Method (2001)	0.678	0.260	0.424	0.626
UWA-05 Method (2005)	2.317	0.276	1.396	0.603
Zhou et al. Method (1982)	0.597	0.286	0.351	0.587
Proposed Method (2006)	**0.964**	**0.230**	**0.649**	**0.673**

There are three steps involved in the method. The first is to resample with replacement 21 λs from the original samples, which means picking λ one by one and after each pick it is placed back into the pool for the next pick. Therefore, in this new set of samples, some λ's may appear more than once, and some not at all. The second step is to calculate the mean and standard deviation of the new sample set. The last step is to repeat the first and second steps numerous times (at least 1,000). Finally, one obtains the distribution of the mean and standard deviations of the new sample sets. From these one can determine how representative the samples are to the population.

Figures 4-25, 4-26, and 4-27 show the results of the Bootstrap analysis for the proposed method for Florida soils. It can be seen that the standard deviation of the resampled mean and resample standard deviation are quite small (0.061, 0.042 respectively). Figures 4-28, 4-29, and 4-30 shows the analysis for the proposed method for Louisiana soil. It also shows very small standard deviation (0.042, 0.027) for the resample mean and standard deviation. Therefore, the proposed method does provide a high level of predictive quality.

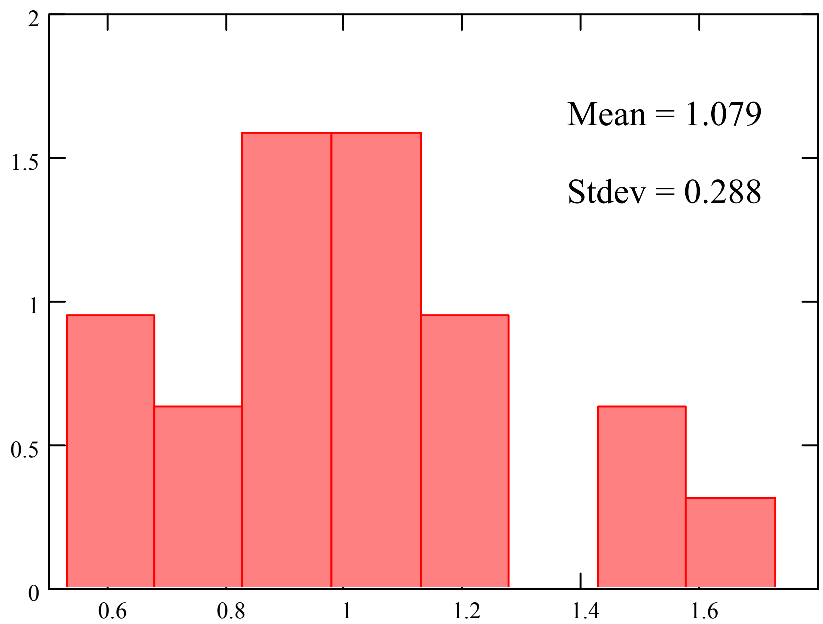

Figure 4-25. Frequency of λ of the Proposed Method for Florida soil

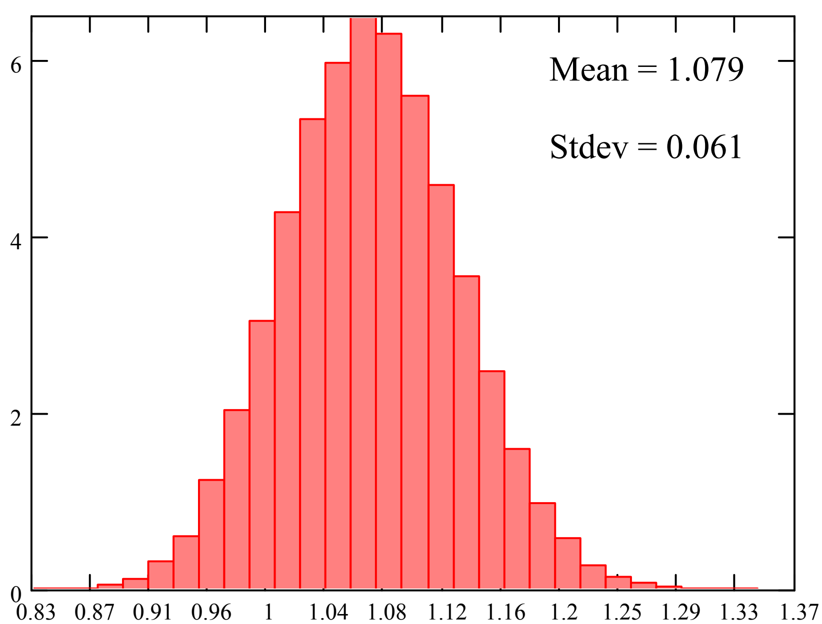

Figure 4-26. Frequency of the sample means using Bootstrap method for Florida soil (100,000 re-sampling runs, Proposed Method)

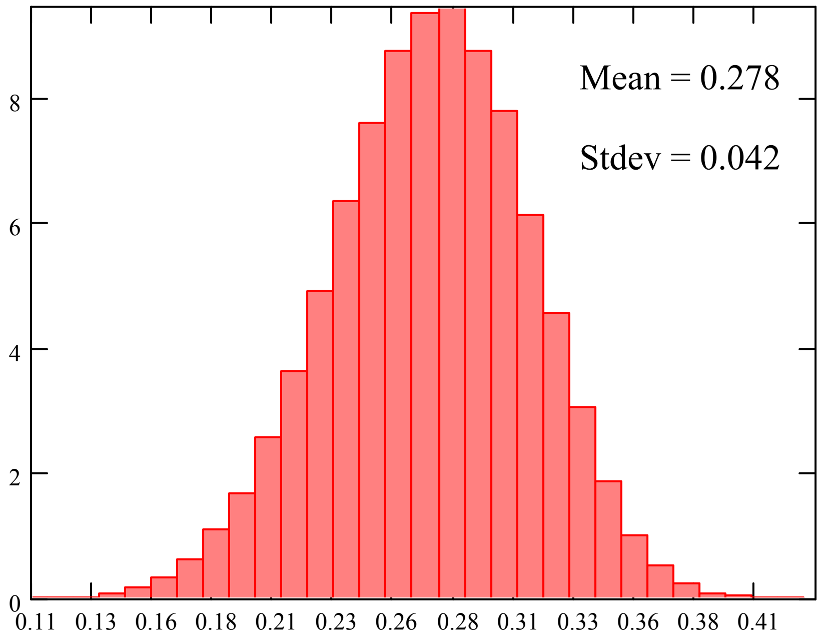

Figure 4-27. Frequency of the sample standard deviations using Bootstrap method for Florida soil (100,000 re-sampling runs, Proposed Method)

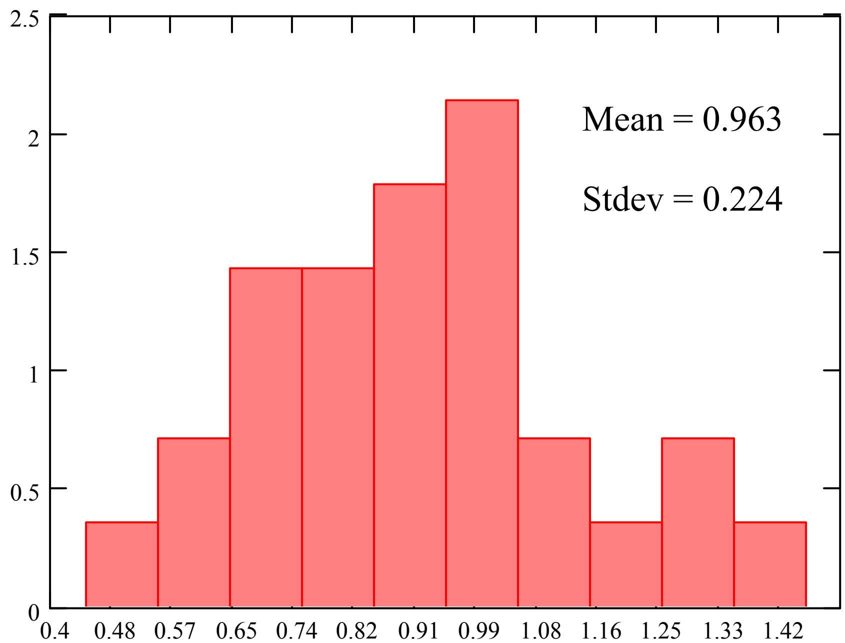

Figure 4-28. Frequency of λ of the proposed method for Louisiana soil

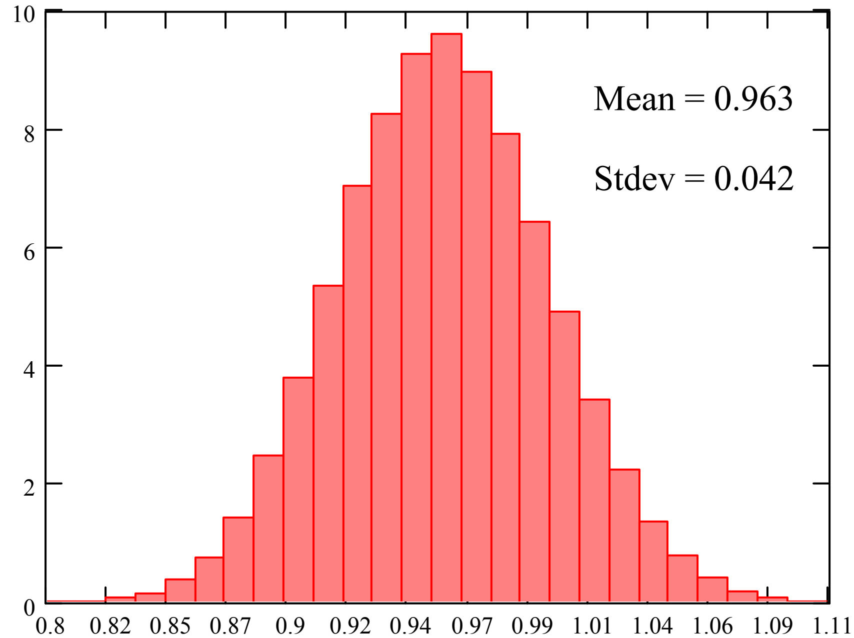

Figure 4-29. Frequency of the sample means using Bootstrap method for Louisiana soil (100,000 re-sampling runs, Proposed Method)

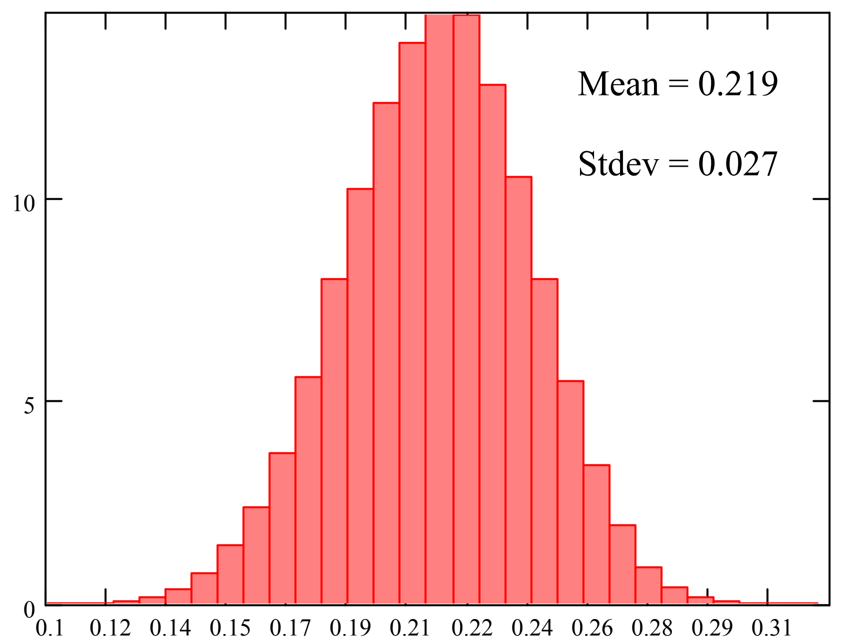

Figure 4-30. Frequency of the sample standard deviations using Bootstrap method for Louisiana soil (100,000 re-sampling runs, Proposed Method)

Figures 4-31, 4-32, and 4-33 show the frequency diagram for the original sample, resampled mean, and resampled standard deviation for Schmertmann's method for Florida soils. As it shows, the standard deviation of resample mean and resample standard deviation are somewhat larger (0.148, 0.243), which means that the sample may not be representative of the population. In other words, in order to perform a more accurate analysis of Schmertmann's method, more data are required.

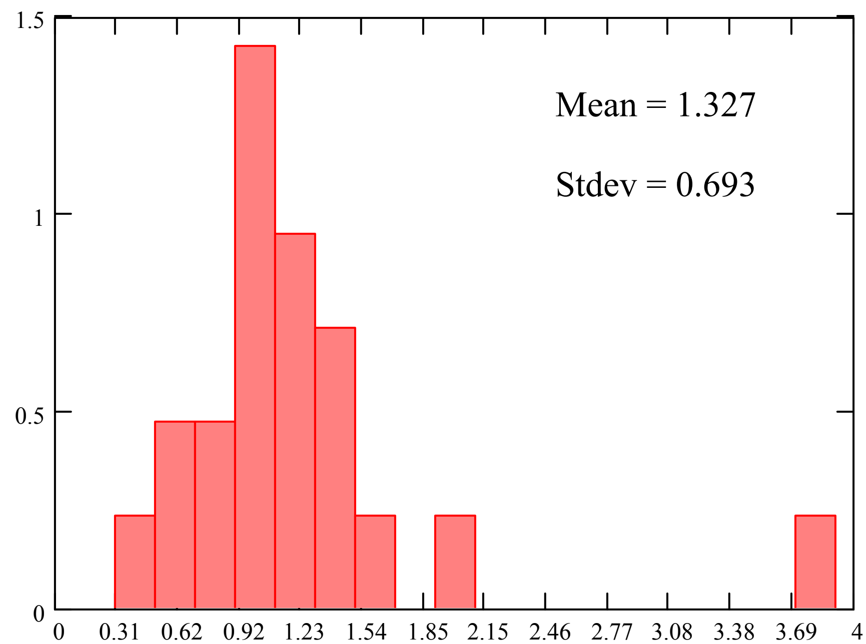

Figure 4-31. Frequency of λs of the Schmertmann's method for Florida soil

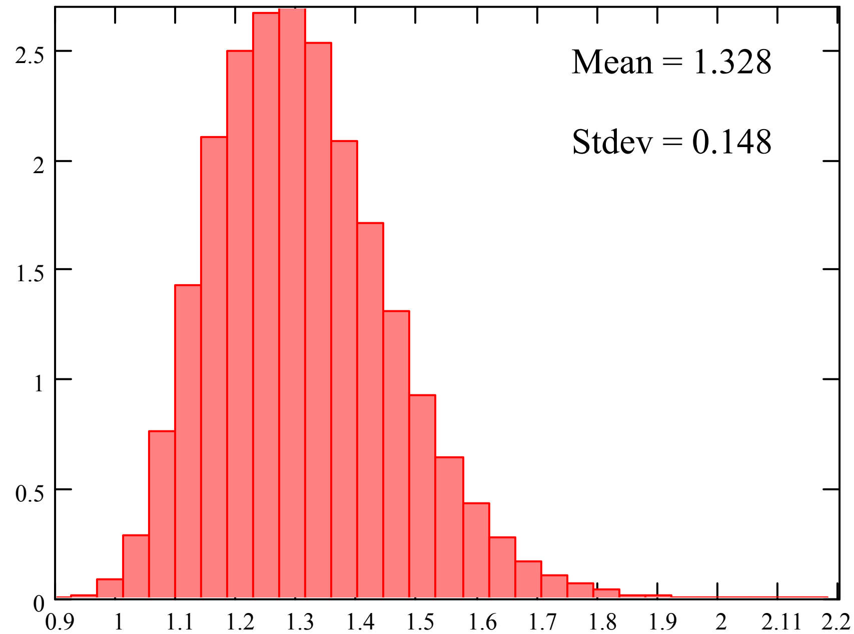

Figure 4-32. Frequency of the sample means of Schmertmann's method using the Bootstrap method for Florida soil (100,000 re-sampling runs)

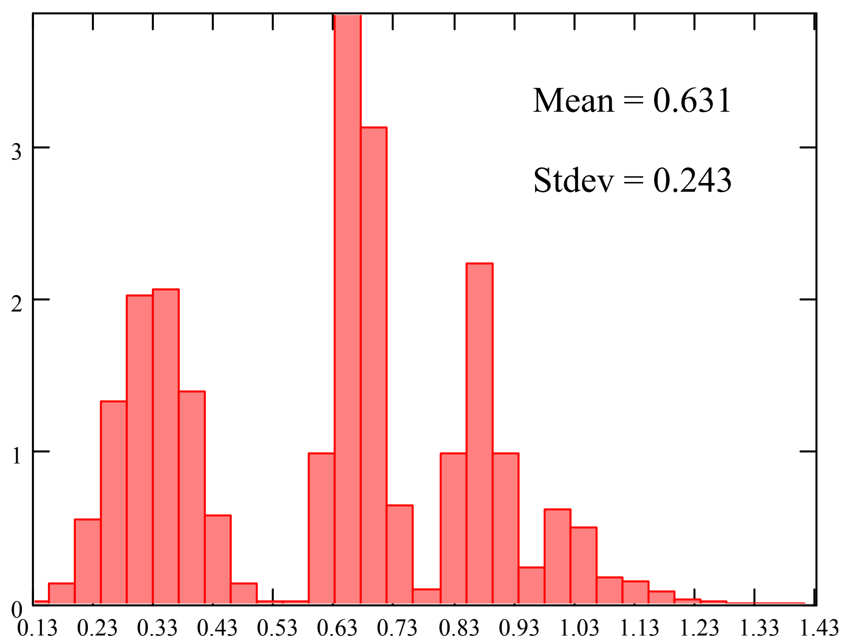

Figure 4-33. Frequency of the sample standard deviations of Schmertmann's method using the Bootstrap method for Florida soil (100,000 re-sampling runs)

Finally, the Bootstrap method was applied to the LCPC method. As can be seen, its mean and standard deviation are very similar, both qualitatively and quantitatively to the Proposed Method. However, when the Coefficient of Variation (CV) is computed, the Proposed Method is the superior one compared to the LCPC formulation. That is to say, dividing the standard deviation by the mean for the three methods (x 100%) yields the following:

Proposed Method: CV = 26.7%   LCPC = 30.9%   Schmertmann = 52.2%

These analyses show that, based on the limited amount of data, the Proposed Method is statistically superior to the other two.

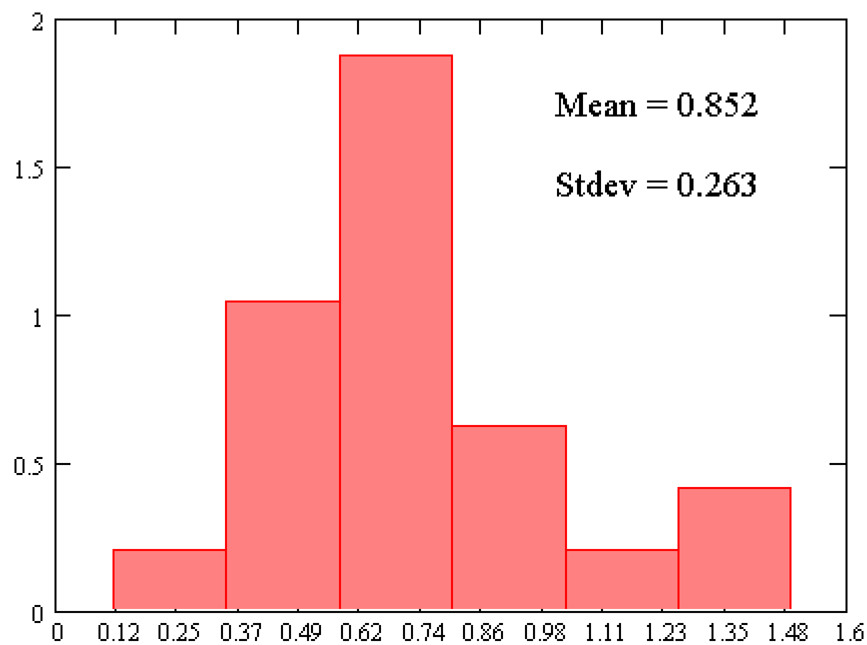

Figure 4-34. Frequency Distribution of the LCPC method's λs for Florida soil

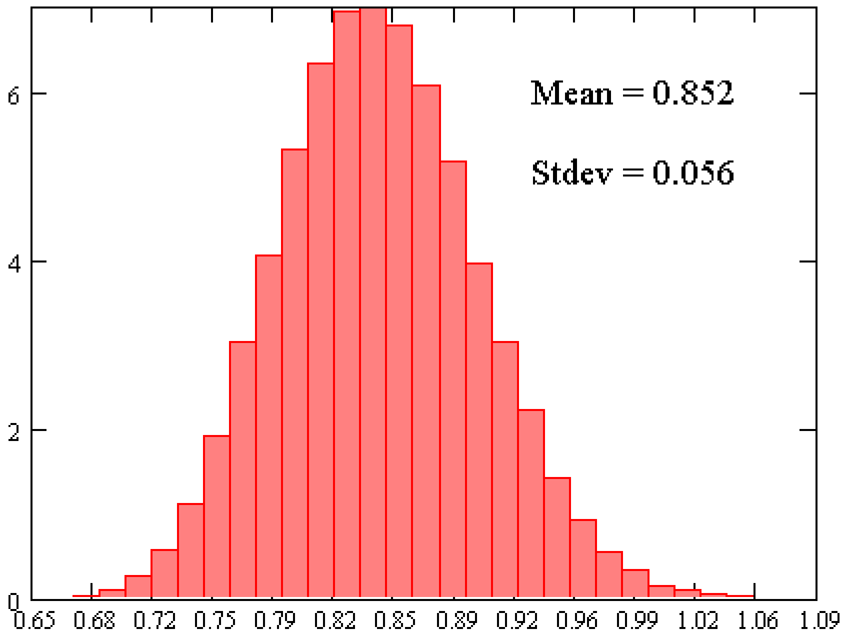

Figure 4-35. Frequency of the sample means using Bootstrap method for Florida soil (100,000 re-sampling runs, LCPC method)

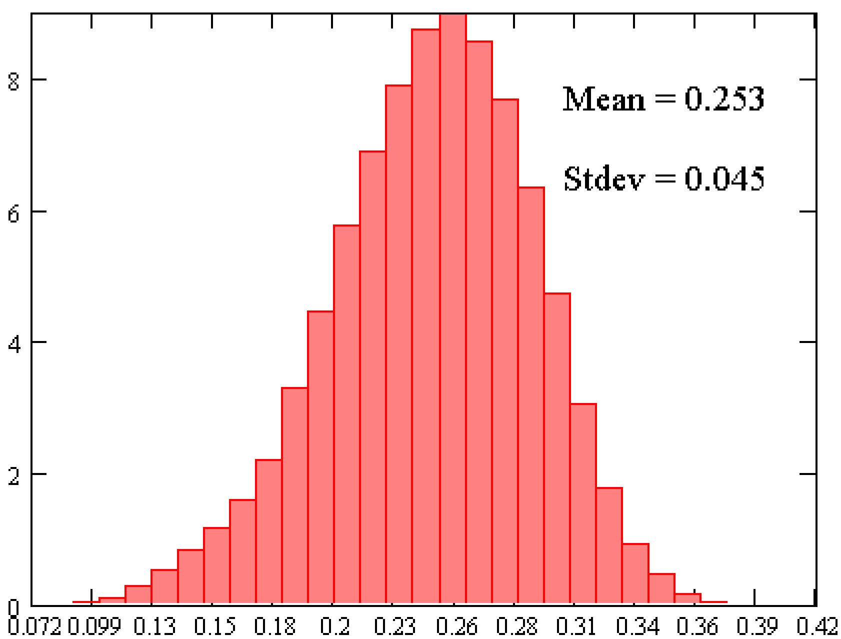

Figure 4-36. Frequency of the sample standard deviations using Bootstrap method for Florida soil (100,000 re-sampling runs, LCPC method)

CHAPTER 5
CONCLUSIONS AND RECOMMENDATIONS

A total of 21 cases (load test data with CPT close to it) in Florida and 28 cases in Louisiana have been used to assess LRFD resistance factors, Φ, for 14 pile axial capacity prediction methods based on CPT results. One of the best methods, the Philipponnat Method, was chosen and modified to form the proposed UF method. Ten field sites were revisited with paired CPT and DTP tests performed. This was an attempt to develop identifiers of cemented sand, which is the one of the most challenging soil types for geotechnical engineers.

Based on the analysis of the test data and resistance factors of each method, the following conclusions can be drawn:

- Current pile axial capacity prediction methods using CPT results overestimate pile capacities in cemented soils. This issue needs to be addressed with additional testing.
- Of the fourteen pile axial capacity prediction methods analyzed, the Philipponnat Method, LCPC Method and MTD Method were shown to have the highest Φ / λ value, indicating more accurate results.
- The proposed UF method has the highest Φ/λ for Florida soil and second highest for Louisiana soil (0.62 for Florida soil and 0.67 for Louisiana soil) among all the methods. In addition, it has the lowest coefficient of variation for Florida soil and second lowest for Louisiana soil (0.27 for Florida soil and 0.23 for Louisiana soil). Therefore, the proposed UF method works very well for both sands (Florida soil) and clays (Louisiana soil).
- The Dual Tip Penetrometer can be a potential tool to identify cemented soil by using the identifier, T2/T1. The following ranges of T2/T1 for different soil types

are shown below, based on limited test data (10 cases) and more data need to be collected to confirm these figures.

≈ 0.5	Non-Cemented Sand (Loose and Medium Dense Sand)
= 0.3~0.5	Lightly Cemented Sand
≈ 1	Strongly Cemented Sand,
= 0.5~1	Silty Sand, Sandy Silt and Silty Clay
< 0.5	Highly Sensitive Clay
> 1	Dense Silty Sand
≥1	Clayey Silt, Silty Clay and Clay

- Using the bootstrap method on the limited field data shows that the standard deviation of the resampled mean and resampled standard deviation are quite small for the proposed method. This means that the proposed method provides a higher predictive quality.

Future Work

Due to the time and budget limitations, there still needs work to confirm the above conclusions. For example:

- More bridge sites should be revisited and tested with both the CPT and DTP. Table 5-1 shows the bridge sites where load test data are available.
- Validate the cemented sand identification values from the DTP (T2/T1), and compare them with SPT & CPT data.
- Evaluate the proposed pile capacity method based on a larger CPT, DTP, and load test database. This will provide confidence in recommending a realistic LRFD resistance factor, Φ, and in turn further the state of geotechnical engineering practice.

Table 5-1. Bridge sites where load test data are available

Cemented Sand Site

Load Test No.	Site Name	Project Number	Pier (Bent/Slab) No.	Station	Pile Embeded Length (ft)	Desired CPT Depth (ft)
1	Cape Canaveral	89-1199.1	T-1	N1533290 E631461	46	53
2			T-6	N1533447 E631541	67	72
3			T-7	N153325 E631568	46.2	53
4			T-14	N1533572 E631617	36	43
5	Marco Island	76-610968-01	TP-2	N/A	33	38
6			TP-10	N/A	63	68
7	Siesta Key Sarasota	N/A	N/A	N/A	16.3	20.3
8	St. John's River(ASCE)	N/A	3A	N/A	36.5	44
9			3B	N/A	46	53
10			3C	N/A	60	65
11	Blount Island Marine Terminal	N/A	B-20	N2909 W6492	64	70
12			B-21	N4080 W6905	46	53
13	West Palm Beach I-95	93220-3473	B-4 (Pier-4)	264+27.23	52.6	59
14			B-9 (Pier-9)	271+25.67	45.8	52
15			C-2 (Pier-2)	1981+87.41	43	49

Non-Cemented Sand Site

Load Test No.	Site Name	Project Number	Pier (Bent/Slab) No.	Station	Pile Embeded Length (ft)	Desired CPT Depth (ft)
1	49th Street Bridge	N/A	TP-1	240+10	41.2	50
2			TP-38	378+29	23.6	32
3	Ballona Creek	N/A	Pile #2	N/A	64	68
4			Pile#3	N/A	49.2	58
5			Pile #4	N/A	23.8	30
6	Beaches of Longboat	N/A	N/A	N/A	47.3	54
7	I-275, 34th Street Pinellas	N/A	N/A	N/A	103.6	114
8	I-295/103rd Street	N/A	Pier 1R	216+14.25	85.7	94
9	I-295/CSX	N/A	Bent 2R	N/A	61.3	70
10	I-295/I10	N/A	Pier 1	494+00	53.4	64
11	I-295/Melvin RD	N/A	Pier 2E	244+05	89.3	100
12	I-295/MEM. PK	N/A	Bent 2W	429+35	80.8	91
13	I-295/Ortega River	N/A	Pier 3R	64+80	80	90
14	Julington Creek	N/A	Bent 32	45+00	61	67
15	NW Conn. OC Retrofit	N/A	Pile #2	N/A	52.3	61

APPENDIX A
MATHCAD PROGRAM

Pile Capacity Prediction Methods

Schmertmann Method (1978)

exchange := 0.164042ft

Ultimate Pile Capacity Based on CPT data Schmertmann Method (1978)

ORIGIN ≡ 1

Input Data:

CPT := C:\..\CPT.xls — DATA input

D := 18in — Diameter or Edge Length of the Pile

L := 48.5ft — Embedment of the Pile

CPT =

	1	2	3	4
1	0	0	0	0
2	0.16	23.09	0.198	0.858
3	0.33	30.21	0.325	1.076
4	0.49	34.84	0.365	1.048
5	0.66	46.72	0.388	0.83
6	0.82	55.85	0.46	0.824
7	0.98	69.86	0.477	0.683
8	1.15	77.52	0.509	0.656
9	1.31	89.36	0.604	0.676
10	1.48	97.08	0.66	0.68
11	1.64	103.23	0.697	0.675
12	1.8	111.71	0.735	0.658
13	1.97	115.18	0.82	0.712
14	2.13	115.03	0.854	0.742
15	2.3	111.57	0.87	0.78
16	2.46	107.59	0.738	0.686

Average q_c over a distance of yD below the pile tip: qc ave_below(CPT,D,L,y)

```
qc_ave_below(CPT,D,L,y) := | n ← ceil(L / exchange)
                           | i ← 0
                           | qc_below_1 ← 0
                           | while CPT_(n+i,1) ≤ (L + y·D)/ft
                           |     | qc_below_1 ← qc_below_1 + CPT_(n+i,2)
                           |     | i ← i + 1
                           | i ← i − 1
                           | counter ← i
                           | qc_below_2 ← 0
                           | qc_below_min ← CPT_(n+i,2)
                           | while i ≥ 0
                           |     | if qc_below_min ≤ CPT_(n+i,2)
                           |     |     | qc_below_2 ← qc_below_2 + qc_below_min
                           |     |     | i ← i − 1
                           |     | otherwise
                           |     |     | qc_below_min ← CPT_(n+i,2)
                           |     |     | qc_below_2 ← qc_below_2 + qc_below_min
                           |     |     | i ← i − 1
                           | qc_ave_below ← (qc_below_1 + qc_below_2) / (2(counter + 1))
                           | return qc_ave_below
```

```
qc1(L) :=  | yy ← 0
           | qc1 ← qc_ave_below(CPT,D,L,0)
           | for  y ∈ 0.7,0.71 .. 4
           |   if  qc1 ≥ qc_ave_below(CPT,D,L,y)
           |       | qc1 ← qc_ave_below(CPT,D,L,y)
           |       | yy ← y
           | return (qc1
           |         yy)
```

$$qc1(L) = \begin{pmatrix} 121.258 \\ 3.75 \end{pmatrix}$$

```
qc2(L) :=  | return "L is too short"   if  L ≤ 8D
           | n ← floor(L / exchange)
           | nn ← ceil(L / exchange)
           | qc1 ←  | yy ← 0
           |        | qc1 ← qc_ave_below(CPT,D,L,0.7)
           |        | for  y ∈ 0.7,0.71 .. 4
           |        |   if  qc1 ≥ qc_ave_below(CPT,D,L,y)
           |        |       | qc1 ← qc_ave_below(CPT,D,L,y)
           |        |       | yy ← y
           |        | yy
           | qc_below_min ←  | i ← 0
           |                 | while  CPT_(nn+i,1) ≤ (L + qc1·D) / ft
           |                 |     | b_(i+1) ← CPT_(nn+i,2)
           |                 |     | i ← i + 1
           |                 | min(b)
           | qc_above_min ← qc_below_min
           | qc_above ← 0
           | i ← 0
           | while  CPT_(n−i,1) ≥ (L − 8·D) / ft
           |    | if  qc_above_min ≤ CPT_(n−i,2)
           |    |     | qc_above ← qc_above + qc_above_min
           |    |     | i ← i + 1
           |    | otherwise
           |    |     | qc_above_min ← CPT_(n−i,2)
           |    |     | qc_above ← qc_above + qc_above_min
           |    |     | i ← i + 1
           | qc_ave_above ← qc_above / i
           | return  qc_ave_above
```

$$qc2(L) = 67.893$$

Calculation of the average cone tip resistance in Schmertmann method:

$qc1(L)_1 = 121.258$

$qc2(L) = 67.893$

$$qt(L) := \text{if}\left(\frac{qc1(L)_1 + qc2(L)}{2} \le 150, \frac{qc1(L)_1 + qc2(L)}{2}, 150\right)\cdot\frac{ton}{ft^2} \qquad qt(L) = 94.575\,\frac{ton}{ft^2}$$

Tip resistance:

$A := D^2 \qquad A = 2.25\,ft^2$

$Qt(L) := A\cdot qt(L) \qquad Qt(L) = 212.795\,ton$

Side Friction(Schmertmann method):

Calculate αc for Concrete & Timber Piles:

$$n := \text{ceil}\left(\frac{L}{exchange}\right) \qquad n = 296$$

$$\alpha_C(f_s) := 0.2049\cdot(f_s\cdot 0.9765)^5 - 1.1778\cdot(f_s\cdot 0.9765)^4 + 2.2795\cdot(f_s\cdot 0.9765)^3 - 1.3222\cdot(f_s\cdot 0.9765)^2 - 0.7543\cdot(f_s\cdot 0.9765) + 1.25$$

$\alpha_C(0.35) = 0.914$

Calculate αs for concrete pile:

$$\alpha_S(L) := \text{if}\left[\frac{L}{D} < 25, -9\cdot 10^{-5}\cdot\left(\frac{L}{D}\right)^3 + 0.0062\cdot\left(\frac{L}{D}\right)^2 - 0.151\cdot\frac{L}{D} + 2.132, 0.83\right]$$

$\alpha_S(L) = 0.83$

Calculate Ultimate Side Friction: Qs

```
Qs(L1,L2,SoilType) := | n ← ceil(L1/exchange)
                      | Qs ← 0·ton
                      | As ← 4·D·exchange
                      | i ← 0
                      | while L1 + i·exchange ≤ L2
                      |   | if SoilType = 2
                      |   |   | y ← CPT[n+i,1]·ft
                      |   |   | f ← if(y ≤ 8·D, αS(L)·(y/(8·D))·CPT[n+i,3], αS(L)·CPT[n+i,3])·ton/ft^2
                      |   |   | f ← if(f ≤ 1.2·ton/ft^2, f, 1.2·ton/ft^2)
                      |   |   | Qs ← Qs + f·As
                      |   |   | i ← i + 1
                      |   | otherwise
                      |   |   | f ← if(αC(CPT[n+i,3])·CPT[n+i,3] ≤ 1.2, αC(CPT[n+i,3])·CPT[n+i,3], 1.2)·ton/ft^2
                      |   |   | Qs ← Qs + f·As
                      |   |   | i ← i + 1
                      | return Qs
```

SoilType: 1 for cohessive soil, 2 for cohesionless soil

$L1 := 4ft$ $L2 := 5.8ft$ $L3 := 27.9ft$ $L4 := 36.5ft$ $L5 := L$

Layer1 :

$SoilType := 2$

$Q_{s1} := Q_s(0.01ft, L1, SoilType)$ $Q_{s1} = 2.177\,ton$

Layer2 :

$SoilType := 1$

$Q_{s2} := Q_s(L1, L2, SoilType)$ $Q_{s2} = 5.633\,ton$

Layer3 :

$SoilType := 2$

$Q_{s3} := Q_s(L2, L3, SoilType)$ $Q_{s3} = 43.393\,ton$

Layer4 :

$SoilType := 1$

$Q_{s4} := Q_s(L3, L4, SoilType)$ $Q_{s4} = 6.687\,ton$

Layer5 :

$SoilType := 2$

$Q_{s5} := Q_s(L4, L5, SoilType)$ $Q_{s5} = 25.765\,ton$

$Qs := Q_{s1} + Q_{s2} + Q_{s3} + Q_{s4} + Q_{s5}$ $Qs = 83.655\,ton$

$Q_{Davisson} := Qs + \frac{Qt(L)}{3}$ $Q_{Davisson} = 154.587\,ton$

De Ruiter and Beringen Method (1979)

exchange := 0.164042ft

Ultimate Pile Capacity Based on CPT data de Ruiter and Beringen Method (1979)

ORIGIN ≡ 1

Input Data:

CPT := C:\..\CPT.xls

DATA input

D := 18in

Diameter or Edge Length of the Pile

L := 48.5ft

Length of the Pile

Average q_c over a distance of yD below the pile tip: qc ave_below(CPT,D,L,y)

CPT =

	1	2	3	4
1	0	0	0	0
2	0.16	23.09	0.198	0.858
3	0.33	30.21	0.325	1.076
4	0.49	34.84	0.365	1.048
5	0.66	46.72	0.388	0.83
6	0.82	55.85	0.46	0.824
7	0.98	69.86	0.477	0.683
8	1.15	77.52	0.509	0.656
9	1.31	89.36	0.604	0.676
10	1.48	97.08	0.66	0.68
11	1.64	103.23	0.697	0.675
12	1.8	111.71	0.735	0.658
13	1.97	115.18	0.82	0.712
14	2.13	115.03	0.854	0.742
15	2.3	111.57	0.87	0.78
16	2.46	107.59	0.738	0.686

```
qc_ave_below(CPT,D,L,y) :=  | n ← ceil( L / exchange )
                            | i ← 0
                            | qc_below_1 ← 0
                            | while  CPT_{n+i,1} ≤ (L + y·D) / ft
                            |     | qc_below_1 ← qc_below_1 + CPT_{n+i,2}
                            |     | i ← i + 1
                            | i ← i − 1
                            | counter ← i
                            | qc_below_2 ← 0
                            | qc_below_min ← CPT_{n+i,2}
                            | while  i ≥ 0
                            |     | if  qc_below_min ≤ CPT_{n+i,2}
                            |     |     | qc_below_2 ← qc_below_2 + qc_below_min
                            |     |     | i ← i − 1
                            |     | otherwise
                            |     |     | qc_below_min ← CPT_{n+i,2}
                            |     |     | qc_below_2 ← qc_below_2 + qc_below_min
                            |     |     | i ← i − 1
                            | qc_ave_below ← (qc_below_1 + qc_below_2) / (2(counter + 1))
                            | return  qc_ave_below


qc1(L) :=  | yy ← 0.7
           | qc1 ← qc_ave_below(CPT,D,L,0.7)
           | for  y ∈ 0.7,0.71 .. 4
           |   if  qc1 ≥ qc_ave_below(CPT,D,L,y)
           |       | qc1 ← qc_ave_below(CPT,D,L,y)
           |       | yy ← y
           | return ( qc1 )
           |        ( yy  )
```

```
qc2(L) := | return "L is too short"   if  L ≤ 8D
          | n ← floor(L / exchange)
          | nn ← ceil(L / exchange)
          | qc1 ← | yy ← 0.7
          |       | qc1 ← qc_ave_below(CPT,D,L,0.7)
          |       | for  y ∈ 0.7,0.71 .. 4
          |       |   if  qc1 ≥ qc_ave_below(CPT,D,L,y)
          |       |       | qc1 ← qc_ave_below(CPT,D,L,y)
          |       |       | yy ← y
          |       | yy
          | qc_below_min ← | i ← 0
          |                | while  CPT_(nn+i,1) ≤ (L + qc1·D) / ft
          |                |     | b_(i+1) ← CPT_(nn+i,2)
          |                |     | i ← i + 1
          |                | min(b)
          | qc_above_min ← qc_below_min
          | qc_above ← 0
          | i ← 0
          | while  CPT_(n−i,1) ≥ (L − 8·D) / ft
          |     | if  qc_above_min ≤ CPT_(n−i,2)
          |     |     | qc_above ← qc_above + qc_above_min
          |     |     | i ← i + 1
          |     | otherwise
          |     |     | qc_above_min ← CPT_(n−i,2)
          |     |     | qc_above ← qc_above + qc_above_min
          |     |     | i ← i + 1
          | qc_ave_above ← qc_above / i
          | return  qc_ave_above
```

$qc2(L) = 67.893$

Calculation of the average cone tip resistance in Schmertmann method:

$qc1(L)_1 = 121.258$

$qc2(L) = 67.893$

$SoilType := 2$ 1 for clay and 2 for sand

$N_c := 9$

$N_k := 20$

$$qt(L) := if\left(SoilType = 1, \frac{N_c}{N_k} \cdot \frac{qc1(L)_1 + qc2(L)}{2}, \frac{qc1(L)_1 + qc2(L)}{2}\right)$$

$$qt(L) := if(qt(L) \le 150, qt(L), 150) \cdot \frac{ton}{ft^2} \qquad qt(L) = 94.575 \frac{1}{ft^2} ton$$

Tip resistance:

$A := D^2 \qquad A = 2.25 ft^2$

$Qt(L) := A \cdot qt(L) \qquad Qt(L) = 212.795\, ton$

Side Friction(de Ruiter and Beringen method):

Calculate Ultimate Side Friction: Qs

$PileType := 1$ 1 for compression pile, 2 for tension pile

$$Q_s(L1, L2, SoilType, beta) := \left| \begin{array}{l} n \leftarrow ceil\left(\frac{L1}{exchange}\right) \\ m \leftarrow floor\left(\frac{L2}{exchange}\right) \\ A_s \leftarrow 4 \cdot D \cdot (L2 - L1) \\ q_{csum} \leftarrow 0 \\ \text{for } j \in n..m \\ \quad q_{csum} \leftarrow q_{csum} + CPT_{j,2} \\ q_{cside} \leftarrow \frac{q_{csum}}{m - n + 1} \\ f_s \leftarrow if\left(\frac{beta}{N_k} \cdot q_{cside} \le 1.2, \frac{beta}{N_k} \cdot q_{cside}, 1.2\right) \text{ if } SoilType = 1 \\ \text{otherwise} \\ \quad \left| \begin{array}{l} f_{smin} \leftarrow mean(submatrix(CPT, n, m, 3, 3)) \\ f_s \leftarrow min\left(f_{smin}, 1.2, if\left(PileType = 1, \frac{q_{cside}}{300}, \frac{q_{cside}}{400}\right)\right) \end{array} \right. \\ Q_s \leftarrow f_s \cdot A_s \cdot \frac{ton}{ft^2} \\ \text{return } Q_s \end{array} \right.$$

SoilType: 1 for cohessive soil, 2 for cohesionless soil

$L1 := 4ft$ $L2 := 5.8ft$ $L3 := 27.9ft$ $L4 := 36.5ft$ $L5 := L$

Layer1 : $SoilType := 2$

$Q_s(0.01ft, L1, SoilType, 1) = 5.732\,ton$ $Q_{s1} := Q_s(0.01ft, L1, SoilType, 1)$

Layer2 : $SoilType := 1$

$Q_s(L1, L2, SoilType, 1) = 12.96\,ton$ $Q_{s2} := Q_s(L1, L2, SoilType, 1)$

Layer3 : $SoilType := 2$

$Q_s(L2, L3, SoilType, 1) = 30.996\,ton$ $Q_{s3} := Q_s(L2, L3, SoilType, 1)$

Layer4 : $SoilType := 1$

$Q_s(L3, L4, SoilType, 1) = 13.841\,ton$ $Q_{s4} := Q_s(L3, L4, SoilType, 1)$

Layer5 : $SoilType := 2$

$Q_s(L4, L5, SoilType, 1) = 20.062\,ton$ $Q_{s5} := Q_s(L4, L5, SoilType, 1)$

$Qs := Q_{s1} + Q_{s2} + Q_{s3} + Q_{s4} + Q_{s5}$ $Qs = 83.591\,ton$

$Q_{Davisson} := Qs + \frac{Qt(L)}{3}$ $Q_{Davisson} = 154.523\,ton$

Penpile Method (1980)

exchange := 0.164042ft

Ultimate Pile Capacity Based on CPT data Penpile Method (Clisby et al. 1978)

ORIGIN ≡ 1

Input Data:

CPT := C:\..\CPT.xls	DATA input
D := 18in	Diameter or Edge Length of the Pile
L := 48.5ft	Length of the Pile

Calculation of the average cone tip resistance using Penpile Method (Clisby et al. 1978):

the average of the three tip resistance close to the tip

$$qc_{ave\_tip}(D,L) := \left| \begin{array}{l} n \leftarrow \text{ceil}\left(\frac{L}{\text{exchange}}\right) \\ qc_{ave} \leftarrow \frac{CPT_{n-1,2} + CPT_{n,2} + CPT_{n+1,2}}{3} \quad \text{if } n - \frac{L}{\text{exchange}} \le 0.5 \\ qc_{ave} \leftarrow \frac{CPT_{n-2,2} + CPT_{n-1,2} + CPT_{n,2}}{3} \quad \text{otherwise} \\ \text{return } qc_{ave} \end{array} \right.$$

$qc_{ave\_tip}(D,L) = 143.153$

SoilType := 2 1 for clay, 2 for sand

$k_b := \text{if}(\text{SoilType} = 1, 0.25, 0.125)$

$$qt(L) := qc_{ave\_tip}(D,L) \cdot k_b \cdot \frac{\text{ton}}{\text{ft}^2}$$

Tip resistance:

$A := D^2 \qquad A = 2.25\,\text{ft}^2$

$Qt(L) := A \cdot qt(L) \qquad Qt(L) = 40.262\,\text{ton}$

Side Friction Penpile Method (Clisby et al. 1978):

$L1 := 0.1\text{ft}$ Input the soil layer

$L2 := 36\text{ft}$

$$fs_{ave\_side}(L1, L2) := \left| \begin{array}{l} n \leftarrow \text{ceil}\left(\frac{L1}{\text{exchange}}\right) \\ i \leftarrow 0 \\ k \leftarrow 0 \\ fs \leftarrow 0 \\ \text{while } CPT_{n+i,1} \le \frac{L2}{\text{ft}} \\ \quad \left| \begin{array}{l} fs \leftarrow fs + CPT_{n+i,3} \\ i \leftarrow i + 1 \end{array} \right. \\ fs_{ave} \leftarrow \frac{fs}{i} \\ \text{return } fs_{ave} \end{array} \right.$$

$fs_{ave\_side}(L1, L2) = 0.406$

$$f(L1,L2) := \frac{\dfrac{fs_{ave\_side}(L1,L2)}{0.072}}{1.5 + 0.1 \cdot \dfrac{fs_{ave\_side}(L1,L2)}{0.072}} \cdot 0.072 \cdot \frac{ton}{ft^2} \qquad f(L1,L2) = 0.197\,\frac{ton}{ft^2}$$

Calculate Ultimate Side Friction: Qs

$$Q_s(L1,L2) := f(L1,L2) \cdot 4 \cdot D \cdot (L2 - L1)$$

$$Q_s(L1,L2) = 42.402\,ton$$

$L1 := 4ft$ $\quad$ $L2 := 5.8ft$ $\quad$ $L3 := 27.9ft$ $\quad$ $L4 := 36.5ft$ $\quad$ $L5 := L$

Layer1 :

$Q_{s1} := Q_s(0.01ft, L1)$ $\qquad$ $Q_{s1} = 5.976\,ton$

Layer2 :

$Q_{s2} := Q_s(L1, L2)$ $\qquad$ $Q_{s2} = 3.857\,ton$

Layer3 :

$Q_{s3} := Q_s(L2, L3)$ $\qquad$ $Q_{s3} = 26.877\,ton$

Layer4 :

$Q_{s4} := Q_s(L3, L4)$ $\qquad$ $Q_{s4} = 3.695\,ton$

Layer5 :

$Q_{s5} := Q_s(L4, L5)$ $\qquad$ $Q_{s5} = 14.669\,ton$

$Qs := Q_{s1} + Q_{s2} + Q_{s3} + Q_{s4} + Q_{s5}$ $\qquad$ $Qs = 55.074\,ton$

$$Q_{Davisson} := Qs + \frac{Qt(L)}{3} \qquad Q_{Davisson} = 68.495\,ton$$

Prince and Wardle Method (1982)

$exchange := 0.164042ft$

Ultimate Pile Capacity Based on CPT data Prince and Wardle (1982)

$ORIGIN \equiv 1$ For Clayey Soil Only

Input Data:

CPT := C:\..\CPT.xls DATA input

$D := 18in$ Diameter or Edge Length of the Pile

$L := 48.5ft$ Length of the Pile

Calculation of the average cone tip resistance using Prince and Wardle (1982):

$$qc_{ave\_side}(L1, L2) := \left| \begin{array}{l} n \leftarrow \mathrm{ceil}\left(\frac{L1}{exchange}\right) \\ i \leftarrow 0 \\ k \leftarrow 0 \\ qc \leftarrow 0 \\ \text{while } CPT_{n+i,1} \le \frac{L2}{ft} \\ \quad \left| \begin{array}{l} qc \leftarrow qc + CPT_{n+i,2} \\ i \leftarrow i + 1 \end{array} \right. \\ qc_{ave} \leftarrow \frac{qc}{i} \\ \text{return } qc_{ave} \end{array} \right.$$

$$qc_{ave\_tip}(D, L) := \frac{qc_{ave\_side}(L - 8D, L) + qc_{ave\_side}(L, L + 4D)}{2}$$ Influnce zone is 8D above and 4D below the pile tip

$qc_{ave\_tip}(D, L) = 112.721$

$k_b := 0.35$ 0.35 for driven pile 0.3 for jacked pile

$qt(L) := \mathrm{if}\left(qc_{ave\_tip}(D, L) \cdot k_b \le 150, qc_{ave\_tip}(D, L) \cdot k_b, 150\right) \cdot \frac{ton}{ft^2}$ $qt(L) = 39.452 \frac{1}{ft^2} ton$

Tip resistance:

$A := D^2$ $A = 2.25 ft^2$

$Qt(L) := A \cdot qt(L)$ $Qt(L) = 88.768 ton$

Side Friction(Prince and Wardle (1982)):

$L1 := 3.8ft$ Input the soil layer

$L2 := 11.2ft$

$$fs_{ave\_side}(L1, L2) := \left| \begin{array}{l} n \leftarrow \text{ceil}\left(\dfrac{L1}{exchange}\right) \\ i \leftarrow 0 \\ k \leftarrow 0 \\ fs \leftarrow 0 \\ \text{while } CPT_{n+i,1} \le \dfrac{L2}{ft} \\ \quad \left| \begin{array}{l} fs \leftarrow fs + CPT_{n+i,3} \\ i \leftarrow i + 1 \end{array} \right. \\ fs_{ave} \leftarrow \dfrac{fs}{i} \\ \text{return } fs_{ave} \end{array} \right.$$

$fs_{ave\_side}(L1, L2) = 0.578$

Calculate Ultimate Side Friction: Qs

$k_s := 0.53$ k_s=0.53 for driven piles, 0.62 for jacked piles, and 0.49 for bored piles

$f_s(L1, L2, k_s) := \text{if}\left(fs_{ave\_side}(L1, L2) \cdot k_s \le 1.2, fs_{ave\_side}(L1, L2) \cdot k_s, 1.2\right) \cdot \dfrac{ton}{ft^2}$ $f_s(L1, L2, k_s) = 0.306 \dfrac{ton}{ft^2}$

$Q_s(L1, L2, k_s) := f_s(L1, L2, k_s) \cdot 4 \cdot D \cdot (L2 - L1)$

$Q_s(L1, L2, k_s) = 13.592\,ton$

$L1 := 4ft$ $L2 := 5.8ft$ $L3 := 27.9ft$ $L4 := 36.5ft$ $L5 := L$

Layer1 : $Q_s(0.01ft, L1, k_s) = 7.272\,ton$ $Q_{s1} := Q_s(0.01ft, L1, k_s)$

Layer2 : $Q_s(L1, L2, k_s) = 6.085\,ton$ $Q_{s2} := Q_s(L1, L2, k_s)$

Layer3 : $Q_s(L2, L3, k_s) = 29.74\,ton$ $Q_{s3} := Q_s(L2, L3, k_s)$

Layer4 : $Q_s(L3, L4, k_s) = 3.262\,ton$ $Q_{s4} := Q_s(L3, L4, k_s)$

Layer5 : $Q_s(L4, L5, k_s) = 16.264\,ton$ $Q_{s5} := Q_s(L4, L5, k_s)$

$Qs := Q_{s1} + Q_{s2} + Q_{s3} + Q_{s4} + Q_{s5}$ $Qs = 62.622\,ton$

$Q_{Davisson} := Qs + \dfrac{Qt(L)}{3}$ $Q_{Davisson} = 92.212\,ton$

Tumay and Fakhroo Method (1982)

$exchange := 0.164042ft$

Ultimate Pile Capacity Based on CPT data Tumay and Fakhroo Method (1982)

For Clayey Soil Only

$ORIGIN \equiv 1$

Input Data:

CPT := C:\..\CPT.xls — DATA input

$D := 18in$ — Diameter or Edge Length of the Pile

$L := 48.5ft$ — Length of the Pile

Average q_c over a distance of yD below the pile tip: qc ave_below(CPT,D,L,y)

$$
\begin{aligned}
qc_{ave\_below}(CPT, D, L, y) := \; & n \leftarrow ceil\left(\frac{L}{exchange}\right) \\
& i \leftarrow 0 \\
& qc_{below\_1} \leftarrow 0 \\
& \text{while } CPT_{n+i,1} \le \frac{L + y \cdot D}{ft} \\
& \quad qc_{below\_1} \leftarrow qc_{below\_1} + CPT_{n+i,2} \\
& \quad i \leftarrow i + 1 \\
& i \leftarrow i - 1 \\
& counter \leftarrow i \\
& qc_{below\_2} \leftarrow 0 \\
& qc_{below\_min} \leftarrow CPT_{n+i,2} \\
& \text{while } i \ge 0 \\
& \quad \text{if } qc_{below\_min} \le CPT_{n+i,2} \\
& \quad \quad qc_{below\_2} \leftarrow qc_{below\_2} + qc_{below\_min} \\
& \quad \quad i \leftarrow i - 1 \\
& \quad \text{otherwise} \\
& \quad \quad qc_{below\_min} \leftarrow CPT_{n+i,2} \\
& \quad \quad qc_{below\_2} \leftarrow qc_{below\_2} + qc_{below\_min} \\
& \quad \quad i \leftarrow i - 1 \\
& qc_{ave\_below} \leftarrow \frac{qc_{below\_1} + qc_{below\_2}}{2(counter + 1)} \\
& \text{return } qc_{ave\_below}
\end{aligned}
$$

$qc1(L) := qc_{ave\_below}(CPT, D, L, 4)$

```
qc2(L) := | return "L is too short"  if  L ≤ 8D
          | n ← floor(L / exchange)
          | nn ← ceil(L / exchange)
          | qc1 ← | yy ← 0.7
          |       | qc1 ← qc_ave_below(CPT,D,L,0.7)
          |       | for  y ∈ 0.7,0.71..4
          |       |   if  qc1 ≥ qc_ave_below(CPT,D,L,y)
          |       |      | qc1 ← qc_ave_below(CPT,D,L,y)
          |       |      | yy ← y
          |       | yy
          | qc_below_min ← | i ← 0
          |                | while  CPT_(nn+i,1) ≤ (L + qc1·D) / ft
          |                |    | b_(i+1) ← CPT_(nn+i,2)
          |                |    | i ← i + 1
          |                | min(b)
          | qc_above_min ← qc_below_min
          | qc_above ← 0
          | i ← 0
          | while  CPT_(n−i,1) ≥ (L − 8·D) / ft
          |    | if  qc_above_min ≤ CPT_(n−i,2)
          |    |    | qc_above ← qc_above + qc_above_min
          |    |    | i ← i + 1
          |    | otherwise
          |    |    | qc_above_min ← CPT_(n−i,2)
          |    |    | qc_above ← qc_above + qc_above_min
          |    |    | i ← i + 1
          | qc_ave_above ← qc_above / i
          | return  qc_ave_above
```

$qc2(L) = 67.893$

Calculation of the average cone tip resistance in Tumay and Fakhroo Method:

$qc1(L) = 122.554$

$qc2(L) = 67.893$

$$qt(L) := \text{if}\left(\frac{qc1(L) + qc2(L)}{2} \le 150, \frac{qc1(L) + qc2(L)}{2}, 150\right) \cdot \frac{\text{ton}}{\text{ft}^2} \qquad qt(L) = 95.224 \frac{\text{ton}}{\text{ft}^2}$$

Tip resistance:

$A := D^2 \qquad A = 2.25\,\text{ft}^2$

$Qt(L) := A \cdot qt(L) \qquad Qt(L) = 214.253\,\text{ton}$

Side Friction(Tumay and Fakhroo Method):

Calculate Ultimate Side Friction: Qs

$L1 := 3.8\text{ft}$ Input the soil layer

$L2 := 11.2\text{ft}$

$$
Q_s(L1, L2) := \left|
\begin{array}{l}
n \leftarrow \text{ceil}\left(\dfrac{L1}{\text{exchange}}\right) \\
m \leftarrow \text{floor}\left(\dfrac{L2}{\text{exchange}}\right) \\
A_s \leftarrow 4 \cdot D \cdot (L2 - L1) \\
f_{ssum} \leftarrow 0 \\
\text{for } j \in n..m \\
\quad f_{ssum} \leftarrow f_{ssum} + CPT_{j,3} \\
f_{sa} \leftarrow \dfrac{f_{ssum}}{m - n + 1} \\
m \leftarrow 0.5 + 9.5 \cdot e^{-9 \cdot f_{sa}} \\
f_s \leftarrow \text{if}\left(m \cdot f_{sa} \le 0.72, m \cdot f_{sa}, 0.72\right) \\
Q_s \leftarrow f_s \cdot A_s \cdot \dfrac{\text{ton}}{\text{ft}^2} \\
\text{return } Q_s
\end{array}
\right.
$$

$Q_s(L1, L2) = 14.242\,\text{ton}$

$L1 := 4ft$ $L2 := 5.8ft$ $L3 := 27.9ft$ $L4 := 36.5ft$ $L5 := L$

Layer1 :

$Q_s(0.01ft, L1) = 7.532\,ton$ $Q_{s1} := Q_s(0.01ft, L1)$

Layer2 :

$Q_s(L1, L2) = 5.951\,ton$ $Q_{s2} := Q_s(L1, L2)$

Layer3 :

$Q_s(L2, L3) = 39.846\,ton$ $Q_{s3} := Q_s(L2, L3)$

Layer4 :

$Q_s(L3, L4) = 23.086\,ton$ $Q_{s4} := Q_s(L3, L4)$

Layer5 :

$Q_s(L4, L5) = 21.667\,ton$ $Q_{s5} := Q_s(L4, L5)$

$Qs := Q_{s1} + Q_{s2} + Q_{s3} + Q_{s4} + Q_{s5}$ $Qs = 98.081\,ton$

$Q_{Davisson} := Qs + \frac{Qt(L)}{3}$ $Q_{Davisson} = 169.499\,ton$

Aoki and De Alencar Method (1975)

$exchange := 0.164042ft$

Ultimate Pile Capacity Based on CPT data Aoki & de Alencar (1975)

$ORIGIN \equiv 1$

Input Data:

$CPT :=$ C:\..\CPT.xls

DATA input

$D := 18in$

Diameter or Edge Length of the Pile

$L := 48.5ft$

Length of the Pile

Calculation of the average cone tip resistance using Aoki & de Alencar method:

$$
qc_{ave\_side}(L1, L2) := \left|
\begin{array}{l}
n \leftarrow ceil\left(\dfrac{L1}{exchange}\right) \\
i \leftarrow 0 \\
k \leftarrow 0 \\
qc \leftarrow 0 \\
\text{while } CPT_{n+i,1} \le \dfrac{L2}{ft} \\
\quad \left| \begin{array}{l} qc \leftarrow qc + CPT_{n+i,2} \\ i \leftarrow i + 1 \end{array} \right. \\
qc_{ave} \leftarrow \dfrac{qc}{i} \\
\text{return } qc_{ave}
\end{array}
\right.
$$

$qc_{ave\_tip}(D,L) := \dfrac{qc_{ave\_side}(L-8D,L) + qc_{ave\_side}(L,L+4D)}{2}$ Influnce zone is 8D above and 4D below the pile tip

$qc_{ave\_tip}(D,L) = 112.721$

$F_b := 1.75$

$qt(L) := \mathrm{if}\left(\dfrac{qc_{ave\_tip}(D,L)}{F_b} \le 150, \dfrac{qc_{ave\_tip}(D,L)}{F_b}, 150\right)\cdot\dfrac{ton}{ft^2}$ $qt(L) = 64.412\,\dfrac{1}{ft^2}\,ton$

Tip resistance:

$A := D^2$ $A = 2.25\,ft^2$

$Qt(L) := A\cdot qt(L)$ $Qt(L) = 144.927\,ton$

Side Friction(Aoki & de Alencar method):

Calculate Ultimate Side Friction: Qs

$F_s := 3.5$

$f_s(L1,L2,\alpha_s) := \mathrm{if}\left(qc_{ave\_side}(L1,L2)\cdot\dfrac{\alpha_s}{F_s} \le 1.2, qc_{ave\_side}(L1,L2)\cdot\dfrac{\alpha_s}{F_s}, 1.2\right)\cdot\dfrac{ton}{ft^2}$

$Q_s(L1,L2,\alpha_s) := f_s(L1,L2,\alpha_s)\cdot 4\cdot D\cdot(L2-L1)$

The empirical factor α_s values for different soil types

Soil Type	α_s (%)	Soil Type	α_s (%)	Soil Type	α_s (%)
Sand	1.4	Sandy silt	2.2	Sandy clay	2.4
Silty sand	2.0	Sandy silt with clay	2.8	Sandy clay with silt	2.8
Silty sand with clay	2.4	Silt	3.0	Silt clay with sand	3.0
Clayey sand with silt	2.8	Clayey silt with sand	3.0	Silty clay	4.0
Clayey sand	3.0	Clayey silt	3.4	Clay	6.0

$L1 := 4ft$ $L2 := 5.8ft$ $L3 := 27.9ft$ $L4 := 36.5ft$ $L5 := L$

Layer1 : $\alpha_s := 1.7\%$

$Q_{s1} := Q_s(0.01ft, L1, \alpha_s)$ $Q_{s1} = 8.176\,ton$

Layer2 : $\alpha_s := 3.7\%$

$Q_{s2} := Q_s(L1, L2, \alpha_s)$ $Q_{s2} = 4.214\,ton$

Layer3 : $\alpha_s := 1.6\%$

$Q_{s3} := Q_s(L2, L3, \alpha_s)$ $Q_{s3} = 42.258\,ton$

Layer4 : $\alpha_s := 5\%$

$Q_{s4} := Q_s(L3, L4, \alpha_s)$ $Q_{s4} = 3.918\,ton$

Layer5 : $\alpha_s := 1.4\%$

$Q_{s5} := Q_s(L4, L5, \alpha_s)$ $Q_{s5} = 24.311\,ton$

$Qs := Q_{s1} + Q_{s2} + Q_{s3} + Q_{s4} + Q_{s5}$ $Qs = 82.877\,ton$

$Q_{Davisson} := Qs + \dfrac{Qt(L)}{3}$ $Q_{Davisson} = 131.186\,ton$

Philipponnat Method (1980)

$exchange := 0.164042ft$

Ultimate Pile Capacity Based on CPT data Philipponnat Method (1980)

$ORIGIN \equiv 1$

Input Data:

CPT := C:\..\CPT.xls

DATA input

$D := 18in$

Diameter or Edge Length of the Pile

$L := 48.5ft$

Length of the Pile

Calculation of the average cone tip resistance using Philipponnat Method (1980):

$$
qc_{ave\_side}(L1, L2) := \left|
\begin{array}{l}
n \leftarrow ceil\left(\dfrac{L1}{exchange}\right) \\
i \leftarrow 0 \\
k \leftarrow 0 \\
qc \leftarrow 0 \\
\text{while } CPT_{n+i,1} \le \dfrac{L2}{ft} \\
\quad \left| \begin{array}{l} qc \leftarrow qc + CPT_{n+i,2} \\ i \leftarrow i + 1 \end{array} \right. \\
qc_{ave} \leftarrow \dfrac{qc}{i} \\
\text{return } qc_{ave}
\end{array}
\right.
$$

$qc_{ave\_tip1}(D, L) := qc_{ave\_side}(L - 3D, L)$

Average tip resistance within 3D above the pile tip

$qc_{ave\_tip2}(D, L) := qc_{ave\_side}(L, L + 3D)$

Average tip resistance within 3D below the pile tip

$$
qc_{ave\_tip}(D, L) := if\left(qc_{ave\_tip1}(D, L) \le qc_{ave\_tip2}(D, L), \frac{qc_{ave\_tip1}(D, L) + qc_{ave\_tip2}(D, L)}{2}, qc_{ave\_tip2}(D, L)\right)
$$

$qc_{ave\_tip1}(D, L) = 118.409$

$qc_{ave\_tip2}(D, L) = 147.483$

$qc_{ave\_tip}(D, L) = 132.946$

Bearing capacity factor (k_b)	
Soil Type	k_b
Gravel	0.35
Sand	0.40
Silt	0.45
Clay	0.50

$k_b := 0.4$

$qt(L) := if\left(qc_{ave\_tip}(D,L)\cdot k_b \le 150, qc_{ave\_tip}(D,L)\cdot k_b, 150\right)\cdot\frac{ton}{ft^2}$ $\qquad qt(L) = 53.178\,\frac{1}{ft^2}\,ton$

Tip resistance:

$A := D^2 \qquad A = 2.25\,ft^2$

$Qt(L) := A\cdot qt(L) \qquad Qt(L) = 119.651\,ton$

Side Friction(Philipponnat Method (1980)):

Calculate Ultimate Side Friction: Qs

$L1 := 0ft$ Input the soil layer

$L2 := 36ft$

$F_s := 100$

$f_s(L1,L2,\alpha_s,F_s) := if\left(qc_{ave\_side}(L1,L2)\cdot\frac{\alpha_s}{F_s} \le 1.27, qc_{ave\_side}(L1,L2)\cdot\frac{\alpha_s}{F_s}, 1.27\right)\cdot\frac{ton}{ft^2}$ $\qquad f_s(L1,L2,\alpha_s,F_s) = \blacksquare\,\frac{ton}{ft^2}$

$Q_s(L1,L2,\alpha_s,F_s) := f_s(L1,L2,\alpha_s,F_s)\cdot 4\cdot D\cdot(L2 - L1)$

$Q_s(L1,L2,\alpha_s,F_s) = \blacksquare\,ton$

α_s is equal to 1.25 for prestressed concrete driven piles

$L1 := 4ft \qquad L2 := 5.8ft \qquad L3 := 27.9ft \qquad L4 := 36.5ft \qquad L5 := L$

Layer1 : $\alpha_s := 1.25 \qquad F_s := 150$

$Q_{s1} := Q_s(0.01ft, L1, \alpha_s, F_s) \qquad Q_{s1} = 14.027\,ton$

Layer2 : $\alpha_s := 1.25 \qquad F_s := 60$

$Q_{s2} := Q_s(L1, L2, \alpha_s, F_s) \qquad Q_{s2} = 8.305\,ton$

Empirical factor F_s	
Soil Type	F_s
Clay and calcareous clay	50
Silt, sandy clay, and clayey sand	60
Loose sand	100
Medium dense sand	150
Dense sand and gravel	200

Layer3 : $\alpha_s := 1.25$ $F_s := 150$

$$Q_{s3} := Q_s(L2, L3, \alpha_s, F_s) \qquad Q_{s3} = 77.032\,\text{ton}$$

Layer4 : $\alpha_s := 1.25$ $F_s := 50$

$$Q_{s4} := Q_s(L3, L4, \alpha_s, F_s) \qquad Q_{s4} = 6.856\,\text{ton}$$

Layer5 : $\alpha_s := 1.25$ $F_s := 150$

$$Q_{s5} := Q_s(L4, L5, \alpha_s, F_s) \qquad Q_{s5} = 50.648\,\text{ton}$$

$$Qs := Q_{s1} + Q_{s2} + Q_{s3} + Q_{s4} + Q_{s5} \qquad Qs = 156.869\,\text{ton}$$

$$Q_{Davisson} := Qs + \frac{Qt(L)}{3} \qquad Q_{Davisson} = 196.753\,\text{ton}$$

LCPC (Bustamante and Gianeselli) Method (1982)

$exchange := 0.164042ft$

Ultimate Pile Capacity Based on CPT data Bustamante and Gianeselli (1982)

$ORIGIN \equiv 1$

Input Data:

$CPT :=$ C:\..\CPT.xls — DATA input

$D := 18in$ — Diameter or Edge Length of the Pile

$L := 48.5ft$ — Length of the Pile

Calculate the equivalent average cone tip resistance around the pile tip $q_{eq}(CPT,D,L)$

$$
qc_{eq\_side}(L1,L2) := \left|
\begin{array}{l}
n \leftarrow \mathrm{ceil}\left(\dfrac{L1}{exchange}\right) \\
i \leftarrow 0 \\
k \leftarrow 0 \\
qc \leftarrow 0 \\
qc_{eq} \leftarrow 0 \\
\text{while } CPT_{n+i,1} \le \dfrac{L2}{ft} \\
\quad \left| \begin{array}{l} qc \leftarrow qc + CPT_{n+i,2} \\ i \leftarrow i+1 \end{array} \right. \\
qc_{ave} \leftarrow \dfrac{qc}{i} \\
\text{for } m \in n..n+i-1 \\
\quad \text{while } CPT_{m,2} \ge 0.7 \cdot qc_{ave} \wedge CPT_{m,2} \le 1.3 qc_{ave} \\
\qquad \left| \begin{array}{l} qc_{eq} \leftarrow qc_{eq} + CPT_{m,2} \\ k \leftarrow k+1 \\ \text{break} \end{array} \right. \\
qc_{eq} \leftarrow \dfrac{qc_{eq}}{k} \\
\text{return } qc_{eq}
\end{array}
\right.
$$

$qc_{eq\_tip}(D,L) := qc_{eq\_side}(L - 1.5D, L + 1.5D)$

$qc_{eq\_tip}(D,L) = 140.821$

Calculate unit tip bearing capacity qt and Tip resistance Qt:

$SoilType := 2$ 1 for clay and silt, 2 for sand and gravel, 3 for Chalk

$k_b(L) := \mathrm{if}(SoilType = 1, 0.6, \mathrm{if}(SoilType = 2, 0.375, 0.4))$ $k_b(L) = 0.375$

$q_t(D,L) := qc_{eq\_tip}(D,L) \cdot k_b(L) \dfrac{ton}{ft^2}$ $q_t(D,L) = 52.808 \dfrac{ton}{ft^2}$

$A := D^2$ $A = 2.25 ft^2$

$Qt(D,L) := A \cdot q_t(D,L)$ $Qt(D,L) = 118.817\, ton$

Side Friction(Bustamante and Gianeselli):

Calculate fmax(tsf):

$$qc_{clay\_slit} := \begin{pmatrix} 0 \\ 5 \\ 10 \\ 20 \\ 30 \\ 40 \\ 50 \\ 60 \\ 70 \\ 80 \end{pmatrix} \qquad qc_{sand\_gravel} := \begin{pmatrix} 0 \\ 25 \\ 50 \\ 100 \\ 150 \\ 200 \\ 250 \\ 300 \\ 350 \\ 400 \end{pmatrix} \qquad qc_{chalk} := \begin{pmatrix} 0 \\ 10 \\ 20 \\ 30 \\ 60 \\ 90 \\ 120 \\ 150 \\ 180 \\ 210 \\ 250 \end{pmatrix}$$

$$f_{max\_clay\_silt} := \begin{pmatrix} 0 & 0 & 0 & 0 & 0 \\ 0.209 & 0.375 & 0.5 & 0.5 & 0.739 \\ 0.304 & 0.591 & 0.774 & 0.774 & 1 \\ 0.357 & 0.765 & 1 & 1 & 1.387 \\ 0.365 & 0.865 & 1.113 & 1.17 & 1.6 \\ 0.375 & 0.87 & 1.174 & 1.261 & 1.739 \\ 0.375 & 0.883 & 1.209 & 1.339 & 1.865 \\ 0.375 & 0.913 & 1.23 & 1.374 & 1.922 \\ 0.375 & 0.922 & 1.261 & 1.404 & 2 \\ 0.375 & 0.957 & 1.291 & 1.439 & 2.043 \end{pmatrix} \cdot \frac{ton}{ft^2}$$

$f_{max\_clay\_silt}^{\langle 2 \rangle} =$

	1
1	0
2	0.375
3	0.591
4	0.765
5	0.865
6	0.87
7	0.883
8	0.913
9	0.922
10	0.957

$\frac{ton}{ft^2}$

$$f_{max\_sand\_gravel} := \begin{pmatrix} 0 & 0 & 0 & 0 & 0 \\ 0.22 & 0.4 & 0.513 & 0.513 & 0.681 \\ 0.309 & 0.634 & 0.832 & 0.832 & 1.10 \\ 0.366 & 0.796 & 1.094 & 1.194 & 1.623 \\ 0.377 & 0.89 & 1.215 & 1.361 & 1.937 \\ 0.387 & 0.932 & 1.257 & 1.461 & 2.094 \\ 0.398 & 0.937 & 1.283 & 1.492 & 2.188 \\ 0.403 & 0.942 & 1.298 & 1.524 & 2.262 \\ 0.408 & 0.953 & 1.309 & 1.555 & 2.304 \\ 0.408 & 0.953 & 1.325 & 1.565 & 2.314 \end{pmatrix} \cdot \frac{ton}{ft^2}$$

$$f_{max\_chalk} := \begin{pmatrix} 0 & 0 & 0 & 0 \\ 0.14 & 0.21 & 0.307 & 0.307 \\ 0.202 & 0.378 & 0.514 & 0.575 \\ 0.246 & 0.492 & .656 & .809 \\ .327 & .699 & .951 & 1.305 \\ .367 & .802 & 1.128 & 1.577 \\ .376 & .864 & 1.243 & 1.765 \\ .386 & .9 & 1.305 & 1.901 \\ .394 & .924 & 1.358 & 1.984 \\ .404 & .934 & 1.399 & 2.057 \\ .41 & .944 & 1.441 & 2.151 \end{pmatrix} \cdot \frac{ton}{ft^2}$$

$L1 := 0.1ft$

$L2 := 36ft$

$qc_{eq\_side}(L1, L2) = 57.052$

$SoilType := 2$ 1 for clay and silt, 2 for sand and gravel, 3 for chalk

$CurveNo := 2$

$$f_{max}(SoilType, CurveNo, L1, L2) := \begin{cases} \text{linterp}\left(qc_{clay\_slit}, f_{max\_clay\_silt}{}^{\langle CurveNo \rangle}, qc_{eq\_side}(L1, L2)\right) & \text{if } SoilType = 1 \\ \text{linterp}\left(qc_{sand\_gravel}, f_{max\_sand\_gravel}{}^{\langle CurveNo \rangle}, qc_{eq\_side}(L1, L2)\right) & \text{if } SoilType = 2 \\ \text{linterp}\left(qc_{chalk}, f_{max\_chalk}{}^{\langle CurveNo \rangle}, qc_{eq\_side}(L1, L2)\right) & \text{otherwise} \end{cases}$$

$$f_{max}(SoilType, CurveNo, L1, L2) = 0.657 \frac{ton}{ft^2}$$

Calculate Ultimate Side Friction: Qs

$Q_s(L1, L2, SoilType, CurveNo) := f_{max}(SoilType, CurveNo, L1, L2) \cdot 4 \cdot D \cdot (L2 - L1)$

$Q_s(L1, L2, SoilType, CurveNo) = 141.485\,ton$

SoilType: 1 for cohessive soil, 2 for cohesionless soil, 3 for Chalk

$L1 := 0.5ft$ $L2 := 1.1ft$ $L3 := 2.9ft$ $L4 := 4ft$ $L5 := 5.8ft$ $L6 := 18.9ft$ $L7 := 20.6ft$ $L8 := 21.4ft$ $L9 := 22.3ft$

$L10 := 22.9ft$ $L11 := 26.9ft$ $L12 := 27.3ft$ $L13 := 27.9ft$ $L14 := 36.5ft$ $L15 := 39.7ft$ $L16 := 40.3ft$ $L17 := L$

Layer1 : $SoilType := 2$ $CurveNo := 1$

$Q_{s1} := Q_s(0.01ft, L1, SoilType, CurveNo)$ $Q_{s1} = 0.597\,ton$

Layer2 : $SoilType := 1$ $CurveNo := 2$

$Q_{s2} := Q_s(L1, L2, SoilType, CurveNo)$ $Q_{s2} = 3.193\,ton$

Layer3 : $SoilType := 2$ $CurveNo := 3$

$Q_{s3} := Q_s(L2, L3, SoilType, CurveNo)$ $Q_{s3} = 11.75\,ton$

Layer4 : $SoilType := 1$ $CurveNo := 2$

$Q_{s4} := Q_s(L3, L4, SoilType, CurveNo)$ $Q_{s4} = 5.952\,ton$

Layer5 : $SoilType := 2$ $CurveNo := 2$

$Q_{s5} := Q_s(L4, L5, SoilType, CurveNo)$ $Q_{s5} = 5.582\,ton$

Layer6 : $SoilType := 2$ $CurveNo := 2$

$Q_{s6} := Q_s(L5, L6, SoilType, CurveNo)$ $Q_{s6} = 52.706\,ton$

Layer7 : $SoilType := 1$ $CurveNo := 3$

$Q_{s7} := Q_s(L6, L7, SoilType, CurveNo)$ $Q_{s7} = 13.456\,ton$

Layer8 : $SoilType := 2$ $CurveNo := 2$

$Q_{s8} := Q_s(L7, L8, SoilType, CurveNo)$ $Q_{s8} = 3.16\,ton$

Layer9 : $SoilType := 1$ $CurveNo := 1$

$Q_{s9} := Q_s(L8, L9, SoilType, CurveNo)$ $Q_{s9} = 1.95\,ton$

Layer10 : $SoilType := 2$ $CurveNo := 2$

$Q_{s10} := Q_s(L9, L10, SoilType, CurveNo)$ $Q_{s10} = 2.337\,ton$

Layer11 : $SoilType := 2$ $CurveNo := 3$

$Q_{s11} := Q_s(L10, L11, SoilType, CurveNo)$ $Q_{s11} = 26.835\,ton$

Layer12 : $SoilType := 1$ $CurveNo := 2$

$Q_{s12} := Q_s(L11, L12, SoilType, CurveNo)$ $Q_{s12} = 2.209\,ton$

Layer13 : $SoilType := 2$ $CurveNo := 1$

$Q_{s13} := Q_s(L12, L13, SoilType, CurveNo)$ $Q_{s13} = 0.765\,ton$

Layer14 : $SoilType := 1$ $CurveNo := 1$

$Q_{s14} := Q_s(L13, L14, SoilType, CurveNo)$ $Q_{s14} = 11.466\,ton$

Layer15 : $SoilType := 2$ $CurveNo := 1$

$Q_{s15} := Q_s(L14, L15, SoilType, CurveNo)$ $Q_{s15} = 3.326\,ton$

Layer16 : $SoilType := 2$ $CurveNo := 2$

$Q_{s16} := Q_s(L15, L16, SoilType, CurveNo)$ $Q_{s16} = 2.285\,ton$

Layer17 : $SoilType := 1$ $CurveNo := 3$

$Q_{s17} := Q_s(L16, L17, SoilType, CurveNo)$ $Q_{s17} = 68.007\,ton$

$$Qs := Q_{s1} + Q_{s2} + Q_{s3} + Q_{s4} + Q_{s5} + Q_{s6} + Q_{s7} + Q_{s8} + Q_{s9} + Q_{s10} + Q_{s11} + Q_{s12} + Q_{s13} + Q_{s14} + Q_{s15} + Q_{s16} + Q_{s17}$$

$Qs = 215.574\,ton$

$Q_{Davisson} := Qs + \dfrac{Qt(D, L)}{3}$ $Q_{Davisson} = 255.18\,ton$

Almeida et al. Method (1996)

exchange := 0.164042ft

Ultimate Pile Capacity Based on CPT data Almeida et al. Method (1996)

ORIGIN ≡ 1

Input Data:

CPT := C:\..\CPT.xls

DATA input

D := 18in

Diameter or Edge Length of the Pile

L := 48.5ft

Length of the Pile

h := 5 water table

Calculation of the average cone tip resistance:

$$
qc_{ave\_side}(L1,L2) := \left|
\begin{array}{l}
n \leftarrow \mathrm{ceil}\left(\dfrac{L1}{exchange}\right) \\
i \leftarrow 0 \\
k \leftarrow 0 \\
qc \leftarrow 0 \\
\text{while } CPT_{n+i,1} \le \dfrac{L2}{ft} \\
\quad \left| \begin{array}{l} qc \leftarrow qc + CPT_{n+i,2} \\ i \leftarrow i + 1 \end{array} \right. \\
qc_{ave} \leftarrow \dfrac{qc}{i} \\
\text{return } qc_{ave}
\end{array}
\right.
$$

$qc_{ave\_tip1}(D,L) := qc_{ave\_side}(L - 8D, L)$

Average tip resistance within 8D above the pile tip

$qc_{ave\_tip2}(D,L) := qc_{ave\_side}(L, L + 3D)$

Average tip resistance within 3D below the pile tip

$$
qc_{ave\_tip}(D,L) := \frac{qc_{ave\_tip1}(D,L) + qc_{ave\_tip2}(D,L)}{2}
$$

$qc_{ave\_tip1}(D,L) = 84.414$

$qc_{ave\_tip2}(D,L) = 147.483$

$qc_{ave\_tip}(D,L) = 115.949$

$k_2 := 2.7$

$$\sigma_{v0\_tip} := \frac{95 \cdot h + 115\left(\frac{L}{ft} - h\right)}{2000} \qquad \sigma_{v0\_tip} = 2.739$$

$$qt(L) := \text{if}\left(\frac{qc_{ave\_tip}(D,L) - \sigma_{v0\_tip}}{k_2} \le 150, \frac{qc_{ave\_tip}(D,L) - \sigma_{v0\_tip}}{k_2}, 150\right) \cdot \frac{ton}{ft^2} \qquad qt(L) = 41.93 \frac{1}{ft^2} ton$$

Tip resistance:

$A := D^2 \qquad A = 2.25\,ft^2$

$Qt(L) := A \cdot qt(L) \qquad Qt(L) = 94.342\,ton$

Side Friction:

Calculate Ultimate Side Friction: Qs

$L1 := 0.01ft$ Input the soil layer

$L2 := 21.8ft$

$\sigma_{v0} := 0.5$

$\sigma_{v0\_ef} := 0.293$

$$f_s(L1, L2, \sigma_{v0}, \sigma_{v0\_ef}) := \min\left[\left[\text{if}\left[qc_{ave\_side}(L1,L2) - \sigma_{v0} \le 0, 0, \frac{\left(qc_{ave\_side}(L1,L2) - \sigma_{v0}\right)}{11.8 + 14 \cdot \log\left(\frac{qc_{ave\_side}(L1,L2) - \sigma_{v0}}{\sigma_{v0\_ef}}\right)}\right], 1.2\right]\right] \cdot \frac{ton}{ft^2}$$

$$Q_s(L1, L2, \sigma_{v0}, \sigma_{v0\_ef}) := f_s(L1, L2, \sigma_{v0}, \sigma_{v0\_ef}) \cdot 4 \cdot D \cdot (L2 - L1)$$

$$Q_s(L1, L2, \sigma_{v0}, \sigma_{v0\_ef}) = 156.888\,\text{ton}$$

$$\text{overburden}(\text{Depth1}, \text{Depth2}) := \left| \begin{array}{l} \text{Depth} \leftarrow \dfrac{\text{Depth1} + \text{Depth2}}{2 \cdot \text{ft}} \\ \sigma_{v0} \leftarrow \text{if}\left[\text{Depth} \le h, \dfrac{95 \cdot \text{Depth}}{2000}, \dfrac{95 \cdot h + 115(\text{Depth} - h)}{2000}\right] \\ \sigma_{v0\_ef} \leftarrow \text{if}\left[\text{Depth} \le h, \dfrac{95 \cdot \text{Depth}}{2000}, \dfrac{95 \cdot h + (115 - 62.4)(\text{Depth} - h)}{2000}\right] \\ \text{out} \leftarrow \text{augment}(\sigma_{v0}, \sigma_{v0\_ef}) \end{array} \right.$$

α_s is equal to 1.25 for prestressed concrete driven piles

$L0 := 0.01\text{ft}$ $L1 := 4\text{ft}$ $L2 := 5.8\text{ft}$ $L3 := 27.9\text{ft}$ $L4 := 36.5\text{ft}$ $L5 := L$

Layer1 : $Q_{s1} := Q_s\left(L0, L1, \text{overburden}(L0, L1)_{1,1}, \text{overburden}(L0, L1)_{1,2}\right)$ $Q_{s1} = 28.728\,\text{ton}$

Layer2 : $Q_{s2} := Q_s\left(L1, L2, \text{overburden}(L1, L2)_{1,1}, \text{overburden}(L1, L2)_{1,2}\right)$ $Q_{s2} = 9.307\,\text{ton}$

Layer3 : $Q_{s3} := Q_s\left(L2, L3, \text{overburden}(L2, L3)_{1,1}, \text{overburden}(L2, L3)_{1,2}\right)$ $Q_{s3} = 159.12\,\text{ton}$

Layer4 : $Q_{s4} := Q_s\left(L3, L4, \text{overburden}(L3, L4)_{1,1}, \text{overburden}(L3, L4)_{1,2}\right)$ $Q_{s4} = 9.186\,\text{ton}$

Layer5 : $Q_{s5} := Q_s\left(L4, L5, \text{overburden}(L4, L5)_{1,1}, \text{overburden}(L4, L5)_{1,2}\right)$ $Q_{s5} = 86.4\,\text{ton}$

$Qs := Q_{s1} + Q_{s2} + Q_{s3} + Q_{s4} + Q_{s5}$ $Qs = 292.741\,\text{ton}$

$Q_{Davisson} := Qs + \dfrac{Qt(L)}{3}$ $Q_{Davisson} = 324.188\,\text{ton}$

MTD (Jardine and Chow) Method (1996)

$exchange := 0.164042ft$

Ultimate Pile Capacity Based on CPT data MTD Method (1996)

ORIGIN ≡ 1

Input Data:

CPT := C:\..\CPT_PP.xls

DATA input

$D := 18in$

Diameter or Edge Length of the Pile

$L := 48.5ft$

Length of the Pile

Calculation of the average cone tip resistance:

$$qc_{ave\_side}(L1, L2) := \left| \begin{array}{l} n \leftarrow ceil\left(\frac{L1}{exchange}\right) \\ i \leftarrow 0 \\ k \leftarrow 0 \\ qc \leftarrow 0 \\ \text{while } CPT_{n+i,1} \le \frac{L2}{ft} \\ \quad \left| \begin{array}{l} qc \leftarrow qc + CPT_{n+i,2} \\ i \leftarrow i + 1 \end{array} \right. \\ qc_{ave} \leftarrow \frac{qc}{i} \\ \text{return } qc_{ave} \end{array} \right.$$

$qc_{ave\_tip}(D, L) := qc_{ave\_side}(L - 1.5D, L + 1.5D)$

Average tip resistance within 1.5D above and below the pile tip

$qc_{ave\_tip}(D, L) = 140.821$

$Soiltype := 2$

1 for cohessive soil, 2 for cohesionless soil

$k_{sand} := if\left(D \le 1.95m, 1 - 0.5 \cdot \log\left(\frac{D}{1.4in}\right), 0.13\right)$

$k_{sand} = 0.445$

$k_{clay} := 1.3$

0.8 for drained loading,1.3 for undrained loading

$qt(L) := \text{if}\left(\text{Soiltype} = 1, k_{clay}\, qc_{ave\_tip}(D, L), k_{sand}\, qc_{ave\_tip}(D, L)\right)\cdot\frac{ton}{ft^2}$ $\quad qt(L) = 62.725\,\frac{1}{ft^2}\,ton$

Tip resistance:

$A := D^2 \qquad A = 2.25\,ft^2$

$Qt(L) := A\cdot qt(L) \qquad Qt(L) = 141.132\,ton$

Side Friction:

Calculate Ultimate Side Friction: Qs

$SoilType := 2$ 1 for cohessive soil, 2 for cohesionless soil

$L1 := 5.8ft$ Input the soil layer

$L2 := 27.9ft$

$f_L := 0.8$

$WT := 5$ water table

$\delta_f := 11.31\cdot\frac{\pi}{180} \qquad \tan(\delta_f) = 0.2$

For fs Calculation in Clay

$qc_{ave\_side}(L1, L2) = 69.712$

$$\sigma_{v0}(L1, L2) := \left| \begin{array}{l} Depth \leftarrow \frac{L1 + L2}{2\cdot ft} \\ \sigma_{v0} \leftarrow \text{if}\left[Depth \le WT, \frac{95\cdot Depth}{2000}, \frac{95\cdot WT + 115(Depth - WT)}{2000}\right] \\ out \leftarrow \sigma_{v0} \end{array} \right. \qquad \sigma_{v0}(L1, L2) = 0.919$$

$$\sigma_{v0\_ef}(L1, L2) := \left| \begin{array}{l} Depth \leftarrow \frac{L1 + L2}{2\cdot ft} \\ \sigma_{v0\_ef} \leftarrow \text{if}\left[Depth \le WT, \frac{95\cdot Depth}{2000}, \frac{95\cdot WT + (115 - 62.4)(Depth - WT)}{2000}\right] \\ out \leftarrow \sigma_{v0\_ef} \end{array} \right. \qquad \sigma_{v0\_ef}(L1, L2) = 0.549$$

$$R_f(L1,L2) := \begin{array}{|l} n \leftarrow \mathrm{ceil}\left(\frac{L1}{exchange}\right) \\ i \leftarrow 0 \\ k \leftarrow 0 \\ R_f \leftarrow 0 \\ \text{while } CPT_{n+i,1} \le \frac{L2}{ft} \\ \quad \begin{array}{|l} R_f \leftarrow R_f + \frac{CPT_{n+i,3}}{CPT_{n+i,2}} \cdot 100 \\ i \leftarrow i+1 \end{array} \\ R_f \leftarrow \frac{R_f}{i} \\ \text{return } R_f \end{array}$$

$$R_f(L1,L2) = 0.636$$

$$S_t(L1,L2) := \frac{10}{R_f(L1,L2)} \qquad S_t(L1,L2) = 15.735$$

$$YSR(L1,L2) := 0.04427 \cdot \left(\frac{qc_{ave\_side}(L1,L2)}{\sigma_{v0\_ef}(L1,L2)}\right)^{1.667} \qquad YSR(L1,L2) = 142.179$$

$$K_c(L1,L2) := \left(2.2 + 0.016 \cdot YSR(L1,L2) - 0.870 \cdot \log\left(S_t(L1,L2)\right)\right) \cdot YSR(L1,L2)^{0.42} \cdot \left(\mathrm{if}\left(\frac{L - \frac{L1+L2}{2}}{D} \le 8, 8, \frac{L - \frac{L1+L2}{2}}{D}\right)\right)^{-0.20}$$

$$f_{s\_clay}(L1,L2,\delta_f) := f_L \cdot K_c(L1,L2) \cdot \sigma_{v0\_ef}(L1,L2) \cdot \tan(\delta_f) \cdot \frac{ton}{ft^2} \qquad f_{s\_clay}(L1,L2,\delta_f) = 1.315 \frac{ton}{ft^2}$$

For fs Calculation in Sand

$$\sigma_{rc}(L1,L2) := 0.029 \cdot qc_{ave\_side}(L1,L2) \cdot \left(\frac{\sigma_{v0\_ef}(L1,L2)}{1.0581}\right)^{0.13} \cdot \left(\mathrm{if}\left(\frac{L - \frac{L1+L2}{2}}{D} \le 8, 8, \frac{L - \frac{L1+L2}{2}}{D}\right)\right)^{-0.38} \qquad \sigma_{rc}(L1,L2) = 0.58$$

$$G(L1,L2) := qc_{ave\_side}(L1,L2) \cdot \left(0.0203 + 0.00125 \cdot \frac{qc_{ave\_side}(L1,L2)}{\sqrt{1.0581 \cdot \sigma_{v0\_ef}(L1,L2)}} - 1.216 \cdot 10^{-6} \cdot \frac{qc_{ave\_side}(L1,L2)^2}{1.0581 \cdot \sigma_{v0\_ef}(L1,L2)}\right)^{-1} \qquad G(L1,L2$$

$$\Delta\sigma_{rd}(L1,L2) := \frac{4 \cdot G(L1,L2) \cdot 3 \cdot 10^{-5} \cdot m}{D} \qquad \Delta\sigma_{rd}(L1,L2) = 0.147$$

$$\sigma_{rf}(L1,L2) := \sigma_{rc}(L1,L2) + \Delta\sigma_{rd}(L1,L2) \qquad \sigma_{rf}(L1,L2) = 0.73$$

$$f_{s\_sand}(L1,L2,\delta_f) := \sigma_{rf}(L1,L2) \cdot \tan(\delta_f) \cdot \frac{ton}{ft^2}$$

$$Q_s(L1,L2,SoilType,\delta_f) := \mathrm{if}\left(SoilType = 1, f_{s\_clay}(L1,L2,\delta_f), f_{s\_sand}(L1,L2,\delta_f)\right) \cdot 4 \cdot D \cdot (L2 - L1)$$

$$Q_s(L1,L2,SoilType,\delta_f) = 19.353\,ton$$

α_s is equal to 1.25 for prestressed concrete driven piles

$L0 := 0.01ft$ $L1 := 4ft$ $L2 := 5.8ft$ $L3 := 27.9ft$ $L4 := 36.5ft$ $L5 := L$ $L6 := L$

Layer1 : $SoilType := 2$ $\delta_f := 30 \cdot \frac{\pi}{180}$

$Q_{s1} := Q_s(0.01ft, L1, SoilType, \delta_f)$ $Q_{s1} = 6.663\,ton$

Layer2 : $SoilType := 1$ $\delta_f := 11.31 \cdot \frac{\pi}{180}$

$Q_{s2} := Q_s(L1, L2, SoilType, \delta_f)$ $Q_{s2} = 9.742\,ton$

Layer3 : $SoilType := 2$ $\delta_f := 30 \cdot \frac{\pi}{180}$

$Q_{s3} := Q_s(L2, L3, SoilType, \delta_f)$ $Q_{s3} = 55.866\,ton$

Layer4 : $SoilType := 1$ $\delta_f := 11.31 \cdot \frac{\pi}{180}$

$Q_{s4} := Q_s(L3, L4, SoilType, \delta_f)$ $Q_{s4} = 7.015\,ton$

Layer5 : $SoilType := 2$ $\delta_f := 30 \cdot \frac{\pi}{180}$

$Q_{s5} := Q_s(L4, L5, SoilType, \delta_f)$ $Q_{s5} = 55.718\,ton$

Layer6 : $SoilType := 1$ $\delta_f := 11.31 \cdot \frac{\pi}{180}$

$Q_{s6} := Q_s(L5, L6, SoilType, \delta_f)$ $Q_{s6} = 0\,ton$

Layer7 : $SoilType := 2$ $\delta_f := 30 \cdot \frac{\pi}{180}$

$Q_{s7} := Q_s(L6, L, SoilType, \delta_f)$ $Q_{s7} = 0\,ton$

$Qs := Q_{s1} + Q_{s2} + Q_{s3} + Q_{s4} + Q_{s5} + Q_{s6} + Q_{s7}$ $Qs = 135.005\,ton$

$Q_{Davisson} := Qs + \frac{Qt(L)}{3}$ $Q_{Davisson} = 182.049\,ton$

Eslami and Fellenius Method (1997)

$exchange := 0.164042ft$

Ultimate Pile Capacity Based on CPT data Eslami and Fellenius (1996)

$ORIGIN \equiv 1$

Input Data:

CPT := C:\..\CPT_PP.xls

DATA input

Diameter or Edge Length of the Pile

$D := 18in$

Length of the Pile

$L := 48.5ft$

Calculation of the average cone tip resistance using Eslami and Fellenius (1996)

$$qc_{eg}(L1, L2) := \left| \begin{array}{l} n \leftarrow ceil\left(\frac{L1}{exchange}\right) \\ i \leftarrow 0 \\ k \leftarrow 0 \\ qc \leftarrow 1 \\ \text{while } CPT_{n+i,1} \le \frac{L2}{ft} \\ \quad \left| \begin{array}{l} qc \leftarrow qc \cdot \left(CPT_{n+i,2} - CPT_{n+i,4}\right) \\ i \leftarrow i + 1 \end{array} \right. \\ qc_{ave} \leftarrow \sqrt[i]{qc} \\ \text{return } qc_{ave} \end{array} \right.$$

$qc_{eg\_tip1}(D, L) := qc_{eg}(L - 2D, L + 4D)$

Influnce zone is 2D above and 4D below the pile tip when the pile is installed through a dense soil into a weak soil

$qc_{eg\_tip2}(D, L) := qc_{eg}(L - 8D, L + 3.8D)$

Influnce zone is 8D above and 4D below the pile tip when the pile is installed through a weak soil into a dense soil

$C_t := 1$

$qt1(L) := qc_{eg\_tip1}(D, L) \cdot C_t \cdot \frac{ton}{ft^2}$

$qt1(L) = 133.647 \frac{ton}{ft^2}$

$qt2(L) := qc_{eg\_tip2}(D,L)\cdot C_t\cdot\frac{ton}{ft^2}$ $\qquad qt2(L) = 79.763\frac{ton}{ft^2}$

Tip resistance:

$A := D^2 \qquad A = 2.25\,ft^2$

$Qt1(L) := A\cdot qt1(L) \qquad Qt1(L) = 300.706\,ton$

$Qt2(L) := A\cdot qt2(L) \qquad Qt2(L) = 179.467\,ton$

Side Friction(Eslami and Fellenius (1996)):

$$qc_{e\_side}(L1,L2) := \left| \begin{array}{l} n \leftarrow ceil\left(\frac{L1}{exchange}\right) \\ i \leftarrow 0 \\ k \leftarrow 0 \\ qc \leftarrow 0 \\ \text{while } CPT_{n+i,1} \le \frac{L2}{ft} \\ \quad \left| \begin{array}{l} qc \leftarrow qc + \left(CPT_{n+i,2} - CPT_{n+i,4}\right) \\ i \leftarrow i+1 \end{array}\right. \\ qc_e \leftarrow \frac{qc}{i} \\ \text{return } qc_e \end{array}\right.$$

Calculate Ultimate Side Friction: Qs

$$Q_s := \left| \begin{array}{l} n \leftarrow ceil\left(\frac{L}{exchange}\right) - 1 \\ Q_s \leftarrow 0 \\ \text{for } i \in 1..n \\ \quad \left| \begin{array}{l} q_E \leftarrow CPT_{i,2} - CPT_{i,4} \\ f_S \leftarrow CPT_{i,3} \\ Q_s \leftarrow Q_s \ \text{ if } f_S \le 0 \\ \text{otherwise} \\ \quad \left| \begin{array}{l} Q_s \leftarrow Q_s + 0.08\cdot q_E\cdot 4\cdot D\cdot exchange \ \text{ if } q_E \le 10.4 \wedge f_S \le 0.21 \\ Q_s \leftarrow Q_s + 0.05\cdot q_E\cdot 4\cdot D\cdot exchange \ \text{ if } q_E \le 10^{0.288\cdot\log(f_S)+1.2121} \wedge f_S > 0.21 \\ Q_s \leftarrow Q_s + 0.025\cdot q_E\cdot 4\cdot D\cdot exchange \ \text{ if } q_E > \max\left(10.4, 10^{0.288\cdot\log(f_S)+1.2121}\right) \wedge q_E \le 10^{0.456\cdot\log(f_S)+1.5358} \\ Q_s \leftarrow Q_s + 0.01\cdot q_E\cdot 4\cdot D\cdot exchange \ \text{ if } q_E > \max\left(10.4, 10^{0.456\cdot\log(f_S)+1.5358}\right) \wedge q_E \le 10^{0.493\cdot\log(f_S)+1.9946} \\ Q_s \leftarrow Q_s + 0.004\cdot q_E\cdot 4\cdot D\cdot exchange \ \text{ if } q_E > \max\left(10.4, 10^{0.493\cdot\log(f_S)+1.9946}\right) \end{array}\right. \end{array}\right. \\ \text{return } Q_s\cdot\frac{ton}{ft^2} \end{array}\right.$$

$Q_s = 106.448\,ton$

$Q_{Davisson1} := Q_s + \frac{Qt1(L)}{3} \qquad Q_{Davisson1} = 206.683\,ton$

Influnce zone is 2D above and 4D below the pile tip when the pile is installed through a dense soil into a weak soil

$Q_{Davisson2} := Q_s + \frac{Qt2(L)}{3} \qquad Q_{Davisson2} = 166.271\,ton$

Influnce zone is 8D above and 4D below the pile tip when the pile is installed through a weak soil into a dense soil

Powell et al. Method (2001)

$exchange := 0.164042ft$

Ultimate Pile Capacity Based on CPT data Almeida et al. Method (1996)

$ORIGIN \equiv 1$

Input Data:

CPT := C:\..\CPT.xls

DATA input

$D := 18in$

Diameter or Edge Length of the Pile

$L := 48.5ft$

Length of the Pile

$h := 5$ water table

Calculation of the average cone tip resistance:

$$qc_{ave\_side}(L1, L2) := \begin{array}{|l} n \leftarrow ceil\left(\frac{L1}{exchange}\right) \\ i \leftarrow 0 \\ k \leftarrow 0 \\ qc \leftarrow 0 \\ \text{while } CPT_{n+i,1} \le \frac{L2}{ft} \\ \quad \begin{array}{|l} qc \leftarrow qc + CPT_{n+i,2} \\ i \leftarrow i + 1 \end{array} \\ qc_{ave} \leftarrow \frac{qc}{i} \\ \text{return } qc_{ave} \end{array}$$

$qc_{ave\_tip1}(D, L) := qc_{ave\_side}(L - 8D, L)$ Average tip resistance within 8D above the pile tip

$qc_{ave\_tip2}(D, L) := qc_{ave\_side}(L, L + 3D)$ Average tip resistance within 3D below the pile tip

$$qc_{ave\_tip}(D, L) := \frac{qc_{ave\_tip1}(D, L) + qc_{ave\_tip2}(D, L)}{2}$$

$$qc_{ave\_tip1}(D,L) = 84.414$$

$$qc_{ave\_tip2}(D,L) = 147.483$$

$$qc_{ave\_tip}(D,L) = 115.949$$

$N_k := 15$ Cone factor: 15 for general clays, 10 for sensitive clays

$$k_2 := \frac{N_k}{9}$$

$$\sigma_{v0\_tip} := \frac{95 \cdot h + 115\left(\frac{L}{ft} - h\right)}{2000} \qquad \sigma_{v0\_tip} = 2.739$$

$$qt(L) := \mathrm{if}\left(\frac{qc_{ave\_tip}(D,L) - \sigma_{v0\_tip}}{k_2} \le 150, \frac{qc_{ave\_tip}(D,L) - \sigma_{v0\_tip}}{k_2}, 150\right) \cdot \frac{ton}{ft^2} \qquad qt(L) = 67.926 \frac{1}{ft^2} ton$$

Tip resistance:

$A := D^2 \qquad A = 2.25\,ft^2$

$Qt(L) := A \cdot qt(L) \qquad Qt(L) = 152.833\,ton$

Side Friction:

Calculate Ultimate Side Friction: Qs

$L1 := 0.01ft$ Input the soil layer

$L2 := 21.8ft$

$\sigma_{v0} := 0.5$

$\sigma_{v0\_ef} := 0.293$

$$f_s(L1, L2, \sigma_{v0}, \sigma_{v0\_ef}) := \min\left[\left[\mathrm{if}\left[qc_{ave\_side}(L1,L2) - \sigma_{v0} \le 0, 0, \frac{\left(qc_{ave\_side}(L1,L2) - \sigma_{v0}\right)}{10.5 + 13.3 \cdot \log\left(\frac{qc_{ave\_side}(L1,L2) - \sigma_{v0}}{\sigma_{v0\_ef}}\right)}\right]\right], 1.2\right] \cdot \frac{ton}{ft^2}$$

$Q_s(L1, L2, \sigma_{v0}, \sigma_{v0\_ef}) := f_s(L1, L2, \sigma_{v0}, \sigma_{v0\_ef}) \cdot 4 \cdot D \cdot (L2 - L1)$

$Q_s(L1, L2, \sigma_{v0}, \sigma_{v0\_ef}) = 156.888\,\text{ton}$

α_s is equal to 1.25 for prestressed concrete driven piles

$L0 := 0.01ft$ $L1 := 4ft$ $L2 := 5.8ft$ $L3 := 27.9ft$ $L4 := 36.5ft$ $L5 := L$

Layer1 : $Q_{s1} := Q_s\left(L0, L1, \text{overburden}(L0, L1)_{1,1}, \text{overburden}(L0, L1)_{1,2}\right)$ $Q_{s1} = 28.728\,\text{ton}$

Layer2 : $Q_{s2} := Q_s\left(L1, L2, \text{overburden}(L1, L2)_{1,1}, \text{overburden}(L1, L2)_{1,2}\right)$ $Q_{s2} = 9.972\,\text{ton}$

Layer3 : $Q_{s3} := Q_s\left(L2, L3, \text{overburden}(L2, L3)_{1,1}, \text{overburden}(L2, L3)_{1,2}\right)$ $Q_{s3} = 159.12\,\text{ton}$

Layer4 : $Q_{s4} := Q_s\left(L3, L4, \text{overburden}(L3, L4)_{1,1}, \text{overburden}(L3, L4)_{1,2}\right)$ $Q_{s4} = 10.05\,\text{ton}$

Layer5 : $Q_{s5} := Q_s\left(L4, L5, \text{overburden}(L4, L5)_{1,1}, \text{overburden}(L4, L5)_{1,2}\right)$ $Q_{s5} = 86.4\,\text{ton}$

$Qs := Q_{s1} + Q_{s2} + Q_{s3} + Q_{s4} + Q_{s5}$ $Qs = 294.27\,\text{ton}$

$Q_{Davisson} := Qs + \frac{Qt(L)}{3}$ $Q_{Davisson} = 345.214\,\text{ton}$

UWA-05 Method (2005)

exchange := 0.164042ft   ORIGIN ≡ 1

Ultimate Pile Capacity Based on CPT data UWA-05 method (2005)

Input Data:

CPT := C:\..\CPT.xls   DATA input

Diameter or Edge Length of the Pile

D := 18in

Length of the Pile

L := 48.5ft

water table

WT := 5

$\Delta r := 0.02mm$ rough of driven piles

$\delta_f := 29 \cdot \frac{\pi}{180}$ $\tan(\delta_f) = 0.554$

Calculation of the average cone tip resistance using UWA-05 method (2005)

Average q_c over a distance of yD below the pile tip: qc ave_below(CPT,D,L,y)

```
qc_ave_below(CPT,D,L,y) := | n ← ceil( L / exchange )
                           | i ← 0
                           | qc_below_1 ← 0
                           | while CPT_(n+i,1) ≤ (L + y·D) / ft
                           |     | qc_below_1 ← qc_below_1 + CPT_(n+i,2)
                           |     | i ← i + 1
                           | i ← i − 1
                           | counter ← i
                           | qc_below_2 ← 0
                           | qc_below_min ← CPT_(n+i,2)
                           | while i ≥ 0
                           |     | if qc_below_min ≤ CPT_(n+i,2)
                           |     |     | qc_below_2 ← qc_below_2 + qc_below_min
                           |     |     | i ← i − 1
                           |     | otherwise
                           |     |     | qc_below_min ← CPT_(n+i,2)
                           |     |     | qc_below_2 ← qc_below_2 + qc_below_min
                           |     |     | i ← i − 1
                           | qc_ave_below ← (qc_below_1 + qc_below_2) / (2(counter + 1))
                           | return qc_ave_below
```

```
qc1(L) := | yy ← 0
          | qc1 ← qc_ave_below(CPT,D,L,0.7)
          | for y ∈ 0.7,0.71..4
          |   if qc1 ≥ qc_ave_below(CPT,D,L,y)
          |       | qc1 ← qc_ave_below(CPT,D,L,y)
          |       | yy ← y
          | return (qc1, yy)
```

$$qc1(L) = \begin{pmatrix} 121.258 \\ 3.75 \end{pmatrix}$$

```
qc2(L) := | return "L is too short"  if  L ≤ 8D
          | n ← floor(L / exchange)
          | nn ← ceil(L / exchange)
          | qc1 ← | yy ← 0
          |       | qc1 ← qc_ave_below(CPT, D, L, 0.7)
          |       | for  y ∈ 0.7, 0.71 .. 4
          |       |   if  qc1 ≥ qc_ave_below(CPT, D, L, y)
          |       |       | qc1 ← qc_ave_below(CPT, D, L, y)
          |       |       | yy ← y
          |       | yy
          | qc_below_min ← | i ← 0
          |                | while  CPT_(nn+i,1) ≤ (L + qc1·D) / ft
          |                |     | b_(i+1) ← CPT_(nn+i,2)
          |                |     | i ← i + 1
          |                | min(b)
          | qc_above_min ← qc_below_min
          | qc_above ← 0
          | i ← 0
          | while  CPT_(n−i,1) ≥ (L − 8·D) / ft
          |    | if  qc_above_min ≤ CPT_(n−i,2)
          |    |     | qc_above ← qc_above + qc_above_min
          |    |     | i ← i + 1
          |    | otherwise
          |    |     | qc_above_min ← CPT_(n−i,2)
          |    |     | qc_above ← qc_above + qc_above_min
          |    |     | i ← i + 1
          | qc_ave_above ← qc_above / i
          | return  qc_ave_above
```

$qc2(L) = 67.893$

Calculation of the average cone tip resistance in UWA-05 method:

$qc1(L)_1 = 121.258$

$qc2(L) = 67.893$

$qt(L) := 0.6 \cdot \frac{qc1(L)_1 + qc2(L)}{2} \cdot \frac{ton}{ft^2}$ $\qquad qt(L) = 56.745 \frac{ton}{ft^2}$

Tip resistance:

$$A := D^2 \qquad A = 2.25\,\text{ft}^2$$

$$Qt(L) := A\cdot qt(L) \qquad Qt(L) = 127.677\,\text{ton}$$

Side Friction(UWA-05 (2005)):

$$\sigma_{v0\_ef}(\text{Depth}) := \text{if}\left[\text{Depth} \le \text{WT}, \frac{95\cdot\text{Depth}}{2000}, \frac{95\cdot\text{WT} + (115 - 62.4)(\text{Depth} - \text{WT})}{2000}\right] \qquad \sigma_{v0\_ef}\left(CPT_{74,1}\right) = 0.421$$

$$\text{int}(\text{Depth}) := \begin{array}{|l} \text{out} \leftarrow \text{ceil}(\text{Depth}) \quad \text{if} \quad \text{ceil}(\text{Depth}) - \text{Depth} \le 0.5 \\ \text{out} \leftarrow \text{floor}(\text{Depth}) \quad \text{otherwise} \end{array}$$

$$q_c(\text{Depth}) := CPT_{\text{int}\left(\frac{\text{Depth}\cdot\text{ft}}{\text{exchange}}\right)+1,2} \qquad q_c\left(CPT_{74,1}\right) = 61.17$$

$$G(\text{Depth}) := \text{if}\left[q_c(\text{Depth}) \ne 0, q_c(\text{Depth})\cdot 185\cdot\left(\frac{\frac{q_c(\text{Depth})}{1.0581}}{\sqrt{\frac{\sigma_{v0\_ef}(\text{Depth})}{1.0581}}}\right)^{-0.7}, 0\right]$$

G

Calculate Ultimate Side Friction: Qs

$$Q_s := \begin{array}{|l} n \leftarrow \text{ceil}\left(\frac{L}{\text{exchange}}\right) - 1 \\ Q_s \leftarrow 0 \\ \text{for } i \in 2..n \\ \quad \begin{array}{|l} q_c \leftarrow CPT_{i,2} \\ LL \leftarrow CPT_{i,1} \\ f_s \leftarrow \left[0.03\cdot q_c\cdot\left(\max\left(\frac{L}{\text{ft}} - LL, 2\right)\right)^{-0.5} + 4\cdot G(LL)\cdot\frac{\Delta r}{D}\right]\cdot\tan\left(\delta_f\right) \\ Q_s \leftarrow Q_s + f_s\cdot 4\cdot D\cdot\text{exchange} \end{array} \\ \text{return } Q_s\cdot\frac{\text{ton}}{\text{ft}^2} \end{array} \qquad Q_s = 99.895\,\text{ton}$$

$$Q_{Davisson} := Q_s + \frac{Qt(L)}{3} \qquad Q_{Davisson} = 142.454\,\text{ton}$$

Zhou et al. Method (1982)

$exchange := 0.164042ft$

Ultimate Pile Capacity Based on CPT data Zhou et al. Method (1982)

$ORIGIN \equiv 1$

Input Data:

CPT := C:\..\CPT.xls

DATA input

Diameter or Edge Length of the Pile

$D := 18in$

Embedment of the Pile

$L := 48.5ft$

Calculation of the average cone tip resistance using Zhou et al. Method (1982):

$$qc_{ave\_side}(L1,L2) := \left| \begin{array}{l} n \leftarrow ceil\left(\frac{L1}{exchange}\right) \\ i \leftarrow 0 \\ k \leftarrow 0 \\ qc \leftarrow 0 \\ \text{while } CPT_{n+i,1} \le \frac{L2}{ft} \\ \quad \left| \begin{array}{l} qc \leftarrow qc + CPT_{n+i,2} \\ i \leftarrow i+1 \end{array} \right. \\ qc_{ave} \leftarrow \frac{qc}{i} \\ \text{return } qc_{ave} \end{array} \right.$$

$$f_{s\_ave}(L1,L2) := \left| \begin{array}{l} n \leftarrow ceil\left(\frac{L1}{exchange}\right) \\ i \leftarrow 0 \\ k \leftarrow 0 \\ f_s \leftarrow 0 \\ \text{while } CPT_{n+i,1} \le \frac{L2}{ft} \\ \quad \left| \begin{array}{l} f_s \leftarrow f_s + CPT_{n+i,3} \\ i \leftarrow i+1 \end{array} \right. \\ f_{s\_ave} \leftarrow \frac{f_s}{i} \\ \text{return } f_{s\_ave} \end{array} \right.$$

$qc_{ave\_tip1}(D,L) := qc_{ave\_side}(L-4D,L)$ Average tip resistance within 4D above the pile tip

$qc_{ave\_tip2}(D,L) := qc_{ave\_side}(L,L+4D)$ Average tip resistance within 4D below the pile tip

$$qc_{ave\_tip}(D,L) := \text{if}\left(qc_{ave\_tip1}(D,L) \le qc_{ave\_tip2}(D,L), \frac{qc_{ave\_tip1}(D,L) + qc_{ave\_tip2}(D,L)}{2}, qc_{ave\_tip2}(D,L)\right)$$

$qc_{ave\_tip1}(D,L) = 110.233$

$qc_{ave\_tip2}(D,L) = 141.028$

$qc_{ave\_tip}(D,L) = 125.631$

$fs_{ave\_tip}(D,L) := f_{s\_ave}(L-4D,L+4D)$ $\quad fs_{ave\_tip}(D,L) = 0.897$ $\quad \dfrac{fs_{ave\_tip}(D,L)}{qc_{ave\_tip}(D,L)} = 7.141 \times 10^{-3}$

$$\alpha := \text{if}\left[qc_{ave\_tip}(D,L) \ge 2\cdot 10.4427 \wedge \frac{fs_{ave\_tip}(D,L)}{qc_{ave\_tip}(D,L)} \le 0.014, 0.71\cdot\left(\frac{qc_{ave\_tip}(D,L)}{10.4427}\right)^{-0.25}, 1.07\cdot\left(\frac{qc_{ave\_tip}(D,L)}{10.4427}\right)^{-0.35}\right]$$

$qt(L) := \alpha\cdot qc_{ave\_tip}(D,L)\cdot\dfrac{ton}{ft^2}$ $\quad qt(L) = 47.894\,\dfrac{1}{ft^2}\,ton$

Tip resistance:

$A := D^2$ $\quad A = 2.25\,ft^2$

$Qt(L) := A\cdot qt(L)$ $\quad Qt(L) = 107.762\,ton$

Side Friction(Zhou et al. Method):

$$\beta(n) := \text{if}\left[CPT_{n,3} \le 0, 0, \min\left[\text{if}\left[CPT_{n,2} \ge 2\cdot 10.4427 \wedge \frac{CPT_{n,3}}{CPT_{n,2}} \le 0.014, 0.23\cdot\left(\frac{CPT_{n,3}}{10.4427}\right)^{-0.45}, 0.22\cdot\left(\frac{CPT_{n,3}}{10.4427}\right)^{-0.55}\right], 2.5\right]\right]$$

Calculate Ultimate Side Friction: Qs

```
Qs := | n ← 2
      | Q_s ← 0ton
      | A_s ← 4·D·exchange
      | i ← 0
      | while i·exchange ≤ L
      |    | Q_s ← Q_s + β(n + i)·(ton/ft^2)·CPT_(n+i,3)·A_s
      |    | i ← i + 1
      | return Q_s
```

$Qs = 115.574\,ton$

$Q_{Davisson} := Qs + Qt(L)$ $\quad Q_{Davisson} = 223.336\,ton$

Calculation of LRFD Resistance Factor

ORIGIN ≡ 1

LRFD Phi factors
(First Order Second Moment Approach)

Input Data: $\gamma_D := 1.25$ $\gamma_L := 1.75$ $Q_D := 2$ $Q_L := 1$ $\frac{Q_D}{Q_L} = 2$

$\lambda_{QD} := 1.08$ $\lambda_{QL} := 1.15$ $COV_{QD} := 0.128$ $COV_{QL} := 0.18$

$\beta_T := 2.5$

DATA :=

C:\..\Phi_factor_data.xls

$n := 28$

$$\lambda_R := \begin{array}{|l} \text{for } i \in 1..n \\ \quad \lambda_i \leftarrow \frac{DATA_{i,2}}{DATA_{i,1}} \\ \lambda_R \leftarrow \text{mean}(\lambda) \\ \text{return } \lambda_R \end{array}$$

$\lambda_R = 0.838$

DATA =

	1	2
1	195	139
2	104	55
3	151.5	125
4	135	105
5	113	116
6	61	115
7	140	105
8	184	165
9	103	90
10	103	90
11	111	82
12	127	95
13	108	70
14	122	85
15	143	80
16	167	140

$$\Phi := \left|\begin{array}{l} \text{for } i \in 1..n \\ \quad \lambda_i \leftarrow \dfrac{DATA_{i,2}}{DATA_{i,1}} \\ \lambda_R \leftarrow \text{mean}(\lambda) \\ COV_R \leftarrow \dfrac{\sqrt{\dfrac{n}{n-1}\cdot \text{var}(\lambda)}}{\text{mean}(\lambda)} \\ \Phi \leftarrow \dfrac{\lambda_R\cdot\left(\gamma_D\cdot\dfrac{Q_D}{Q_L}+\gamma_L\right)\cdot\sqrt{\dfrac{1+\dfrac{\dfrac{Q_D^{\,2}}{Q_L^{\,2}}\cdot\lambda_{QD}^{\,2}\cdot COV_{QD}^{\,2}+\lambda_{QL}^{\,2}\cdot COV_{QL}^{\,2}}{\dfrac{Q_D^{\,2}}{Q_L^{\,2}}\cdot\lambda_{QD}^{\,2}+2\cdot\dfrac{Q_D}{Q_L}\cdot\lambda_{QD}\cdot\lambda_{QL}+\lambda_{QL}^{\,2}}}{1+COV_R^{\,2}}}}{\left(\lambda_{QD}\cdot\dfrac{Q_D}{Q_L}+\lambda_{QL}\right)\cdot e^{\beta_T\cdot\sqrt{\ln\left[\left(1+COV_R^{\,2}\right)\cdot\left(1+\dfrac{\dfrac{Q_D^{\,2}}{Q_L^{\,2}}\cdot\lambda_{QD}^{\,2}\cdot COV_{QD}^{\,2}+\lambda_{QL}^{\,2}\cdot COV_{QL}^{\,2}}{\dfrac{Q_D^{\,2}}{Q_L^{\,2}}\cdot\lambda_{QD}^{\,2}+2\cdot\dfrac{Q_D}{Q_L}\cdot\lambda_{QD}\cdot\lambda_{QL}+\lambda_{QL}^{\,2}}\right)\right]}}} \\ \text{return } \Phi \end{array}\right.$$

$$\Phi_{\lambda R} := \frac{\Phi}{\lambda_R}$$

$$COV_R := \left|\begin{array}{l} \text{for } i \in 1..n \\ \quad \lambda_i \leftarrow \dfrac{DATA_{i,2}}{DATA_{i,1}} \\ \lambda_R \leftarrow \text{mean}(\lambda) \\ COV_R \leftarrow \dfrac{\sqrt{\dfrac{n}{n-1}\cdot \text{var}(\lambda)}}{\text{mean}(\lambda)} \\ \text{return } COV_R \end{array}\right.$$

$\Phi = 0.452$ $\quad COV_R = 0.32$ $\quad \Phi_{\lambda R} = 0.539$

Bootstrap Analysis

Schmertmann Method (Florida Soil)

$ORIGIN \equiv 1$

Data := E:\Histogram_Schmertmannmethod.xls

$m := rows(Data)$ $\quad m = 21$ $\quad mean(Data) = 1.327$

$min(Data) = 0.475$

$max(Data) = 3.93$

$$stdev(Data) \cdot \sqrt{\frac{m}{m-1}} = 0.693$$

$a := 0$

$b := 4$

$n := 20$

$j := 1 .. n + 1$

$$h := \frac{b-a}{n}$$

$$int_j := a + (j-1) \cdot h$$

$$f := \frac{hist(int, Data)}{m \cdot h}$$

Data =

	1
1	1.25
2	0.737
3	0.475
4	1.121
5	1.602
6	1.039
7	1.252
8	1.169
9	0.673
10	1.54
11	1.183
12	1.431
13	2.096
14	1.157
15	1.389
16	1.441

int =

	1
1	0
2	0.2
3	0.4
4	0.6
5	0.8
6	1
7	1.2
8	1.4
9	1.6
10	1.8
11	2
12	2.2
13	2.4
14	2.6
15	2.8
16	3

f =

	1
1	0
2	0
3	0.238
4	0.476
5	0.476
6	1.429
7	0.952
8	0.714
9	0.238
10	0
11	0.238
12	0
13	0
14	0
15	0
16	0

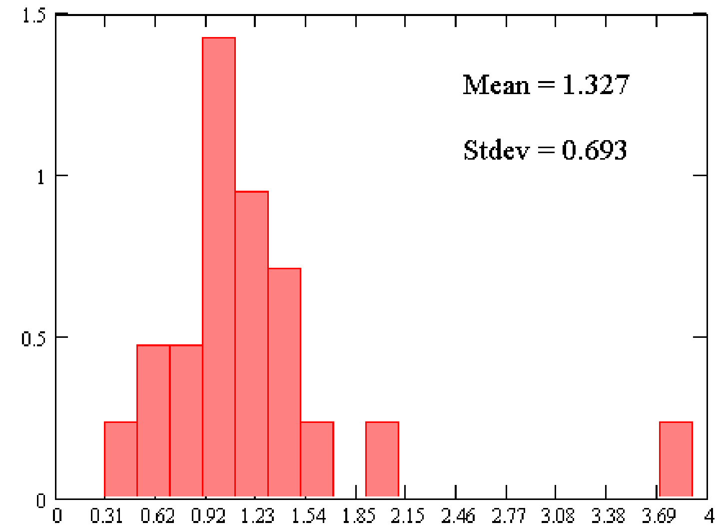

$$
\begin{array}{l}
\text{Mean} := \left|
\begin{array}{l}
\text{Index} \leftarrow \text{ceil}(\text{runif}(100000 \cdot m, 0, m)) \\
\text{for } i \in 1..100000 \\
\quad \left|
\begin{array}{l}
\text{for } j \in 1..m \\
\quad RD_j \leftarrow \text{Data}_{\left[\text{Index}_{m \cdot (i-1)+j}\right]} \\
\text{Mean}_i \leftarrow \text{mean}(RD)
\end{array}
\right. \\
\text{return Mean}
\end{array}
\right.
\end{array}
$$

$$
\begin{array}{l}
\text{Stdev} := \left|
\begin{array}{l}
\text{Index} \leftarrow \text{ceil}(\text{runif}(100000 \cdot m, 0, m)) \\
\text{for } i \in 1..100000 \\
\quad \left|
\begin{array}{l}
\text{for } j \in 1..m \\
\quad RD_j \leftarrow \text{Data}_{\left[\text{Index}_{m \cdot (i-1)+j}\right]} \\
\text{Stdev}_i \leftarrow \text{stdev}(RD) \cdot \sqrt{\dfrac{m}{m-1}}
\end{array}
\right. \\
\text{return Stdev}
\end{array}
\right.
\end{array}
$$

Mean =

	1
1	1.379
2	1.661
3	1.467
4	1.923
5	1.398
6	1.412
7	1.457
8	1.179
9	1.057
10	1.196
11	1.597
12	1.125
13	1.314
14	1.159
15	1.143
16	1.413

Stdev =

	1
1	0.687
2	1.01
3	0.946
4	0.856
5	1.032
6	0.368
7	0.921
8	1.15
9	0.708
10	0.418
11	0.65
12	0.896
13	0.216
14	0.285
15	0.714
16	0.745

$Truemean := mean(Mean)$ $Truemean = 1.328$

$TrueStdev := mean(Stdev)$ $TrueStdev = 0.631$

$Stdevmean := stdev(Mean)$ $Stdevmean = 0.148$

$Stdevstdev := stdev(Stdev)$ $Stdevstdev = 0.243$

$m := rows(Mean)$

Mean Analysis:

$min(Mean) = 0.895$

$max(Mean) = 2.206$

$a := min(Mean)$

$b := max(Mean)$

$n := 30$

$j := 1 .. n + 1$

$$h := \frac{b - a}{n}$$

$$int_j := a + (j - 1) \cdot h$$

$$f := \frac{hist(int, Mean)}{m \cdot h}$$

$c := max(f)$ $c = 2.704$

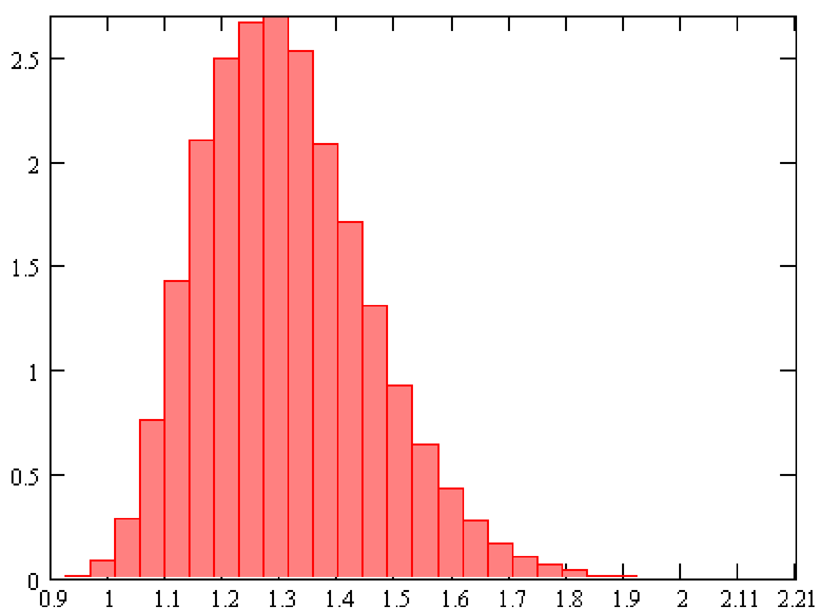

Standard Deviation Analysis:

$\min(\mathrm{Stdev}) = 0.129$

$\max(\mathrm{Stdev}) = 1.428$

$a := \min(\mathrm{Stdev})$

$b := \max(\mathrm{Stdev})$

$n := 30$

$j := 1..n + 1$

$$h := \frac{b - a}{n}$$

$\mathrm{int}_j := a + (j - 1)\cdot h$

$$f := \frac{\mathrm{hist}(\mathrm{int}, \mathrm{Stdev})}{m\cdot h}$$

$c := \max(f)$ $\quad c = 3.885$

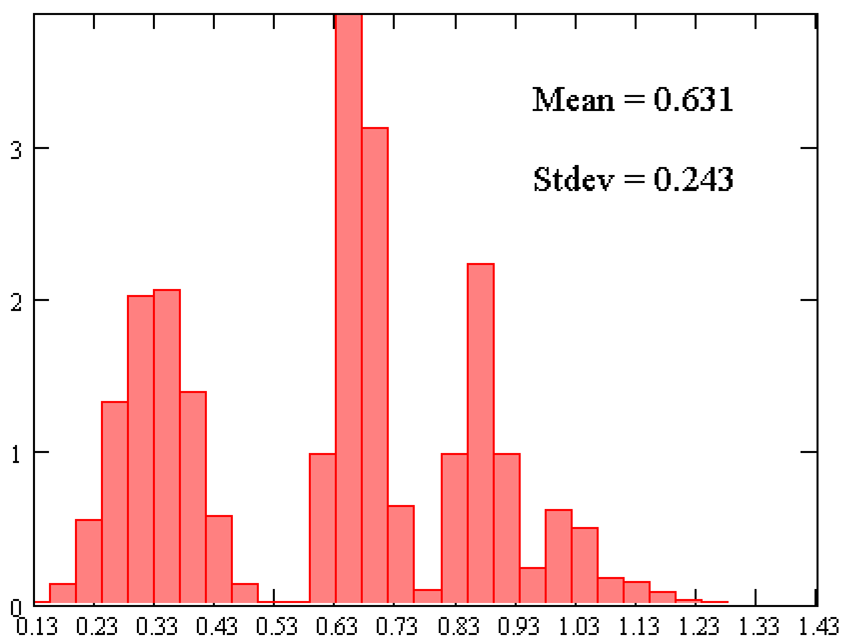

The Proposed Method (Florida Soil)

ORIGIN ≡ 1

Data :=

E:\Histogram_UF method_Florida soil.xls

$\text{mean}(\text{Data}) = 1.079$

$m := \text{rows}(\text{Data})$ $\quad m = 21$ $\quad \text{stdev}(\text{Data}) \cdot \sqrt{\dfrac{m}{m-1}} = 0.288$

$\min(\text{Data}) = 0.613$

$\max(\text{Data}) = 1.701$

$a := 0.6$

$b := 1.8$

$n := 8$

$j := 1 .. n + 1$

$$h := \frac{b - a}{n}$$

$$\text{int}_j := a + (j - 1) \cdot h$$

$$\text{Frequency} := \frac{\text{hist}(\text{int}, \text{Data})}{m \cdot h}$$

Data =

	1
1	0.921
2	0.971
3	0.72
4	0.94
5	1.182
6	0.869
7	1.01
8	0.791
9	0.68
10	1.277
11	1.261
12	1.055
13	1.584
14	0.954
15	1.195
16	1.066

$$\text{int} = \begin{pmatrix} 0.6 \\ 0.75 \\ 0.9 \\ 1.05 \\ 1.2 \\ 1.35 \\ 1.5 \\ 1.65 \\ 1.8 \end{pmatrix} \qquad \text{Frequency} = \begin{pmatrix} 0.952 \\ 0.635 \\ 1.587 \\ 1.587 \\ 0.952 \\ 0 \\ 0.635 \\ 0.317 \end{pmatrix}$$

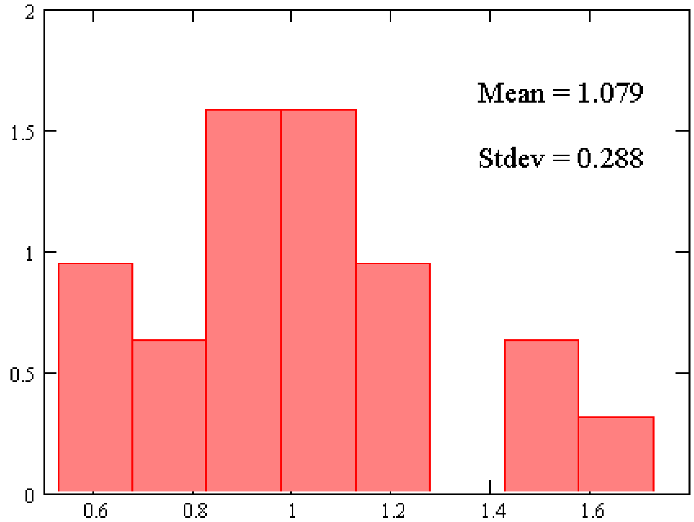

$$\text{Mean} := \left| \begin{array}{l} \text{Index} \leftarrow \text{ceil}(\text{runif}(100000\cdot m, 0, m)) \\ \text{for } i \in 1..100000 \\ \quad \left| \begin{array}{l} \text{for } j \in 1..m \\ \quad RD_j \leftarrow \text{Data}_{\left[\text{Index}_{m\cdot(i-1)+j}\right]} \\ \text{Mean}_i \leftarrow \text{mean}(RD) \end{array} \right. \\ \text{return Mean} \end{array} \right.$$

$$\text{Stdev} := \left| \begin{array}{l} \text{Index} \leftarrow \text{ceil}(\text{runif}(100000\cdot m, 0, m)) \\ \text{for } i \in 1..100000 \\ \quad \left| \begin{array}{l} \text{for } j \in 1..m \\ \quad RD_j \leftarrow \text{Data}_{\left[\text{Index}_{m\cdot(i-1)+j}\right]} \\ \text{Stdev}_i \leftarrow \text{stdev}(RD)\cdot\sqrt{\dfrac{m}{m-1}} \end{array} \right. \\ \text{return Stdev} \end{array} \right.$$

Mean =

	1
1	1.11
2	1.212
3	1.109
4	1.249
5	1.094
6	1.151
7	1.102
8	1.069
9	0.936
10	1.04
11	1.173
12	1.008
13	1.126
14	1.024
15	1.032
16	1.14

Stdev =

	1
1	0.306
2	0.314
3	0.305
4	0.302
5	0.314
6	0.283
7	0.304
8	0.34
9	0.298
10	0.246
11	0.251
12	0.273
13	0.226
14	0.248
15	0.332
16	0.311

$m := \text{rows}(\text{Mean})$

$Truemean := mean(Mean)$ $\quad Truemean = 1.079$

$Stdevmean := stdev(Mean)$ $\quad Stdevmean = 0.061$

$TrueStdev := mean(Stdev)$ $\quad mean(Stdev) = 0.278$

$Stdevstdev := stdev(Stdev)$ $\quad Stdevstdev = 0.042$

Mean Analysis:

$min(Mean) = 0.832$

$max(Mean) = 1.369$

$a := min(Mean)$

$b := max(Mean)$

$n := 30$

$m := rows(Mean)$ $\quad m = 1 \times 10^5$

$j := 1 .. n + 1$

$$h := \frac{b - a}{n}$$

$int_j := a + (j - 1) \cdot h$

$$Frequency := \frac{hist(int, Mean)}{m \cdot h}$$

$c := max(Frequency)$ $\quad c = 6.528$

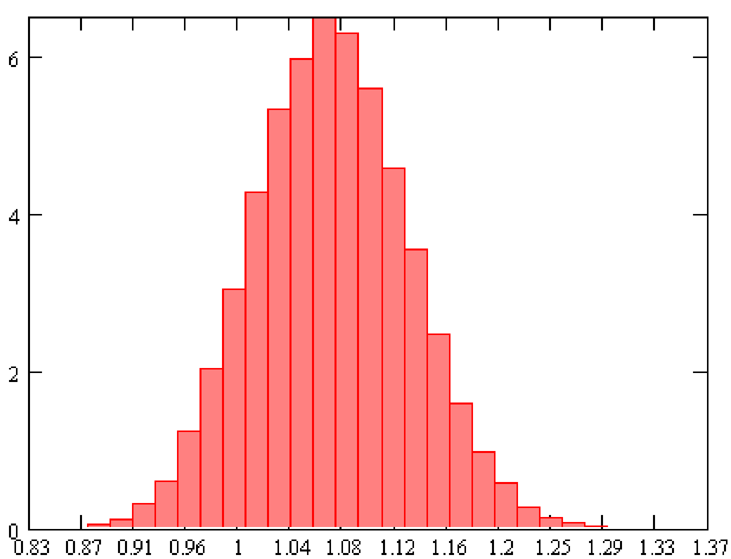

Standard Deviation Analysis:

$\min(\text{Stdev}) = 0.105$

$\max(\text{Stdev}) = 0.435$

$a := \min(\text{Stdev})$

$b := \max(\text{Stdev})$

$n := 30$

$j := 1 .. n + 1$

$$h := \frac{b - a}{n}$$

$int_j := a + (j - 1) \cdot h$

$$f := \frac{\text{hist}(int, \text{Stdev})}{m \cdot h}$$

$c := \max(f) \qquad c = 9.481$

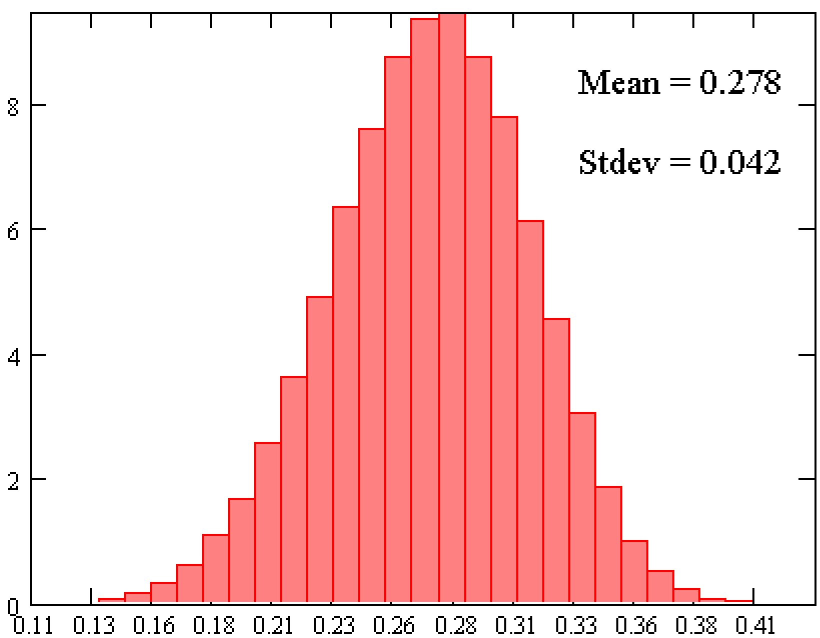

REFERENCES

AASHTO. (1996/2000). “LRFD Bridge Design Specifications.” 2nd LRFD Edition—2000 Interim Revisions, AASHTO, Washington, DC.

Ahmadi, M.M., Byrne, P.M., and Campanella, R.G. (2005). “Cone tip resistance in sand: modeling, verification, and applications.” *Can. Geotech. J.*, 42, 977–993.

Almeida, M.S.S., Danziger, F.A.B., and Lunne, T. (1996). “Use of the piezocone test to predict the axial capacity of driven and jacked piles in clay.” *Can. Geotech. J.*, 33 (1), 23-41.

Aoki, N., and De Alencar, D. (1975). “An approximate method to estimate the bearing capacity of piles.” *Proc., 5th Pan-American Conf. of Soil Mechanics and Foundation Engineering*, Buenos Aires, Vol. 1, 367–376.

Baldi, G., Bellotti, R., Ghionna, V.N., Jamiolkowski, M., and LoPresti, D.C.F. (1989). “Modulus of sands from CPT and DMT.” *Proc., 12th International Conf. on Soil Mechanics and Foundation Engrg.* A.A. Balkema, Rotterdam, The Netherlands, Vol. 1, 165–170.

Baldi, G., Bellotti, R., Ghionna, V.N., Jamiolkowski, M. and Pasqualini, E. (1981). “Cone resistance of a dry medium sand.” *Proc. 10th International Conf. on Soil Mechanics and Foundation Engrg.*, Stockholm, Vol. 2, 427-432.

Baligh, M.M., Vivatrat, V., and Ladd, C.C. (1980). “Cone penetration in soil profiling.” *J. of Geotech. Engrg. Div.*, ASCE, Vol. 106, GT4, 447-461.

Briaud, J.L. “Introduction to soil moduli.” Dept. of Civil Engineering, Texas A&M Univ., College Station, Tx, USA. < http://ceprofs.civil.tamu.edu/briaud/Intro%20to%20Moduli/Intro%20to%20Moduli.pdf>

Bustamante, M., and Gianeselli, L. (1982). “Pile bearing capacity predictions by means of static penetrometer CPT.” *Proc., 2nd European Symp. on Penetration Testing*, ESOPT-II, Amsterdam, The Netherlands, Vol. 2, 493–500.

Campanella, R. G. (1995). “Interpretation of piezocone test data for geotechnical design.” The University of British Columbia, Vancouver, B.C. Canada, Soil Mechanics Series Nos. 157 & 158.

Campanella, R. G., and Robertson, P. K. (1988). “Current status of the piezocone test.” *Proc., 1st Int. Symp. on Penetration Testing*, ISOPT-1, Orlando, Fla., Vol. 1, 93–116.

Chapman, G.A. and Donald, I.B. (1981). “Interpretation of static penetration tests in sand.” *10th International Conf. on Soil Mechanics and Foundation Engrg.*, Stockholm, Vol. 2, 455-458.

Clisby, M. B., Scholtes, R. M., Corey, M. W., Cole, H. A., Teng, P., and Webb, J. D. (1978). “An evaluation of pile bearing capacities.” *Final Report*, Mississippi State Highway Department, Volume 1.

Clough, G.W., Sitar, N., Bachus, R.C. and Rad, N.S. (1981). "Cemented sands under static loading." *J. of the Geotech. Engrg. Division*, ASCE, 107 (GT6), 799-817.

Davisson, M. T. (1972). "High capacity piles." *Proc., Lecture Series on Innovation in Foundation Construction*, American Society of Civil Engineers, ASCE, New York, 81–112.

De Ruiter, J., and Beringen, F. L. (1979). "Pile foundations for large North Sea structures." *Mar. Geotech.*, 3(3), 267–314.

Dobry R and Vucetic M. (1987). "State-of-the-art report: dynamic properties and response of soft clays deposits." *Proc., the Int. Symp. on Geotech. Engrg. of Soft Soils*, Mexico City, 51–87.

Douglas, B. J., and Olsen, R. S. (1981). "Soil classification using electric cone penetrometer." *Symp. on Cone Penetration Testing and Experience*, ASCE, New York, 209–227.

Durgunoglu, H.T., Mitchell, J.K. (1975). "Static penetration resistance of soils 1 – analysis." *Proc. of the Conf. on Insitu Measurement of Soil Properties*, 151 – 171.

Eslami, A., and Fellenius, B. H. (1997). "Pile capacity by direct CPT and CPTU methods applied to 102 case histories." *Can. Geotech. J.*, 34, 886–904.

Florida Department of Transportation. (2007). "Standard specifications for road and bridge construction 2007." Sec. 455-2.2.1. Tallahassee, Fla. <http://www.dot.state.fl.us/Specificationsoffice/2007BK/TOC.htm>

Gens, A. and Nova, R. (1993). "Conceptual bases for a constitutive model for bonded soils and weak rocks." *Geotech. Engrg. of Hard Soils and Soft Rocks*, Edited by A. Anagnostopoulos, F. Schlosser, N. Kalteziotis, and R. Frank. A.A. Balkema, Rotterdam, 485–494.

Greig, J.W., Campanella, R.G. and Robertson, P.K. (1986). "Comparison of field vane results with other in situ test results." *Soil Mechanics Series No. 106*, Dept. of Civil Engineering, Univ. of British Columbia, Vancouver.

Hardin, B.O. and Drnevich, V.P. (1972). "Shear modulus and damping in soils: Design equations and curves." *Proc. of ASCE, J. of the Soil Mechanics and Foundation Div.,* Vol. 98, SM7, 667-692.

Jamiolkowski, M., Lancellotta, R., Tordella, L. and Battaglio, M. (1982). "Undrained strength from CPT." *Proc. of the European Symp. on Penetration Testing*, ESOPT II, Amsterdam, Vol. 2, 599-606.

Janbu, N., Senneset, K. (1974). "Effective stress interpretation of in-situ static penetration tests." *Proc. of the European Symp. on Penetration Testing*, National Swedish Building Research, Stockholm, Sweden, Vol. 2(2),181–193.

Jardine, R. J., and Chow, F. C. (1996). “New design methods for offshore piles.” *MTD Publ. No. 96/103,* Centre for Petroleum and Marine Technology (CPMT), London, U.K.

Joustra, K. and de Gijt, J.G. (1982). “Results and interpretation of cone penetration tests in soils of different mineralogic composition.” *Proc. of the 2nd European Symp. on Penetration Testing*, ESOPT II, Amsterdam, The Netherlands, Vol. 2, 615-626.

Ladd, C.C. and Foott, R. (1974). “New design procedure for stability of soft clays.” *J., Geotech. Engrg. Div.*, ASCE, Vol. 100, No. GT7, 763-786.

Lehane, B.M., Schneider, J.A., and Xu, X. (2005b). “CPT based design of driven piles in sand for offshore structures.” *UWA Report, GEO: 05345*.

Leroueil, S., Vaughan, P. R. (1990). “General and congruent effects of structure in natural soils and weak rocks.” *Geotechnique*. Vol. 40, 467-88.

Lunne, T. and Kleven, A. (1981). “Role of CPT in North Sea foundation engineering.” *Symp. on Cone Penetration Testing and Experience, Geotech. Engrg. Div.*, ASCE, 49-75.

Lunne, T., Robertson, P.K. and Powell, J.J.M. (1997). “Cone penetration testing in geotechnical practice.” *Blackie Academic and Professional*.

Martin, G. R. and Douglas, B. J. (1981). “Evaluation of the cone penetrometer for liquefaction hazard assessment.” *Open File No. 81-284,* Dept. of the Interior, U.S. Geological Survey, Menlo Park, California.

Parkin, A., Holden, J., Aamot, K., Last, N. and Lunne, T. (1980). “Laboratory investigations of CPT’s in sand.” *Report 52108-9,* Norwegian Geotechnical Institute, Oslo.

Philipponnat, G. (1980). “Methode pratique de calcul d’un pieu isole a l’aide du penetrometre statique.” *Rev. Fr. Geotech.*, 10, 55–64.

Powell, J. J. M., Lunne, T., and Frank, R. (2001). “Semi empirical design procedures for axial pile capacity in clays.” *Proc. XV ICSMGE*, Istanbul.

Price, G., and Wardle, I. F. (1982). “A comparison between cone penetration test results and the performance of small diameter instrumented piles in stiff clay.” *Proc. of the 2nd European Symp. on Penetration Testing*, Amsterdam, The Netherlands, Vol. 2, 775–780.

Puppala , A.J., Acar, Y.B. and Tumay, M.T. (1995). “Cone penetration in very weakly cemented sand.” *J. Geotech. Engrg.*, Vol. 121, No. 8, 589-600.

Puppala, A.J., Arslan, S., Tumay, M.T. and Yalcin, B.A. (1998). “Cone penetration testing in cemented soils: Comparisons between field and laboratory chamber test results.” *Proc. of the 1st International Conf. on Site Characterization*, Atlanta, Ga.

Rad, N.S., and Tumay, M.T. (1986). “Effect of cementation on the cone penetration resistance of sand.” *Use of In Situ Tests in Geotech. Engrg*, ASCE, 926-948.

Rix, G. J. and Stokoe, K. H. (1991). "Correlation of initial tangent modulus and cone penetration resistance." *Calibration Chamber Testing*, Elsevier Science, New York, 351-361.

Robertson, P.K. (1990). "Soil classification using the cone penetration test." *Can. Geotech. J.*, Vol. 27, No. 1, 151- 158.

Robertson, P.K. and Campanella, R.G. (1983a). "Interpretation of cone penetration tests-part I (sand)." *Can. Geotech. J.*, Vol. 20, No. 4, 718-733.

Robertson, P.K. and Campanella, R.G. (1983b). "Interpretation of cone penetration tests-part II (clay)." *Can. Geotech. J.*, Vol. 20, No. 4, 734-745.

Robertson, P.K., Campanella, R.G., Gillespie, D. and Grieg, J. (1986). "Use of piezometer cone data." *Proc., in-situ '86, ASCE Specialty conf.*, Blacksburg, Va, United States, 1263–1280.

Schmertmann, J.H. (1975). "Measurement of In-situ shear strength." *Proc. of the Specialty Conference on In Situ Measurement of Soil Properties,* ASCE, Vol. 2, 57-138, Raleigh, Nc.

Schmertmann, J.H. (1978a). "Guidelines for cone penetration test, performance and design." *Rep. No. FHWA-TS-78-209*, U.S. Department of Transportation, Washington, D.C., 145.

Seed, H.B. and Idriss, I.M. (1970). "Soil moduli and damping factors for dynamics response analysis." *Rep. No. EERC 70-10*, Univ. of California, Berkeley, Ca.

Styler, M.A. (2006). "Development and implementation of the DIGGS format to perform LRFD resistance factor calibration of driven concrete piles in Florida." Master's thesis, Univ. of Florida, Gainesville, Fla.

Sun, J.I., Golesorkhi, R., and Seed, H.B. (1988). "Dynamic moduli and damping ratio for cohesive soils." *Rep. No. UCB/EERC-88/15*, Earthquake Engineering Research Center, University of California, Berkeley, Ca.

Titi, H. H., and Abu-Farsakh, M. Y. (1999). "Evaluation of bearing capacity of piles from cone penetration test data." *Rep. No. FHWA/LA.99/334*, Louisiana Transportation Research Center, Baton Rouge, La.

Tumay, M. T., and Fakhroo, M. (1982). "Friction pile capacity prediction in cohesive soils using electric quasi-static penetration tests." *Interim Research Rep. No. 1*, Louisiana Department of Transportation and Development, Research and Development Section, Baton Rouge, La.

Veismanis, A. (1974). "Laboratory investigation of electrical friction-cone penetrometers in sand." *Proc. of the European Symp. on Penetration Testing*, ESOPT I, Stockholm, Vol. 2.2.

Vesic, A.S. (1963). "Bearing capacity of deep foundations in sands." *Highway Research Rep. 39*, Highway Research Board, National Research Council, Washington, D.C.

Villet, W.C.B. and Mitchell, J.K. (1981). “Cone resistance, relative density and friction angle.” *Symp. on Cone Penetration Testing and Experience*, Geotech. Engrg. Division, ASCE, 178-208.

Vucetic, M. and Dobry, R. (1991). ”Effect of soil plasticity on cyclic response.” *J. of Geotech. Engrg*, 117(1), 89-107.

Zhou, J., Xie, Y., Zuo, Z.S., Luo, M.Y. and Tang, X.J. (1982). “Prediction of limit load of driven pile by CPT.” *Proc. of the 2nd European Symp. on Penetration Testing*, Amsterdam, The Netherlands, Vol. 2, 957-961.